Studies of enzyme kinetics and aspects of enzyme structure *in vivo* using NMR and molecular genetics

A thesis submitted in partial fulfilment of the requirements for the Degree of Doctor of Philosphy

by

Simon–Peter Williams, M.A.

Green College, Oxford

Trinity Term, 1992

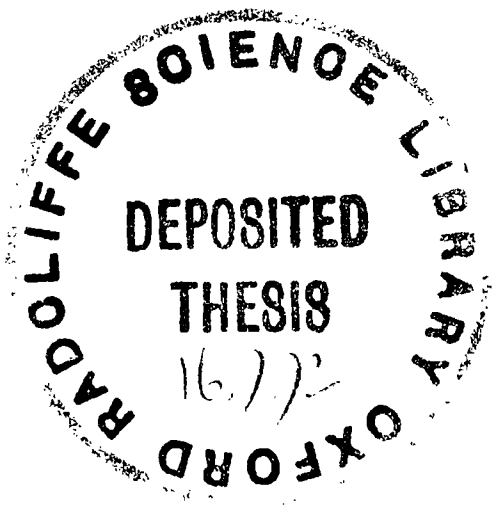

Simon-Peter Williams
Green College, Oxford

ABSTRACT

D.Phil thesis
Trinity Term, 1992

Studies of enzyme kinetics and aspects of enzyme structure *in vivo* using NMR and molecular genetics

A quantitative understanding of metabolic control depends on a knowledge of the enzymes involved. The extrapolation of studies *in vitro* to the intact cell is controversial because the intracellular environment is relatively poorly characterised, particularly with respect to the interactions between weakly-associated enzymes.

There is a clear need to study enzymes directly in the cell, yet there are few suitable techniques. Metabolites have been very successfully studied in cells by the non-invasive technique of nuclear magnetic resonance (NMR). NMR studies of enzymes in the cell have, however, been prevented by difficulties in assigning the resonances from the many proteins within the cell.

A method for studying a specific enzyme in the cell has been developed, using *Saccharomyces cerevisiae* and phosphoglycerate kinase (PGK) as a model system. Using an inducible expression system, PGK was synthesised in the cell without significant synthesis of other proteins. With 5-fluorotryptophan in the growth medium, fluorine-labelled PGK was formed *in situ*. Fluorine is an excellent label for NMR since it is absent from most cells and has a high receptivity to NMR detection.

^{19}F NMR was used to study PGK in the intact cell. Comparisons with measurements *in vitro* showed that PGK was exposed to only a small fraction of the total intracellular [ADP], implying some form of compartmentalisation. The NMR relaxation properties observed *in vivo* and *in vitro* were compared with theoretical predictions. This showed that PGK was not part of a complex in the cell and that the viscosity of the cytoplasm, relative to water, was c. 4 at 30 °C. Fluorine-labelled pyruvate kinase and hexokinase have also been prepared; the spectra of these proteins *in vitro* are responsive to their ligands, and further work will study these proteins *in vivo*.

NMR techniques were also applied to study the kinetics of PGK in the cell. PGK and GAPDH catalyse an ATP$\leftrightarrow P_i$ exchange which is near-equilibrium in wild-type cells. ^{31}P magnetisation transfer experiments in genetically manipulated cells showed that the reaction becomes unidirectional if the PGK activity is reduced by 95 %. Net flux is reduced by less than 30 %. In low-PGK cells, the ATP$\leftrightarrow P_i$ exchange from oxidative phosphorylation can be isolated from that of glycolysis, facilitating direct measurements of the P:O ratio. In the cells studied, the P:O ratio was 2 to 3.

Brief Table of Contents

Dedication

I'd just like to stop and remember all those who have not had the opportunities life has afforded me, and especially those who gave up their own opportunities for the sake of others.

Acknowledgements

This is definitely a "work of many parts", and several places too.

I am greatly indebted to Kevin Brindle for rescuing me from the abacus abyss, and particularly to my mother, Bridget Harris, Carole Howells, Claire Dickinson and Corinne Spickett for encouraging me to step back. Thanks to Corinne, Ro, and Peta for looking after me when I still had rows of figures etched on my brain, and Siân, James, Kate, Kevin and Sandra for looking after me when I still had spires etched on my brain.

I am very grateful for the support of all my friends in Oxford, London and Manchester, particularly during the Great Data Famine of '89-'91 and the migration North. Green College provided me with friends, surroundings, and food that made life much more pleasant and easy. Rusholme was an education in itself. Thanks to Margaret for showing me the better bits of Manchester, or at least the better cocktail bars.

Professional acknowledgements are in the text, but I am particularly grateful to Siân, Kevin and Sandra for inculcating in me some sense of good laboratory practice. Corinne and Ro ("poor old Ro") were invaluable in finding my laboratory feet too. James set an example in the laboratory (and pub) that can only be described as marvellous.

My finances were supported through a SERC Quota award, two different scholarships at Green College, and especially my parents. I could have got at least as much again if Kevin had used the swear-box properly on magnet days.

Abbreviations used

3PG, 3PGA	3-phosphoglycerate
3,4-DCI	3,4-dichloroisocoumarin
Å	Ångstrom(s), 10^{-10} m
α/β/γ-ATP, NTP etc.	the α,β or γ phosphate of adenosine triphosphate, etc.
ADP	adenosine diphosphate
AMP	adenosine monophosphate
ATP	adenosine triphosphate
AXP	adenosine mono- di- or triphosphate
BSA	bovine serum albumin
CIAP	calf intestinal alkaline phosphatase
CSA	chemical shift anisotropy
D_2O	deuterium oxide, ^2H_2O
DHAP	dihydroxyacetone phosphate
DTT	dithiothreitol, Cleland's reagent
E64	trans-epoxysuccinyl-L-leucylamido(4-guanidino)butane
EDTA	ethylenediaminetetracetic acid
F6P	fructose-6-phosphate
FBP, Fru-1,6-BP	fructose-1,6-bisphosphate ("fructose diphosphate, FDP")
FPhe	m-fluorophenylalanine
FTrp	5-fluorotryptophan
G3P	glycerol-3-phosphate
G3PDH	glycerol-3-phosphate dehydrogenase
G6P	glucose-6-phosphate
G6PDH	glucose-6-phosphate dehydrogenase
g	the force due to the Earth's gravity, or in context
g	gram, 10^{3} kilogram
GAP, GA3P	glyceraldehyde-3-phosphate
GAPDH	glyceraldehyde-3-phosphate dehydrogenase
GOD	glucose oxidase
GTP	guanosine triphosphate
HEPES	N-2-hydroxyethylpiperazine-N'-2-ethanesulphonic acid

HPLC	high pressure/performance liquid chromatography
HK, HXK	hexokinase
kb, kbp	kilobases, kilobase pairs
kDa	kilodaltons
LDH	lactate dehydrogenase
M	mol dm^{-3}
MDP	methylene diphosphonate
MES	2-(N-morpholino)ethanesulphonic acid
ml	millilitre, 10^{-6} m^3
MOPS	3-(N-morpholino)propanesulphonic acid
NAD, NAD^+	nicotinamide adenine dinucleotide (β form)
NADH	reduced nicotinamide adenine dinucleotide (β form)
NDP	nucleotide diphosphate
NMR	nuclear magnetic resonance
NOE	nuclear Overhauser effect
NTP	nucleotide triphosphate
Pa	Pascal(s)
PAGE	polyacrylamide gel electrophoresis
PCA	perchloric acid
PDE	phosphodiesters
PEG	polyethylene glycol
PEP	phospho*enol*pyruvate
PGI	phosphoglucose isomerase
PGK	3-phosphoglycerate kinase
Phe	phenylalanine
P_i	inorganic phosphate, orthophosphate
PIPES	Piperazine-N,N'-bis[2-ethanesulphonic acid]
PK, PYK	pyruvate kinase
PME	phophomonoesters
PMSF	phenylmethyl sulphonyl fluoride
POD	peroxidase
ppm	parts per million
R_1	spin-lattice or longitudinal relaxation rate constant
R_2	spin-spin or transverse relaxation rate constant

rpm	revolutions per minute
s	second(s)
SDS	sodium dodecyl sulphate (lauryl sulphate)
T_1	spin-lattice or longitudinal relaxation time constant
T_2	spin-spin or transverse relaxation time constant
TEMED	N,N,N',N'-tetraethylmethylenediamine
TIM, TPI	triose phosphate isomerase
Tris	tris(hydroxymethyl)aminomethane
Trp	tryptophan
Tyr	tyrosine
U	enzyme activity unit, μmol product per minute
% v/v	percentage by volume
% w/v	percentage weight by volume

Full Table of Contents

1 Introduction

1.1 The importance of enzymology

A quantitative understanding of metabolism depends on our knowledge of the enzymes involved. An understanding of the control of metabolism is a prerequisite for its rational manipulation for investigative, therapeutic or commercial purposes.

One of the most active research areas in enzymology concerns the behaviour of whole systems of enzymes acting together. The problem has received much attention through both theory (Kacser and Burns 1973; Heinrich and Rapoport 1974; Torres *et al.* 1986; Kacser and Porteous 1987; Acerenza and Kacser 1990) and experiment (Weber and Bernhard 1982; Srivastava and Bernhard 1986; Srere 1987; Srere and Ovadi 1990; Sumegi *et al.* 1990).

Although the combined properties of enzymes in solution can lead to complex phenomena, such as the well-known oscillations in metabolite concentrations (Hess 1973), much of the interest has focused on the existence and operation of weakly-associated multienzyme complexes. These complexes may be defined by specific interactions between proteins or by their co-localisation on cytoskeletal or membrane structures.

However defined, it is thought that some synergy may arise from the direct interaction of several enzymes; complexes may possess important kinetic or regulatory properties because of their supposed ability to "channel" metabolites directly from one active site to the next (Srere 1987; Jackson *et al.* 1990; Srere and Ovadi 1990; Ovádi 1991).

The paper by Ovádi (1991) is a review article at the beginning of an excellent special issue of the *Journal of Theoretical Biology*. Nearly thirty articles on metabolite channelling have been brought together by Athel Cornish-Bowden in this volume. Many of the articles are critical of the evidence for the existence of metabolite channelling, or question its importance even if it does occur. Clearly, the field remains controversial.

The difficulty in devising convincing models or experiments originates from a failure to understand the intracellular environment, as experienced by the enzymes in question, in sufficient detail. An experimental approach to overcoming this limitation is, clearly, to perform experiments in which the enzymes are studied *in situ* in the intact cell.

Not many techniques allow the non-invasive study of a chosen enzyme in the intact cell. The aim of the work undertaken in this thesis was to develop and apply the non-invasive techniques of nuclear magnetic resonance in ways that may increase the understanding of the intracellular environment.

1.2 Non-invasive probes of the intracellular environment

Studies of optically active molecules in the intact cell have a long history (Keilin 1925; Millikan 1937) and continue to be important (Gyubi *et al.* 1988; Campbell 1990). These rely on observing the absorbance, fluorescence, or luminescence of naturally occurring or artificially introduced molecules in the cell. Some of the studies with fluorophores have shown great sensitivity - even allowing fluorescent probes of viscosity to be observed in single cells (Dix and Verkman 1990).

Optical techniques are necessarily limited in their application by the poor tissue penetration depth of visible light. Their use is confined to looking at thin layers of cells or only the surface of bulky tissues, although

improvements in image intensifying and other technologies will probably widen their use.

The potential for the application of nuclear magnetic resonance spectroscopy in biological systems has long been recognised (see, for example, (Gadian 1982)). In this context, the ability to gather data throughout a relatively large, opaque sample, such as a human being, is a distinct advantage over optical techniques. Conversely, there seems little prospect of collecting data from a defined area the size of a cell with NMR techniques. Nevertheless, NMR studies of living tissues have been immensely useful and are capable of yielding a great deal of information about the intracellular environment (Gadian 1982; Iles *et al.* 1982; Avison *et al.* 1986; Radda 1986; Brindle and Campbell 1987).

1.3 Types of NMR experiment *in vivo*

The applications of NMR to the study of intact tissues are diverse. NMR can be used to measure steady-state concentrations of metabolites and the time courses of their turnover (Arnold *et al.* 1984). Isotopic labelling experiments enable the fate of a molecule to be followed through time (den Hollander *et al.* 1986). Magnetisation transfer techniques enable relatively fast reaction rates to be measured (Brindle and Campbell 1987), such as the flux between γ-ATP and the phosphate of phosphocreatine. NMR has also been used to study membrane potentials and cell volumes (London and Gabel 1989) and the intracellular viscosity (Endre *et al.* 1983).

Diverse and powerful though these applications are, studies of small molecules in the cell do not necessarily improve our understanding of the immediate environment of a particular protein. In principle, this information is at least partly accessible through NMR studies of the protein itself. In

practice, this has only been possible in some special cases (Brown *et al.* 1977; Wang *et al.* 1990) because of the difficulties of assigning the observed resonances in the cell to a particular protein species.

The work in this thesis has primarily been concerned with developing a methodology to allow the introduction of NMR-observable labels into a defined protein in the intact cell, and then to use the non-invasive techniques of NMR to study the labelled protein *in situ* in the intact cell.

1.4 Yeast glycolysis as a model system for studying enzymology *in vivo*

All the work done in this thesis employed the baker's yeast *Saccharomyces cerevisiae* as a model organism, although the techniques developed clearly have application in other systems including mammalian cells. Yeast conveniently combines properties of bacterial and mammalian cells, in that it is simple to grow and to genetically manipulate, yet it has the complexity of function of a eukaryote (Botstein and Fink 1988), and indeed has been regarded as a paradigm for the tumour cell. Yeast is capable of using glucose through glycolysis at a great rate, and so one might expect it to be adapted by evolution to use this glucose in an efficient manner. One might, therefore, expect any rate-enhancing multienzyme complexes to be apparent in this organism.

1.5 NMR, genetic engineering, and molecular modelling combined

Metabolic control theory shows how the influence of each component in a metabolic pathway can be isolated and characterised, and suggests a methodology for performing experiments to determine the influence of each

activity in the pathway (Kacser and Burns 1973; Heinrich and Rapoport 1974; Kacser and Burns 1979; Kacser and Porteous 1987). The experiments require changing the activity of a single enzyme in the pathway and evaluating the resultant change in pathway flux.

The techniques of molecular genetics offer the prospect of specifically manipulating enzyme activities in a way that is far more powerful than conventional inhibitor studies (Nimmo and Cohen 1987). In combination with NMR studies of the changes in fluxes, this allows non-invasive assessments of the rôle of different enzymes in the cell (Brindle *et al.* 1991).

Molecular genetics also suggests a method for introducing an NMR-detectable label into a specific protein in the intact cell. If the synthesis of a particular protein could be elevated when other proteins were not being synthesised, then a labelled amino acid present in the cell could be incorporated exclusively into the target protein. Inducible expression systems make this possible (Sykes and Weiner 1980), and molecular genetics can be used to apply this principle to any chosen protein (Brindle *et al.* 1989).

NMR has the potential to reveal the motional properties of the nuclei observed (Harris 1986). There are many modes of motion in a macromolecule, and they can not all be understood analytically. Some of the motions in a protein can, however, be modelled by iterative computation on a large scale.

Molecular dynamics modelling, from structures obtained by crystallography, high-resolution NMR or even by prediction, should allow calculations of the motions within the protein. A knowledge of the motions involved allows the prediction of the expected NMR spectra from the molecule under different conditions, at different temperatures and viscosities, for example.

Comparisons of predicted and observed NMR spectra from the intact cell could give information about the protein *in situ*, whether it was part of a larger complex, or associated with a membrane or the cytoskeleton, for example. It is hoped that the combination of NMR, molecular genetics and molecular modelling will allow some further questions about the operation of enzymes in the intact cell to be answered.

2 Materials and Methods

2.1 Conventions used

Abbreviations used in the protocols are expanded in the Abbreviations section preceding Chapter 1.

2.2 Suppliers of materials

2.2.1 General reagents

Reagents were obtained in analytical grade from various sources. The water used was double glass-distilled or purified (Millipore MilliQ™) water.

The principal suppliers were :

Aldrich Chemical Company Ltd., Gillingham, Dorset, England

BDH Ltd, Poole, Dorset, England

Boehringer Mannheim UK, Lewes, East Sussex

Sigma Chemical Company Ltd., Poole, Dorset, England

2.2.2 Growth media

Dehydrated yeast and *E. coli* growth media and agar were obtained from Difco Laboratories Ltd., East Molesey, Surrey. The Bacto™ range of products referred to in the media recipes is produced by Difco.

2.2.3 Biochemicals

Enzymes were obtained from Boehringer Mannheim or Sigma. Where activities of coupling enzymes are quoted in an assay protocol, the specific

activity of the enzyme used was taken from the manufacturer's product information. Nucleotides, hexose and triose sugars and their derivatives were also obtained from Boehringer or Sigma. β–NADH, notoriously difficult to store (Fawcett *et al.* 1961) was obtained pre-weighed in glass vials from Sigma. The snail gut preparation Glusulase™ was obtained from NEN Du Pont (UK) Ltd.

2.2.4 The yeast strains used

All the strains used for this work were haploid forms of the yeast *Saccharomyces cerevisiae*

AH22	**a**	can^R, his4-519, leu2-3, leu2-112
BC3		his 3-15, leu2-3, leu2-112, trp1-1, ura3-52 pgk::TRP1
BJ2168	**a**	gal2, leu2-3, leu2-112, pep4-3, prb1-1122, prc1-407, trp1=,ura3-52,
DBY745	α	ade1-100, leu2-3, leu2-112, ura3-52
FY3-1		trp1, ade1-100, his3-11, his3-15, leu2-3, leu2-112
FY7-11		trp1, ade1-100, leu2-3, leu2-112, ura3-52
RH1319	**a**	aro3-2, aro4-1
RH1320	α	aro3-2, aro4-1, leu2-2

These strains were obtained from

Dr Alan Kingsman, University of Oxford (AH22, DBY745, FY3-1, FY7-11),

Dr Peter Piper, University College, London. (BC3),

Dr John Rosamond, University of Manchester (BJ2168),

Dr Peter Niederberger, Nestlé Research Center, Vevey (RH1319), and

Dr Gerhard Braus, ETH, Zurich (RH1320).

2.3 The plasmid vectors used and prepared

All the plasmids used can function as "shuttle vectors" as they possess both yeast and *E. coli* replication origins and selection markers. The plasmids carry the yeast *LEU2* gene which expresses ß-isopropyl-malate dehydrogenase to complement the deficient *leu2* gene in the chromosomal DNA of the yeast strains used. They also carry an *E. coli* gene conferring resistance to ampicillin.

The pMA and pYC plasmids have been prepared, characterised and comprehensively described by groups in Oxford and London (Ogden *et al.* 1986; Piper *et al.* 1988).

2.3.1 Acknowledgements

pR21M and pD372N have kindly been made available by Drs. Jennifer Littlechild and Herman Watson, Bristol. The pMA and pKV plasmids were kindly provided by Dr. Alan Kingsman, Oxford. The pYC plasmids were kindly provided by Dr. Peter Piper, London.

2.3.2 A glossary of the plasmids used

See the Figure 2.1 for outline maps of the important plasmids described below. Table 2.1 summarises the nature of the plasmids used, in alphabetical order.

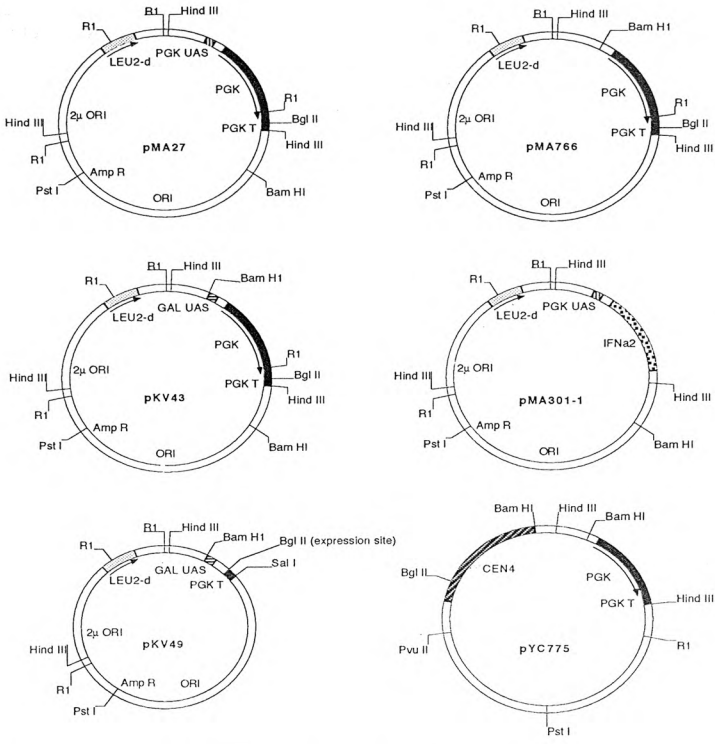

Schematic maps of the plasmid vectors used in this work.

The construction and function of these plasmids and some others based on those shown are discussed in the text. Text inside the circles gives the abbreviated name of the gene or region of the plasmid. Text outside the circles shows the restriction enzyme cut sites. The UAS regions are upstream activator sequences. PGK T is the terminator region of the PGK gene. ORI is the origin of replication in *E. coli*. 2μ ORI is the origin of replication from the natural yeast plasmid 2μ circle. PGK is the coding sequence for PGK, IFNa2 that for human interferon α2. The LEU2-d gene is the LEU2 gene with a partial promoter deletion to reduce its efficiency. CEN4 is a fragment of a yeast centromeric origin of replication.

Figure 2.1

Table 2.1

Plasmid name	Expression product	Promoter type	Expression level (c.f. wild type)
pBF72	PK	PGK/GAL UAS	up to 25
pD372N	PGK D372N	PGK	x 20
pKV43	PGK	PGK/GAL UAS	up to 25
pKV49	none	PGK/GAL UAS	—
pMA3a	none	—	—
pMA27	PGK	PGK	x 20
pMA301-1	Interferon	PGK	—
pMA766	PGK	PGK, no UAS	x 5
pMA777	PGK	modified PGK	1 to 2 x
pR21M	PGK R21M	PGK	x 20
pYC763	PGK	modified PGK	20 %
pYC767	PGK	modified PGK	50 %
pYC775	PGK	modified PGK	5 %

Alphabetical list of the plasmids used in this work and their important characteristics.
PGK is phosphoglycerate kinase, PK is pyruvate kinase. All the plasmids use derivatives of the yeast PGK promoter. Some have been made galactose-inducible by the substitution of the Upstream Activator Sequence from the GAL1-10 gene in place of the native PGK UAS.

2.3.2.1 pMA27

pMA27 expresses high levels of PGK constitutively (Mellor *et al.* 1983). It contains a 2.95 kb Hind III fragment that has the very efficient PGK promoter directing PGK synthesis. When transformed into the yeast strain AH22, for example, it causes up to twenty-fold normal expression levels of PGK protein. PGK normally represents some 3 to 5% of the total soluble cell protein in untransformed cells, and can rise to become as much as 50% of the total soluble cell protein depending on the cell type and growth conditions.

2.3.2.2 *pMA301-1*

pMA301-1 is a derivative of pMA27 in which the PGK coding sequence has been replaced by that of human interferon α2. The PGK promoter sequences are retained but transcription levels are lower than in pMA27 since they are influenced by the coding sequence itself (Mellor *et al.* 1985). The interferon product only reaches 1 to 3% of total soluble cell protein.

2.3.2.3 *pR21M and pD372N*

pR21M is a derivative of pMA27 in which the coding sequence for PGK has been mutagenised to express the site-specific mutants R21M and D372N respectively (Minard *et al.* 1990).

2.3.2.4 *pMA3a*

pMA3a is a vector that contains no expression cassette. It is equivalent to pMA27 but without the Hind III fragment that carries the PGK gene sequences. It does, however, express the products of its selectable markers *LEU2-d* and *Amp*^{r}.

2.3.2.5 *pMA766*

pMA766 is based on pMA27. The UAS region of the PGK promoter, at -402 to -479, has been deleted to reduce the promoter strength. Transformed into AH22 cells it causes around five times wild type expression levels of PGK protein.

2.3.2.6 *pKV43*

pKV43 is similar to pMA27 but with the upstream activator sequence from the *GAL1-10* gene in place of the *PGK* UAS. A 144 bp *GAL1-10* UAS fragment was inserted at the unique Bam HI site in pMA766. The promoter is thus galactose-inducible and glucose-repressible.

2.3.2.7 *pKV49*

pKV49 is similar to pMA27 but it does not contain the PGK coding sequence (Cousens *et al.* 1990). The *PGK* UAS sequence of the native promoter has been replaced with the 144 bp UAS region from the *GAL1-10* gene. The Bal31 nuclease used to remove the coding sequence also removed part of the native 3' UTR including the transcription terminator region. A sequence incorporating the PGK transcription terminator and a translation stop codon ATG has been inserted just downstream of the unique Bgl II site that is used as the coding sequence insertion point.

2.3.2.8 *pBF72*

pBF72 was constructed by inserting the coding sequence for pyruvate kinase (PK) into the pKV49 vector such that the PK coding sequence is transcribed in a galactose-inducible manner under the direction of the efficient hybrid PGK/GAL-UAS promoter.

2.3.2.9 *pMA777*

pMA777 is similar to pMA766 but with a different deletion in the promoter region. When transformed into the *pgk*$^-$ yeast strain BC3 the PGK expression level is comparable to the level expressed from the chromosome in the parental diploid BC2.2 yeast strain (Piper *et al.* 1988). Because of this similarity, this expression level was considered to be approximately wild type for this yeast strain and this plasmid was used to obtain "control" expression levels for the pYC plasmids.

2.3.2.10 *pYC775, pYC763*

The pYC vectors contain yeast CEN4 centromeric sequences in place of the replicative 2μ sequences found in the other vectors. This keeps the copy number as low as 1 to 3 copies per cell. pYC775 and pYC763 each have the

PGK coding sequence under the control of different weakened promoters, based on pMA775 and pMA763 respectively (Ogden *et al.* 1986). The low copy number and the inefficient promoters result in very low levels of PGK expression, approximately 2 to 5% of control expression from pMA777 transformed into yeast strain BC3.

2.4 Plasmid preparation, analysis and storage

2.4.1 Plasmid production and isolation

Plasmids were prepared in *E. coli* according to standard procedures (Sambrook *et al.* 1989). Briefly, the transformations used a calcium chloride treatment to make the cells competent, and the plasmid preparations employed caesium chloride density gradient centrifugation to isolate circular superhelical plasmid DNA.

The isolated plasmid DNA, either fully purified by an alkaline-lysis method or partly purified in small-scale rapid-boiling "minipreps", was analysed by restriction fragment analysis with agarose gel electrophoresis to confirm that the correct material was used for the subsequent yeast transformations.

2.4.2 Restriction enzyme digests

The digests were performed in 0.5 ml plastic microcentrifuge tubes with a total reaction volume of 30 μl. The reaction mixture comprised 10 μl of miniprep sample, 3 μl of reaction buffer concentrate (supplied with the restriction enzyme), 0.1 to 0.2 μl of restriction enzyme stock (typically 1 to 2 units) and water.

The mixture was incubated at 37 °C for 1 to 2 hours before analysis by electrophoresis. The gel loading buffer used contained a small quantity of

RNAse A, sufficient to degrade the RNA contaminants in the mixture within seconds.

2.4.3 Fragment analysis by agarose electrophoresis

DNA fragments were separated by electrophoresis on 1 % agarose slab gels after RNAse treatment as described by Maniatis *et al.* (Sambrook *et al.* 1989).

2.4.4 Long-term plasmid storage

Long-term storage stocks of plasmid DNA were made by transferring 5 μl of a 1 to 2 μg/μl DNA solution into a 500 μl microcentrifuge tube, adding 10 μl of ethanol and 0.5 μl of 3 M sodium acetate. The mixture was frozen at minus 20 °C after centrifuging at c. 15000 g at 4 °C for 10 to 15 minutes.

2.4.5 Plasmid assembly by ligation

2.4.5.1 Linearisation of pKV49

Plasmid pBF72 was prepared by inserting the pyruvate kinase coding sequence into the Bgl II expression site of vector pKV49 such that the transcription of pyruvate kinase was under the control of a galactose-inducible promoter. DNA containing the pyruvate kinase coding sequence was kindly provided by Alistair Brown, Edinburgh, and this was modified by Peta Braddock, Oxford, to give a fragment for expression. The protocol followed to effect this ligation is described below.

5 μl of pKV49 stock (approximately 10 μg) was resuspended to 100 μl with 10 μl of 10X restriction enzyme buffer (as directed by the supplier) and 5 μl of Bgl II restriction enzyme stock (50 units, Boehringer product). The mixture was incubated at 37 °C for 2 hours to cut the pKV49 at its single Bgl II site.

At the end of the incubation period, 5 units of calf intestinal alkaline phosphatase (CIAP) was added to the reaction mixture to remove the terminal 5'-phosphate groups from the linearised DNA. This prevents recircularisation. The mixture was held at 37 °C for 20 minutes.

100 μl of water, 100 μl of STE-saturated phenol, and 100 μl of chloroform were added to the reaction mixture and the whole was twice shaken and centrifuged (5 min, 15000 g benchtop microcentrifuge) to remove the proteins in the mix.

The upper, aqueous DNA-containing layer was removed to a clean 1.5 ml microcentrifuge plastic tube. The DNA was precipitated by adding 1/10 volume 3M sodium acetate and 2 vols. ethanol. The mixture was left on ice for 30 minutes and then centrifuged (15 min, 15000 g) at 4 °C.

The ethanol was removed from the DNA pellet with a fine, flame-drawn Pasteur pipette. The surface of the pellet was gently rinsed with 200 μl of 70% ethanol/30% STE. The pellet was resedimented by centrifugation as before.

The supernatant was removed from the pellet with a fine pipette as before, and dried for 2 minutes in a vacuum dessicator.

The linearised pKV49 stock solution was prepared by overlaying the pellet with 20 μl STE, allowing it to resuspend at room temperature for 30 minutes and then transferring the tube to storage at 4 °C.

The linearisation of pKV49 was confirmed by electrophoretic analysis of 2 μl of the stock solution on a 1 % agarose minigel against the uncut plasmid and 3 μl of a set of rewarmed linear phage λ Hind III/Eco RI fragments (Boehringer). The concentration of the stock was also determined by comparing band intensities of the pKV49 and λ bands and correcting for the different fragment sizes.

2.4.5.2 *Ligation of linear pKV49 and the PK coding sequence.*

A sticky-end ligation procedure was carried out as follows.

Approximately 0.2 μg of linearised pKV49 was incubated with one to two times its molar concentration of the 1.76 kbp PK coding fragment. The ligation was carried out in 20 μl of pH 7.5 ligation buffer containing 60 mM Tris, 10 mM $MgCl_2$, 1 mM EDTA, 10 mM DTT and 2 mM ATP. The reaction was catalysed by 2 units of T4 ligase, approximately 0.5 μl of stock solution.

The reaction mixture was incubated in a water bath in a cold room overnight at 12 °C and then the ligase was inactivated by heating the mixture to 70 °C for 10 minutes. 10 μl of the reaction mixture was removed from the tube and used to transform *E. coli* cells as described above.

2.4.5.3 *Selection of the plasmid with correctly-oriented insert*

It is possible to distinguish plasmids with no insert, the correctly- and incorrectly-oriented inserts on the basis of their Eco RI restriction maps. This is possible since the insertion site on the vector lies at a unique site with respect to the Eco RI sites in the vector and the fragment itself is cut into two unequal fragments by Eco RI. Single transformants were restreaked for single colonies on ampicillin plates.

Plasmid DNA from 24 different transformants was isolated and analysed as described below.

Rapid boiling minipreps were used to prepare DNA samples from the transformants. The DNA was digested by Eco RI and the fragments separated by electrophoresis.

All pKV49-based constructs produced fragments of 2.45, 1.0 and 0.75 kbp. The size of the remaining fragments depends on the insert at the Bgl II site.

For each possible outcome of the ligation, the additional fragment sizes for each insert, in kbp, are shown in Table 2.2.

Table 2.2

Insert orientation	Size of extra fragment(s), kbp
No insert	4.5
Correct insert	4.26 and 2.0
Inverted insert	5.5 and 0.76

Selection of the correctly-oriented pyruvate kinase insert into pKV49.
The absence of an insert into the vector pKV49 or its presence and orientation was determined by examining the EcoRI restriction map. The insert gives rise to unique bands that were used to calculate the orientation.

Each transformant was classified as having no insert, the correct or the inverted insert on the basis of the restriction digest pattern. Analysis of 24 transformants showed that five had no fragment, eleven had the inverted fragment and eight had the pyruvate kinase fragment correctly inserted into pKV49. One of these correct-insert transformants was chosen and restreaked for single colonies on ampicillin plates. One of these colonies was used to produce a larger quantity of purified plasmid DNA for the yeast transformation.

The stock of plasmid produced was examined in a double Eco RI / Bgl II digest to confirm its identity before proceeding to use the stock for the yeast transformations.

2.5 Storage, growth and manipulation of yeast

2.5.1 Growth media

2.5.1.1 Preparation and storage

All these media were prepared and autoclaved for 20 minutes after reaching 115°C (15 psi) and then used when cool or stored at 4°C in at least partial darkness until required, normally within four weeks. Additions of amino acid stocks etc. were made immediately prior to inoculation. Proportions are quoted w/v for solid ingredients, v/v for liquids.

2.5.1.2 Defined minimal media

"YNB" media comprised 0.67% Bacto™ Yeast Nitrogen Base in water. "YNBD" also contained 2% glucose ("dextrose"). "YNB Gal" contained 1% Bacto™ galactose instead of the glucose used in YNBD. YNB media are of defined composition, containing minerals and vitamins and simple salts, and they omit the purines, pyrimidines and all of the casamino acids (Difco Laboratories 1963).

2.5.1.3 Complete media

"YEP" based media comprised 2% Bacto™ Peptone and 1% Difco Bacto™ Yeast Extract in water. "YEPD" also contained 2% glucose that was added prior to autoclaving. "YEPGE" contained 3% glycerol and 2% pure ethanol. The glycerol was added prior to autoclaving, the ethanol just before the media was inoculated.

2.5.1.4 Yeast sporulation medium

Fogel's sporulation medium was prepared as in (Sharman *et al.* 1986) The ingredients are given w/v, made up in water:

Potassium acetate 1%, yeast extract 0.1%, glucose 0.05%, agar 2%.
The medium was supplemented with only those amino acids etc. required for auxotrophic complementation, and only with 25% of the amount used in defined growth media.

2.5.1.5 Solid media

Agar plates were prepared by including 2% Bacto™ agar by weight in the appropriate liquid medium before autoclaving. After partial cooling the media supplements such as amino acids were added as required. Approximately 20 ml medium per 8 cm plate was poured into plates once it had cooled enough to be hand-held. Once set and cool, plates were stored at 4 °C in at least partial darkness until required.

2.5.2 Media supplements

2.5.2.1 Amino acids

Defined minimal media were supplemented with the amino acids and bases required for a particular cell type to grow. Where indicated, a cocktail of amino acids and base substances was added to the solid and liquid YNB media to produce "SC-leu", synthetic complete medium without leucine, that was suitable for growing all the leucine auxotrophs used. The additions beyond strict requirements also promote more rapid growth.

Stocks of individual amino acids were made at 100 times final medium concentration in water. After autoclaving at 115 °C for 15-20 minutes, these stocks were stored at room temperature (Sharman *et al.* 1986) and renewed approximately each month. All the amino acids were purchased as the L-enantiomer in analytical grade, except the fluorinated amino acids which were purchased as the racemic mixture.

The 100 times stock SC-leu cocktail is described below, in percent proportions w/v. These are based variously on the free amino acid, the hydrochloride, or the sodium or potassium salt as available. The quantities are in such excess that more precise definition is unnecessary, although the same preparation of each ingredient was always used. The mixture was prepared by weighing the compounds into an autoclavable bottle and dispersing in water before autoclaving at 115 °C for 15-20 minutes. The stock was used "as is" without control of the pH.

Adenine	0.2	Arginine	0.2	Aspartate	1
Glutamate	1	Histidine	0.2	Isoleucine	3
Lysine	0.3	Methionine	0.2	Phenylalanine	0.5
Serine	3.5	Threonine	2	Tyrosine	0.3
Uracil	0.2	Valine	1.5		

This mixture was fully dissolved only for a few days after autoclaving though subsequent precipitation had no effect on cell growth (Kingsman *et al*, Oxford, personal communication).

Stocks of individual compounds were made at the concentrations shown for that amino acid in the table above. Not shown are Tryptophan and Leucine which were always prepared as 0.2 % (100x) single-compound stocks. The SC cocktail can not be used where leucine is to be added to the medium since the mixture forms leucine-uptake inhibitors on autoclaving. This renders the preparation ineffective for *leu* complementation (Kingsman *et al*, personal communication). Tryptophan is readily oxidised and the stock renewed more frequently than the other compounds.

2.5.2.2 5-fluorotryptophan

5-fluorotryptophan was obtained either from Aldrich Chemical Co. or from Sigma Chemical Co. and used without further purification. The powdered material was dissolved into water some hours before use. The solution contained some black insoluble matter that was removed by filtering through a 5μ pore-size membrane filter. The solution was made up to 0.4 % w/v and then sterilised in 50 ml aliquots by filtration through a sterile 0.2μ pore-size membrane filter into a sterile 50 ml plastic tube.

2.5.2.3 Glyphosate

Technical grade glyphosate was obtained as a generous gift from the Monsanto Company, Inc., St. Louis, Missouri, through Dr. Gary Jacobs. It was stored desiccated at room temperature and the stock solution prepared just before use. Glyphosate was dissolved in 1M sodium hydroxide solution to a final concentration of 20% w/v and then sterilised by filtration through a 0.2μ pore-size membrane filter.

2.5.3 Storage of yeast

Yeast were prepared for long-term storage by overnight (16-20 h) growth at 30 °C of a single colony in 1 ml of YEPD in a small plastic screw-capped tube. An equal volume of sterile glycerol was added before vortex mixing and storing the tube at $^{-}$70 °C.

Yeast were recovered from glycerol by removing some of the frozen mixture and using it to inoculate an appropriate agar plate which was incubated at 30 °C. When this preliminary plate had grown, a single colony was then restreaked onto a fresh plate for use.

Agar plates were used to maintain populations of single yeast colonies that were used for growing yeast for the experiments. New plates were prepared approximately each month from the previous plates. Yeast were freshly obtained from the glycerol stocks approximately each six months.

2.5.4 Incubation

Yeast were grown aerobically at 30 °C in glass conical flasks with polyurethane foam bungs to maintain sterility. The cultures were shaken to maintain aerobiosis either in an orbital incubator or on a reciprocating shaker. 50 and 100 ml cultures were grown in 250 ml flasks, 500 ml cultures in 2 litre flasks, and 1 or 2 litre cultures in 5 litre flasks.

2.5.5 Cell counting

The cell densities of liquid cultures were determined directly in a hemacytometer counting chamber.

2.5.5 Transformation

Yeast transformations were performed using a protocol derived from Hinnen *et al.* (Hinnen *et al.* 1978). All the solutions were sterilised by autoclaving. Autoclaved plastic vessels were used throughout for the steps after harvesting. The polyethylene glycol used for resealing the spheroplasts was known as PEG-4000 but it has since been shown to have a lower average molecular weight of 3350 (Sigma Chemical Co. product P3640 product information). The steps involved were as follows, and all are at room temperature.

A single colony of yeast was taken from a freshly-restreaked YEPD agar plate and grown overnight in 50 ml YEPD medium. This preculture was used to

inoculate 100 ml YEPD medium at 10^4 cells per ml. This culture was grown overnight until the cell density had increased to no more than 1.5 x 10^7 per ml, typically 0.7 x 10^7.

The culture was harvested by centrifugation (5 min, 2000 g benchtop centrifuge) in two sterile plastic 50 ml tubes, and each pellet washed in 10 ml 1M sorbitol before pooling and resedimenting. The cell pellet was resuspended into 10 ml 1M sorbitol and 0.2 ml Glusulase™ added to digest the cell wall. The cells were incubated at 30 °C for one hour with occasional agitation.

The degree of spheroplast formation was checked by comparing cell counts of 10 μl of cell suspension resuspended either in 1M sorbitol or in water. The spheroplasting process was halted when 80 to 90% or more of the cells had been converted to spheroplasts.

The spheroplasts were harvested by centrifugation (as before) and washed twice by resuspension and resedimentation in 10 ml 1M sorbitol. The pellet was then resuspended in 1 ml of 1M sorbitol containing 10 mM calcium chloride buffered at pH 7.5 with 10 mM Tris.

The spheroplasts were divided into 100 μl aliquots in 1.5 ml microcentrifuge tubes. 2 μg circular plasmid DNA (usually 1 to 5 μl of plasmid stock, never more than 15 μl) was added and gently mixed into the spheroplast suspension. The mixture was incubated at room temperature for 10 to 20 minutes before adding 1 ml of 44% w/v PEG-4000. The spheroplasts and PEG-4000 were gently mixed and allowed to stand for 8 to 10 minutes at room temperature

The spheroplasts were sedimented by spinning briefly (15 to 30 seconds) in a benchtop microcentrifuge and then resuspended in 1.2 ml 1M sorbitol. Part of this suspension was used to make serially diluted suspensions of

spheroplasts in 1M sorbitol, typically using 50 μl in 1 ml to make 1/20, 1/400 dilutions.

The transformed spheroplasts were regenerated into whole cells by incubating them in a selective (*leu* deficient) agar containing 3% w/v agar and 1M sorbitol to prevent osmotic shock. Auxotrophic growth supplements were added individually once the autoclaved agar had cooled to 50 °C. Control plates were prepared by adding leucine to the agar before mixing with spheroplasts. 1.0 to 1.2 ml of neat or diluted spheroplast suspension was then mixed with 18 to 20 ml of molten regeneration agar at 50 °C and poured into a Petri dish to cool.

Once cool, the plates were incubated at 30 °C for several days during which time yeast colonies would form in the agar. The control plates were examined to confirm that the spheroplasts had survived satisfactorily and to gauge the likely time of colony appearance in the selective media, usually a day later than the control plates.

Transformants were picked out of the regeneration agar, restreaked onto selective media and grown to give single colonies. Several transformants were usually stored immediately as glycerol stocks and characterised to confirm that the transformation had been functionally successful. After initial characterisation, one transformant clone was chosen for subsequent experiments and more glycerol stocks of that clone prepared for routine use.

I am extremely grateful to Siân Davies for succeeding in transforming BJ2168 with pKV43 and pBF72 at a critical time when I inexplicably could not.

2.5.6 Yeast crossing

Yeast crossing to produce a strain *aro3, aro4, leu* was attempted by making a diploid strain from the haploids AH22 (a, *his, leu*) and RH1319 (α, *aro3, aro4*) and then sporulating the diploid.

The diploid was prepared by mixing a large loopful of each yeast together on a fresh YEPD plate and incubating the plate overnight at 30 °C. The yeast mix was depleted of haploids by repetitively growing single colonies on unsupplemented selective YNBD medium so that only the diploids would thrive.

Spores were prepared by transferring growing diploid yeast to Fogel's sporulation medium. The sporulation medium was incubated for 3 to 5 days, during which time the distinctive spore-containing asci structures formed and could be seen under the microscope. The asci spontaneously broke apart to release the spores, which could also be seen under the microscope, after a few days more incubation.

The random spore mixture was restreaked onto YEPD for single colonies and replica plated onto selective media designed to identify colonies of haploid yeast arising from the desired *aro leu* phenotype.

Unfortunately, the cross appeared to be sterile or the spores were of very low viability and no appropriate haploid was obtained by this method. The production of the desired *aro leu* haploid subsequently became unnecessary first because of the use of glyphosate as an aromatic amino acid biosynthesis inhibitor, and later when Gerhard Braus was able to provide a *leu* derivative of RH1319, called RH1320, from his laboratory.

2.6 Perifusion of yeast

Yeast were maintained in a stationary-phase metabolic steady-state by immobilising them in fine agarose threads and perifusing the threads with a defined medium at a constant temperature. The medium flow rate was sufficiently high to be non-limiting with respect to oxygen and glucose utilisation but not so high as to mechanically compact the threads. With 4 g cells in a 20 mm NMR tube, this was typically 25 ml per minute.

2.6.1 Cell Harvesting

50 or 100 ml yeast cultures were harvested by centrifugation (5 min, 2000 g benchtop centrifuge) in one or two 50 ml plastic tubes. Centrifugation was performed in a 4 °C cold room and the pellet(s) put on ice pending subsequent operations.

1 and 2 litre yeast cultures were harvested after cooling the cultures in their growth flasks for 30 to 60 minutes in a 4 °C cold room. The media was transferred to 500 ml nominal volume polypropylene centrifuge pots and centrifuged at 4 °C in a pre-cooled Beckman JA10 rotor (15 min, 5000 g). The pellets were then pooled and washed by resuspension and resedimentation once in chilled water and once in chilled substrate-free perifusion buffer.

Approximately 5 g cells were transferred to each of two 50 ml plastic tubes and washed twice in chilled substrate-free buffer by resuspension to 30 to 40 ml and resedimentation (5 min, 2000 g benchtop centrifuge).

Cells being frozen for later assay or for preparative enzyme extraction were transferred into 50 ml plastic tubes and frozen at −20 °C.

PERIFUSION BUFFER 50 mM MES, 2 mM KCl, 2 mM $MgSO_4$, 1.7 mM NaCl, pH 6.0 at 30°C.

2.6.2 Immobilisation in agarose threads

Immobilisation was achieved by mixing cells with low-gelling-temperature agarose and extruding the mix through a 0.5 mm i.d. tube. This technique has previously been used with yeast and mammalian cells and was first described in (Foxall *et al.* 1984). The protocol used was as follows.

Approximately 5 g yeast cells were resuspended in about 40 ml chilled substrate-free buffer and transferred to a clean, dry pre-weighed 50 ml plastic tube. The cells were sedimented by centrifugation (5 min., 2000 g benchtop centrifuge) and the supernatant discarded as soon as the centrifugation was complete. Leaving the pellet under the supernatant leads to variable water content in the pellet. The inside of the tube was wiped dry and the tube re-weighed to determine the weight of the packed wet yeast pellet. Yeast was removed from the tube until exactly 4 g remained. If necessary, the yeast was collected at the bottom of the tube by mixing with 40 ml substrate-free buffer and centrifuging as before.

The 4 g yeast in the 50 ml tube was placed in a water bath at 37 °C and allowed approximately 10 minutes to warm through. The yeast was then mixed with 4 ml of 1.8% w/v molten low-gelling-temperature agarose (Sigma type VII product A4018), also at 37 °C. The agarose was prepared by boiling briefly 0.18 g agarose in 10 ml substrate-free buffer before transferring to the 37 °C water bath. Mixing was achieved by repeated drawing into and expelling from a 5 ml syringe, holding the mixture in the palm of the hand all the while to keep it warm.

The agarose and cell mixture was taken up in 1.5 to 2.0 ml aliquots in a 2 ml plastic syringe and extruded through a 0.6 mm I.D. 23-gauge needle along approximately 30 to 40 cm of smooth-bore 0.5 mm I.D. polypropylene tubing (Portex PP-50). The tubing was immersed briefly in ice-water to gel

the agarose in the tube and the gel in the tube was extruded into a 20 mm NMR tube filled with chilled substrate-free buffer. This chilling - extrusion process was repeated until all of the mixture had been processed into fine threads. The 2 ml syringe was held in the palm of the hand throughout to keep the agarose mixture warm and molten.

The agarose threads were compacted gently and slowly under a perforated vortex plug to a standard depth of 65 mm measured to the bottom of the NMR tube (wall thickness 1 mm) from the bottom of the vortex plug. This corresponds to a volume of 16.5 ml, a cell density of approximately 0.25 g/ml that was constant in all experiments.

2.6.3 Perifusion system

Yeast were perifused on especially designed and constructed apparatus that was intended to hold the yeast at a constant temperature of 30 °C while recirculating a perifusion buffer through the thread bed at flow rates around 25 to 30 ml/min. The buffer was gassed by sparging and circulated through gas-impermeable lines to allow the efficient establishment of aerobiosis or anaerobiosis as required. The apparatus was built to allow the yeast to be perifused in a 20 mm NMR tube within the bore of an 89 mm (wide-bore) superconducting magnet. It was possible to sample the medium as it flowed both into and away from the thread bed to make measurements of the oxygen consumption across the thread bed.

The medium reservoir was separated from the tube containing the threads by up to 8 metres of tubing to allow the pumps and other equipment to be kept at a safe distance from the magnet. Heat exchange to warm the perifusion medium took place within the bore of the magnet, just prior to the flow reaching the thread bed. The system was calibrated to ensure the

temperature in the NMR tube was a constant 30 °C. Oxygen electrode experiments were used to confirm that nitrogen-sparged oxygen-free medium pumped through the delivery tubing (1/16" wall thickness Tygon S50-HL Class VI polythene) arrived at the NMR tube containing no detectable oxygen under the experimental conditions.

Experiments were performed with exactly one litre of perifusion medium at the start of the experiment. Samples of the medium, approximately 1 ml, were withdrawn from the reservoir at six to eight recorded times over the course of the perifusion. The sampling interval was approximately 30 to 60 minutes, depending on the duration of the perifusion. The samples were frozen at $^{-}$20 °C until they were assayed, usually one to two days after the perifusion. The samples were assayed for glucose, ethanol and, if required, ethanal (acetaldehyde). The assays were used to determine the rates of glucose utilisation and ethanol production, and the NAD^{+}/NADH ratio from the ethanol/ethanal ratio (Brindle 1988).

2.6.4 Preparation of cell extracts following perifusion

Perchloric acid extracts of the yeast were made as follows.

The NMR tube was rapidly removed from the perifusion apparatus. The vortex plugs and cotton wool were removed quickly and all the threads, together with any residual perifusion buffer, cast into a porcelain mortar thoroughly pre-cooled with liquid nitrogen. Liquid nitrogen was poured into the mortar and the threads were spread around to aid rapid freezing on the pestle and mortar surfaces. This whole process typically took ten seconds. The frozen threads were then ground, with the addition of more liquid nitrogen as required, until the threads were reduced to a fine powder.

The powder was covered in liquid nitrogen once more and 5 ml of 3M perchloric acid added dropwise to the mortar. The frozen droplets of PCA were ground into the powdered agarose threads and the whole carefully transferred by spatula into a 50 ml plastic tube.

The frozen powder was allowed to thaw to a slush before the tube and contents were frozen in liquid nitrogen once more, and thawed again. The freeze-thawing process was repeated one more time.

The thawed suspension was centrifuged at room temperature for ten minutes at 2000 g in a benchtop centrifuge. The supernatant was transferred to a clean tube along with a few ml of water used to wash the surface of the pellet. 0.2 g disodium EDTA was added to the mixture before subsequent neutralisation.

The pH of the crude extract was adjusted to approximately 6 with cold 5M potassium hydrogen carbonate solution. The potassium chlorate that forms during the neutralisation precipitated out and could be removed by benchtop centrifugation as before. This crude extract could be frozen in liquid nitrogen overnight if required. Overnight freezing had the added benefit of improving the precipitation of insoluble material that could be removed by centrifugation once thawed.

The supernatant from the neutralised extract was transferred to a clean 50 ml plastic tube and mixed with 3 to 4 ml of Chelex™ mixed ion exchange resin to remove paramagnetic metal ions that would compromise subsequent NMR experiments. After standing for a few minutes, the extract was centrifuged briefly (1 min, 2000 g) to sediment the Chelex™ resin. The supernatant was transferred to a 250 ml round-bottomed flask for shell-freezing in a bath of liquid nitrogen. The Chelex™ resin was washed twice

by resuspension and resedimentation in 20 ml water. The washings were added to the flask for freezing.

The extract was shell-frozen, around the wall of the 250 ml flask, by spinning the flask on the surface of a bath of liquid nitrogen. The frozen extract was then freeze-dried and stored frozen at -20 °C until reconstituted.

2.7 Assays of enzymes and metabolites

Enzyme assays were performed on fresh cell extracts made by mechanical disruption of the yeast cells. Metabolites were determined in perchloric acid extracts of cells. Activities and concentrations are reported throughout as the amount per ml of cell water or equivalently as the average concentration in the cell water, calculated on the basis that 1.67 g of packed wet-weight yeast contained 1.0 ml cell water (Gancedo and Gancedo 1973).

2.7.1 Cell harvesting

50 or 100 ml cultures were harvested by benchtop centrifugation (5 min, 2000 g). The cell pellets were put on ice and washed twice by resuspension in and resedimentation from chilled extraction buffer.

2.7.2 Cell preparation and disruption

A standard cell disruption procedure was used for all assays. The extraction buffers used are described with the assay protocols. The disruption protocol is described below.

Approximately 100 to 200 mg of washed yeast (a small spatula tip) was transferred to a clean, dry, pre-weighed 2 ml microcentrifuge plastic tube,

mixed with approximately 1 ml chilled extraction buffer and centrifuged in a benchtop microcentrifuge (5 min., 15000 g)

The supernatant was removed as soon as possible to help give consistency of the pellet water content, and any residual droplets wiped from the tube walls. The tube was re-weighed and the increase in weight ascribed to the wet-weight of the yeast in the tube. 5 μl of chilled extraction buffer were added for each mg of yeast and the yeast was resuspended by vortex mixing before placing on ice.

200 μl of the yeast suspension was transferred to another clean, dry 2 ml microcentrifuge tube. 0.5 to 1mm diameter glass beads were added to the meniscus of the yeast suspension. The beads were pre-cooled to 4 °C to prevent them warming the suspension.

The yeast - bead mixtures were then vortexed, up to eight tubes at a time with a vortex adapter, for 2 minutes before returning to ice. Effective vortexing was indicated by the glass beads rising up the tube wall at least half way, which did not occur if too few or too many beads were present.

The disrupted cell suspension was separated from the beads by piercing the bottom of the tube with a drawing pin and using a syringe plunger in the tube to push the liquid through into a clean plastic microcentrifuge tube. The cell debris was removed from the extract by centrifugation in a benchtop microcentrifuge (5 min, 15000 g). Usually, 50 μl of the supernatant was removed and diluted with 950 μl extraction buffer to give a 1/20 extract that was used for subsequent dilution and assay. The extracts were kept on ice. Subsequent calculations were based upon the undiluted extracts being yeast cell water diluted 1 in 10.02 (6 x 1.67).

2.7.3 Enzyme assay protocols

All enzyme assays that employed the production or utilisation of β–NAD(P)H as an indicator reaction were analysed on the basis that the extinction coefficient at 340 nm, ε_{340}, of β-NAD(P)H was 6.22 at all the pH, ionic strength and temperature combinations used. This introduces only a very small error, less than 1%, to the subsequent calculations (Bergmeyer and Gawehn 1978).

The extracts were diluted so as to cause a change in the A_{340} of approximately 0.02 to 0.2 OD units per minute, and the reactions were followed over a time course of several minutes. The rate was determined by reference to the slope of the reaction progress curve at its earliest part. In practice, the reaction conditions used meant that the reactions proceeded linearly for more than a minute.

2.7.3.1 3-phosphoglycerate kinase, PGK

3-Phosphoglycerate kinase (PGK, EC 2.7.2.3) was determined via the coupled reaction with glyceraldehyde-3-phosphate dehydrogenase (GAPDH, EC 1.2.1.12). The assay was performed in the backward ADP-forming direction using GAPDH as a "following" indicator reaction since there are complications in following the kinetics of the forward reaction (Bücher 1947; Bücher 1955; Bergmeyer and Gawehn 1978).

$$\text{GA3-P} + \text{NAD}^+ + \text{P}_i \xleftrightarrow{\text{(GAPDH)}} \text{1,3-BPG} + \text{NADH} + \text{H}^+$$

$$\text{1,3-BPG} + \text{Mg.ADP} \xleftrightarrow{\text{(PGK)}} \text{Mg.ATP} + \text{3-PG}$$

Provided that the GAPDH activity is considerably in excess of the PGK activity, the PGK activity is rate-limiting and can be followed spectrophotometrically from the decrease in absorbance of the NADH at 340 nm.

The assay was performed using extracts prepared in an extraction buffer of 50 mM HEPES, 5 mM EDTA, 2 mM DTT at pH 7.5. The assay buffer was 100 mM HEPES, 6.25 mM $MgCl_2$, 0.5 mM EDTA, 2 mM DTT at pH 7.5. The assay mixture comprised 800 μl of the assay buffer mixed with 200 μl of reagents to give a 1 ml reaction volume containing 10 mM 3PGA, 4mM ATP, 5mM $MgCl_2$, 0.15 mM NADH, and approximately 5 units of GAPDH.

The GAPDH stock was prepared by diluting 30 μl of the Boehringer rabbit muscle preparation to 500 μl with assay buffer. The enzyme was supplied in 1.8 M ammonium sulphate, resulting in a carry-through to the cuvette of some 5.4 mM. The activity was based on the catalogue rather than measured activity since consistency of the sulphate concentration was more important than the precise coupling enzyme activity.

The reaction mixture's absorbance at 340 nm was monitored for a minute in the absence of any cell extract to confirm that no contaminating reactions were taking place. The reaction was started by the addition of 10 μl of diluted cell extract to the cuvette and thoroughly mixing. The small additional volume of extract was ignored in subsequent calculations of the activity.

2.7.3.2 Glyceraldehyde-3-phosphate dehydrogenase, GAPDH

GAPDH was measured using PGK as a preceding reaction to supply the 1,3-bisphosphoglycerate. Approximately 15 units of PGK were used in each cuvette, carrying with it 6.3 mM ammonium sulphate. The other reagent concentrations and buffer conditions were exactly as for PGK. The same extract preparation was used to measure both PGK and GAPDH. Two extraction and assay conditions have thus been used for GAPDH as well as for PGK, and experiments were performed to reconcile the activities reported in the two assay systems.

2.7.3.3 *Pyruvate kinase, PK*

Pyruvate kinase (PK, EC 2.7.1.40) was assayed in a coupled reaction with lactate dehydrogenase (LDH, EC 1.1.1.27) as a following indicator reaction,

$$\text{PEP} + \text{ADP} \xrightarrow[\text{(PK)}]{} \text{pyruvate} + \text{ATP}$$

$$\text{pyruvate} + \text{NADH} + \text{H}^+ \xrightarrow[\text{(LDH)}]{} \text{NAD}^+ + \text{lactate}$$

The protocol employed followed that of Murcott et al. (Murcott *et al.* 1991) to facilitate the comparison of results with other workers in the field. Details of the extraction and assay protocols were kindly provided by the authors prior to publication.

Yeast pyruvate kinase is cold-labile, so once the initial cell extract had been prepared as described above, it was kept not on ice but at room temperature.

The extraction buffer contained 20% v/v glycerol to stabilise the tetrameric pyruvate kinase. Glycerol is commonly used to stabilise oligomeric proteins in solution (Scopes 1987; Deutscher 1990). It reduces the water activity and raises the relative viscosity of the extraction medium to approximately 2, a value similar to that of cytoplasm (Endre *et al.* 1983). The extraction buffer comprised 100 mM Tris, 100 mM KCl, 5 mM EDTA, 2 mM DTT and 20% v/v glycerol at a pH of 7.5. Protease inhibitors were omitted from the small-scale extracts used only for assays of total activity in crude cell extracts. This was thought to be acceptable since all the extracts were performed on a protease deficient yeast strain (BJ2168) and the assays were performed promptly after making the extracts.

The assay buffer was pH 6.2 100 mM MES, 125 mM KCl, 20 mM $MgCl_2$, 0.25 mM EDTA and 2 mM DTT. The reaction mixture comprised 800 μl of assay buffer and reagents to a total volume of 1 ml containing 6 mM ADP, 6 mM PEP, 0.25 mM NADH, and approximately 2 units of LDH. To avoid interference

from sulphate ions, the LDH stock used was a preparation of about 2000 units per ml in glycerol (Sigma product L2518).

This assay protocol does not employ fructose-1,6-bisphosphate as an activator, unlike some other published protocols (Roschlau and Hess 1972), since at the high ADP concentrations used the activity is already near-maximal.

The reaction mixture's absorbance at 340 nm was monitored for a minute in the absence of any cell extract to confirm that no contaminating reactions were taking place. The reaction was started by the addition of 10 μl of diluted cell extract to the cuvette and thoroughly mixing. The small additional volume of extract was ignored in subsequent calculations of the activity.

2.7.4 Metabolite assays

2.7.4.1 Fructose-1,6-bisphosphate (FBP), dihydroxyacetone phosphate (DHAP) and glyceraldehyde-3-phosphate (GA3P)

A three-part protocol (Bergmeyer and Gawehn 1978) was followed to determine FBP, DHAP and GA3P in the same reaction. The conversion of DHAP to L-glycerol-3-phosphate (G3P) by glycerol-3-phosphate dehydrogenase (G3PDH, EC 1.1.1.8) was used as an indicator reaction by monitoring the decline in [NADH]-dependent absorbance at 340 nm.

$$DHAP + NADH + H^+ \xleftrightarrow[(G3PDH)]{} G3P + NAD^+$$

Addition of triosephosphate isomerase (TIM, EC 5.3.1.1) once the DHAP in the sample is depleted allowed the determination of glyceraldehyde-3-phosphate (GA3P) by its conversion to DHAP and subsequent reduction by the glycerol-3-phosphate dehydrogenase indicator reaction.

$$GA3P \leftrightarrow DHAP$$
(TIM)

Likewise, subsequent addition of aldolase (EC 4.1.2.13) allowed FBP to be determined by its conversion to DHAP and GA3P.

$$FBP \leftrightarrow GA3P + DHAP$$
(aldolase)

The protocol followed is described below.

The reaction buffer recipe has been changed slightly from the Bergmeyer protocol to allow the same buffer to be used for this and the other sugar assays. The reaction buffer comprised 250 mM TEA, 10 mM $MgCl_2$, 2 mM EDTA and 1.5 mM DTT at pH 7.6.

850 μl buffer, 50 μl of 4 mM NADH in 5 % $NaHCO_3$ and 100 μl sample were mixed in a 1 ml cuvette.

The absorbance at 340 nm ("A1") was monitored for a minute to ensure no contaminating reactions were taking place. 0.2 units of G3PDH in 10 μl were added, mixed, and the reaction monitored until a new constant absorbance value ("A2") was reached, typically after 10 minutes.

One unit of TIM in 10 μl was added, mixed, and the monitoring process repeated. The absorbance typically reached a new steady value ("A3") in five minutes. 0.1 units of aldolase in 10 μl were then mixed into the reaction mixture. A new steady absorbance value ("A4") was reached after approximately ten minutes.

The absorbance changes at each stage were used to calculate the concentrations of DHAP (A1 - A2), GA3P (A2 - A3) and FBP (A3 - A4). The calculation allowed for the fact that each FBP molecule gives rise to two glycerol-3-phosphate molecules, using two NADH in the process.

2.7.4.2 *Fructose-6-phosphate (F6P) and glucose-6-phosphate (G6P)*

F6P and G6P were assayed in the same reaction by a protocol from (Bergmeyer and Gawehn 1978).

The indicator reaction is the conversion of glucose-6-phosphate to 6-phosphogluconolactone by glucose-6-phosphate dehydrogenase (G6PDH, EC 1.1.1.49).

$$G6P + NADP^+ \xleftrightarrow[(G6PDH)]{} 6\text{-phosphogluconolactone} + NADPH + H^+$$

The phosphogluconate degrades to 6-phosphonogluconate spontaneously in water, driving the reaction to completion.

F6P was determined after the G6P by the addition of phosphoglucose isomerase (PGI, EC 5.3.1.9).

$$F6P \xleftrightarrow[(PGI)]{} G6P$$

The reaction volume of 1 ml comprised 850 µl of the sugar assay reaction buffer (see above), 50 µl sample and 100 µl of reagents. The assay contained 0.4 mM $NADP^+$ and 5 mM $MgCl_2$.

The absorbance of the mixture at 340 nm was monitored for a minute to ensure that no contaminating reactions were taking place. The absorbance was noted ("A1") before the addition and mixing in of 0.5 units G6PDH in 10 µl.

The absorbance was allowed to reach a new steady level ("A2"), which took approximately 10 minutes. One unit of PGI in 10 µl was added and mixed in to catalyse the conversion of F6P. The absorbance value was allowed to reach a new steady level ("A3") which took approximately 20 minutes.

The G6P concentration in the sample was proportional to the first absorbance change, A1 - A2, and the F6P to the second, A2 - A3.

2.7.4.3 3-phosphoglycerate

Samples were assayed for 3-phosphoglycerate (3PGA) using a protocol by Bergmeyer (Bergmeyer and Gawehn 1978).

Because intracellular 3PGA concentrations are typically very low, two successive indicator reactions are used to improve the assay sensitivity.

$$3PGA + ATP \leftrightarrow 1,3\text{-}BPG + ADP$$
(PGK)

$$1,3\text{-}BPG + NADH + H^+ \leftrightarrow GA3P + P_i + NAD^+$$
(GAPDH)

$$GA3P \leftrightarrow DHAP$$
(TIM)

$$DHAP + NADH + H^+ \leftrightarrow \text{glycerol-3-phosphate} + NAD^+$$
(G3PDH)

The reaction mixture comprised 700 μl of sugar assay buffer (see above), 50 μl sample (containing no more than 50 μM 3-PGA) and reagents to 1 ml total volume. The mixture contained 200 μM NADH, 7 mM ATP, 4 units GAPDH, 25 units TIM, 1 unit G3PDH and 20 units PGK.

The assay was performed by mixing all the reagents except the PGK and monitoring the absorbance at 340 nm for a several minutes. The absorbance value declined slightly over this period. The assay reaction was started by the addition of the 20 units PGK in 10 μl and mixing thoroughly. The absorbance was monitored for a further ten to twenty minutes, until a new steadily but slowly declining rate was achieved.

The progress curve was extrapolated back to the time of the addition of the PGK to the reaction mixture. The extrapolated difference in the absorbance

values was used to determine the amount of NADH utilised and thus calculate the quantity of 3PGA in the sample, taking into account that two NADH were utilised for each 3PGA in the sample.

2.7.4.4 Glucose

Glucose assays were performed using an assay kit from Sigma Chemical Co., Sigma Diagnostics Procedure No. 510.

The assay was based on the glucose oxidase (GOD, EC 1.1.3.4) reaction coupled to a peroxidase (POD, EC 1.11.1.7) indicator reaction.

$$\text{Glucose} + 2\ H_2O + O_2 \xleftrightarrow[\text{(GOD)}]{} \text{Gluconic acid} + 2\ H_2O_2$$

$$H_2O_2 + \underset{\text{(colourless)}}{\text{reduced dye}} \xleftrightarrow[\text{(POD)}]{} \underset{\text{(brown)}}{\text{oxidised dye}} + H_2O$$

The dye used in the kit was o-dianisidine dihydrochloride, and the stock solution was made by rehydration of material supplied in the kit. The concentration of the brown oxidised dye is proportional to the glucose concentration in the original sample. The brown dye can be quantitated by measuring the optical absorbance at 425 nm against a blank sample containing water in place of the sample or standard solution.

The assay was calibrated each time it was used by constructing an absorbance vs glucose concentration curve from samples of known glucose concentration. The 5.55 mM standard glucose solution used was supplied in the kit. Five standards in the range 0 to 5.55 mM glucose were used to construct the calibration curve, and all samples were diluted if necessary to lie within this range. Typically, the samples of reservoir buffer from a perifusion experiment were diluted 1 in 10 in water.

2.7.4.5 *Ethanol*

Ethanol was assayed using alcohol dehydrogenase (ADH, EC 1.1.1.1) as an NAD^+-linked indicator reaction. The reaction equilibrium lies heavily in the direction of ethanol and NAD^+, so semicarbazide is used to trap the ethanal produced and pull the reaction to completion.

$$CH_3CH_2OH + NAD^+ \xleftrightarrow[(ADH)]{} CH_3CHO + NADH + H^+$$

$$[H^+].[NADH].[CH_3CHO] \;/\; [NAD^+].[CH_3CH_2OH] = 1.19 \times 10^{-11} \text{ at } 30\ ^\circ C.$$

The reaction buffer was 75 mM sodium pyrophosphate, 75 mM semicarbazide-HCl and 25 mM glycine, at pH 8.7. The reaction mixture was prepared by mixing 4.8 ml buffer, 100 μl sample, 100 μl 25 mM NAD^+ (final concentration 0.5 mM NAD^+), and approximately 240 units of ADH in 20 μl water (1 mg of Boehringer lyophilised preparation). The samples were perifusion reservoir buffer diluted in water 1 in 2 (early time points) to 1 in 10 (late time points) as appropriate. The reaction mixture was incubated in the dark for approximately 70 minutes, until the reaction was essentially complete.

The NADH concentration in the sample was determined by measuring the absorbance of the reaction mixture at 340 nm against a blank reaction mixture prepared with water instead of sample. The final concentration of NADH in the reaction mixture was taken to equal the starting ethanol concentration of the sample. The reaction volume was taken to be 5 ml, ignoring the 20 μl of ADH added to start the reaction.

2.7.4.6 *Ethanal (acetaldehyde)*

Ethanal was determined using the alcohol dehydrogenase reaction described in the ethanol assay. The reaction equilibrium lies heavily in favour of ethanol production (Brindle 1988, and references therein), so the reaction

can be performed in a simple buffer (50 mM HEPES, pH 7.5) without product-trapping reagents. The reaction mixture of 1 ml contained 0.5 ml sample, approximately 120 units of ADH (0.5 mg Boehringer lyophilisate) and 0.2 mM NADH.

Samples were typically undiluted perifusion reservoir buffer, containing more ethanol than ethanal. The equilibrium position lies so far toward ethanol production ([EtH]/[EtOH], at pH 7.2 = 1.89×10^{-4}) that the presence of the c. 25 mM ethanol in the sample does not interfere with the determination of the c. 0.1 mM ethanal in the sample.

The reaction was followed at room temperature by monitoring the decline in absorbance at 340 nm as the reaction proceeded to completion, in approximately 30 minutes. The change in NADH concentration was taken to equal the ethanal concentration in the sample.

2.7.4.7 Oxygen

Oxygen was measured by a polarographic technique with a Clark-type electrode produced by the Yellow Springs Instrument Co. (YSI 5331 oxygen probe). This system comprised concentric platinum cathode and silver anode bridged by an alkaline saturated potassium chloride solution and surrounded by a Teflon™ membrane.

According to the information from the manufacturer's data sheet, the electrode current was simply proportional to the dissolved oxygen concentration under the conditions in which it was used.

The electrode was used to measure oxygen in a stream of the yeast perifusion buffer before and after flowing through the cell bed. The electrode generates a current linearly proportional to the oxygen consumption of around 0.003 μA in nitrogen, 0.3μA in air and 1.6 μA in pure oxygen. This current was

amplified and displayed on an arbitrary scale. The amplification of the small currents involved gave rise to a slightly noisy signal, limiting the accuracy of measurement to about five per cent. Measurements were made at the air-conditioned temperature of approximately 20 °C, assuming air-saturated water contained 0.279 μmol dioxygen per ml under typical atmospheric pressure and at 20 °C (Gnaiger and Forstner 1983).

The oxygen consumption of the yeast in the perifusion system (2.4 ml cell water in 4 g cells) was thus calculated from the electrode readings of inlet and outlet buffers and of air-saturated water, and knowledge of the flow rate (ml per second) of the perifusion buffer through the cell bed as follows

$$(\text{In-Out})/\text{Water} \times 0.279 \times \text{Flow} \times 1/2.4\ \mu\text{mol}\ O_2.s^{-1}.(\text{ml cell water})^{-1}$$

2.7.4.8 Protein

Protein concentrations were determined using a kit from Bio-Rad Laboratories. The assay is based on that developed by Bradford (Bradford 1976) in which protein binds under acidic conditions to Coomassie Brilliant Blue G-250 dye and causes a change in the absorbtion maximum of the dye from 465 to 595 nm. The assay is relatively insensitive to interference from non-proteins in the sample, but it does give slightly different responses to different protein species. All protein assays were performed by reference to a calibration curve constructed from assays of known concentrations of bovine serum albumin, BSA. The BSA standard was supplied as part of the kit and a new calibration curve was constructed each time an assay was performed. Samples were diluted in water to bring them into the appropriate protein concentration range for the assay if necessary. None of the samples contained reagents reported as interfering with the assay.

2.8 Enzyme purification

Enzyme purifications were adapted from the literature to take account of the different starting material available. Modifications were necessary because this work was concerned with isolating protein from yeast cells that were relatively difficult and expensive to prepare compared to traditional commercial yeast sources such as pressed yeast cake.

The modifications required scaling the protocols down to work with smaller starting quantities of yeast that were expressing a higher proportion of the target protein. The protocols used here also place a greater emphasis on the choice of cell strain and disruption protocols to avoid proteolytic artefacts in the target protein, something that has been notoriously difficult with pyruvate kinase in particular (Murcott *et al.* 1991). Later preparations were carried out with a yeast strain deficient in general degradative proteases (BJ2168, *pep4, prb, prc*) which greatly helps overcome proteolysis problems. Some changes in the detailed materials specified were also necessary to take account of availability.

All the modifications and optimisations were made with reference to standard works in protein purification (Scopes 1987; Deutscher 1990), and I am particularly grateful for advice from Terry Butters and Jean Rotsaert, both of the Monsanto Glycobiology Unit, Oxford.

2.8.1 Cell Harvesting, storage and disruption

Yeast were harvested from one or more 1000 ml cultures by centrifugation (15 min., 5000 g in a Beckman JA10, 4 °C) and washed by resuspension and resedimentation in water once or twice and then the cell pellets were stored in 50 ml plastic tubes, frozen at -20 °C until required. This was often several months later, since it took many weeks to grow sufficient yeast for a

preparation using the minimal-medium method used in the early part of this work (see Chapter 3). Typically, approximately 50 to 100 g yeast formed the starting material.

The cell pellets were thawed and washed twice by sedimentation and resuspension in chilled extraction buffer. The extraction buffer composition is given with each protein protocol. The glass beads used were pre-chilled to -20 °C and approximately 0.5 to 1.0 mm in diameter when new. Repeated use grinds the beads to a smaller size, and they were replaced when visibly worn. Glass beads were washed in conc. nitric acid and then copious amounts of water before each use. The washed cells were processed as follows to prepare a basic yeast extract.

A cell slurry was made by mixing 2 parts v/v of extraction buffer with one of wet yeast pellet. The extraction buffer at this stage already contained DTT and protease inhibitors as appropriate.

Approximately 50 ml of cell suspension was transferred to a 6 cm diameter 250 ml nominal volume wide-necked polythene container. Glass beads were added almost to the meniscus of the cell suspension. The slurry, about 6 cm deep, in the plastic container was placed in a small ice bath. The subsequent operations were performed behind a Perspex™ safety screen.

A two-blade plastic impellor (Deansgate Model Shop, Manchester) approximately 45 mm in diameter was inserted in to the cell - bead slurry on a stainless steel drive shaft connected to a Black & Decker variable-speed power drill. The impellor was driven at approximately 2000 rpm in the direction causing the beads to be pushed downwards.

The cells, still in the ice bath, were mechanically disrupted by rapid stirring with the impellor for two 3 minute periods with a 4 minute rest period on ice

between. It had been determined by experiment that this releases at least 95 % of the PGK measured in the small-scale extracts described earlier.

The cell extract was separated from the glass beads by filtration through a stainless steel gauze in a filter. The filtrate was collected directly into a centrifuge pot in an ice bath. Residual extract was washed from the beads with a further two volumes of chilled extraction buffer. The beads were mixed again with more cell suspension as required.

The disrupted cell extract was centrifuged (15 min., 14000 g, JA14 rotor, 4 °C) to remove crude cell and bead debris and the supernatant centrifuged again (60 min., 30000 g, 4 °C) to remove any remaining debris.

A neutralised solution of 100 mg/ml protamine sulphate was added to the supernatant in a conical flask on ice. Approximately 20 mg protamine sulphate were added per gram of yeast in the starting material. The mixture was swirled occasionally (i.e. not stirred with a magnetic stirrer) on ice for 30 minutes. The protamine-nucleic acid complex was precipitated by centrifugation (30 min., 14000 g JA14 rotor 4 °C). This relatively large quantity of protamine was added to precipitate the large quantity of highly sheared nucleic acid material that is released when yeast are mechanically disrupted (Scopes 1987).

The supernatant was decanted into a measuring cylinder to determine its volume and then returned to storage on ice, or at room temperature for PK purifications. This was considered to be the basic yeast extract from which PGK or PK would be purified.

2.8.2 Phosphoglycerate kinase, PGK

Phosphoglycerate kinase was purified from the basic extract essentially as by Fifis and Scopes (Fifis and Scopes 1978). The material was kept on ice throughout the procedure until the column steps and all centrifugations were at 4 °C.

The extraction buffer used was pH 7.5 50 mM sodium phosphate, 5 mM EDTA, 1 mM 1,10-phenanthroline and 2.5 mM dithiothreitol (DTT). A cocktail of protease inhibitors was also added. The cocktail provided Pepstatin A to 1-2 μM, E64 to 10 μM and 3,4-DCl to 100 μM concentration in the extract. PMSF, which has been widely used, was omitted from the cocktail since it is relatively inefficient and its action is reversed by the reducing agent DTT. Note that in the crude extract, the chelating agents are fulfilling an anti-metalloproteinase function and are not merely duplicating the anti-oxidative function of DTT.

The extract was brought to 50 % saturation with ammonium sulphate (enzyme grade, low in heavy metals) by the slow addition of 314 grams of solid powdered ammonium sulphate per litre of extract. The mixture was stirred vigorously throughout the addition and for a further 30 minutes before centrifuging (30 min., 15000 g). The pH was adjusted to 7.5 again if necessary after the addition of the ammonium sulphate with 2M Tris base solution or 2M MES acid solution as appropriate.

The volume of the supernatant was measured and then the supernatant was brought to 75 % saturation with ammonium sulphate by the slow addition of 171 grams solid powdered ammonium sulphate per litre of extract. The pH was re-adjusted to 7.5 if necessary, and the mixture stirred on ice for 30 minutes before centrifuging as before.

The PGK-rich pellet was put on ice and the supernatant adjusted to pH 4.3 with cold 5M lactic acid solution, pH 3.5. After stirring for 30 minutes, the mixture was centrifuged as before if there was any indication of a further precipitate. The pellets were combined and processed further if required as follows. Subsequent operations were carried out at approximately 20 °C until the final step.

The ammonium sulphate pellet was redissolved into approximately 100 ml of 10 mM MES, 2 mM DTT adjusted to pH 6.0 with 2M Tris base. The solution was filtered through a 5 μm pore membrane filter, then desalted by passage at 10 ml per minute down a 50 mm diameter 240 mm bed height column of Pharmacia Sephadex™ G-50 M equilibrated with the same buffer. As with subsequent column steps, the eluate flowed through a 280 nm UV detector and on to a fraction collector. Fractions containing more than approximately 1 mg protein per ml were collected and pooled.

The pooled protein was filtered through a 5 μm pore membrane filter, diluted with the elution buffer to a concentration of 5 to 10 mg per ml and then run on to a 26 mm diameter 300 mm bed height weak cation exchange resin. This was a column of a porous polymer carboxymethyl-substituted ion exchange resin, TSK Fractogel™ CM-650. This column was operated at a flow rate of 2 ml per minute. The column was previously equilibrated in the same buffer. Under these conditions the PGK protein bound to the resin and other proteins were washed through in a further 150 ml (one column volume) of the starting buffer.

The column was washed with one column volume of a pre-elution buffer of 10 mM MOPS, 3 mM potassium acetate and 2mM DTT adjusted to pH 7.0 with 2M Tris. This releases some further protein but only a little PGK. The ionic

strength and pH of this buffer are designed to be the same as that in the next step.

The PGK was eluted by an affinity process from the column with two column volumes of 10 mM MOPS, 0.5 mM 3-phosphoglycerate, 2 mM DTT adjusted to pH 7.0 with 2M Tris. Since the pH and ionic strength are unchanged, the process should be specific for 3-phosphoglycerate-binding proteins, i.e. PGK.

Fractions containing at least 1 mg protein per ml were pooled and precipitated by bringing the solution to 75 % saturation in ammonium sulphate by the slow addition of 515 grams solid powdered ammonium sulphate per litre of solution. The pH was readjusted to 7.0 if necessary and the mixture stirred for 30 minutes before centrifuging (30 min., 15000 g).

The pellet was resuspended in a minimum volume, typically 10 to 15 ml, with 50 mM HEPES, 5 mM EDTA, 2 mM DTT at pH 7.5. The mixture was filtered through a 5 μm pore size membrane filter and then loaded onto a 26 mm diameter 900 mm bed height gel filtration column. The column was packed with an inert porous polymer resin, TSK Fractogel™ HW50-S, which has a bead size 25 to 40 μm and an effective relative molecular weight fractionation range of 1000 to 80000. The column was eluted at a flow rate of 0.5 ml per minute. PGK was by far the largest peak eluting from the column, and fractions containing more than approximately 1 mg protein per ml were collected and pooled.

The purified PGK was concentrated at 4 °C in 200 and then 50 ml Amicon stirred ultrafiltration cells with a YM30 low-protein-binding 30 kDa nominal exclusion weight membrane until it reached a concentration of around 25 to 30 mg per ml. For longer term storage, this solution was brought to approximately 75 % saturation in ammonium sulphate by the slow

addition of 0.5 g solid powdered ammonium sulphate per ml of solution and then stored at 4 °C.

2.8.3 Pyruvate kinase

Pyruvate kinase was purified from the basic yeast extract essentially as by Murcott et al., a protocol specifically developed for the efficient purification of PK from a highly expressed recombinant system (Murcott *et al.* 1991). The protocol was kindly made available by the authors prior to publication. All procedures were carried out at room temperature.

The extraction buffer used was 100 mM Tris, 100 mM KCl, 5 mM EDTA, 2 mM DTT and 20% v/v glycerol at a pH of 7.5.

The extract was brought to 40 % saturation in ammonium sulphate by the slow addition of 243 grams solid powdered ammonium sulphate per litre of extract. The pH was readjusted to 7.5 if necessary with 2M Tris base. The solution was allowed to equilibrate while stirring for a further 30 minutes before centrifuging (30 min., 15000 g).

The pellet was discarded while the supernatant was brought to 60 % saturation in ammonium sulphate by the slow addition of 130 grams solid powdered ammonium sulphate per litre of extract. The pH was readjusted to 7.5 if necessary with 2M Tris base. The solution was allowed to equilibrate while stirring for a further 30 minutes before centrifuging (30 min., 15000 g).

The pellet was resuspended in a minimum volume, typically 50 ml, of 50 mM Tris, 50 mM KCl, 5 mM EDTA, 2 mM DTT and protease inhibitors as described in the basic extraction protocol, section x. The solution was filtered through a 5 μm pore membrane filter, then desalted by passage at

10 ml per minute down a 50 mm diameter 240 mm bed height column of Pharmacia Sephadex™ G-50 M equilibrated with the same buffer.

Fractions containing more than approximately 1 mg protein per ml were collected and pooled. The pooled protein was filtered through a 5 μm pore membrane filter and loaded onto a column of Pharmacia Q-Sepharose™ equilibrated in the resuspension buffer. The column was 26 mm in diameter and the bed height was 300 mm. The column was operated isocratically at a flow rate of 0.5 ml per minute. PK principally elutes in the break-through volume.

Eluate fractions containing more than approximately 1 mg protein per ml were collected and pooled. The pooled protein was precipitated by bringing the solution to 75 % saturation in ammonium sulphate by the slow addition of 0.5 g powdered solid ammonium sulphate per ml of solution. After equilibrating while stirring for 30 minutes, the protein precipitate was sedimented by centrifugation (30 min., 20000 g, 20 °C)

The protein pellet was resuspended in a minimum volume, typically 5 or 10 ml, of extraction buffer (omitting the protease inhibitors) loaded onto a gel filtration column equilibrated in the same buffer. The column was a 26 mm diameter 700 mm bed height column of a porous polymer resin, TSK Fractogel™ HW55-S. This had an effective relative molecular weight fractionation range of 2000 to 800000, and a bead size of 25 to 40 μm.

The PK activity was eluted as the principal peak and concentrated by ultrafiltration or ammonium sulphate precipitation as described for PGK. The ammonium sulphate precipitate was stored at 4 °C since the protein was not significantly cold-labile under these conditions (Fiona Stuart, Edinburgh, personal communication).

2.8.4 Electrophoresis

2.8.4.1 PAGE-SDS

Polyacrylamide gel electrophoresis with the denaturing detergent SDS was performed according to the discontinuous system of Laemmli (Laemmli 1970; Hames and Rickwood 1990). Nearly all proteins denatured with SDS under reducing conditions are unfolded and bind the detergent in proportion to their relative molecular weights. Under these conditions they are charged, and migrate in an electric field, in proportion to their relative molecular weights. Complications can arise, particularly with glycosylated proteins or with some unusually stable proteins, but the proteins examined in this work are not known to belong to either of these categories.

2.8.4.2 Native gel PAGE

Non-denaturing or "native" gels were run with the Pharmacia Phast™ system using pre-cast gels. These gels were silver-stained.

2.8.4.3 Isoelectric focusing

IEF was performed using pre-cast Pharmacia PhastGel™ IEF media, covering pH ranges 3 to 9, 5 to 8 or 4 to 6.5. Desalted samples and Pharmacia pI standards were run using a protocol from the system owner's handbook.

2.8.4.4 Coomassie blue gel staining

Proteins in polyacrylamide gels were stained with Coomassie Brilliant Blue by soaking for approximately 15 minutes in a solution of 50 % v/v methanol, 10 % v/v acetic acid, 40 % v/v water and 0.1 % w/v Coomassie Blue. Excess stain was removed by rinsing and then soaking with repeated volumes of a solution of 10 % v/v methanol and 10 % v/v acetic acid in water.

2.8.4.5 Silver gel staining

Phast™ system gels were stained by the protocol described in the Phast™ system Owner's Handbook.

2.8.5 Electrospray MS

I am extremely grateful to Andy Pitt, Cambridge, for running a sample of purified fluorinated PGK on an electrospray mass spectrometer. The sample used was 250 pmol in 10 μl of 15 mM Tris-HCl, pH 8.5. The sample was run on a BioQ instrument from VG Instruments.

3 Labelling a single protein in the intact cell

3.1 The choice of a model protein to label and a cell type to work in

Developing a new technique is aided by working on a well-characterised system. The system should be easy to manipulate experimentally and relatively simple, to aid the interpretation of results. These criteria apply both to the protein to be labelled and the cell in which it is produced.

These considerations led to the baker's yeast, *Saccharomyces cerevisiae*, as an experimental organism. It constitutes a homogeneous tissue that is relatively simple to manipulate genetically, easy to grow in large quantities and has been very widely studied (Botstein and Fink 1988).

The protein chosen for these studies was phosphoglycerate kinase (PGK) (EC 2.7.2.3), widely studied in many kinetic and structural contexts. Its basic properties have been reviewed in a chapter of *The Enzymes* (Scopes 1973).

Some work was done with pyruvate kinase and some preliminary further work with hexokinase. The discussion here concentrates on the expression of PGK since it has been studied in greater detail by other workers and is the main object of this work.

Together with glyceraldehyde-3-phosphate dehydrogenase (GAPDH, EC 1.2.1.12), the enzyme preceding it in the glycolytic pathway, PGK catalyses an important coupled reaction that links the phosphorylation potential, [ATP]/[ADP][Pi], to the redox state of the cell, the NAD^+/NADH ratio.

$$GA3\text{-}P + NAD^+ + P_i \leftrightarrow 1,3\text{-}BPG + NADH + H^+$$

$$1,3\text{-}BPG + Mg.ADP \leftrightarrow Mg.ATP + 3\text{-}PG$$

PGK is a 45 kDa monomer with no disulphide bridges. It is a relatively stable protein, making its purification and characterisation *in vitro* easier. It is the only monomeric enzyme in the glycolytic pathway in yeast and has no known physiological effectors.

ADP and ATP are important in many aspects of cellular energy metabolism. ATP is often present in the cell in sufficient concentration, several mM (Gancedo and Gancedo 1973), to allow its observation in the intact cell by ^{31}P NMR.

High resolution x-ray crystal structures have been determined for yeast and horse muscle PGK (Banks *et al.* 1979; Watson *et al.* 1982), and for a number of site-directed mutants of yeast PGK (Herman Watson *et al.*, personal communication). PGK has also been investigated by high resolution ^{1}H NMR spectroscopy in solution (Fairbrother *et al.* 1988; Wilson *et al.* 1988; Fairbrother *et al.* 1989a; Fairbrother *et al.* 1989b; Fairbrother *et al.* 1990b; Fairbrother *et al.* 1990a). These studies have looked at the protein in the presence of various substrates and other ligands. The enzyme—substrate interactions have also been investigated by ^{31}P NMR spectroscopy (Rao and Oesper 1961; Rao *et al.* 1978; Ray and Rao 1988a; Ray and Rao 1988b; Ray *et al.* 1990).

These structural studies suggest that PGK may undergo a large conformational change, a "hinge-bending" motion, upon binding its ligands (Banks *et al.* 1979; Blake *et al.* 1986). Kinetic studies of native, mutant and chimeric human/yeast PGKs have probed the structural interactions that may be responsible for the conformational change (Adams and Pain 1986; Mas *et*

al. 1986; Tompa *et al.* 1986; Mas *et al.* 1987; Mas *et al.* 1988; Mas and Resplandor 1988).

Some aspects of the enzyme's structure have been examined with tryptophan fluorescence (Wasylewski and Eftink 1987), photochemically-induced dynamic nuclear polarisation (photo-CIDNP) (Scheffler and Cohn 1986) and low- and high-temperature denaturation (Griko *et al.* 1989).

Extensive studies of the kinetic properties of native yeast PGK have been undertaken, particularly by Larsson-Raznikiewicz. Many binding, kinetic and inhibitory parameters have been determined (Larsson-Raznikiewicz and Malmstrom 1961; Larsson-Raznikiewicz 1964; Larsson-Raznikiewicz 1970; Larsson-Raznikiewicz and Arvidsson 1971; Scopes 1978b; Scopes 1978a). The thermodynamic parameters governing some of the enzyme-substrate interactions have also been characterised (Hu and Sturtevant 1987).

The kinetics of the GAPDH:PGK couple has also been studied in detail experimentally and theoretically; there is an active debate in the literature about substrate-channelling at this step in the glycolytic pathway (Weber and Bernhard 1982; Srivastava and Bernhard 1986; Sukhodelets *et al.* 1988; Kvassman and Petterson 1989b; Kvassman and Petterson 1989a; Vas and Batke 1990).

This detailed understanding of PGK should be helpful in understanding the relationships between protein, labels and ligands. The operation of any multi-enzyme complex involving PGK would also, presumably, involve protein-protein interactions that may be amenable to study by a novel labelling technique.

3.2 Choosing the type of label to use

3.2.1 Approaches to labelling a protein

To observe a single protein species in the intact cell it is clearly necessary that it has some distinguishing property. One might selectively introduce a label into the protein of interest. Suitable labels might be fluorescent, radioactive or detectable by magnetic resonance, and might be biosynthetically incorporated into the protein covalently or as labelled cofactors that bind tightly to the protein.

Chemical derivatisation of a purified protein *in vitro* offers many labelling strategies. Human insulin, for example, is produced commercially by the enzymatic modification of porcine insulin (Turnock 1991) and there are techniques for incorporating non-coded amino acids or amino acid derivatives into proteins synthesised by *in vitro* translation systems. These and other approaches to protein labelling have been reviewed briefly by Offord (Offord 1991).

Such schemes would lack specificity and generality if applied to a complex mixture of proteins in the cell, even if the cell survived exposure to the reagents used. It might be possible to prepare labelled proteins *in vitro* for uptake by pinocytosis, or even by microinjection in suitable cell types. However, such techniques do not seem to offer the prospect of a generally applicable labelling methodology.

3.2.2 The choice of fluorotryptophan as the label for these studies

The labelling strategy adopted was to use a fluorine label biosynthetically incorporated into the protein as the fluorinated amino acid 5-fluorotryptophan. Tryptophan was chosen for these studies since it was

available in several fluorinated forms and because its rarity in proteins (Reeck 1976) should lead to relatively simple labelling patterns.

Fluorine was chosen as the labelling atom since it is highly amenable to study by NMR, a technique that can be applied noninvasively, and because it is likely to be a relatively non-perturbing label (Gerig 1989). The fluorine atom is not much larger than the hydrogen atom, the Van der Waals radii being about 1.20 and 1.35 Å respectively, although the electronic properties are somewhat different.

Fluorine-19 occurs with 100% natural abundance, and is detected by NMR with a sensitivity nearly as great as that of the proton. Sensitivity is a particularly important issue with NMR since it is inherently insensitive, requiring samples of around 0.5 to 1 ml and tens of micromolar. This limitation is particularly apparent in comparison to techniques involving fluorphores (see, for example, (Dix and Verkman 1990) where micromolar quantities of flurophore are studied in single cells to determine the cytoplasmic viscosity).

Fluorine NMR signals are exquisitely sensitive to the environment of the fluorine nucleus. The chemical shift range of fluorine is very great, around 100 ppm, which makes it possible to distinguish subtly different environments (Gerig 1989). Most cells contain no fluorine, so a fluorinated label can be observed without background signals arising from other cellular components. These important properties have been exploited in a study of cell volume and membrane potentials using trifluoroacetate and trifluoroacetamide (London and Gabel 1989).

Fluorine labels should thus be sensitive probes of changes within a protein in the cell.

3.2.3 Precedents for the study of fluorinated proteins

Fluorotryptophan, fluorophenylalanine and fluorotyrosine have previously been used to non-selectively label proteins in *E.coli*. Individual proteins have been purified from the cells and studied *in vitro* (reviewed by Sykes and Weiner 1980). Many fluorinated proteins have been studied, including alkaline phosphatase (Hull and Sykes 1974), the *lac* repressor (Jarema *et al.* 1981), the membrane-bound D-lactate dehydrogenase (Ho *et al.* 1989), the galactose chemosensory receptor (Luck and Falke 1991), the cAMP receptor protein (Sixl *et al.* 1990), and the H^+-ATPase (Kim *et al.* 1990).

Purifying a protein from a globally-labelled organism has also been used to isolate haemoglobins (Gerig *et al.* 1983; Gamcsik *et al.* 1987) and GAPDH (Mark Boulton and Kevin Brindle, personal communication) from rabbits fed on a diet containing fluorophenylalanine. Fluorinated proteins have also been prepared by chemical modification *in vitro*. For example, ^{19}F-labelled lysozyme has been prepared by trifluoroacetylation of the ε-amino groups of the six native lysines (Adriaensens *et al.* 1988).

Efforts to improve the specificity and efficiency of the labelling process have included depleting the growth medium of the natural amino acid and adding the fluorinated amino acid when the target protein is being actively synthesised (Sykes and Weiner 1980). Ho *et al.* achieved this for lactate dehydrogenase simply by starvation of the cells followed by feeding lactate to induce protein synthesis. Sykes *et al.* achieved a similar result with alkaline phosphatase by depleting the growth medium of phosphate. Most previous studies have used auxotrophic cell types to encourage the uptake of label, but the work of Kim *et al.* made use of glyphosate to inhibit endogenous aromatic amino acid production (Kim *et al.* 1990). Many studies have used cells carrying plasmids to direct the overproduction of the target protein.

3.3 Three strategies for the incorporation of the label

3.3.1 General considerations

3.3.1.1 The uptake of labelled compounds from the medium

A simple protocol to make cells to utilise a fluorinated amino acid seems beyond reach if they can not assimilate it from their growth medium. Three approaches have been used to try to encourage this assimilation, all aimed at increasing the cell's dependence on exogenous tryptophan. The approaches include the use of auxotrophic yeast strains and an inhibitor of endogenous tryptophan synthesis. As they constitute an important experimental variable, each of these approaches is detailed and discussed in Section 3.3.2 after some further general discussion.

3.3.1.2 Galactose–induction of protein synthesis

The second problem with attempting to label a protein *in vivo* is the difficulty of ensuring specificity of the labelling process. This problem has been tackled by arranging that the protein of interest was the predominant one being synthesised when the label was present in the growth medium.

This selective synthesis has been possible with a galactose-inducible expression vector, pKV43, which directs the synthesis of phosphoglycerate kinase only in the presence of galactose and absence of glucose. Simple manipulation of the growth medium makes it possible to control the expression of PGK. The plasmid pKV43 is described in the Materials and Methods section, Chapter 2.

3.3.1.3 *The induction process in practice*

Yeast was grown into late-log or early stationary phase on a glucose-containing medium. At this point, cell growth was essentially complete and the cells possessed a full complement of normal cellular proteins that had been synthesised in the absence of label. The 5-fluorotryptophan and galactose were now added to the growth medium. In the absence of glucose and presence of galactose, the target protein alone was now synthesised in the presence of 5-fluorotryptophan.

The mechanism by which galactose-induction takes place is well understood (Johnston 1987). Galactose in the cytoplasm is transported either non-specifically or specifically by the GAL2 transport protein. In the cell, galactose binds to the GAL80 protein causing it to dissociate from the GAL4 protein. GAL4, a positive regulatory factor required for the activation of transcription, is thus freed to bind to the GAL1-10 UAS sequence in the promoter region of the gene, activating transcription. The molecular recognition involved in the GAL4-DNA binding is now understood in some detail (Baleja *et al.* 1992; Kraulis *et al.* 1992; Marmorstein *et al.* 1992).

3.3.1.4 *Criteria for judging the outcome of the labelling process*

The success of a labelling depends on two principal factors, the total quantity of target protein produced and the degree of labelling. The extent to which the protein is labelled will depend on the ratio of the labelled and unlabelled amino acids available for protein synthesis. The combination of amino-acyl tRNA synthetase and translational editing will further discriminate against derivatised amino acids and reduce the fractional labelling achieved.

A high degree of labelling is clearly desirable, but there may be unwanted physiological responses, for example, to the overproduction of a particular protein that make it impossible to produce detectably large quantities in the

cell. On the other hand, the cell may already produce large quantities of the target protein and tolerate well a small proportional increase in the protein concentration, large enough in absolute terms to facilitate the monitoring of the label *in vivo* by NMR.

3.3.2 The strategies adopted to encourage cells to take up fluorotryptophan from the growth medium

3.3.2.1 The choice of yeast strains

PGK was expressed from a plasmid maintained in the cell population by leucine selection, so all the yeast strains used carried a *leu* mutation. Some yeast strains, such as AH22, have ~~also~~ been found to be unsuitable for work with galactose-inducible plasmids as they did not seem to allow the efficient expression of the inducible gene (Alan Kingsman, Oxford, personal communication), although the *gal2* galactose transport mutation does not prevent efficient galactose induction in strains such as BJ2168 (Adams 1989). This problem further restricted the choice of yeast strains for this work.

3.3.2.2 Labelling strategy 1 (Trp auxotroph, defined medium)

The first approach to forcing the cell to take up labelled tryptophan from the medium was to use a yeast strain auxotrophic for tryptophan and grown in a defined medium. This work was done with the yeast strain FY3-1 (*trp, leu, ade, his*). This strain was chosen because it had the *trp* phenotype and was known to work with galactose-inducible plasmids.

This approach seemed to offer the best prospects for achieving labelling since the cells were absolutely dependant on exogenous tryptophan.

3.3.2.3 *Labelling strategy 2 (Inhibition of Trp synthesis in defined medium)*

The second approach to encourage the uptake of labelled amino acid from the medium was to use a yeast strain prototrophic for tryptophan but grown in the presence of glyphosate, an inhibitor of aromatic amino acid biosynthesis (Bode *et al.* 1986). This work was done with the yeast strain DBY745 (*ade, leu, ura*). This strain was chosen because it was a parent of the strain FY3-1 and because it was known to be a successful host of galactose-inducible plasmids (Alan Kingsman, Oxford, personal communication).

This approach offered the prospect of labelling with the other aromatic amino acids, since glyphosate acts on the shikimate pathway to block tryptophan, tyrosine and phenylalanine production.

3.3.2.4 *Labelling strategy 3 (Trp prototroph, complete medium)*

The third approach to encourage the uptake of labelled amino acid from the medium was using a tryptophan auxotroph grown on complete media to high cell densities. Once grown, the cells were induced with galactose added to the same medium. This relied on the growth of the cells to deplete the medium of tryptophan. It was anticipated that the cells would then take up exogenous tryptophan in preference to biosynthesis. This work was done with the yeast strain BJ2168 (*ura, leu, trp*).

This method was the last to be tried since problems of plasmid loss were anticipated on complete medium. In practice, it was found that the measured plasmid loss was minimal over the 24 hour growth period. This was in accord with work examining the stability of 2μ plasmids in complete media (Futcher and Cox 1984).

3.3.2.5 *Other possible strategies*

The depletion of tryptophan in a complete medium by enzymatic means, or the use of a defined medium with further additional supplements are also possible. Preliminary further work has shown that incubation of the growth medium with tryptophanase results to a near-doubling of the fractional labelling achieved in complete medium, to over 60 %. This promising result has yet to be pursued in detail.

3.4 Methods

3.4.1 Introduction to the methods

3.4.1.1 *Refer to Chapter 2, the Materials and Methods section*

The detailed descriptions of the yeast strains, plasmids, media and other reagents used are given in the Materials and Methods section, Chapter 2. Details of the growth conditions and other practical details are also contained in the Materials and Methods section.

Some of the protocols refer to the addition of amino acids to the medium without explicitly detailing the concentrations involved. Except where stated otherwise, amino acids and other growth supplements were always added to media to the same concentrations as those described in the Media Supplements section of Chapter 2, Materials and Methods.

3.4.1.2 *Important definitions*

The synonymous terms "induction level" and "induction factor" are used extensively in the remainder of this chapter. They are defined as the ratio of the PGK activities in the cells before and after induction by incubation on galactose. This was originally measured as the ratio of the "before" and

"after" relative activities of PGK and GAPDH, or later simply as the ratio of the "before" and "after" PGK (or PK as appropriate) activities, normalised to one ml of cell water.

Transformed yeasts are referred to simply as the strain name followed by the plasmid name, e.g. "BJ2168 pKV43" means cells of the yeast strain BJ2168 carrying the plasmid pKV43, the yeast having been transformed with that plasmid.

3.4.2 Early induction protocol with FY3–1 A tryptophan auxotroph induced in defined medium

The first induction protocol used the tryptophan auxotroph FY3-1 transformed with the galactose-inducible PGK-producing plasmid pKV43. The induction protocol used was based upon that suggested by the originators of the strain and vector (Alan Kingsman *et al.*, Oxford, personal communication) and refined experimentally by Mark Boulton and Kevin Brindle.

The protocol had to be adapted because the fluorotryptophan label was toxic to the cells under some circumstances, particularly if added to the medium too soon. The optimal timing of the fluorotryptophan addition was found to be almost coincident with the onset of galactose-induced protein synthesis, typically after 12 hours with galactose, when the induction level was approximately 1.5.

The final protocol was as follows.

A single colony of FY3-1 pKV43 was inoculated into a 50 ml culture of the defined SC-leu medium ("synthetic complete" without leucine). This preculture was grown for 24 hours, when the cell density was approximately 8×10^7 per ml.

The culture was used to inoculate several, typically three, 5 litre flasks containing 2 litres of the complete YEPD medium at a cell density of 4 x 10^5 per ml. After 10 hours, the cell density was measured approximately each hour. The cells were grown until the cell density had reached 3 to 4 x 10^7 per ml. This took between 12 and 20 hours, typically 14.

The cells were harvested by centrifugation (30 min., 5000 g, 4 °C) in sterilised 1 litre nominal volume polypropylene pots. The long spin time was necessary as the cells did not sediment effectively from low cell densities in the large centrifuge pots.

The cells were thoroughly washed free of residual YEPD medium by resuspension and resedimentation twice in approximately 500 to 1000 ml of chilled sterile water. A third wash was performed in sterile 50 ml plastic tubes centrifuged at 2000 g in a benchtop centrifuge.

The cell density of the final suspension was typically 2 to 4 x 10^9 per ml. This suspension was used to inoculate a number of, typically 6, 5 litre flasks containing 2 litres of YNB Gal medium. This was supplemented with the SC cocktail of media supplements but with only 0.5 % the normal amount of tryptophan supplement.

The cells were grown for 12 hours, after which time 1 % v/v of filter-sterilised 0.4 % w/v DL-5-fluorotryptophan was added to each two litre culture. A sample of the medium was taken for subsequent enzyme assay.

The cells were grown for a further 36 hours before harvesting by centrifugation (30 min., 5000 g, 4 °C) in 1 litre nominal volume polypropylene pots. The harvested cells were washed and perifused, or stored frozen for subsequent use.

3.4.3 Later induction protocol with DBY745

The use of glyphosate to inhibit endogenous tryptophan synthesis

The basic principle of the galactose-induced overproduction was combined with the addition of glyphosate at various concentrations and times to inhibit endogenous tryptophan production. I am grateful to Iain Campbell, Oxford, for suggesting this use of glyphosate. A number of different protocols were tried and developed. These are minor variants in the media and timing of the protocol described for FY3-1 pKV43 (section 3.4.2) and each experiment is described in the results section.

3.4.4 Final induction protocol with BJ2168

A tryptophan auxotroph induced in complete medium

A newly-published and procedurally very simple induction protocol (Broker *et al.* 1991) was employed to great effect with this yeast strain. Variations of the basic protocol were necessary to effect labelling, however. The modifications are discussed in the Results section. The final protocol was as follows.

A single colony of BJ2168 pKV43 was inoculated into 50 ml of YNBD medium supplemented with uracil and tryptophan. This preculture was incubated for 24 hours.

One ml of the preculture was used to inoculate a 100 ml starter culture of YNBD medium supplemented with uracil and tryptophan. The culture was incubated for 48 hours and then poured into one litre of YEPD medium in a 5l flask.

The YEPD culture was incubated with shaking for 24 hours and then brought to 2 % in galactose by the addition of 22 g galactose. The galactose was

dispersed in water to 100 ml and autoclaved. The galactose remained dissolved once autoclaved.

Six hours after the addition of galactose, 0.2 g 5-fluorotryptophan filter-sterilised in 50 ml water was added to the culture.

The culture was incubated for a total of 72 hours after the first addition of galactose. The cultures were chilled for 30 to 60 minutes before harvesting the cells in 500 ml nominal volume polypropylene pots by centrifugation (15 min., 5000 g, 4 °C).

3.5 Results from the three labelling strategies

3.5.1 Results from the early induction protocol with FY3–1 A tryptophan auxotroph induced in defined medium

3.5.1.1 Growth yields

The yield from FY3-1 on the galactose-containing medium was very poor, a significant handicap in accumulating enough material to prepare purified labelled enzyme. Growth yields were typically 0.7 to 1.0 g per litre of culture, using an inoculum of 2×10^7 cells per ml in the galactose medium. This limited the total batch yield attainable since it was, for technical reasons, impossible to culture more than 24 litres at a time, and impractical to culture more than the routine quantity of 12 litres. For comparison, yields of 10 g or more wet weight yeast per litre of medium were routinely achieved with the strain AH22 on glucose-containing media.

The cell density remains low (2.0 to 2.3 $\times 10^7$ per ml) in the galactose medium since in galactose the cells do not multiply significantly. Indeed, this is a prerequisite for a specific labelling strategy, and would not be a handicap

in itself if a higher cell density could be used (10^8 per ml, for example, as in glucose-grown stationary phase cultures).

Some variations in the protocol aimed at increasing the batch growth yields were tried. Increasing the cell density in the galactose medium beyond 2×10^7 per ml markedly reduced the level of PGK induction, and was counter-productive. The trade-off between extra cells and less PGK per cell was approximately equal at just 3×10^7 per ml, and at an inoculation density of 4×10^7 per ml the induction of PGK became negligible.

Incubating less than two litres of medium in a flask did not allow the use of proportionately higher cell densities or achieve higher levels of induction. It was thought that the volume of medium in the flask might have been important since the quantity of liquid in a conical flask determines the surface area to volume ratio and hence the aeration of the medium in the flask. Aerobiosis is known to be important for efficient galactose induction (Broker *et al.* 1991).

3.5.1.2 *Induction levels*

The induction levels achieved over the first six months of operating this protocol are given in Table 3.1 below.

Table 3.1

Cell batch number	Induction factor (induced/wild type PGK activity)
1	9.5
2,3	5.9, 5.8
4,5,6	5.6, 6.2, 6.4
7	5.0
8	9.4
9	8.7
10	5.4
11	10.8
12	7.0

The PGK induction factors achieved using the yeast strain FY3-1 and plasmid pKV43; earlier experiments.
Each value is the induction level for a particular batch of cells; where two or three batches are shown on the same line, more than one cell batch was prepared simultaneously.

The average induction level over this period was thus approximately 7.3.

The induction levels achieved using the protocol described above were, unfortunately, somewhat unpredictable despite rigid adherence to the protocol. It was observed that the cell densities reached after a particular time of growth depended on the age of the starting yeast colony and was difficult to control. It was found that the time taken for the cells to reach a density of 4×10^7 per ml in the YEPD medium varied between 12 and 20 hours, depending on the growth rate of the preculture and the age of the agar plate. The protocol seemed to work best with second-generation agar plates

around a month old, which gave rise to YEPD cultures that reached 4 x 10^7 per ml in about 14 hours.

Unfortunately, these factors did not seem to vary in any reproducible, meaningful or predictable fashion, and were not fully investigated. The experiments were suspended for about two months while some equipment was constructed. After the break, the protocol could not be made to work reliably with large-scale cultures. Eventually, the protocol seemed to "break down" and became totally irreproducible, as illustrated in Table 3.2 below.

Table 3.2

Cell batch number	Induction factor (induced/wild type PGK activity)
13	1
14	7
15	4
16	4
17	5
18 and subsequent batches	c. 1

The PGK induction factors achieved using the yeast strain FY3-1 and plasmid pKV43; later experiments.
The details are as described in the legend to Table 3.1. An induction factor of 1 corresponds to no induction, i.e. no increase in the PGK activity

Many factors surrounding the protocol were scrutinised to no avail.

It was confirmed that the plasmid presence in the cell population was greater than 90 % by comparing the viability of the cells on media with or without the plasmid selection marker leucine. After growth on the YEPD, the presence remained at over 80 %. The integrity of the plasmid, at least at a gross level, was confirmed with a restriction digest of plasmids rescued from the yeast (Sandra Fulton, Oxford, personal communication). The yeast stocks were

renewed by retrieving yeast from a different glycerol stock than had been used originally.

It was confirmed that the cells had not become petite (deficient in mitochondria) by assaying cell extracts for the predominantly mitochondrial enzymes cytochrome c oxidase and citrate synthase. The activities were not significantly different from those of the yeast AH22 pMA3a (Corinne Spickett, Oxford, personal communication), that were then being used in the lab for mitochondrial studies. The cells were also capable of growth on glycerol-ethanol.

The degree of shaking during incubation, anaerobiosis from wetting of the culture's foam bungs, glassware washing, glucose caramelisation during autoclaving, the number and temperature of the sterile washes and the incubation temperature were all considered as being causes of the induction failure. None was found to be responsible, but as the protocol was not to work again it could have been one or a combination of these factors.

For several months, induction levels of 8 to 10 could be obtained in small-scale (50 ml) experiments but not in the large-scale experiments needed to produce cells for NMR experiments. It was not clear whether this was due to the scale of the experiment *per se*, or the fact that the small-scale flasks of galactose medium were produced in advance from different stocks of dehydrated media concentrates. Glucose assays were performed on various media and media components. The results are shown in Table 3.3 below.

Table 3.3

Sample assayed	Glucose concentrations
1% Difco galactose batch 1 (KMB)	0.22 mM
1% Difco galactose batch 2 (KMB)	0.45 mM
1 % Difco galactose batch 3 (AJK)	0.22 mM
1 % Sigma low-glucose galactose	0.15 mM
1% Difco Yeast Nitrogen Base	none detected

Glucose concentrations of the galactose and Yeast Nitrogen Base components of the media used for PGK induction with FY3-1.
The initials KMB and AJK refer to the source laboratory of the galactose tested, either Brindle or Kingsman.

These glucose levels were thought insufficient to explain the failure of the induction protocol since the protocol had worked in the 0.45 mM glucose-containing solutions. It has since become apparent that the glucose content at such low levels is unlikely to cause any failure of the induction in any case (since the cells themselves will efficiently remove it from the medium).

Glycerol stocks of FY3-1 and the related strain FY7-11 (also *trp* but not *his*) were obtained from Fiona Yull, Oxford, and re-transformed with the plasmid pKV43. With fluorotryptophan, the new transformants achieved induction levels of 2.4 to 3.0 in both strains, not enough to consider using these new transformants for routine experiments.

3.5.1.3 Fraction of the protein labelled with fluorotryptophan

The proportion of the PGK containing fluorine was determined by comparing the concentration of enzyme with the concentration of fluorotryptophan as measured in a fully-relaxed fluorine NMR spectrum. This suggested that approximately 60 % of the PGK tryptophans were replaced with 5-fluorotryptophan. Mark Boulton had determined a similar figure for the

enzyme prepared in his preliminary work (Kevin Brindle, Oxford, personal communication).

3.5.2 Results from the induction in DBY745 Inhibiting endogenous tryptophan synthesis with glyphosate

Except where stated otherwise, all the experiments used media with mixtures or single amino acids at the same final concentration as that provided by the SC-leu growth medium supplement cocktail. This is fully described in Chapter 2, the Materials and Methods section.

3.5.2.1 Basic induction of PGK synthesis

Experiments showed that PGK induction factors of up to twenty-fold could be achieved by growing them in SC-leu defined minimal medium, harvesting them under sterile conditions, and resuspending them in YNB Gal medium at cell densities as high as 5×10^7 per ml. However, these cells grew poorly on the SC-leu minimal medium (to approximately 5×10^7 per ml after 24 or even 48 hours). The final induction protocol used with this yeast used YEPD complete medium to rapidly grow cells that were then washed and resuspended in YNB Gal medium at a cell density of 2×10^7 per ml. This method is similar to that described in section 3.4.2.

3.5.2.2 Finding conditions to allow glyphosate action

A preliminary experiment was carried out in SC-leu medium with varying glyphosate concentrations. The glyphosate concentrations used were in the range reported as inhibitory to growth in other yeasts (Bode *et al.* 1986). The cell densities after 24 hours in the presence of 0, 0.25, 0.5 or 1 g/l glyphosate were all comparable at around 10^8 cells per ml. The glyphosate had no gross effect on the growth rate.

The effect of glyphosate on whole cells is compromised by compounds competitively reducing its uptake (Bode *et al.* 1985). As well as its action being negated by the presence of the aromatic amino acids Trp, Tyr and Phe, other compounds including glutamate and glutamine, aspartate and asparagine, arginine, serine, lysine, leucine, valine and pyruvate are also effective. Many of these compounds are present in the SC-leu medium.

To find conditions under which glyphosate was effective and the cells would grow, further growth inhibition experiments were carried out in YNBD medium with various combinations and concentrations of supplementing compounds. These experiments are detailed in Table 3.4 below.

Fortunately, the auxotrophic markers were compounds not inhibitory to the action of glyphosate. All further work used adenine and uracil as the only basic growth supplements since there was no apparent benefit in adding those other components of the SC-leu cocktail that do not reverse the action of glyphosate. The cells grew slower than with the SC-leu cocktail, but reached the same cell density after 48 hours.

Table 3.4

Growth supplement in the medium	Glyphosate concentration in the medium, grams per litre.			
	None	0.1	1.0	3.0
0.1 % v/v SC-leu cocktail	+++	+++	+++	++
1 % v/v "Aa OK" cocktail	+++	+++	+	—
1 % v/v Ade Ura mix	+++	+++	+	—
0.1 % v/v Ade Ura mix	++	+	—	—

Growth levels of cultures grown with various concentrations and combinations of glyphosate and growth medium supplements.
Cultures of the yeast DBY745 (*ade, ura*) containing the plasmid pKV43 were grown on YNBD medium with four different growth medium supplements and in the presence of four different glyphosate concentrations. Growth levels at 24 hours (results not shown) and 48 hours (results shown above) were estimated visually from the cloudiness of the culture by looking through the culture medium at a simple pattern drawn beneath the flask. The cell densities were simply scored from - (no growth) through +, ++, to +++. Cell counting with a hemacytometer established that +++ corresponded to cell densities over 5×10^7 per ml. For normal media, the addition of the SC-leu supplement was 1 % v/v. The Ade Ura mix contained adenine and uracil at the same concentration as those compounds were in the SC-leu cocktail. The "Aa OK" cocktail was a subset of compounds from the SC-leu cocktail, and comprised those compounds not thought to inhibit glyphosate action (Bode *et al.* 1985), viz. Ade, His, Ile, Met, Thr and Ura.

It was concluded that glyphosate could be made to inhibit growth, and thus presumably tryptophan synthesis, in these cells.

Compared to untreated cells, glyphosate-treated cells appeared smaller under the microscope and yielded smaller cell pellets (about half the volume) when harvested from a given volume of medium, even though the number of cells per unit volume was the same.

Further experiments established that the growth inhibition could be reversed by the addition to the medium of tryptophan or tyrosine alone (besides the

adenine and uracil required by the cells), or more effectively with all three aromatic amino acids together.

Presumably, the inhibition is somewhat incomplete and providing even one amino acid in the medium allows the "leak" to meet a significant part of the cells requirements for the other two amino acids. Perhaps unsurprisingly, fluorotryptophan alone abolished glyphosate's inhibitory action much less effectively than tryptophan alone. Fluorotyrosine alone was ineffective at reversing the inhibition.

3.5.2.3 The effect of glyphosate on the induction of PGK

The next series of experiments, looked at the effect of glyphosate on the induction levels of PGK. The aim was to find a set of conditions compatible with labelling. It was thought that the presence of glyphosate to block endogenous tryptophan synthesis would prevent induction unless tryptophan, or fluorotryptophan, was supplied in the medium.

One experiment examined the effect of glyphosate on the time course of the PGK induction process. The detailed conditions and the results are given in Table 3.5, below.

Table 3.5

Medium conditions in which the induction was taking place	Time interval between transferring the cells to galactose medium and adding glyphosate alone or glyphosate and tryptophan or fluorotryptophan to the medium		
	12 hours		0 hours
	PGK activity	Induction factor	Induction factor
Pre-galactose cells	900	1.0	1.0
No glyph., Trp or FTrp	9800	11	12
1 g/l glyphosate	14400	16	11
2 g/l glyphosate	15600	17	19
1 g/l glyph. and Trp	12200	14	10
1 g/l glyph. and FTrp	14900	17	5

PGK activities and induction levels after incubation with different combinations of glyphosate, tryptophan and fluorotryptophan.
DBY745 (ade, ura) cells were grown on complete medium then washed and transferred to YNB Gal medium. Cells were inoculated at a density of 2 x 10^7 per ml and incubated for 45 hours with Ade/Ura as growth supplements. Glyphosate and fluorotryptophan were added to the medium either at the time of inoculation or 12 hours later, the time induction was just beginning (the induction factor being less than 2). L-Tryptophan was added at the same concentration as described for the SC-leu medium in the Materials and Methods section, Chapter 2. Twice the quantity of fluorotryptophan was used because this material was supplied as the DL racemate. The cells were harvested after 45 hours and assayed for PGK. PGK activities are expressed in units of activity per ml of cell water.

The higher induction levels achieved at the 2 as opposed to 1 gram per litre of glyphosate were not investigated further. They were presumed to erroneous or relate to non-specific effects such as the pH difference caused by adding different amounts of the acidic 200 g/l glyphosate stock solution, which was acidic even though it was prepared in 1M sodium hydroxide solution.

The low induction level (5-fold) seen with fluorotryptophan given at the time of inoculation is thought to be due to the toxic effects of this compound interfering with the synthesis of proteins in the cell.

It was concluded that it was not feasible to eliminate induction by simply adding glyphosate to the YNB Gal medium, despite the growth inhibition experiments showing that the endogenous tryptophan supply was severely reduced by glyphosate. Presumably, the tryptophan requirement for the induction was very low compared to that for growth, and the demand could be met by endogenous reserves or an imperfectly blocked shikimate pathway.

Although outright inhibition of induction was impossible, the induced PGK may well have been fluorine-labelled. The presence of glyphosate in the medium from the time of inoculation was expected to improve the fractional labelling achieved, and so the use of glyphosate was continued.

The induction protocol used for subsequent experiments followed that described for FY3-1 in section 3.4.2 except for the composition of the induction medium. Each litre of YNB Gal medium contained two grams of glyphosate from the time of inoculation. Only adenine and uracil were used as growth supplements rather than the complete SC-leu cocktail to avoid blocking the uptake of glyphosate. This protocol gave induction levels of up to ten-fold in the presence of fluorotryptophan added 12 hours after inoculation.

3.5.2.4 A different induction protocol

Induction of PGK in complete medium, simply adding galactose to the culture as described for BJ2168 cells (section 3.4.4), was also tried with the DBY745 cells. The induction level achieved, approximately 3, was poorer than that obtained with the defined media protocol using glyphosate. The absolute PGK

levels and the induction factors attained were also significantly lower for the DBY745 strain than for BJ2168 (induction factors of 3 for DBY and 9 for BJ under identical conditions).

Since the BJ2168 strain showed more promise as a vehicle for the induction experiments, no further work carried out with DBY745.

3.5.2.5 Incorporation of label

The DBY745 pKV43 cells were not used for *in vivo* NMR or protein purification experiments, since they were effectively superseded by the BJ2168 cells described in section 3.5.3. However, crude cell extracts and simple ammonium sulphate concentrates were examined by NMR. The spectra observed were consistent with those seen previously with fluorotryptophan-labelled PGK in extracts of the FY3-1 yeast strain. The spectra showed the same ATP dependence as previously observed with partly purified labelled PGK. All these observations supported the view that the induced PGK had been successfully and specifically labelled in this cell type.

It has not been conclusively demonstrated that the use of glyphosate does increase the proportion of the PGK that is labelled with fluorotryptophan. It has been established that glyphosate can be made to inhibit endogenous tryptophan biosynthesis in a manner that is at least partly relieved by fluorotryptophan, offering the prospect of increased fractional labelling.

3.5.3 Results from the induction in BJ2168

A tryptophan auxotroph induced in complete medium

3.5.3.1 Growth yields

Growth yields were excellent with this technique, not surprisingly, since the cells were grown and induced on complete medium. The cultures had cell

densities of 2 x 10^8 per ml, giving 25 to 30 grams of cells per litre of culture medium after 24 hours. This compares well with the best yield of approximately 20 grams per litre that could be achieved with AH22 and other strains used in the lab.

As has been known in the brewing industry for a long time, one benefit of growing cells at these cell densities is that the culture becomes largely resistant to superinfection by common airborne bacteria. That may become important if the process was scaled up. Another benefit is the reduced requirement for large-scale incubation facilities, since large quantities of yeast for NMR and protein purification can be produced quickly in relatively small cultures volumes. Up to 150 grams of induced yeast can be produced in a week with this technique from just six litres of complete medium, compared to the three to four months, over a hundred litres of defined medium and fifty litres of complete medium required with the FY3-1 technique.

3.5.3.2 Induction levels

Early experiments performed without the addition of fluorotryptophan established that the basic protocol worked well with both the PGK-producing plasmid pKV43 and the pyruvate kinase-producing plasmid pBF72. Preliminary further work has shown that it also works well with hexokinase expressed from a similar pKV49-based vector.

These first experiments were performed with cells grown on YEPD medium for 28 hours as opposed to the 24 hours used in the final protocol, hence the time course and outcome of the induction are somewhat different to data subsequently presented for cells grown according to the final protocol. The results are given in Table 3.6 below.

Table 3.6

Hours in galactose medium	PGK activity	Induction factor for PGK	PK activity	Induction factor for PK
0	1082	1.0	1300	1.0
18	1272	1.2	1970	1.5
46	5803	5.4	8336	6.4
68	9377	8.7	13467	10.4

Induction levels of PGK and pyruvate kinase (PK) as a function of the incubation time in galactose.
One litre cultures of BJ2168 cells with either plasmid pKV43 (PGK) or pBF72 (PK) were grown in 5 litre flasks for 28 hours and then galactose was added to 2 % w/v. Samples of the cells were taken at the times indicated and assayed for PGK or PK as appropriate. Enzyme activities are expressed as units of activity per ml of cell water.

Subsequent experiments established the final induction level was higher in cells that were incubated for 24, rather than 28, hours on the YEPD before the addition of galactose. The time of onset of induction was also much more rapid with these cells. For example, cells producing pyruvate kinase reached 6650 units per ml cell water (an induction factor of 5.1) after just eight hours. PGK-producing cells showed a similarly accelerated induction process when incubated on YEPD for 24 rather than 28 hours. The induction time course for PGK production in cells incubated on YEPD for 24 hours is shown below in Table 3.7.

Table 3.7

Time, hours	0	2	4	6	8	10	24
Induction level	1.0	1.7	4.5	7.5	9	11	26

The onset of the induction of PGK in cells grown for 24 hours before the addition of galactose.
Other experimental conditions are as described for the 28-hour experiment in Table 3.6. The induction factors represent the ratio of the PGK activities in the cells before and after incubation on galactose. The time is that since the addition of galactose to the medium.

Incubation on YEPD for 26 hours before adding galactose gave a result intermediate between that of 24 and 28 hours, but the effect of this incubation time was not fully investigated. It was concluded simply that the timing of this step is a critical determinant of the induction timing and the final induced protein levels reached.

Presumably, the age and condition of the starter culture also influenced the growth of the cells on the YEPD medium, so that the timing of this step also depended on the age of the agar plates used for each experiment. The time course of the induction was not as reproducible as its outcome, a reflection of the difficulties in starting each induction with exactly equivalent cell populations. These sorts of difficulties were also encountered with the FY3-1 cells, and may be a general difficulty of working with yeast.

The final protocol employed two preculture phases, the second growing the cells for 48 hours, well into stationary phase. It was anticipated that this step would help to ensure some uniformity of the cells used to inoculate the YEPD culture and that this protocol would thus be more robust than the protocol used for FY3-1 induction.

Another factor influencing the final induction levels reached is the quantity and frequency of galactose additions to the medium. Again, this was not investigated rigorously but there was some evidence that cultures with 2 % w/v galactose added more than once induced more PGK in 72 hours than cultures given only one aliquot of galactose.

There did not seem to be a significant difference between giving galactose twice (at 0 and 24 hours) after growth on YEPD as opposed to three times (0, 24, and 48 hours). Either of these conditions resulted in cells with PGK activities over 20000 units per ml of cell water, over 1 mM PGK protein in the cell water. This compares with activities of approximately 10 to 20000 for

cells given just one aliquot of galactose. It may be that these effects also depend critically on the period of growth in the complete medium, but the combination of these factors has not been investigated.

The protocol adapted for routine use employed only one addition of galactose since cells produced this way gave good NMR signals but were, presumably, less physiologically disturbed by the overproduction of the PGK.

3.5.3.3 Fraction of the protein labelled

Fluorinated PGK produced by induction in BJ2168 was purified and its fluorine content determined in a fully-relaxed fluorine-19 NMR spectrum. The fluorine content was compared with the protein content of the sample to calculate the fractional replacement of tryptophan by fluorotryptophan.

There was no significant difference between the fluorine content of the two tryptophan residues, reflecting the random incorporation of the label into the protein. The proportion of the protein that was fluorinated was approximately 25 to 30 %. The time course of the induction for the batch of cells used to prepare this PGK sample showed that only about one half of the total PGK was produced in the presence of fluorotryptophan, so the PGK produced in the presence of the label was c.50 % labelled.

The overall labelling figure might be improved by altering the amount of fluorotryptophan used and particularly by optimising the time interval between the additions of galactose and fluorotryptophan. Some preliminary further work has shown that shortening the incubation time before adding galactose from 24 to as little as 16 hours is very beneficial, but that adding greater amounts of fluorotryptophan has no benefit.

With the FY3-1 induction protocol, the addition of fluorotryptophan was coincident with the onset of PGK induction, the induction factor at 12 hours

post-galactose typically being c. 1.5. The addition of fluorotryptophan at times near the onset of induction in BJ2168 totally abolished the induction.

When fluorotryptophan was added to BJ2168 cultures six hours after galactose, when the induction factor was typically three, there was no apparent effect on the final level of PGK reached. At four hours, however, when the induction factor was approximately two, the addition of fluorotryptophan caused the induction process to fail completely. Preliminary further work has shown that shortening the YEPD incubation step to 16 to 20 hours abolishes this effect, allowing the fluorotryptophan to be added at the same time as the galactose, with a consequent improvement in the fractional labelling achieved.

3.6 Discussion of the results obtained and possible further work

The methods used showed several practical ways to achieve fluorine-labelling of an enzyme in the intact cell. The methods varied in the amount of labelled and unlabelled protein produced within the cell. The growth yields also varied, so the amount of labelled protein produced within a given volume of culture also changed.

The importance of these differences depends on the intended use of the cells. For protein purification, the high yields per culture are important to obtain sufficient enriched starting material. For studies using the labelled protein as a reporter group in the cell, it may be preferable to have lower levels of induction to minimise some of the physiologically disruptive side-effects of expressing a large quantity of protein (Brindle 1988). These might be general effects of protein overexpression, or specific to a particular protein.

Specific difficulties would be particularly important if the expressed protein significantly bound a species in the cell that was only present at low concentrations. This would buffer changes in its concentration, altering the rate of change of concentration in the cell, possibly perturbing events that rely on rapid transients in the concentration of the bound compound. Similar difficulties are encountered with the introduction of fluorescent or NMR probes of intracellular calcium (Kirschenlohr *et al.* 1988) or magnesium (London 1991). The buffering of calcium transients by the probe species 5FBAPTA, for example, is thought to be responsible for perturbations of the cardiac function in hearts loaded with this probe (Kirschenlohr *et al.* 1988).

Further optimisation of the protocols may be possible, especially to change the amounts and proportions of labelled and unlabelled protein produced.

3.6.1 Growth yields

All the methods used were capable of growing the gram-quantities of labelled cells required for NMR experiments, but with rather different degrees of practicability and cost. Only the complete-media method used with BJ2168 was easily capable of growing the hundreds of grams required for large-scale protein purification, and it also gave the highest levels of overproduction within the cell.

The minimal-media induction protocols seemed to support induction only at low cell densities, so these methods were less suitable for growing large quantities of cells. This limitation may be overcome by the addition of trace elements, vitamins, growth factors, etc. to the minimal medium, but the development of this approach may well require many trial-and-error experiments to find the missing factor or combination of factors responsible.

3.6.2 Induction levels

3.6.2.1 The final induction levels achieved

Using the plasmid pKV43, the highest galactose-induced PGK levels seen in BJ2168 are the same as those seen in other cells overproducing PGK from the plasmid pMA27 which expresses PGK efficiently and constitutively. This suggests that the expression systems are operating at their maximum capacity, and these represent the highest PGK levels attainable with this type of plasmid.

For studies of normal cellular metabolism it might be argued that the maximum PGK level attained, of around 50 mg per ml of cell water, is in any case too high. The state of the cells, in terms of growth rates and the concentrations of metabolites, may be altered by the production and presence of large quantities of even unlabelled PGK (Brindle 1988). With other proteins, a similar 20-fold overexpression may not produce nearly as much protein and the total quantity may be tolerated well.

The induction level depends on the amount of galactose given to cultures of BJ2168, but the effect of the galactose concentration used in the minimal media experiments was not investigated. All the minimal medium experiments employed only 1 % galactose, and achieved induction levels of up to ten-fold. Perhaps the higher induction levels attained in the complete media experiments with BJ2168 could be attained in minimal medium with more galactose.

3.6.2.2 The time course of induction

The rapid onset of induction in BJ2168 cells grown on YEPD for 24 hours holds out the prospect of using this or a similar system for acutely elevating enzyme levels for metabolic studies. Some metabolic studies may be

compromised in BJ2168 since it has specific mutations in the general degradative proteolytic functions of the vacuole. The strain is, however, comparable to other strains such as AH22 in terms of the rates of its growth, glucose and oxygen consumption, etc. BJ2168 is well-characterised and widely used for protein production and protein-processing studies (Adams 1989).

The use of a rapid induction process in a cell type with genetically reduced or eliminated background levels of the induced protein would allow cells to be produced with a wide range of defined activities of the induced protein. The acute establishment of a particular enzyme activity, in a range from near-zero to many times higher than the wild type, would be of great value in studies of the control of metabolic processes where conventional constitutive overexpression of an enzyme may be associated with adaptive changes that compromise the experiments.

The rapid induction process and the improvements in the detection of the signal also suggest that it might be possible to monitor the labelling process as it occurs in the cell. Performing the fluorination in the bore of the magnet might allow the observation of proteins as they arise.

It has been reported that the efficacy of the galactose-induction system is somewhat limited by the quantity of the GAL4 transcriptional activator in the cells (Johnston and Hopper 1982; Laughton *et al.* 1984; Johnston 1987), especially when the cell contains multiple copies of the expression plasmid (Baker *et al.* 1987). The presence of galactose-inducible copies of the GAL4 gene can results in the production of substantially more induced target protein (up to 10 times more) than in cells without the extra GAL4 genes. This has been demonstrated both by using a second plasmid population in the cell

(Laughton *et al.* 1984) and by producing a cell type with a regulated GAL4 construct integrated into the genome (Schultz *et al.* 1987).

The utility of regulated GAL4 overexpression may be limited in the case of the PGK and PK proteins expressed under the control of a modified PGK promoter in this work since the PGK promoter is in any case very efficient (Kingsman *et al.* 1990). However, it may be of great value in elevating the expression levels of other galactose-induced proteins that are expressed less efficiently, or in altering the time course of the induction process, presumably hastening it.

Some preliminary further work has shown that cells overexpressing GAL 4 along with yeast hexokinase B contain approximately twice as much hexokinase after 3 days as those expressing hexokinase alone. The fractional labelling of the resultant protein with 5-fluorotryptophan is unchanged. The effect on the time-course of the induction has not yet been investigated.

3.6.3 Fractional labelling

3.6.3.1 Comparison with other work

The fractional fluorotryptophan labelling achieved for PGK with the FY3-1 protocol, using defined medium with a minimal quantity of unlabelled tryptophan, was approximately 60 %. The 25 to 30 % achieved for PGK with BJ2168 in complete media is superficially much worse, but this figure represents labelling of approximately 50 % of the protein produced in the presence of label, and improvements in the protocol may lead to a rise in the overall labelling figure. This prospect of improvement is further supported by the result with pyruvate kinase, which was approximately 75 % labelled.

These fractional labelling figures are comparable to those achieved in a wide range of studies reviewed by Sykes and Weiner (Sykes and Weiner 1980). In

the work reviewed, all based on proteins purified from "globally labelled" organisms, fractional labelling levels ranged from 10 to 100 %, but with the average being around 50 to 75 %. Sykes and Weiner also report that previous workers had found that in *E. coli* it was difficult or impossible to totally substitute fluoroamino acid for the normal amino acid, presumably because the fluoroamino acids disrupt some critical protein function. This finding has been confirmed in this work with yeast.

3.6.3.2 *Determinants of the fractional labelling*

A very important process in reducing the fractional labelling achieved is the specificity of the aminoacyl tRNA synthetase charging. The importance of this phenomenon has been demonstrated *in vitro* with phenylalanine tRNA synthetase (Santi and Danenberg 1971). It was shown that the K_M's for the fluorotyrosines were orders of magnitude higher than for tyrosine, such that if the cell had 97 % 3-fluorotyrosine and just 3% tyrosine, the protein synthesised would contain only 50 % fluorotyrosine. Some workers (Dunn and Leach 1967) obtained evidence with *in vitro* translation systems that the fractional labelling obtained with fluorophenylalanine depended on the codon used for phenylalanine, UUU being more permissive than UUC for fluoroamino acid incorporation. Tryptophan has just one codon, but this finding may be important when carrying out site-directed mutagenesis to introduce a fluorophenylalanine at a site of interest.

The inability to synthesise all the induced protein in the presence of label inevitably increases the pool of unlabelled protein in the cells. Using the complete-medium induction protocol with the BJ2168 strain, the induction level of PGK or PK was already around 3 when the fluorotryptophan was added to the medium. In systems where the total level of overexpression is low, this large unlabelled pool may be a majority of the total protein

produced. Preliminary further work shows that the fluorotryptophan can be introduced at the same time as the galactose if the YEPD incubation time is shortened; following up this finding will clearly be important.

3.6.3.3 Improving the fractional labelling

It may be possible to devise a method to remove much of the unwanted tryptophan, or other labelling species, from the complete medium used for the complete-medium induction of BJ2168. The cells would then depend entirely on exogenous tryptophan, which would presumably allow the use of minimal quantities of normal tryptophan and allow more effective competition from the fluorotryptophan at the time of induction.

Tryptophan, based on the indole ring, is readily oxidised, and it may be possible to break down most of the tryptophan by chemical, or preferably enzymatic, oxidation. The CRC Handbook of Biochemistry and Molecular Biology lists tryptophanase, tryptophan decarboxylase, tryptophan indole lyase, and several tryptophan monooxygenases, amongst the many enzymes of tryptophan metabolism.

Preliminary further experiments have shown that the use of tryptophanase-treated medium can increase the fractional labelling to over 60 %.

3.6.4 Other labelling strategies

3.6.4.1 Other NMR visible nuclei: ^{13}C and ^{15}N

Many biologically important nuclei can be detected by NMR, but the problems of receptivity and of selectivity against the natural background make the rapid observation of nitrogen-15 or carbon-13 labelled proteins impractical *in vivo*. The following calculations give estimates of some of the difficulties involved in studying a labelled amino acid in the intact cell. It is

assumed throughout that signals arising from each of the amino acids can be resolved.

The amino acid species are relatively abundant in a typical cell, especially if the concentration of protein in the cell is considered as part of the amino acid pool. For example, a rat liver cell may contain sufficient protein to be equivalent to 2 M amino acids (Metzler 1977), crudely considered to be equivalent to approximately 100 mM of each of the twenty common amino acids.

The total soluble protein content of yeast cell extracts has been measured in this work as approximately 100 mg per ml of cell water. If a notional "average" 50 kDa protein contained 500 amino acid residues of an average mass of 100 Da each, the 100 mg/ml soluble cell protein would comprise 2 mM protein, or the equivalent of each of the twenty amino acids at an average of 50 mM. Allowing for an equal quantity of insoluble protein, the yeast cell too could well contain the equivalent of 100 mM of each of the amino acids. The calculations below are based on this approximate value of 100 mM for the total concentration of a "typical" amino acid species in the cell.

If a labelled protein was expressed at 1 mM in the cell, about the maximum concentration achieved in this work, then a labelled amino acid confined to one particular protein might represent 1 % of all of that amino acid in the cell.

Carbon-13 has a natural abundance of 1.1 %. Thus, for direct carbon-13 detection, the ratio of the signal intensity from the 1 mM labelled amino acid in the protein to the intensity of the signal from the naturally occurring carbon-13 in the 100 mM total cell content of that amino acid would be one to one. This ratio may be termed the "label to background signal ratio".

Nitrogen-15 has a natural abundance of 0.37 %. For direct nitrogen-15 detection, the ratio of the label to the background signal would be three to one. With either of these nuclei, the label to background signal ratio of the spectrum would be poor and, furthermore, the spectrum would take a long time to acquire given the low receptivity factors of these nuclei (Harris 1986). The receptivity factor of a nucleus is a measure of how efficiently it is detected in the NMR experiment. The factor depends on an inherent property of the nucleus type called the magnetogyric ratio, γ.

Nuclei with magnetogyric ratios close to 1, such as the proton (γ 1.0 by definition) and fluorine-19 (γ0.94), are observed much more efficiently than those that have a low magnetogyric ratio (Harris 1986), such as carbon-13 (γ 0.25) and nitrogen-15 (γ 0.10).The receptivity factor depends on the cube of γ. Ignoring the low natural abundance and considering isotopically pure samples, carbon-13 has a receptivity factor relative to the proton of 1.6 %, and nitrogen-15 has a receptivity factor relative to the proton of only 0.1 % (Harris 1986).

Unfortunately, these factors are exaggerated further by the need to accumulate the NMR spectrum as a series of repeated stimulation—detection steps. The statistical properties of such a summation mean that the signal to noise ratio in the spectrum rises only as the square root of the number of repetitions. The practical effect of this phenomenon is illustrated in the following example.

For a group of interest, perhaps a tryptophan side chain, either with an atom 100 % labelled with a fluorine-19 atom, or an atom 100 % isotopically replaced by a carbon-13 or a nitrogen-15 atom as appropriate, a proton spectrum of the sample might take an hour to acquire. Under the same conditions a fluorine-19 spectrum with the same signal to noise ratio would

take 1.2 hours, a carbon-13 spectrum nearly 2.6 days and a nitrogen-15 spectrum would take almost 6 weeks to acquire. Note that the "noise" in the signal to noise ratio arises from the NMR equipment and is not the background signal from naturally occurring carbon-13 or nitrogen-15.

These times assume that the NMR spectra can be collected at the same repetition rate for all the nuclei. In practice, this is often not so because of the different relaxation properties of the different nuclei, and this effect usually exaggerates rather than diminishes the difficulties of detecting carbon-13 and nitrogen-15. However, there are NMR polarisation transfer techniques such as INEPT and DEPT that can be used to improve the acquisition of carbon-13 and nitrogen-15 spectra (Derome 1987). These methods rely on reducing the receptivity factor to γ^2 rather than γ^3. In practice, this can improve the detection sensitivity by factors of 4 and 10 for carbon-13 and nitrogen-15 respectively. Even with this improvement, the detection sensitivity of these nuclei is very much lower than for the proton or for fluorine.

For carbon-13 and nitrogen-15, the ratio of label to background signal in the spectrum might be improved significantly for a particular case where the labelled amino acid is present in the target protein (still 1 mM, say) but is only present at a low level in the cell as a whole (a lot less than the "average" 100 mM). This would probably be true of tryptophan, a relatively infrequent amino acid in proteins that is typically only 0.5 to 2 % of total cell protein (Reeck 1976). Fluorine-19 has an advantage over carbon-13 and nitrogen-15 labels in this context too since most cells contain no fluorine and there is thus no background signal.

3.6.4.2 *An alternative approach to the direct observation of ^{13}C and ^{15}N labelled proteins*

An interesting though technically challenging experiment would be to perform the inverse detection experiment to observe protons attached to nitrogen-15 attached to carbon-13. This is termed a triple-resonance experiment, and has been used to study proteins *in vitro* (Kay *et al.* 1991). Since the experiment actually observes protons, albeit in a way that selects only those protons attached to ^{15}N attached to ^{13}C, the signal detection has a sensitivity nearer that of proton spectra. The sensitivity is somewhat poorer than for simple proton detection because of the T_2 signal losses during the complex pulse sequence needed for the triple resonance experiment.

The natural abundance background signals from the double-label of the triple resonance experiment would be very low. The natural abundance of carbon-13 adjacent to nitrogen-15 is the product of the single-nucleus factors of 1.1 and 0.37 % respectively, i.e. 41 parts per million. This would dramatically reduce the background signals from the amino acid pool in the cell when compared to observing singly-labelled carbon-13 or nitrogen-15 species.

In the calculation above for direct carbon-13 observation, where a 1 mM ^{13}C-labelled protein was observed in a cell containing a total of 100 mM of each amino acid, the relative intensities of the signals from the labelled protein and from the rest of the amino acid pool were shown to be 1 to 1. With the same assumptions, but observing a doubly-labelled compound in the triple-resonance experiment, the ratio of signal intensities from the labelled protein and the rest of the amino acid pool would be c. 250 to 1.

Nitrogen-15—carbon-13 double-labelled compounds are expensive and few are commercially available. They may, however, avoid the toxicity problems

associated with the use of fluorine-labelled amino acids. The coupling of carbon-13 carboxyl and nitrogen-15 amino groups in peptide bonds could be achieved by using a mixture of singly-labelled ^{13}C-carboxyl- and ^{15}N-amino-labelled amino acids. This would allow the observation of the slow-exchanging amide proton in the protein backbone, through the triple-resonance experiment, provided the overall molecular mobility is sufficient. This would allow the observation of protons exclusively within a protein, without significant interference from free amino acids.

The backbone resonances from a 20 kDa protein have been completely assigned by using a triple-resonance experiment (Kay *et al.* 1991). It might be possible to monitor the whole population of peptide bonds in proteins much larger than 20 kDa, since resolution is relatively unimportant if one is unconcerned with precise assignments. Labelling in this way could conceivably facilitate the direct observation of the population of $^{15}N/^{13}C$ double-labelled peptide bonds as they arose in the cell. This might give information about kinetics of protein turnover in the intact cell.

Labelling amino acid side groups may be more useful for ligand-binding studies since it is the side groups that play the greater rôle in protein-ligand interactions.

3.6.4.3 Uptake of a labelled protein into the cell

It may be possible to label a protein *in vitro* and cause its uptake into the cell. This has the benefit of allowing almost any labelling technique to be used, such as halogenation, acylation, radio- or other isotopic labelling, fluorophore-tagging etc. However, the delivery of the protein to the cell is much more challenging than for proteins produced by biosynthesis. Proteins may be taken up in some cell types by pinocytosis, or even introduced directly by microinjection.

This approach has been employed with a fluorinated glycoconjugate protein introduced into the bloodstream of rats. The label accumulates where the protein is catabolised, in the liver, and ^{19}F NMR can be used to follow protein turnover non-invasively (Daugherty *et al.* 1989).

3.6.5 Overall conclusions

The biosynthetic approach to labelling a protein offers a practical approach to labelling a single protein *in vivo*. The method also opens the possibility of engineering the expressed gene to include leader sequences to direct the labelled protein to a particular intracellular compartment. This would make possible experiments to compare the environment of a protein at different sites in the cell, perhaps to measure ligand concentration gradients, local motional restrictions, etc.

4 Direct observation of proteins in the intact cell

4.1 Introduction

Studying sub-microscopic cell components *in situ* has a long history. Natural chromophores, such as the cytochromes, have been studied in the intact cell for at least seventy years (Keilin 1925). Over 50 years ago, Millikan studied fibres of the leg muscles in cats and correlated the mechanical changes during contraction with rapid changes in the optical spectrum of haemoglobin (Millikan 1937).

More recently, Chance's group has performed time-resolved laser-based optical studies of myoglobin in muscle (Chance *et al.* 1988). They have also performed some elegant studies combining optical studies of the naturally occurring fluorophore, NADH, with simultaneous ^{31}P NMR observations to monitor the redox state and the phosphorylation potential in the gerbil brain (Gyubi *et al.* 1988).

Synthetic fluorophores, such as fluoroscein, have been introduced into cells to study intracellular ion concentrations and fluxes (Ross 1989; London 1991) and cytoplasmic viscosity (Dix and Verkman 1990). Some studies have been performed with luminescent probes, for example, the jellyfish-derived chemiluminescent calcium-binding protein, aequorin. The gene for this protein has been cloned and expressed in plant cells and used to study the intracellular calcium concentrations (Knight *et al.* 1991). In a patent application (Campbell 1990), the authors also suggest engineering aequorin

to be responsive to different ligands and to achieve localisation of the probe in different cellular compartments.

NMR-detectable probes could also be produced by protein engineering. Because the reporter group is a single atom that can be placed near a ligand-binding site, NMR probes may have greater sensitivity to changes in their environment than luminescent probes. They could also be detected in opaque tissues.

Optical studies are necessarily limited by the poor tissue penetration depth of the light used to study chromophores and fluorophores. Despite the exquisite sensitivity of some fluorophores, which enables them to be monitored even in single cells, this is a serious deficiency that limits the application of fluorescent and luminescent probes.

This confinement to studying cells in suspension or layers of cells near the surface of an organ is considerably relaxed for NMR, which can be used to study non-invasively the interiors of animals as large as adult humans (Radda 1986). Some of the calcium-sensitive fluorophores have been systematically modified to give NMR-detectable analogues, such as the "NMRophore" 5FBAPTA, used to study calcium transients in the heart (Kirschenlohr *et al.* 1988).

4.1.1 Precedents for the direct observation of proteins in the intact cell by NMR

There are some precedents for detecting assigned resonances from particular proteins in the intact cell by NMR. Resonances have been detected from the histidines of haemoglobin in erythrocytes (Brown *et al.* 1977), and of myoglobin in the intact human forearm (Jue and Anderson 1990; Wang *et al.* 1990). These cases are unusual in that the protein was observed in a cell

population naturally producing large quantities of a single protein, serendipitously one with groups that give characteristic NMR signals.

Ackerman's group has studied protein turnover *in vivo* by injecting a rat with labelled proteins and recording ^{19}F NMR spectra from the liver (Daugherty *et al.* 1989). The proteins are labelled with slowly-metabolised fluorinated glycoconjugates. These are termed "residualising labels" since they accumulate and can be observed in the tissue in which the protein to which they were attached was catabolised.

Although very important precedents for the study of proteins in the intact cell, none of these previous studies employed a method that could be generally applied to study a chosen protein *in situ* in a variety of cell types. The emphasis of the techniques developed here has been to widen the scope of non-invasive NMR applied to the study of proteins in the intact cell.

4.1.2 The nature of the fluorine–19 NMR spectrum

Fluorine was chosen as the labelling species for these studies because it can be detected in biological systems by NMR without interference from naturally-occurring background signals. The detection sensitivity of fluorine is relatively high, nearly as high as the proton. The chemical shift parameter of its NMR spectrum is very sensitive to subtle changes in its electronic environment. These and other reasons for choosing fluorine were examined in Chapter 3. A more detailed consideration of the electronic factors affecting the fluorine-19 NMR spectrum may help in understanding the spectra obtained from the labelled protein. Section 4.5 considers the interpretation of spectra in more detail.

The principal parameters that may be obtained from a fluorine-19 NMR experiment are the chemical shift, spin-lattice (T_1) and spin-spin (T_2)

relaxation time constants, the linewidths, the coupling constants and the nuclear Overhauser effect. Of these, the chemical shift is often the only readily-observed, accurately-determined parameter when studying a macromolecule in the intact cell, since it is less subject to the difficulties caused by the poor resolution and poor signal-to-noise ratios typical of spectra obtained *in vivo* (Gerig 1989).

Spectra from a given compound in a cellular sample are typically much poorer than from the same material in a simple solution. It is much more difficult to establish an homogeneous magnetic field across a cellular sample than across a simple liquid. A cellular sample inevitably contains many discontinuities and different environments with varying magnetic susceptibilities, and this causes artefactual line-broadening (Fabry and San George 1983). Other factors such as the presence of unchelated paramagnetic ions also contribute to the loss of resolution by increasing the relaxation rates and hence the linewidths. Information such as the fluorine-proton coupling constants is lost altogether, and the accuracy with which other parameters can be obtained is reduced.

The low concentration of fluorinated material in the intact cell makes it difficult to measure the T_1 and T_2 relaxation time constants, since the experiments can take longer to perform than the cells are capable of surviving. The measurement of the T_2 spin-spin relaxation time, which is inversely related to the rotational correlation time of the molecule, is also more challenging in the case of macromolecules. This is because the accurate assessment of the very short-lived signals (of the order of 1 to 10 ms) typically detected from macromolecules is much more difficult than for the relatively long-lived signals (of the order of 1 s) from small molecules.

Although the chemical shift is thus the only information that is likely to be obtained rapidly and reproducibly from a labelled protein in the intact cell, it is perhaps the most useful parameter. The range of chemical shifts observed for different fluorine species is unusually large, up to 800 ppm in all its ionic and molecular forms (Jenkins 1991). The fluorine of 5-fluorotryptophan showed a chemical shift dispersion of greater than 10 ppm at different sites within the *E.coli* galactose chemosensory protein (Luck and Falke 1991).

The theoretical basis for fluorine-19 chemical shifts has not been as well established as that for the proton and carbon-13, perhaps because less is known about the chemistry of the C-F bond than the C-H bond (Gerig 1989). Nevertheless, some important empirically-derived guidelines are available to help interpret chemical shift data from fluorine-19 NMR spectra.

The effects of proteins upon the chemical shifts of fluorinated (Gerig 1989) or phosphorylated (Kirk and Kuchel 1988) small molecules have been discussed. The shifts observed for protein-bound ligands are usually downfield of the free-ligand, but sometimes the direction of the change is different for fluorine and proton in the same position of the same molecule, emphasising the different electronic properties of these two nuclei.

These effects have been explained mainly in terms of altered patterns of hydrogen bonding, van der Waal's interactions, electrostatic interactions, dipolar interactions (including the effect of the α-helical dipole) and the presence of polar groups such as the carbonyl group or aromatic rings. It appears that the changes in the van der Waal's interactions associated with changes in the solvation shell around the fluorinated molecule are quantitatively the most important, and correctly predict that the chemical shift of an aqueous molecule will shift downfield as it is removed to a more hydrophobic environment on the protein surface.

4.2 Fluorotryptophan–labelled PGK studied in the intact cell

4.2.1 Experiments performed

4.2.1.1 Maintenance of the cells in a viable state during observations

Yeast cells were immobilised in fine agarose gel threads and perifused in the bore of the magnet as described in Chapter 2, the Materials and Methods section.

4.2.1.2 Manipulation of the metabolic state of the cells

Cells were mostly studied either while starved (perifused on a substrate-free medium) or supplied with glucose (an initial 50 mmoles of glucose in one litre of recirculating perifusion medium). These experiments were performed either aerobically or anaerobically, as indicated in the following Results section. Some experiments were also performed with cells perifused aerobically with a medium containing ethanol, initially at 2 % v/v.

4.2.2 Results obtained

4.2.2.1 The spectra observed

Fluorine-19 and phosphorus-31 NMR spectra were successfully obtained from the cells containing labelled PGK prepared and perifused as described. Typical fluorine-19 NMR spectra are shown in Figure 4.1. Typical phosphorus-31 spectra are shown Figure 4.2.

Note that the ^{31}P NMR spectra obtained from intact cells were all obtained in the absence of proton decoupling, since little advantage would be gained given that the lines are inherently so broad.

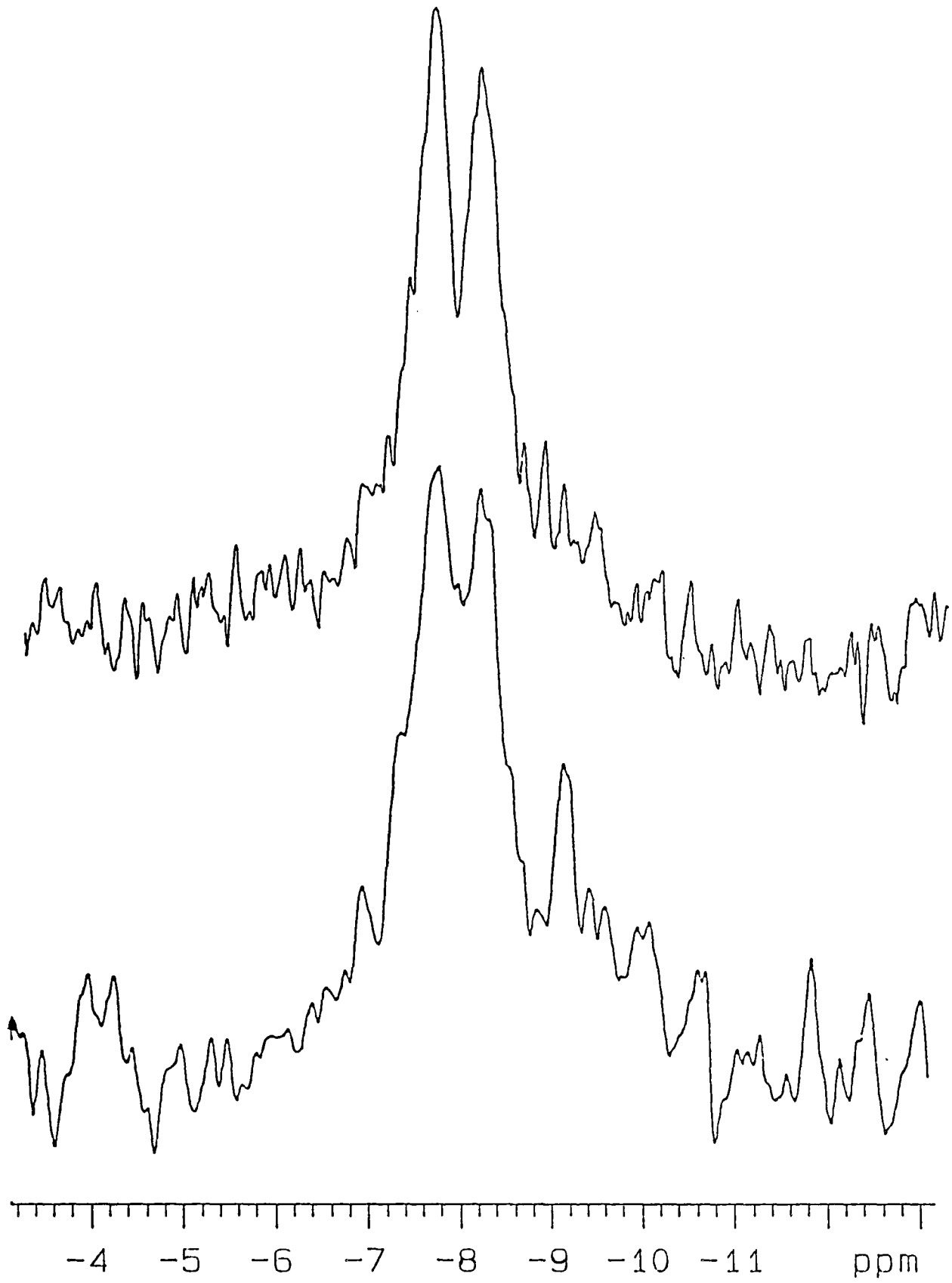

^{19}F NMR spectra of intact yeast cells containing 3-phosphoglycerate kinase labelled with 5-fluorotryptophan.

The spectra were acquired from 4 g cells perifused anaerobically at 30 °C with a 50 mM glucose solution. The interpulse delay was 0.67 s, the spectral width 12000 Hz. Both spectra are presented on the same scale and with 25 Hz exponential line broadening. The chemical shift scale is referred to aqueous *m*-fluorophenylalanine in a coaxial capillary at 0.0 ppm.

The top spectrum was obtained at 9.4 T (^{19}F resonance frequency 376 MHz) from cells of the BJ2168 strain. 2000 scans were accumaulated over 22 minutes. The cells contained approximately 300 μM labelled PGK in the cell water.

The bottom spectrum was obtained at 7 T (^{19}F resonance frequency 282 MHz) from cells of the FY3-1 strain. 24576 scans were accumulated over 4.5 hours. The cells contained approximately 100 μM labelled PGK in the cell water.

Figure 4.1

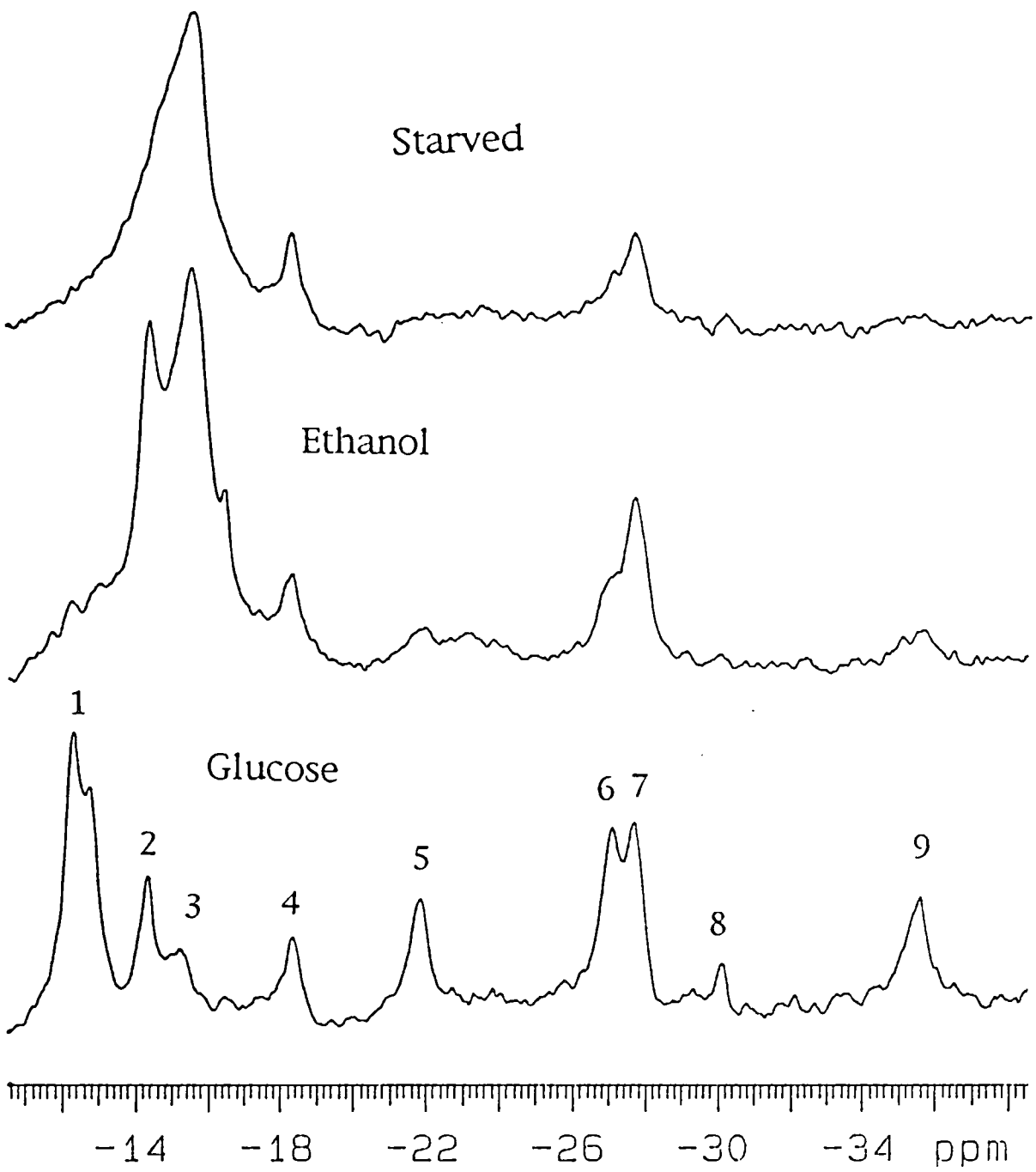

^{31}P NMR spectra of intact yeast cells under different metabolic conditions.
4 g cells were perifused at 30 °C with a medium containing glucose (bottom), ethanol (middle) or no substrate (top). The spectra were acquired with an interpulse delay of 5.4 s and a spectral width of 10000 Hz. 256 scans were collected over 23 minutes. All the spectra are presented on the same scale and are shown with 25 Hz exponential line broadening. The chemical shift values are quoted with reference to MDP at 0.0 ppm. The spectra were obtained from cells of the BJ2168 strain which were expressing high levels of 5-fluorotryptophan-labelled 3-phosphoglycerate kinase. The ethanol-fed cells were aerobic, the others anaerobic. The numbered peaks were assigned by reference to previous work (Brindle, K.M. (1988) Biochemistry 27: 6187-6196, and references therein)

1: phosphomonoesters (particuarly sugar phosphates), 2: cytoplasmic phosphate, 3: vacuolar phosphate, 4: phophodiesters 5: γ-NTP and β-NDP, 6: α-NTP and α-NDP 7: NAD(P)(H), 8: NDP-sugars, 9: β-NTP.

Figure 4.2

The fluorine-19 spectra showed reversible variations in the chemical shifts of the peaks observed depending on whether the cells were perifused with or without the glycolytic substrate glucose. These results are shown below in Tables 4.1 and 4.2 for the two different yeast strains and field strengths used.

A comparison of the ^{19}F NMR signal intensities observed in fully-relaxed spectra of the intact cells and of cell extracts showed that all of the fluorinated PGK was visible in the spectra recorded from the intact cells.

Table 4.1

Perifusion condition	*n*	Downfield PGK peak	Upfield PGK peak	Difference	Third peak
Glucose, 50 mM	5	7.76 ±0.06	8.25 ±0.07	0.49 ±0.09	9.16 ±0.03
Starved	3	7.78 ±0.10	8.06 ±0.06	0.28 ±0.11	9.18 ±0.01
Crude extract of starved cells	2	7.78	8.10	0.32	9.17
Dialysed crude extract	2	7.63	8.50	0.87	(absent)

Chemical shift positions in ppm for the peaks recorded from 5-fluorotryptophan-labelled PGK in intact yeast cells (FY3-1 strain), and in crude cell extracts.
The cells were perifused anaerobically either starved or with 50 mM glucose. The cell extracts were prepared by vortexing the cells with glass beads in 50 mM HEPES/100 mM K acetate/2 mM DTT, pH 7.5. This buffer was also used for dialysis. The NMR spectra were acquired as described in the legend to Figure 4.1. Chemical shifts are upfield from the external reference, p-fluorophenylalanine in a coaxial capillary, at 0.0 ppm. *n* is the number of experiments performed and the figures are means quoted with the standard deviations.

Table 4.2

Perifusion condition	*n*	Downfield PGK peak	Upfield PGK peak	Difference
Glucose, anaerobic	6	7.51 ±0.07	8.06 ±0.04	0.55 ±0.09
Glucose, aerobic	3	7.51 ±0.02	8.08 ±0.02	0.56 ±0.02
Ethanol, aerobic	4	7.57 ±0.04	7.98 ±0.05	0.41 ±0.06
Starved anaerobic	10	7.59 ±0.03	7.93 ±0.03	0.34 ±0.04
Crude extract of starved cells	2	7.58	8.30	0.72
Crude extract after ultrafiltration (30 kDa)	2	7.53	8.46	0.87

Chemical shift positions (ppm) of the peaks recorded from 5-fluorotryptophan-labelled PGK in intact yeast cells (BJ2168 strain), and in crude cell extracts.
The cells were perifused anaerobically either with 50 mM glucose or without any glycolytic substrate. The cell extracts were prepared by vortexing the cells with glass beads in 50 mM HEPES/135 mM K acetate/5 mM EDTA/2 mM DTT, pH 7.5. This buffer was also used for desalting the extract by ultrafiltration over an Amicon YM30 30 kDa membrane. The NMR spectra were acquired as described in the legend to Figure 4.1. Chemical shifts are upfield from p-fluorophenylalanine at 0 ppm. *n* is the number of experiments performed and the figures are means quoted with the standard deviations.

Examination of phosphorus-31 NMR spectra of the same cells showed that there were marked and reversible changes in the concentrations of the phosphorylated metabolites, particularly the nucleotide triphosphates, depending on whether the cells were starved or fed glucose. The concentration of NTP seen in glucose-fed cells was 2 to 3 mM (shown by HPLC of perchloric acid cell extracts to be approximately 80 % ATP, 20 % GTP). There was very little NTP apparent in the spectra of starved cells, too little to reliably quantitate.

4.2.2.2 *Differences between the two cell types*

The spectra obtained were very similar in the two cell types, but the third peak around 9.0 to 9.2 ppm (assigned to free fluorotryptophan or small protein fragments) was essentially absent in the spectra recorded from the BJ2168 cells. This may be because the BJ2168 cells carry mutations in the pathways of general proteolytic degradation (Adams 1989; Jones 1990a; Jones 1990b), perhaps slowing down starvation-induced protein turnover and hence the accumulation of proteolytic fragments of fluorinated PGK.

The signal-to-noise ratio attained in these BJ2168 spectra was much improved over that obtained with the FY3-1 cells. This was due to a combination of factors, but mostly because the cells contained more fluorotryptophan-labelled material to observe. Improvements in the construction of the probehead used for signal detection were also thought to have been important.

The increase in magnetic field strength used to obtain the spectra may also have been beneficial, although consideration of the effect of the chemical shift anisotropy phenomenon (CSA) might lead one to expect that, for fluorine-19, an increase in the field strength to 9.4 T would lead to poorer, not better, spectra than at 7 T. This is discussed further in section 4.5.

The changes in the fluorine-19 and phosphorus-31 NMR spectra that accompanied the change from a glucose-fed to a starved state were the same in both cell types.

The relatively small differences in the absolute chemical shift values presumably reflects differences in the magnetic susceptibility. To study changes in the environment of labelled PGK, it seems most appropriate to examine the chemical shift difference between the upfield and downfield peaks rather than their absolute position.

The concentrations of paramagnetic ions such as Mn^{2+} and the magnetic susceptibilities of the two cell types may be different, as the concentration of polyphosphate is very different in the two cell types. The loss of vacuolar polyphosphates may be associated with the escape of metal ions, ordinarily bound to the vacuolar polyphosphate (Klionsky *et al.* 1990), from the vacuole into the cytoplasm.

4.2.2.3 The linewidths of the peaks

The half-height linewidths of the peaks were measured by fitting Lorentzian lines to the experimental spectra with the utility software provided with the NMR instrument. The data are discussed in section 4.5.

4.3 Fluorotryptophan–labelled pyruvate kinase

4.3.1 Experiments performed

Experiments were performed as described for the PGK-producing cells in section 4.2.1.

4.3.2 Results obtained

4.3.2.1 The failure to observe labelled pyruvate kinase in the intact cell

It proved impossible to record fluorine-19 NMR spectra from 5-fluorotryptophan-labelled pyruvate kinase in the intact cell under conditions in which labelled PGK was clearly visible in similar cells. The BJ2168 cells used contained approximately 0.5 mM pyruvate kinase subunits, each with one tryptophan residue. A signal was easily detected *in vitro* from cell lysates and from pyruvate kinase partially purified from the same batches of cells used for the perifusion experiments.

The fractional labelling estimated from enzyme assays and fully-relaxed NMR spectra was high, about 70 %. The PK gave a single peak *in vitro*, at about 10 ppm upfield of fluorophenylalanine. The chemical shift of the peak changed by approximately 1 ppm in response to millimolar amounts of the allosteric effector fructose-1,6-bisphosphate. Spectra from the labelled pyruvate kinase *in vitro* are shown in Figure 4.4.

4.3.2.2 *Possible explanations*

Sequence-derived MW is 210 kDa

Yeast PK exists as a homotetramer of molecular weight c. 210 to 240 kDa (Murcott *et al.* 1991), and it was thought that the loss of visibility in the cell was due to protein immobilisation or simple viscosity effects. Both these factors would increase the rotational correlation time of the PK, broadening the NMR signal from the 5-fluorotryptophan label. This is discussed further in section 4.5.1. In muscle cells, pyruvate kinase is thought to associate with the cytoskeleton even at high ionic strength (Walsh and Knull 1987; Shearwin and Masters 1990; Shearwin *et al.* 1990).

The effect of viscosity on visibility was investigated using labelled PGK and pyruvate kinase studied *in vitro*. Labelled PGK (45 kDa) was studied *in vitro* at the rotational correlation time expected for labelled pyruvate kinase (240 kDa) in the cell. The solvent viscosity was increased with glycerol until the PGK correlation time *in vitro* was the same as that of pyruvate kinase *in vivo*, assuming the intracellular viscosity is 1.9, relative to physiological saline (Endre *et al.* 1983).

The rotational correlation time for a spherical molecule, τ_c, is given by the Stokes-Einstein relation (Van Holde 1971).

$$\tau_c = 8\pi a^3 \eta / 6kT \qquad \text{(Eq. 4.1)}$$

where a is the Stokes radius, η is the viscosity, k is Boltzmann's constant and T is the temperature in Kelvins. This is equivalent to

$$\tau_c = V\eta / kT \qquad \text{(Eq. 4.2)}$$

where V is the volume of the spherical molecule.

The rotational correlation time of PGK *in vitro* is thus increased to the same value as that expected of PK *in vivo* when the relative viscosity of the medium *in vitro* is 10.1 (240/45 x 1.9), assuming both proteins are globular and their molecular weights are proportional to the cube of their radii. 59 % glycerol was used to achieve the desired viscosity at 30 °C (CRC Handbook 1978).

The resultant spectra are shown in Figure 4.3. The spectra shown contain some distortion, evident where the peaks become asymmetric near their bases. This is caused by the first few points of the free induction decay being artefactually high. The problem may arise from fluorine compounds present in the probe. Increasing the delay between the pulse and collecting the first data point, removal of the first few points from the data set, or replacing the first few points with data calculated from the rest of the data set (linear prediction) improves the spectra but does not eliminate the problem entirely. A very short (200 μs) spin-echo sequence does cure the problem, however, supporting the idea that the problem arises from solid fluorine compounds, perhaps Teflon™. Although a commercial "$^{1}H/^{19}F$" probe, it is clearly not perfect when used for detection at the high gain settings used in these experiments.

The effect of temperature on the visibility of isolated pyruvate kinase in solution was also examined. Spectra were collected in a buffer containing 20 % glycerol at 25, 35 and 45 °C. The spectra collected are shown in Figure 4.4. The effect of temperature on τ_c directly and on τ_c through changing the viscosity have been calculated, and this experiment is equivalent to observing

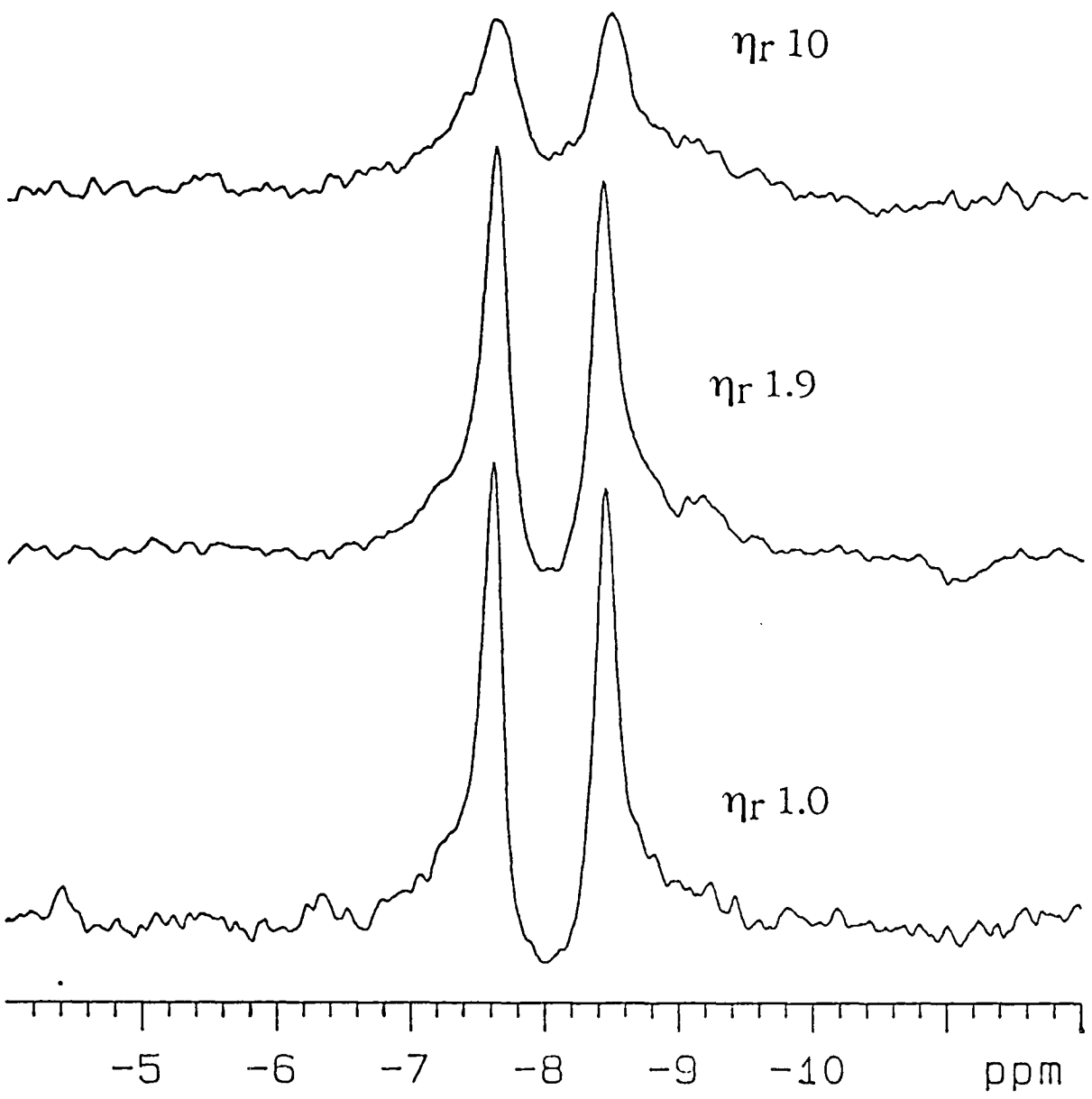

^{19}F NMR spectra of 5-fluorotryptophan-labelled 3-phosphoglycerate kinase in media of different viscosity.
Samples of PGK were studied at 30 °C in aqueous solutions with varying concentrations of glycerol to alter the solution viscosity. The spectra were acquired at viscosities relative to water of 1 (bottom), 1.9 (middle) and 10 (top). These values represent lower and upper limits of the cytoplasmic viscosity (see text). The acquisition employed a 0.67 s interpulse delay, a 9000 Hz spectral width and a pulse angle of 65°. The top two spectra were from 5000 scans accumulated over 56 minutes. The bottom spectrum was from 2000 scans accumulated over 22 minutes. The samples for the top two spectra contained approximatly 30 mg/ml PGK. The sample for the bottom spectrum contained approximately 20 mg/ml PGK. The spectral distortion, evident at the bases of the peaks, arose from fluorinated materials in the NMR probe itself. The distortion can be eliminated by collecting the spectra with a very short (200 μs) spin echo sequence. The spectra have been presented on the basis of equal peak areas, determined by weighing peaks cut from plots of the spectra.

Figure 4.3

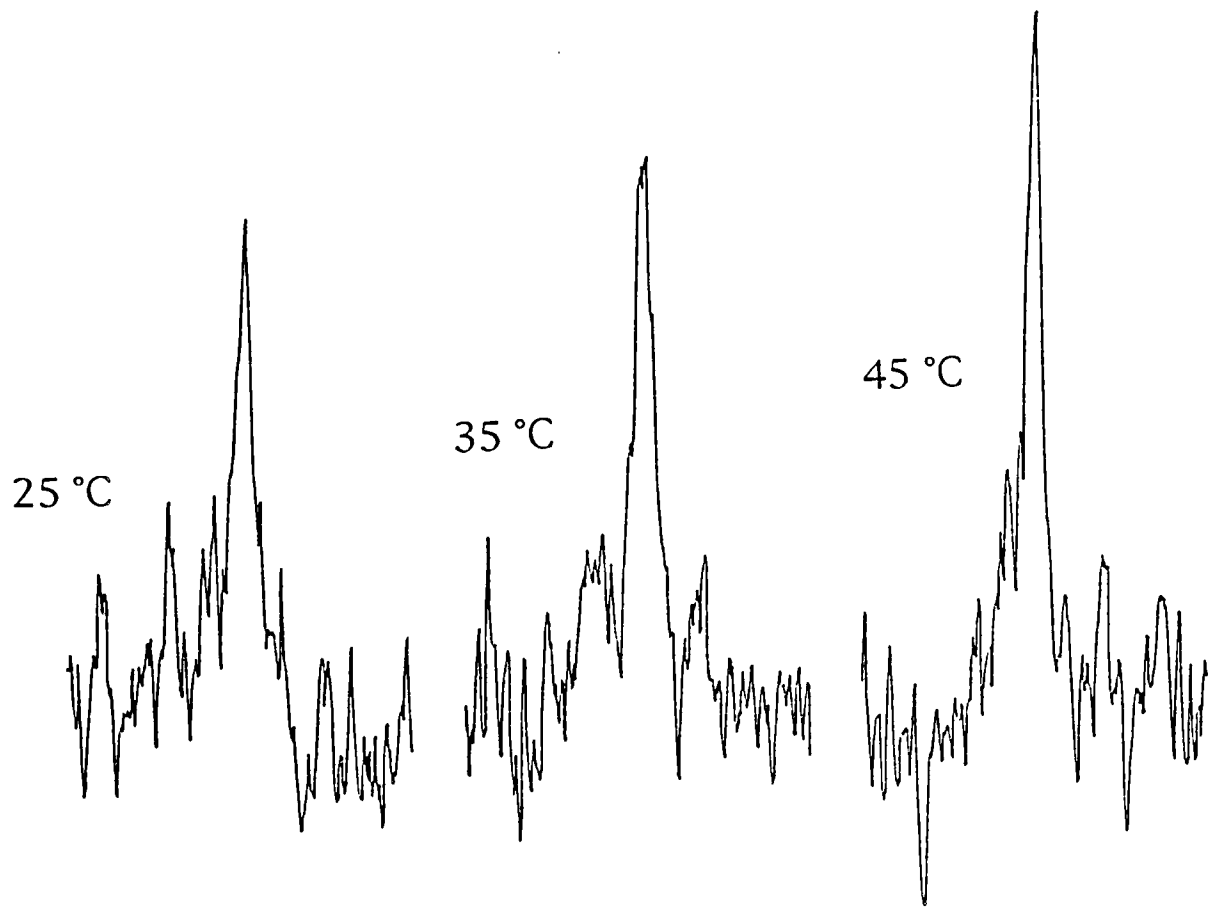

^{19}F NMR spectra of 5-fluorotryptophan-labelled pyruvate kinase at different temperatures.
Spectra were collected at 25, 35 and 45 °C from a solution of labelled pyruvate kinase in a buffer containing 20 % v/v glycerol. The interpulse delay was 0.67 s, the spectral width 12000 Hz. The spectra were collected sequentially with 16000 scans collected over three hours at each temperature. The spectra are displayed on the same scale.

Figure 4.4

PK at 30 °C in media with viscosities relative to saline of 2.2, 1.7 and 1.3 respectively. The calculations assume that the viscosity of the glycerol solution changes with temperature in the same way as does water, i.e. the viscosities (relative to that at 30 °C) at 25, 35 and 45 °C are 1.12, 0.90 and 0.75 respectively (CRC Handbook 1978).

These experiments showed that the resonance peaks from pyruvate kinase *in vivo* would be significantly broader than those from PGK (which is clearly visible in the cell), so the signal to noise ratios attained in a typical 5 hour cell perifusion experiment would be much poorer than for PGK under the same conditions. The failure to observe pyruvate kinase *in vivo* may then reflect the cytoplasmic relative viscosity if it is much higher than the lower estimate of 1.9, but the possibility that PK is subject to further restriction of motion, perhaps by binding to other proteins, has not been excluded.

4.4 Interpretation of the spectra seen in the intact cell

4.4.1 ^{19}F NMR peak assignments

The peaks seen in the fluorine spectra were tentatively assigned from their chemical shifts and their behaviour under different metabolic conditions. Figure 4.5 shows the relative dispositions of the two tryptophan residues, and Figure 4.6 is a colour plate showing the tryptophan residues in the context of the whole protein. In both cases, the data are from the crystal structure (Watson *et al.* 1982). The distances marked on Figure 4.5 are those measured from the proton on carbon 5 of the indole ring to the effective electronic centre of the adenine ring (Giessner-Prettre and Pullman 1970).

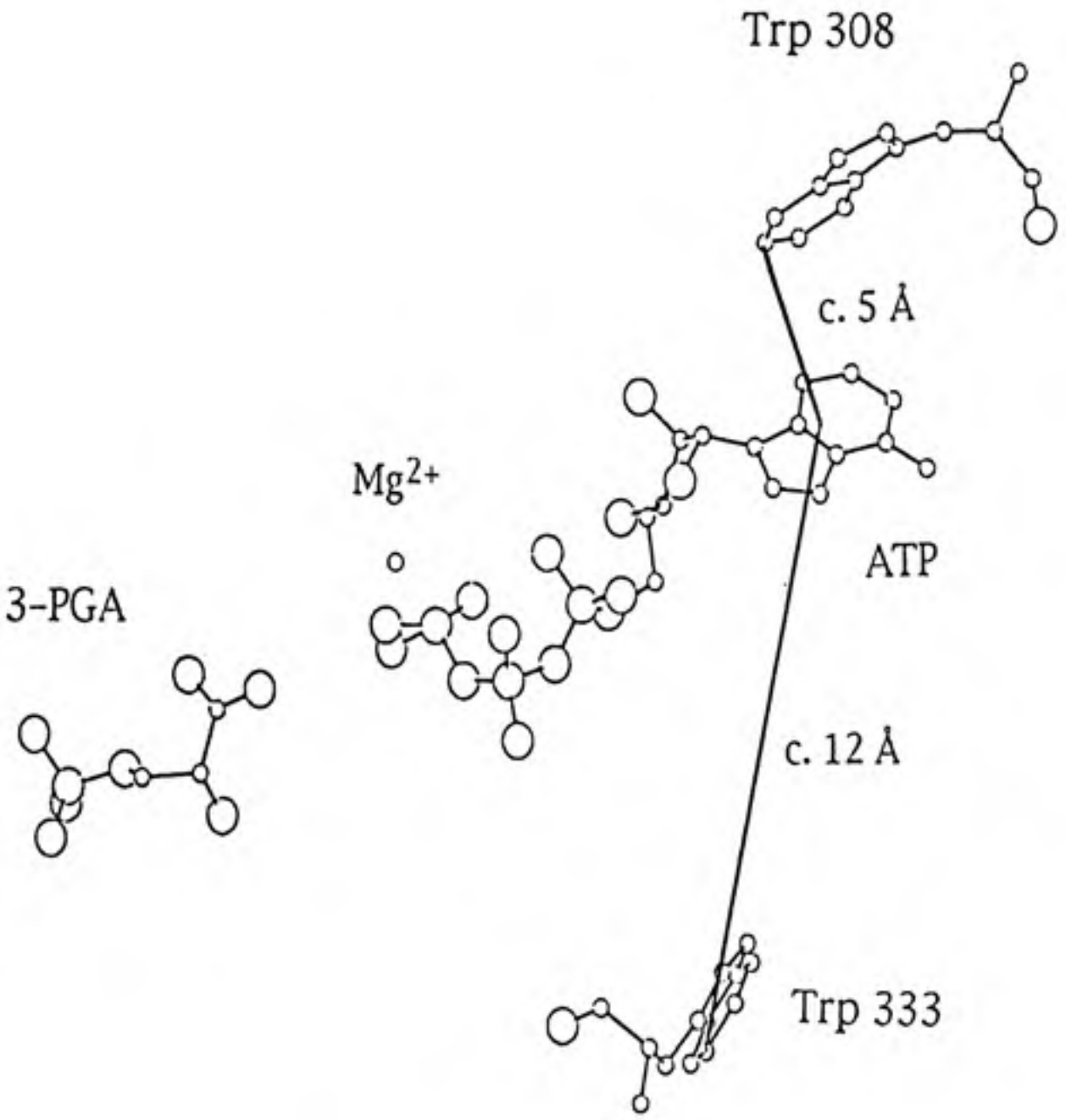

The relative positions of the two tryptophans and the substrate ligands of yeast 3-phosphoglycerate kinase.
The positions of the groups shown have been taken from the crystal structure published by Watson *et al* (1982)(see text). The structure was obtained from a copy of the Brookhaven protein data bank at the SERC Daresbury laboratory. The model was generated by Polygen's Quanta software running on a Silicon Graphics Power Series computer. The distances marked are from the proton on carbon-5 of the indole ring to the effective electronic centre of the adenine ring (see text).

Figure 4.5

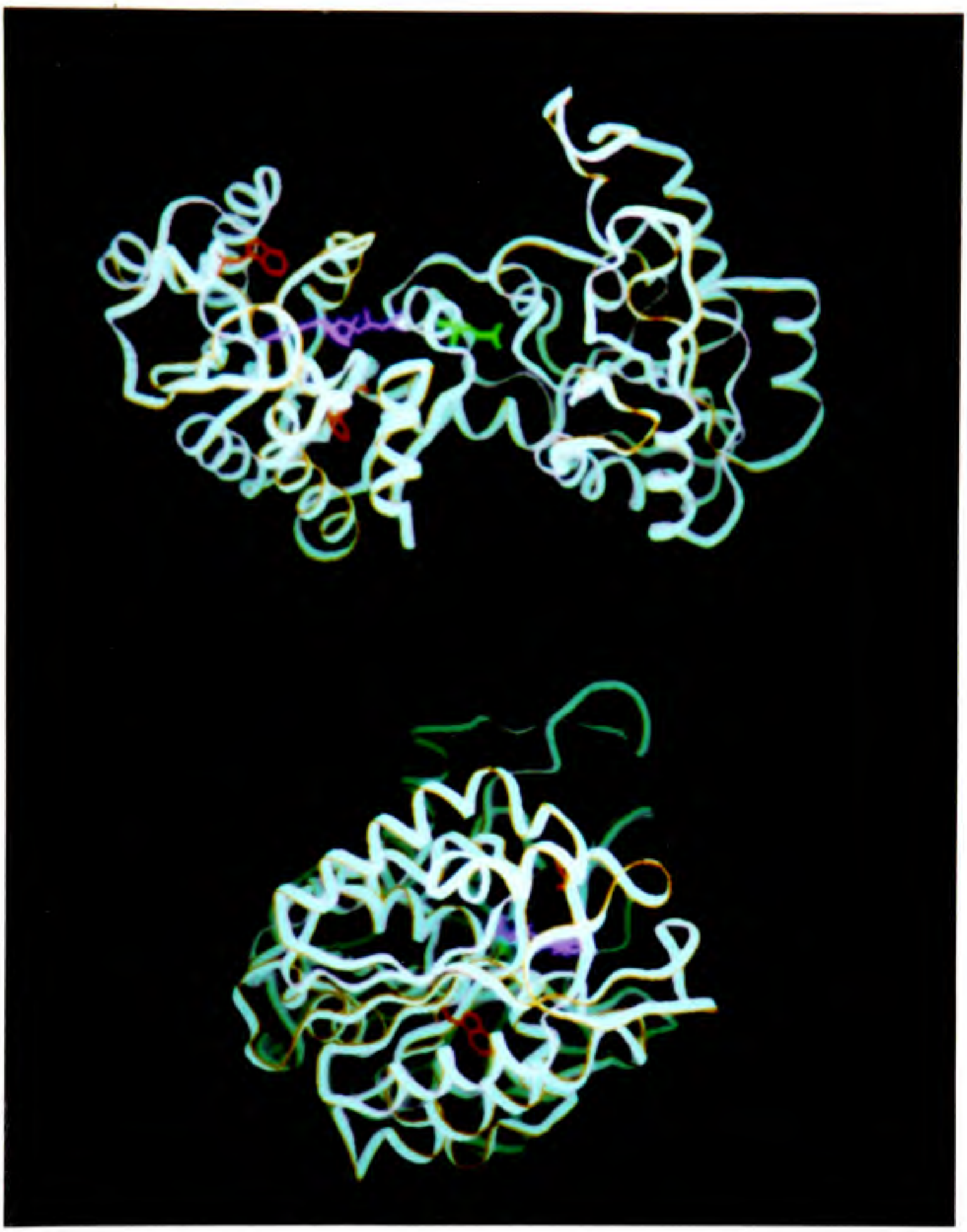

Two views of yeast 3-phosphoglycerate kinase, showing the positions of the two tryptophans and the substrate ligands
The model is based on the crystal structure (Watson *et al.* 1982). The structure was obtained from a copy of the Brookhaven protein data bank at the SERC Daresbury laboratory. The model was generated by Polygen's Quanta software running on a Silicon Graphics Power Series computer. The colour-coding of the relevant groups shown is: red - tryptophan; purple - ATP; bright green - 3-phosphoglycerate; yellow - Mg^{2+}. The bottom view is end-on looking at the C-terminal domain. The top view shows the disposition of the relevant groups more clearly; the C-terminal domain is on the left. The upper of the two (red) tryptophans is Trp 308. Carbon-5 is at approximately "5 o'clock" on the 6-ring as shown. The plane of the adenine ring, at the left of the ATP as shown, is perpendicular to the page.

Figure 4.6

4.4.1.1 *The downfield peaks 7.5 to 8.3 ppm*

Similar spectra were recorded from the intact cells of yeast strains FY3-1 and BJ2168, and from lysates of these cells and of the yeast strain DBY745 (a preliminary experiment described in Chapter 3). In each case, the two peaks around 7.5 to 8 ppm were assigned to the two fluorotryptophans of the fluorinated PGK.

The material causing the peaks around 7.5 to 8 ppm was retained during dialysis or ultrafiltration and had PGK enzymatic activity. It was protein-like in that it was precipitated by perchloric acid and by ammonium sulphate in the 50 to 75 % saturation band at pH 7.5 (Deutscher 1990). The two peaks around 7.5 to 8 ppm only appeared when PGK production was induced in the presence of fluorotryptophan, and the signals were only detectable when PGK had been significantly induced in the presence of fluorotryptophan. A control experiment using the plasmid pMA301-1 to induce low levels of interferon in the presence of fluorotryptophan resulted in cells from which no fluorine-19 NMR signals could be detected.

The downfield protein peak around 7.5 to 7.7 ppm was tentatively assigned to Trp 333, that lies in the C-terminal domain of the protein. The range of chemical shifts exhibited by this peak was smaller than that of the other peak. This suggested that this peak corresponded to the tryptophan less exposed to solvent and more distant from the ligand binding site. The fluorine on carbon 5 of the indole ring lies about 12 Å from the centre of the adenine ring of ATP when it is bound.

The upfield protein peak around 8.0 to 8.3 ppm was tentatively assigned to Trp 308, that lies close to the nucleotide-binding region of the protein partly exposed to the solvent. The fluorine on carbon 5 of the indole ring lies about 5 Å from the centre of the adenine ring of bound ATP, with the phosphate

groups stretching further away from the indole. The position of this peak was more responsive to changes in the cell. This suggested that this peak corresponded to the tryptophan more exposed to solvent and closer to the ligand binding site.

Definitive peak assignments can perhaps best be made by studying a mutant enzyme that has only one or the other tryptophan, which is easily feasible with the techniques of protein engineering and site-directed mutagenesis. This approach has been used before with the *lac* repressor protein (Jarema *et al.* 1981) and lactate dehydrogenase (Rule *et al.* 1987). Mutants of PGK with one or the other tryptophan substituted by a different residue have been prepared by Jennifer Littlechild and co-workers (Jennifer Littlechild, Exeter, personal communication), and these will be used to produce definitive assignments.

4.4.1.2 The upfield peak around 9 ppm

The material causing the peak around 9 ppm has not been definitively assigned, but some experiments have been carried out to try to limit the range of possibilities. It was lost from the cell lysate following dialysis or ultrafiltration, but was not precipitated by 75 % ammonium sulphate or by perchloric acid, which would be expected to precipitate proteins (Deutscher 1990). The relatively upfield chemical shift corresponds to a very polar, water-like environment (see Table 4.3), and the presence of this signal did not correlate with the amount of PGK present in the cells, so it did not seem to arise from PGK protein. All this suggests that the peak arises from free fluorotryptophan or a small peptide containing fluorotryptophan.

Some experiments were carried out with pure 5-fluorotryptophan to establish the range of chemical shifts shown by that compound in different solvents. These data are presented in Table 4.3.

Table 4.3

Solvent description	Chemical shift from FPhe, ppm
Water, H_2O	9.16
Heavy water, D_2O	9.13
Water/methanol 50/50 %	10.05
Methanol	10.87
Ethanol	10.43
iso-Propanol	10.00
n-Butanol	9.77
2M guanidinium chloride, pH 6.5	9.18
MES/HCl, pH 2.0	9.04
Phosphate buffer, 0.1M, pH 7.0	9.16
Borate/KOH buffer, pH 10.1	9.57

The chemical shifts of 5-fluorotryptophan in different solvents
A solution of 5-fluorotryptophan, at an arbitrary concentration between 1 and 10 mM, was prepared in each of the solvents listed in the table. The chemical shift of the FTrp peak seen in the ^{19}F NMR spectrum is upfield of external fluorophenylalanine at 0.0 ppm.

This confirmed that the ^{19}F NMR chemical shift of aqueous 5-fluorotryptophan is similar to that of the upfield peak seen in the cells and cell lysates at around 9 ppm from the FPhe reference. It also emphasised the effect of the solvent on the chemical shift, and suggested that the pH and ionic strength are relatively unimportant. Note that none of these chemical shifts are close to the 7.5 ppm shift seen from fluorotryptophan in PGK.

The large shift seen in going from water to methanol through a water/methanol mixture presumably reflects substantial changes occurring in the organisation of the solvation shell. Once a non-aqueous pattern of solvation is established, the trend from methanol to butanol shows the expected move downfield as the hydrophobicity of the environment increases.

A simple chromatographic procedure was used to help characterise the behaviour of the material responsible for the peak around 9 ppm. The experiments used BJ2168 cells from a batch that exhibited a large peak around 9 ppm, and in which the assayed PGK concentrations were in decline, presumably a factor linked to the appearance of the peak around 9 ppm. The experiments used a C_{18} alkylated resin in a batchwise reverse-phase separation.

Neutralised perchloric acid cell extracts were passed through a Waters C_{18} BondPak™ cartridge, that was then eluted with 70 % aqueous acetonitrile. It is expected that small peptides, c. 5 to 10 amino acids, will bind to the resin in aqueous solvents and be eluted by the acetonitrile (Martin Humphries, Manchester, personal communication). This stepwise elution is commonly used to free synthetic peptides of amino acid impurities. Control experiments with pure 5-fluorotryptophan added to the cell extract or dissolved in a HEPES buffer were carried out in order to validate the procedure. The aqueous run-through and the acetonitrile eluate materials were examined by fluorine-19 NMR to quantitate the 9 ppm peak. The results are shown in Table 4.4.

Table 4.4

Starting material	Sample examined by fluorine-19 NMR	Signal intensity %	Relative signal intensity
1*	original cell extract - solution 1	100	100
	extract after passage through C_{18} cartridge	5	
	acetonitrile eluate of C18 cartridge	85	
2*	original solution 2	100	1650
	solution after passage through C_{18} cartridges	48	
	acetonitrile eluate of C_{18} cartridge	62	
3*	original solution 3	100	290
	solution after passage through C_{18} cartridge	13	
	acetonitrile eluate of C_{18} cartridge	64	

Reverse-phase C_{18} absorption/elution experiments to examine the nature of the material causing the peak around 9 ppm in the ^{19}F NMR spectrum of BJ2168 cells and cell lysates.

* The starting materials were

1) a neutralised PCA extract of 5g of cells
2) run-through eluate from (1) spiked with FTrp to 1 mM
3) HEPES/NaCl buffer containing 100 μM FTrp, pH 7.3.

Neutralised PCA extracts were prepared and diluted to 20 ml with 50 mM HEPES/133 mM NaCl, pH 7.3. These extracts were passed through two 1 ml volume C_{18} cartridges. The cartridges were eluted with 20 ml 70 % acetonitrile. The first eluate was spiked with FTrp to 1 mM and then processed again. The material in the all the solutions had the same chemical shift as added pure 5-FTrp. A control experiment with 20 ml of a 100 μM FTrp solution in the buffer was also performed with one C_{18} cartridge. The intensities in acetonitrile have been multiplied by an experimentally-determined saturation factor of 1.54 to allow direct comparisons of the intensities, necessary because the spectra were not collected under fully-relaxed conditions.

The simple experiments shown in Table 4.4 are inconclusive because the column capacity may have been exceeded in the control experiments (set 2). The experiments have not yet been repeated. The behaviour of the material in the cell extract, mostly binding to the C_{18} resin, is like that expected of a

peptide rather than a free amino acid. However, pure FTrp in a HEPES buffer shows a similar behaviour under the conditions used.

Further, more detailed, analysis of the material in the cell extracts is necessary to fully characterise the material or materials that cause the peak around 9 ppm in the NMR spectra. At present, the material seems likely to be free fluorotryptophan, but may be a small peptide.

4.4.2 The changes in the ^{19}F spectra

There are two important changes that occur in the fluorine-19 NMR spectra of the intact cell. The first concerns the chemical shift positions of the two peaks of fluorotryptophan-labelled PGK, while the second concerns the presence or absence of the upfield peak at around 9 ppm.

4.4.2.1 The two peaks of labelled PGK

The changes in the chemical shifts of the two peaks are caused by changes in the local environment of the fluorine nuclei, either through the proximity of a ligand or solvent molecule, or through a conformational change in the protein. In fed cells, the peaks from the two tryptophans are relatively well-resolved and about 0.6 ppm apart. In starved cells, the peaks are only about 0.3 ppm apart and they considerably overlap one another. These reversible changes in the spectra reflect metabolic changes in the cell upon starvation, and are illustrated in Figure 4.7.

The ligands of PGK are all phosphorylated and include the very important metabolite ATP. It was thus expected that ^{31}P NMR would provide some useful information about the changes occurring within the cell that accompanies the changes seen in the ^{19}F NMR spectra (see Figure 4.2).

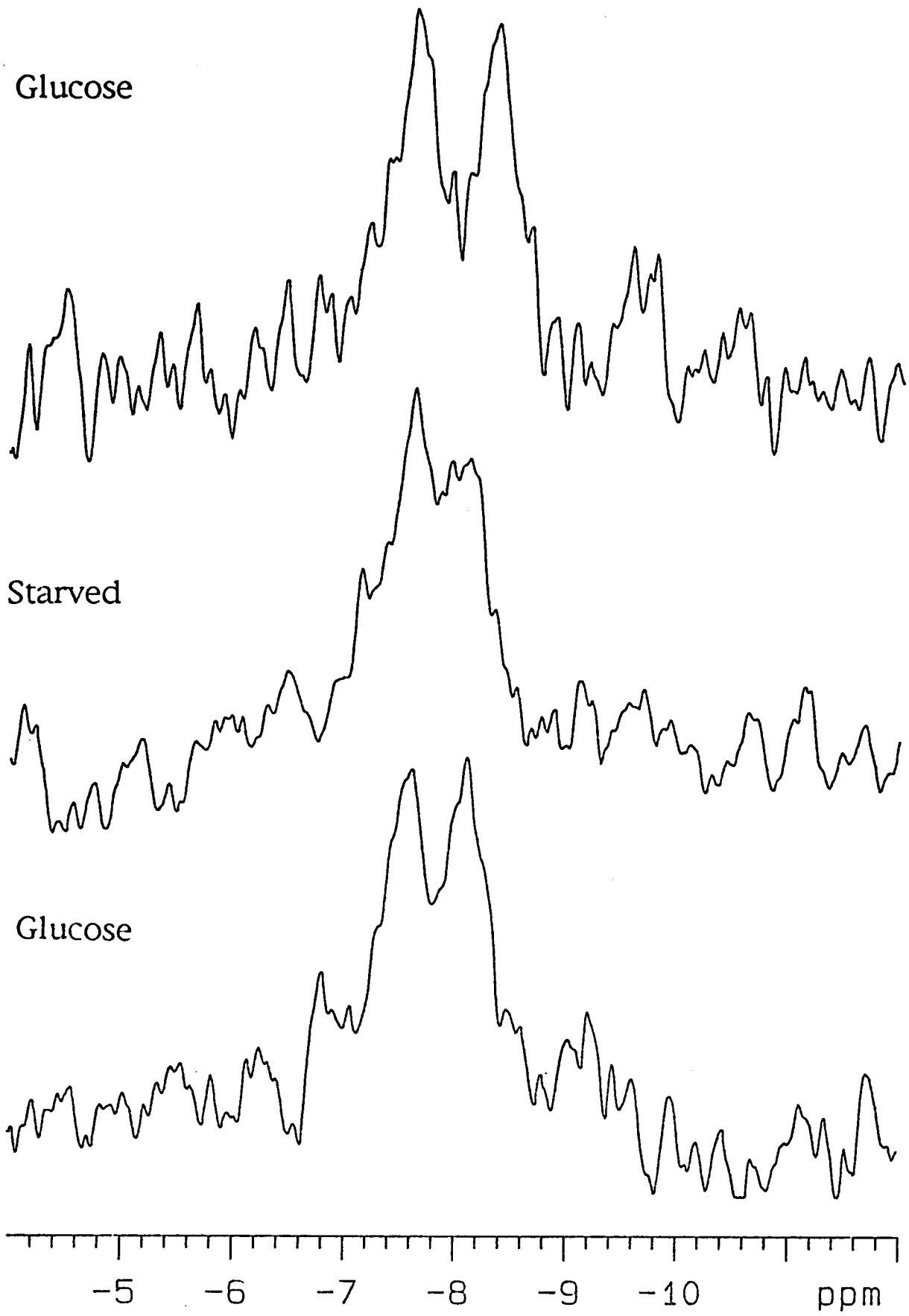

A series of ^{19}F NMR spectra collected from cells perifused first with glucose (bottom), then starved (middle) and then with glucose again (top)

4 g of cells containing 5-fluorotryptophan-labelled 3-phosphoglycerate kinase were perifused at 30 °C. The BJ2168 cells used contained approximately 150 μM labelled PGK. The interpulse delay was 0.67 s, the spectral window 6000 Hz. The cells were perifused with 100 mM glucose for 1 hour, then the first spectrum acquired as 10000 scans over the next two hours. The cells were switched to a substrate-free medium and perifused for an hour before collecting the next spectrum. Lastly, the process was repeated with a medium containing 50 mM glucose.

Figure 4.7

Experiments have been carried out with purified labelled PGK to characterise the relationships between the fluorine chemical shifts and the concentrations of various metabolites. These experiments are the subject of Chapter 5.

4.4.2.2 The upfield peak around 9 ppm

In the FY3-1 cells, the intensity of this peak was very much greater in starved cells than in fed cells. Its magnitude increased at the expense of the PGK peaks during starvation and declined without a change in the PGK peak intensities on re-feeding with glucose, i.e. it appeared to wash out of the cells. It may be that this reflects starvation-induced protein turnover, which occurs on a time scale consistent with the changes in peak intensity, that is a protein half-life of the order of two hours (Bachmair *et al.* 1986; Dice 1987; Chiang and Schekman 1991).

4.4.3 ^{31}P NMR spectra

With both cell types, the principal difference between the starved and fed cells is the absence from the starved cells of sugar phosphates and NTP. There are some other differences, such as the accumulation of P_i in the cytoplasm and in the vacuole.

Perchloric acid cell extracts show that there is some residual ATP in starved cells, approximately 0.5 to 0.7 mM. One might expect to see a signal from a metabolite at this concentration in the intact cell, yet this ATP in the starved cells is not apparent. The signal-to-noise ratio in the spectra from the intact cells prevents one from conclusively ruling out the presence of a broad signal of the correct magnitude, however (see Figure 4.2). Representative ^{31}P NMR spectra of cell extracts are shown in Figure 4.8. Note that all the ^{31}P NMR spectra from cell extracts were obtained with broadband WALTZ-16 proton decoupling (Shaka *et al.* 1983).

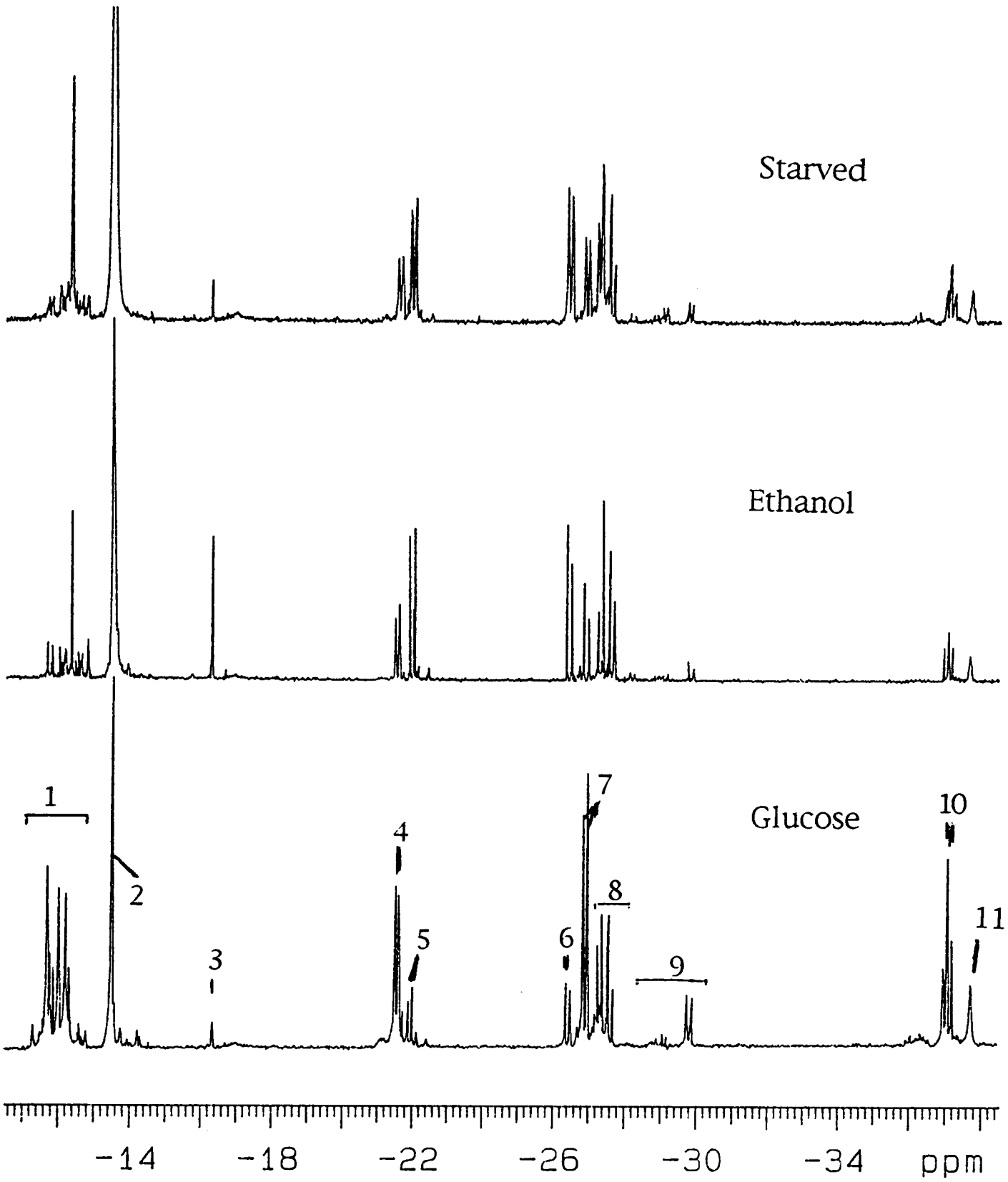

^{31}P NMR spectra of perchloric acid extracts of BJ2168 cells perifused under different metabolic conditions.
Cells were perifused with glucose (bottom), ethanol (middle) or no substrate (top). The lyophilised extracts were reconstituted and examined in a triethanolamine buffer at pH 8.0. ^{31}P NMR spectra were obtained at 30 °C with WALTZ-16 ^{1}H proton decoupling. The interpulse delay was 4.5 s, the pulse angle 60°. The spectral window was 10000 Hz. The spectra are presented on the same scale. The peak assignments have been made with reference to previously published work (Navon *et al.* (1979) Biochemistry 21: 4487-4499) as follows

1: phosphomonoesters (particuarly sugar phosphates), 2: inorganic phosphate, 3: phophodiesters (particularly ethanolamine derivatives), 4: γ-NTP, 5: β-NDP, 6: α-NDP, 7: α-NTP 8: NAD^+, 9: diphosphodiesters (particularly NDP–sugars), 10: β-NTP, 11: polyphosphate inner residues.

Figure 4.8

This observation is consistent with the residual ATP being partly immobilised by viscous or protein-binding effects, perhaps because it is a pool localised within the mitochondria. A similar observation has been made in ischemic rat liver, where cytosolic ATP is depleted leaving an NMR-invisible mitochondrial pool of around 0.8 μmol/g wet weight liver (Murphy *et al.* 1988). There has long been a debate about the NMR observability of ADP, which may become invisible by binding to actin in muscle or by other forms of compartmentation in kidney and liver (Gadian 1982; Iles *et al.* 1982; Stubbs *et al.* 1984; Desmoulin *et al.* 1987).

A comparison of the spectra of the starved and ethanol-fed cells *in vivo* (Figure 4.2) and *in vitro* (Figure 4.8) shows that there is, apparently, greater visibility *in vivo* of the small amount of ATP present in the ethanol-fed as opposed to the starved cells. It might be interesting to determine whether or not this observation was significantly reproducible, and, if so, if it reflects any difference in the compartmentalisation of the ATP in the ethanol-fed aerobic as opposed to the starved anaerobic cells.

4.5 NMR spectra and molecular motion

4.5.1 NMR and relaxation

4.5.1.1 General principles

The NMR spectrum arises from the observation of nuclear spin transitions as the system relaxes back to equilibrium after a perturbation. The peak intensity depends on the number of transitions. The width of a peak in the NMR spectrum ideally depends only on the relaxation parameters for these nuclear spin transitions. In experimental NMR, especially with biological samples, the complications of imperfect magnet homogeneity and especially

imperfect sample homogeneity can dominate the linewidths. Nevertheless, the analysis of the lineshapes and determination of the relaxation time constants can provide useful information about the mobility and environment of a molecule (Sanders and Hunter 1987).

The nuclei of a sample of spin-1/2 nuclei (such as ^{1}H or ^{19}F) at thermal equilibrium in a magnetic field will have a net magnetic moment aligned with the magnetic field. This is conventionally denoted M_0, the equilibrium net z axis magnetisation. The spin of each nucleus will be in one of the two allowed quantised spin states, "high" or "low", precessing around the z axis (the direction of the field). The population of nuclear magnetic moments will be randomly distributed in the xy plane, and thus there is no net magnetisation in the xy plane.

The NMR experiment perturbs the equilibrium by applying an oscillating radio frequency magnetic field perpendicular to the z axis, causing the nuclear magnetic moments to precess about that field and the net magnetisation to "tip" into the xy plane. The intensity of the NMR signal depends on the magnitude of the projection of the net magnetisation vector in the xy plane. The net magnetisation decays both within the xy plane and returns to the z axis, according to processes that are usually modelled by exponential decay processes.

The T_1 relaxation processes result in the return of the net magnetisation to the z-axis. The most important processes governing the rate of this process are dipole-dipole interactions between the relaxing nuclei and the fluctuating magnetic fields around them in the sample. The relaxation is at its most effective when the fluctuating field is at the nuclear spin transition frequency, the Larmor frequency ω_0. This can be achieved if the relaxing molecule is tumbling in space at a frequency equal to ω_0, i.e. when $1/\omega_0 = \tau_c$, the

molecule's average rotational correlation time. When the condition $\omega_o = 1/\tau_c$ is met, the T_1 time constant is at a minimum. When the correlation rate ($1/\tau_c$) and ω_o are mismatched, the relaxation process will be less efficient and the relaxation time constant T_1 will be longer.

The T_2 relaxation processes result in the loss of net magnetisation in the xy plane as the components of the net vector become progressively more incoherent. These processes are the result of interactions along all three axes, and include dipolar interactions as for T_1. They can include additional low-frequency interactions such as chemical exchange or diffusion, and these additional processes imply that the T_2 processes are at least as fast as the T_1 processes, or in terms of the time constants $T_2 \leq T_1$. In a protein, concerted movements of different domains relative to one another can contribute to these relatively slow processes.

The fact that low frequency interactions are involved in T_2 processes means that they continue to become more efficient as the molecule tumbles more slowly; there is no value of τ_c for which the T_2 time constant is minimised. T_2 continues to decline with increasing correlation time, so that large molecules such as proteins typically have short T_2 time constants while having relatively long T_1 values. With small molecules tumbling much more rapidly than the Larmor frequency, i.e. when $\omega_o\tau_c << 1$, the T_2 processes are relatively inefficient and the time constants T_1 and T_2 are nearly equal.

The theory associating linewidths, nuclear relaxation parameters and molecular motion is well-developed for some spin-1/2 nuclei such as carbon-13 and the proton (Wittebort and Szabo 1978; Henry *et al.* 1986). The relaxation time constants T_1 and T_2, and the chemical shift anisotropy (CSA) are functions of the molecular motion in a macromolecule (Wittebort and Szabo 1978). The field strength, the molecule's average rotational correlation

time, τ_c, and the various internal motions are all important in determining the relaxation properties, and hence linewidth, of the observed nucleus.

The magnitude of the CSA effect must be calculated and taken into account before the linewidth can be used to make calculations of molecular motion based on the T_1 and T_2 relaxation time constants. This is not a complication of any practical consequence for ^{13}C and ^{1}H NMR at currently used field strengths, but is a significant problem in high-field ^{19}F NMR spectra, since the fluorine linewidth becomes dominated by the CSA effect (Ho *et al.* 1989).

Calculating the CSA component of the linewidth requires a detailed knowledge of the molecular geometry of the molecule, and of its various modes of motion. This information is used to calculate a spectral density function that determines the chemical shift at different molecular orientations. Even superficially similar molecules such as the different fluorotryptophan isomers (4-, 5-, and 6-F) can have spectral density functions that give rise to significantly different CSA components in their NMR linewidths (for example, 160 vs. 50 Hz for 4- and 5-FTrp respectively under the same conditions at 7T) (Ho *et al.* 1989).

Fluorotryptophan-labelled membrane-bound lactate dehydrogenase has been characterised by Ho and co-workers (Ho *et al.* 1989). Ho states that the most useful information about the molecular motion came from a comparison of the nuclear Overhauser effects (NOEs) from 4-FTrp and 5-FTrp labelled proteins. Ho explains that "it is difficult to calculate meaningful values [of linewidths and NOEs] for comparison with experimental data". The use of two fluorotryptophans obviated the need for a full prediction of the internal motions based on just one isomer. The work presented in this thesis concentrates exclusively on 5-fluorotryptophan since the most informative experiments used by Ho (Nuclear Overhauser Effect spectroscopy) have to

date been unavailable for technical reasons and 4-FTrp is prohibitively expensive.

The very fact that spectra can be recorded from the fluorotryptophan-labelled PGK in the intact cell, however, indicates immediately that the labelled protein is not fully immobilised, as it might be by binding to the cytoskeleton or membranes.

4.5.1.2 *Predicting the linewidths expected from a labelled protein*

Quantitative estimates of the relaxation parameters expected from a fluorotryptophan-labelled protein have been made previously by workers in Ho's laboratory (Post *et al.* 1984). They studied 5-fluorotryptophan-labelled protein J from *S. typhimurium*. Protein J is a histidine-binding 26 kDa monomeric protein. They assumed that the protein was a rigid body undergoing isotropic Brownian rotational diffusion, and on this basis they calculated the expected dipolar and CSA T_1 and T_2 relaxation time constants, and the NOE. All the expressions presented here are those given by Post (Post *et al.* 1984).

The expressions used for the CSA relaxation terms in such a body were those given by Abragam (Abragam 1961).

$$1/T_1 = (6/40)\ \omega_o^2\delta_z^2\ (1+\varepsilon^2/3)\ J(\omega_o) \qquad \text{(Eq. 4.3)}$$

$$1/T_2 = (1/40)\ \omega_o^2\delta_z^2\ (1+\varepsilon^2/3)\ [\ 3J(\omega_o) + 4J(0)\ ] \qquad \text{(Eq. 4.4)}$$

$$\text{where } J(\omega) = 2\tau_c/(1+\omega^2\tau_c^2) \qquad \text{(Eq. 4.5)}$$

ω_o is the resonance frequency of the relaxing nucleus, $J(\omega)$ is the spectral density function at frequency ω, ε is the asymmetry parameter of the traceless CSA tensor, given by $(\delta_x-\delta_y)/\delta_z$. $\delta_{x,y,z}$ are the chemical shifts when the molecule is oriented along the x, y or z axes respectively. The spectral density function used is that for a tumbling sphere. τ_c is the rotational

correlation time of the molecule. Note that the expression increases as the square of the frequency, that is the CSA relaxation rate goes up as the square of the increase in magnetic field strength.

For heteronuclear (^{19}F-^{1}H) dipolar relaxation, Hull and Sykes have shown (Hull and Sykes 1975) that for a fluorine coupled to a large number of protons the process is well-described by a single exponential process whose relaxation rate is the sum of the individual fluorine-proton couplings. The relaxation rates are given by

$$1/T_1 = K\, f(r) \left[J(\omega_H - \omega_F) + 3J(\omega_F) + 6J(\omega_H + \omega_F) \right] \qquad \text{(Eq. 4.6)}$$

$$1/T_2 = (K/2)\, f(r) \left[J(\omega_H - \omega_F) + 3J(\omega_F) + 6J(\omega_H + \omega_F) \ \ldots \right.$$
$$\left. + 4J(0) + 6J(\omega_H) \right] \qquad \text{(Eq. 4.7)}$$

$$\text{where } J(\omega) = \tau_C/(1+\omega^2\tau_C^2) \qquad \text{(Eq. 4.8)}$$

$J(\omega)$ is the spectral density function for an isotropic tumbling motion. K is a constant determined by the magnetic dipoles involved (proton and fluorine-19), and is equal to $\gamma_H^2\gamma_F^2\hbar/20$ where γ_H and γ_F are the gyromagnetic ratios of ^{1}H and ^{19}F respectively, and $\hbar$ is Planck's constant divided by 2π.

The function f(r) depends on the distance, r, between the observed fluorine nucleus and the protons with which it is relaxing. For N equivalent protons at a distance r, f(r) is simply given by

$$f(r) = N/r^6 \qquad \text{(Eq. 4.9)}$$

The fluorine of 5-fluorotryptophan has two equivalent proton neighbours on the ring, each 2.6 Å distant. Since the influence of a relaxing proton depends on a sixth-power relationship, the effect of other protons may be ignored. A more comprehensive treatment is possible, setting f(r) equal to the integrated volume of a sphere starting at distance r (here 2.6 Å) from the fluorine and

stretching to infinity, and containing protons at a density ρ. This gives an expression of

$$f(r) = \rho(4/3)\pi\, r^{-3} \qquad \text{(Eq. 4.10)}$$

The heteronuclear ^{1}H-^{19}F NOE is given by

$$NOE = -(\gamma_H/\gamma_F)\,[\,J(\omega_H - \omega_F) - 6J(\omega_H + \omega_F)\,] \,/\, [\,J(\omega_H - \omega_F) + 3J(\omega_F) + 6J(\omega_H + \omega_F)\,] \qquad \text{(Eq. 4.11)}$$

The NOE expression evaluates to approximately $^{-}1$ (complete abolition of the signal) for any large, rigid, isotropically tumbling molecule. Ho sees its greatest value in studies of large proteins as revealing the presence of rapid internal motions that cause the NOE to differ from $^{-}1$ (Rule *et al.* 1987).

Post (Post *et al.* 1984) showed that these expressions predicted relaxation parameters very close to those actually measured with their 5-fluorotryptophan labelled J protein, and they ascribed the discrepancies to internal motions of the labelled side group and protein.

4.5.1.3 Predicting the relaxation parameters of 5-fluorotryptophan–labelled PGK

The critical factor in evaluating the expressions given above is the rotational correlation time of the molecule. A comprehensive treatment would consider the effect of the ellipsoidal shape on the rotational diffusion. Certainly, the molecule will actually have independent correlation times for rotation about each of the axes. Tao (Tao 1969) has calculated the ratios of the correlation times along the different axes relative to those of a sphere of equivalent volume. For a prolate ellipsoid of axial ratio 2, the correlation times about the long and short axes are 0.8 and 1.5 respectively, relative to a sphere of rotational correlation time 1.

The effect of the protein shape has been discounted in these calculations, however, and the correlation function used is that for an isotropically

tumbling sphere. It is hoped that these limitations can be removed in future work.

For a sphere, the rotational correlation time can be found from the Stokes-Einstein relation given above (section 4.3), but this depends on knowing the radius of the protein. Here, both the radius and the correlation time are taken to be average figures for an equivalent sphere. The radius has been estimated here in two ways, and has been previously measured by small-angle x-ray scattering. The estimates and the measurement are all in good agreement.

Firstly, the crystal structure (Watson *et al.* 1982) has been used to determine the overall dimensions of the molecule by simply measuring the molecule with a molecular modelling program (Polygen's Quanta) on a Silicon Graphics Power Series workstation. The basic shape is that of a prolate ellipsoid, with overall dimensions of approximately 72 x 33 x 33 Å, giving a root mean square radius of approximately 24.6 Å.

Secondly, the radius has been estimated from the molecular weight, according to the generalised expression for a solid sphere (Freifelder 1982)

$$R = (3M_rV/4\pi N_A)^{1/3} \qquad \text{(Eq. 4.12)}$$

where V is the partial specific volume, N_A is Avogadro's number, and M_r is the relative molecular mass. The partial specific volume was taken to be 0.75, a value typical for globular proteins (Van Holde 1971). For PGK, M_r 44.5 kDa, this expression evaluates to 23.7 Å.

A third, perhaps more accurate, estimate of the effective radius could be calculated from the sum of the distance-weighted masses of every atom in the molecule. This is relatively simple with modern molecular modelling programs, but this has not yet been done.

The above values of 24.6 and 23.7 Å are for the anhydrous protein. An estimate of the water content allows the hydrated radius to be calculated. For globular proteins, this is typically 0.2 to 0.3 g water per g protein (Tao 1969). The additional mass caused by this bound water is thus (44 500/6x10^{23}) x 0.2 = 1.483x10^{-20} g. Since the density of water is close to 1, this is equivalent to an increase in volume of 1.483x10^{-20} ml. The hydrated radii on this basis are 25.6 and 26.4 Å respectively.

The experimental determination of the radius of gyration of PGK (Pickover *et al.* 1979) gave a value of approximately 22.5 ± 1 Å, depending on the presence and absence of ligands. These experiments have been used to predict the magnitude of the conformational change that occurs upon binding ligands. The spherical radius, r, and radius of gyration, R_G, are simply related as (Hestenes 1986)

$$R_G = r\,(3/5)^{0.5} \qquad \text{(Eq. 4.13)}$$

This gives an experimental hydrated average effective radius for PGK of about 29 Å.

All the subsequent calculations will assume that PGK can be approximated by a sphere of radius 27 Å, this being the average of the experimental and both the theoretical radii determined above.

The rotational correlation time of a molecule depends critically on the viscosity of its environment. The viscosity caused by the PGK itself, being a compact globular protein, is relatively small. It can be calculated from a knowledge of its concentration and intrinsic viscosity, η_i. The intrinsic viscosity of a typical globular protein may be determined as

$$\eta_i = \nu(V_2+\delta V_1) \qquad \text{(Eq. 4.14)}$$

where V_2 is the partial specific volume (0.75 g/ml), V_1 is the solvent density (1 g/ml for water), δ is a hydration factor (0.2-0.3 for a typical globular protein) and ν, the Simha factor, is a symmetry parameter that depends on the axial ratio of the protein (Van Holde 1971). Since the term in brackets is close to 1, this symmetry parameter dominates. Fortunately, the crystal structure provides a good estimate of this parameter (approximately 2.2) and the intrinsic viscosity of PGK can be confidently estimated as 3.3 g/ml.

The absolute viscosity of a protein solution is found from the specific viscosity, η_{sp}, which is equal to $c\eta_i$, where c is the protein concentration in grams per ml.

$$\eta_{sp} = (\eta - \eta_o)/\eta_o, \qquad \text{(Eq. 4.15)}$$

where η_o is the viscosity of the pure solvent and η is the viscosity of the solution (Van Holde 1971). For a 5 mg/ml protein solution in water at 30 °C (viscosity 0.797 mPa.s), the viscosity is thus 0.811 mPa.s, and at 50 mg/ml the viscosity is 0.929 mPa.s. The influence of the protein concentration on the total viscosity is thus relatively small, which is not unexpected for small non-interacting spheres in solution. PGK is thought not to self-associate in solution (Scopes 1973).

4.5.1.4 *Calculated relaxation parameters for 5-fluorotryptophan–labelled PGK*

The dipolar contributions to the T_1 and T_2 have been calculated for both the two-proton model (Eq. 4.9) and the spherical integral model (Eq. 4.10) discussed above. The radius of the protein has been taken as 27 Å, as discussed in the preceding section. These calculations are for a 30 mg/ml protein solution which is approximately equivalent to the concentration in the cell water after induction (see Chapter 3) and which was used for the *in vitro* experiments (see Chapter 5). Allowing for the viscosity of the protein

solution, this gives a rotational correlation time at 30 °C in a simple aqueous solution of approximately 17 ns.

With simple relaxation by the two nearest protons, providing the repetition rate is slow enough to prevent the relaxing protons being saturated by the cross-relaxation (Hull and Sykes 1975), the dipolar T1 relaxation time constant is predicted to be approximately 1.2 seconds, which represents an upper bound on the likely range of values. Taking into account all the surrounding protons of the protein matrix has been done by using a value for the proton density the same as Post et al. (Post *et al.* 1984) use for their J-protein studies ($\rho = 5.73 \times 10^{22}$ ml^{-1}). It is believed that this value will not be greatly different for PGK (Andy Brass, Manchester, personal communication) since it is mostly determined by factors common to other globular proteins. A better estimate may be obtainable by modelling the hydrated molecule on the basis of the crystal structure and directly determining the proton density in the model, but this has not yet been done.

On this basis, the dipolar T_1 (given by equations 4.3, 4.6 and 4.10) would be approximately 0.6 seconds, which is in excellent agreement with the value determined experimentally under the same conditions, 0.6 s (see section 4.5). The experimental determination of the T_1 is discussed in Chapter 5.

These values and others are tabulated below in Table 4.5.

Table 4.5

Calculated relaxation rate constants and linewidths for a 30 mg/ml solution of PGK at 30 °C.		Basis for calculating dipolar relaxation terms	
Solution viscosity	Parameter calculated	Two nearest protons	Full proton matrix
η_o (0.876 mPa.s)	dipolar contribution to R_1	0.77	1.63
" "	CSA contribution to R_1	0.06	0.06
" "	total R_1	0.83	1.69
" "	dipolar contribution to R_2	11.5	24.2
" "	CSA contribution to R_2	63.5	63.5
" "	total R_2	74.9	87.6
" "	linewidth (total $R_2+\pi$)	24	28
$\eta/\eta_o = 1.9$	linewidth	45	52
$\eta/\eta_o = 10$	linewidth	237	276

Relaxation parameters at 9.4 T (^{19}F NMR frequency 376 MHz) calculated for a 30 mg/ml aqueous solution of PGK at 30 °C assuming an average correlation time of 17 ns at the lowest viscosity.
R_1 and R_2 are the longitudinal and transverse relaxation rate constants, respectively. The familiar relaxation time constants T_1 and T_2 are the reciprocals of these rate constants. All values are in units of s^{-1} (Hz). The values are calculated using the equations and parameters presented in the text.

The linewidths determined through these calculations (R_2/π) are the linewidths for a singlet line in the ^{19}F NMR spectrum. The fluorine of fluorotryptophan is adjacent to and coupled to protons on either side of it on the indole ring. Its spectrum is actually a 1:1:2:2:1:1 multiplet structure reflecting this splitting, although at larger linewidths the components overlap one another to form an envelope that has the general appearance of a Lorentzian line. This is shown in Figure 4.9.

To allow the predicted singlet linewidth to be converted into the width of the overlapped multiplet actually observed in the experiments, a calibration

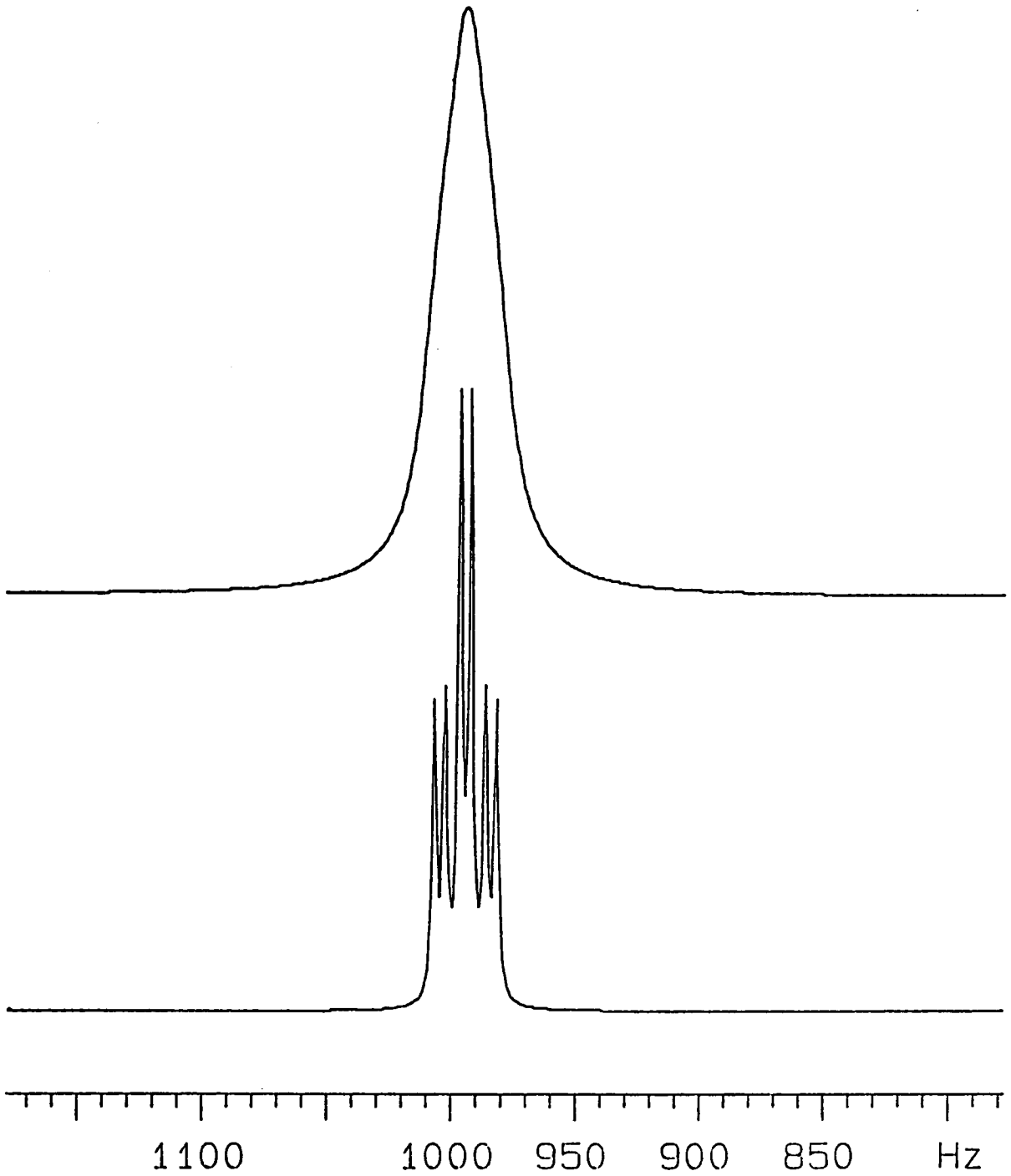

Simulation of the ^{19}F NMR spectrum of 5-fluorotryptophan using different singlet linewidths.
An AMQX system was simulated, where A, M, and Q represent the non-equivalent protons attached to carbons 4, 6 and 7 respectively, and X represents the fluorine attached to carbon 5. The coupling constants, due to Post *et al* (1984)(see text), were: JAX 10.2 Hz, JMX 10.1 Hz, JMQ 8.6 Hz, JAM 1.9 Hz, JQX 4.6 Hz, and JAQ 0.0 Hz. The simulations were performed with Varian's VNMR utility software, specifying frequencies of 0 Hz for A, M and Q and 1000 Hz for X. The spectra differed only in the singlet linewidth. The multiplet produced was examined by integration and shown to be of the 1:1:2:2:1:1 pattern expected. The singlet linewidths of the simulated spectra shown are 15 Hz (top) and 2 Hz (bottom).

Figure 4.9

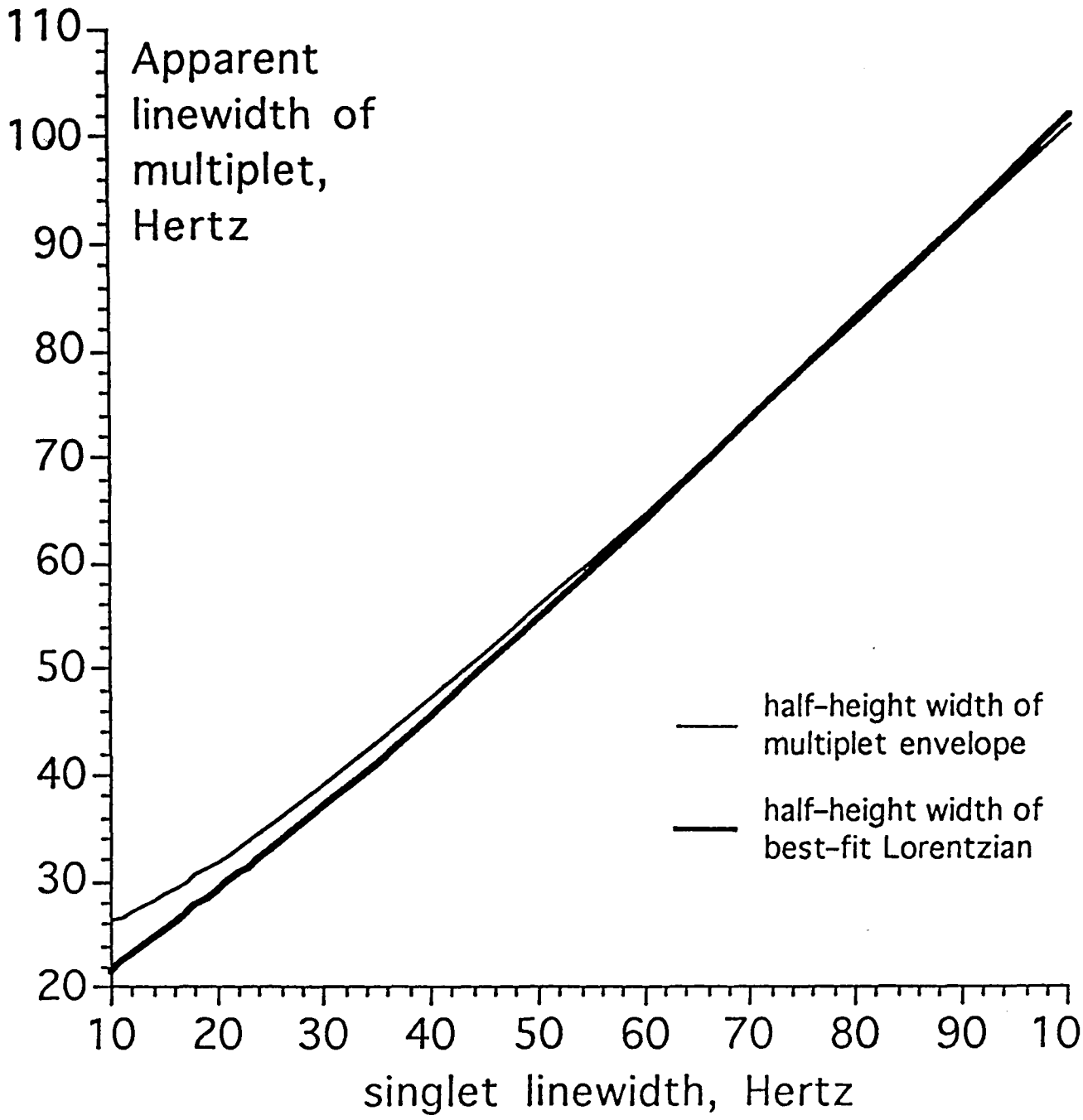

^{19}F NMR linewidth calibration curve: the apparent linewidth of the 5-fluorotryptophan multiplet, treated as if it were a single peak, as a function of the underlying true singlet linewidth.
Spectral simulations (see text and Figure 4.9) were used to generate spectra of 5-fluorotryptophan at different singlet linewidths. For singlet linewidths of 10 Hz and over, the components of the resultant multiplet overlapped enough to give the appearance of a single peak. The apparent linewidth of this single peak was measured both by measuring its width at half-height and by determining the half-height linewidth of the Lorentzian line which most closely resembled it. The best-fit Lorentzian was determined by an iterative least-squares fitting procedure in Varian's VNMR utility software. The graph shows the apparent linewidth as a function of the true singlet linewidth.

Figure 4.10

curve was constructed by measuring the width of the multiplet envelope produced by spectral simulation at different singlet linewidths. The coupling constants used were those of Post et al. (Post *et al.* 1984) who used the same process in their studies of 5-fluorotryptophan-labelled J protein. The calibration curve is shown in Figure 4.10.

The small increase in resolution apparent in moving from 7 T to 9.4 T (see Figure 4.1) is in accord with the predictions. For a typical peak separation of 0.4 ppm, the distance between the peaks is 113 Hz at 7 T, 150 Hz at 9.4 T and 188 Hz at 11.7 T (^{1}H resonance frequency 500 MHz). The linewidths predicted for a molecule with a correlation time of 20 ns are approximately 23, 33 and 36 Hz respectively. Since the increase in separation is greater than the increase in linewidth, some increase in the resolution is expected at 9.4 or even 11.7 T compared to that obtained at 7 T.

4.5.2 The relaxation parameters of labelled PGK determined by experiment

4.5.2.1 Linewidths

The linewidths of the two peaks from 5-fluorotryptophan-labelled PGK recorded at different fields and under different conditions are shown in Tables 4.6 (FY3-1 cells) and 4.7 (BJ2168 cells). The linewidths observed with purified labelled PGK are included for comparison. As can be seen from the spectra, the lineshapes obtained from the labelled PGK *in vivo* are much poorer than those obtained *in vitro*. This is particularly true in the spectra from starved cells where the peaks overlap significantly. Although the errors are not quantitated and thus not shown in the tables, it is clear that the linewidths reported for the purified PGK are much more reliable than those for the PGK in the intact cell.

Table 4.6

Sample or cell condition	Downfield peak	Upfield peak
Glucose-fed cells	140	100
Starved cells	100	130
Purified PGK no ATP	31	36
Purified PGK with 0.5 mM MgATP	37	67
Purified PGK with 1.27 mM MgATP	40	60
Purified PGK with 12.7 mM MgATP	32	58

Half-height linewidths (Hz) of the peaks seen in the 7 T ^{19}F NMR spectrum of labelled PGK in FY3-1 cells or in vitro.
The linewidths were determined by fitting the experimental data to Lorentzian lines with the Bruker utility software Glinfit. The experiments with the purified PGK were performed at room temperature (16 to 20 °C) in a HEPES/acetate buffer, pH 7.2, I=0.15 M.

Table 4.7

Sample or cell condition	Downfield peak	Upfield peak
Glucose-fed cells	135	110
Ethanol-fed cells	200	130
Starved cells	200	110
Purified PGK with no ATP	34	36
Purified PGK at a relative viscosity of 1.9 [1]	49	52
Purified PGK at a relative viscosity of 10.1 [2]	170	150
Purified PGK with 1 mM MgATP	40	120
Purified PGK with 1.4 mM MgADP, 0.7 mM MgATP	50	100

Half-height linewidths (Hz) of the peaks seen in the 9.4 T ^{19}F NMR spectrum of labelled PGK in BJ2168 cells or in vitro.
The experimental data was fitted to Lorentzian lines with the Varian utility software VNMR. The purified PGK was studied at 30 °C in a HEPES/acetate buffer, pH 7.2, I=0.15 M. (1) This represents a lower limit on the estimated intracellular viscosity (Endre *et al.* 1983). (2) This represents an upper limit on the estimated intracellular viscosity (Dix and Verkman 1990). The viscosity experiments were performed in the HEPES buffer with glycerol to increase the solution viscosity.

The main reasons for the difference between the linewidths of the PGK in the intact cell and of the isolated PGK are probably exchange-broadening, sample inhomogeneity, and perhaps the presence of paramagnetic ions such as Mn^{2+}, which all serve to increase the observed linewidth.

Exchange-broadening results from the superposition of the signals from the same nucleus observed in two or more environments. The different environments are, presumably, the enzyme with and without bound magnesium-nucleotide. Since the signals from the enzyme and the Mg-ADP-enzyme can not be resolved, these states are in fast exchange on the NMR time scale. The effect of exchange-broadening can be seen clearly *in vitro* since the enzyme can be studied in the absence of any ligands. This is not possible *in vivo*, since the cell always contains some Mg-ADP and other ligands.

A crude estimate of the expected effect of exchange broadening on the ^{19}F NMR linewidths can be calculated from estimates for the rate constants involved in the exchange process. Given that the K_d for PGK:MgADP is around 50 μM (Scopes 1978a), an equilibrium mixture of 1 mM PGK and 0.5 mM MgADP will contain around 0.5 mM each of PGK^{free} and PGK^{MgADP}, and around 50 μM free MgADP. If the association of the PGK and MgADP is diffusion-limited, the second-order rate constant for the association is likely to be similar to that of other small ligand - protein interactions, around 10^6 to 10^8 $M^{-1}s^{-1}$ (Cantor and Shimmel 1980; Fersht 1984). Taking a value of 10^7 $M^{-1}s^{-1}$, the unimolecular PGK:MgADP dissociation rate constant would be around $10^7 \times 50 \times 10^{-6} = 500$ s^{-1}.

Provided the exchange rate is faster than the frequency difference between the two states, i.e. in the fast-exchange limit, the half-height linewidth

increment, $\Delta\nu_{1/2}$, caused by chemical exchange can be calculated as (Harris 1986)

$$\Delta\nu_{1/2} = \pi(\nu_a - \nu_b)^2 / 2k \qquad \text{(Eq. 4.16)}$$

where ν_a and ν_b are the resonance frequencies (s^{-1}) of the interconverting species *a* and *b* and k is the pseudo-first-order rate constant for the exchange process, here around 500 s^{-1}. The chemical shift of the upfield peak in the ^{19}F NMR spectrum moves from around 8.5 to 8.0 ppm (see Chapter 5) on binding MgADP. At 9.4 T, this corresponds to a frequency difference in the two states of 188 Hz. Eq. 4.16 then evaluates to 110 Hz for the exchange-broadening contribution to the observed linewidth. This is in good agreement with the experimental observations (c. 50 to 100 Hz, see Chapter 5), given the very approximate nature of the rate constant used.

The spectra whose linewidths are reported in Tables 4.6 and 4.7 were acquired from the intact cells over approximately 4 to 12 hours (FY3-1 cells) or 0.5 to 2 hours (BJ2168 cells), or from purified enzyme in approximately 10 to 20 minutes. Some broadening is likely to have occurred as a result of changes in the metabolic state of the cells on this time scale. The broadening may result from a drift in the ligand environment of the protein or the magnetic susceptibility.

The spectra from the purified enzyme were stable over the period of the acquisition, though there was some broadening on prolonged incubation because some of the ATP in the mixtures was hydrolysed slowly to ADP, which binds to the PGK (in the presence of Mg^{2+}) more tightly than ATP. This is discussed further in Chapter 5.

The effect of viscosity on the linewidths is also important in determining the linewidth. The rotational correlation time of the molecule is linearly proportional to the viscosity of the medium, but the influence this has on the

linewidth will depend on the modes of motion within the molecule and the relaxation pathways of the observed nucleus (via the spectral density function) (Wittebort and Szabo 1978).

The effect of the intracellular viscosity on the minimum linewidths of the PGK (i.e. without any exchange-broadening) has been investigated by studying purified PGK in a buffer containing glycerol to increase the viscosity to values corresponding to that in the cytoplasm. Literature values for the cytoplasmic viscosity vary considerably, estimates ranging (relative to physiological saline) from 1.9 (Endre *et al.* 1983) to 10 (Dix and Verkman 1990). The linewidths observed under these conditions vary from 50 Hz (η_r 1.9) to 170 Hz (η_r 10.1) (see Table 4.7 and Figure 4.3).

4.5.2.2 *Relaxation rate constants*

The T_1 relaxation time constants for the two peaks were measured *in vitro* using an inversion recovery experiment (Sanders and Hunter 1987). The series of spectra obtained and the subsequent exponential-fit data analysis are shown in Chapter 5. The T_1s for both PGK peaks were around 0.6 seconds. The experiment was repeated in the presence of Mg-ATP, which made no measurable difference to the results.

The T_2s were to be estimated by the Carr-Purcell-Meiboom-Gill (CPMG) sequence (Sanders and Hunter 1987) since a preliminary spin-echo experiment (Sanders and Hunter 1987) indicated that the T_2 lay in the region of 10 to 20 ms. Unfortunately, technical difficulties prevented these experiments from being completed and they have not yet been repeated.

A short T_2 would be consistent with the peaks arising from a macromolecule, as is the fact that the T_1s measured here at 9.4 T (0.6 s) are longer than those measured at 7 T (0.4 s) (Ho *et al.* 1989). The T_2 for the material in the peak

around 9 ppm appeared to be longer than those of the PGK peaks, although it has not been measured properly; this is consistent with the 9 ppm peak arising from a smaller molecule.

4.5.3 Comparing the results obtained *in vivo*, *in vitro* and by calculation

4.5.3.1 General observations

Allowing for the effects of exchange-broadening and the intracellular viscosity, and the possible importance of paramagnetic ions, there seems to be no evidence in the data presented here for a significant difference in the linewidths, and hence molecular motion, of PGK in isolation and PGK in the intact cell.

The observed linewidths of PGK in the intact cell, around 110 to 130 Hz minimum, correspond to that expected from a molecule with a correlation time of around 70 to 80 ns, ignoring any exchange-broadening. If the radius of PGK is taken as 27Å (see section 4.5.1.3), this puts an upper limit on the intracellular viscosity of approximately 4 mPa.s at 30 °C, a viscosity relative to water of around 4.5. This is not dissimilar to values for the cytoplasmic viscosity determined by other techniques, such as fluorescence photobleaching of labelled dextrans (4 mPa.s at 37 °C) (Luby-Phelps *et al.* 1986) or ESR studies of small molecules (η_r 3 to 6) (Lepock *et al.* 1983; Mastro *et al.* 1984).

The data certainly suggests that the relative viscosity experienced by PGK in the cell is nearer the lower limit of 1.9 (Endre *et al.* 1983) than the upper limit of around 10 (Dix and Verkman 1990), and Dix and Verkman point out themselves that their estimates are higher than many previously published. They ascribe this to immobilisation of their fluorescent probes by binding to cellular proteins.

Alternatively, again ignoring the exchange-broadening contributions, if the relative viscosity of the cytoplasm is as low as 1.9 then the effective radius of PGK would have to be 36 Å to account for the observed linewidths. This is compared to 29 Å measured for PGK (Pickover *et al.* 1979), 31 Å measured for yeast hexokinase (McDonald *et al.* 1979) and 55 Å measured for yeast pyruvate kinase (Müller *et al.* 1972). Using the general expression relating molecular weight and size given by Freifelder (see section 4.5.1.3), a 36 Å radius spherical complex would have a molecular weight of approximately 156 kDa.

Removal of any exchange-broadening effects would make the viscosity appear even lower, or the effective radius of PGK even smaller. The exchange-broadening contribution may be as much as half the total linewidth, as estimated from experiments with labelled PGK *in vitro* (see Table 4.7). This suggests that the bulk of the PGK is not part of any large complex under the experimental conditions, and is unlikely to be bound to another molecule of similar size.

The experimental uncertainties leave open the possibility that at least some of the PGK is bound to another relatively small protein such as the c. 140 kDa GAPDH (Sukhodelets *et al.* 1988). It seems unlikely that much of the PGK is bound to a relatively immobile matrix such as the cytoskeleton, particularly since the NMR signal intensity of the labelled PGK in the intact cell appears to be 100 % of that of the same amount of isolated PGK.

These data suggest that PGK is freely diffusible in the cell, and not part of a large glycolytic complex either in the cytoplasm or on the cytoskeleton (Walsh and Knull 1987). The principal difficulty in extending this conclusion to the normal cell is that the yeast used in this work has a large excess of PGK, from ten to twenty times the wild-type levels. It might be argued that the PGK

observed is indeed outside any complex, yet the relatively small amount of physiologically important material is indeed complexed or compartmentalised.

Further experiments in which the labelled PGK levels are brought closer to the wild-type level are needed. However, the fact that similar results are obtained from cells with four to ten (FY3-1 cells) or ten to twenty (BJ2168 cells) times wild-type levels of PGK suggests that this problem may not be important. If the putative complex of PGK were in the same cellular compartment as the labelled PGK, the complex would be weakly associated and in exchange with the pool of labelled PGK, since a tight complex would presumably be more stable and easier to isolate and characterise than the weak complexes that are the object of much debate (Chock and Gutfreund 1988; Cornish-Bowden 1991; Mendes *et al.* 1992)

4.5.3.2 *The calculated NMR properties of labelled proteins in solution*

The calculations of the expected spectral relaxation properties show which parameters are likely to be most sensitive to changes in the rotational correlation time of the PGK. Further work would concentrate on enhancing the spectral density function used to account for some internal motion of the protein and for its ellipsoid nature. However, the general conclusions from the calculations of the relaxation parameters are likely to be unchanged. The calculations have been used to produce the graphs in Figures 4. 11 to 4.13, which show the predicted behaviour of the relaxation parameters and linewidths as functions of magnetic field strength and of correlation time.

Some experimental results obtained with 5-fluorotryptophan-labelled phosphoglycerate kinase, pyruvate kinase and hexokinase (preliminary data from some further work not presented in full) are tabulated along with the calculated parameters for comparison in Table 4.8 below. Preliminary spectra

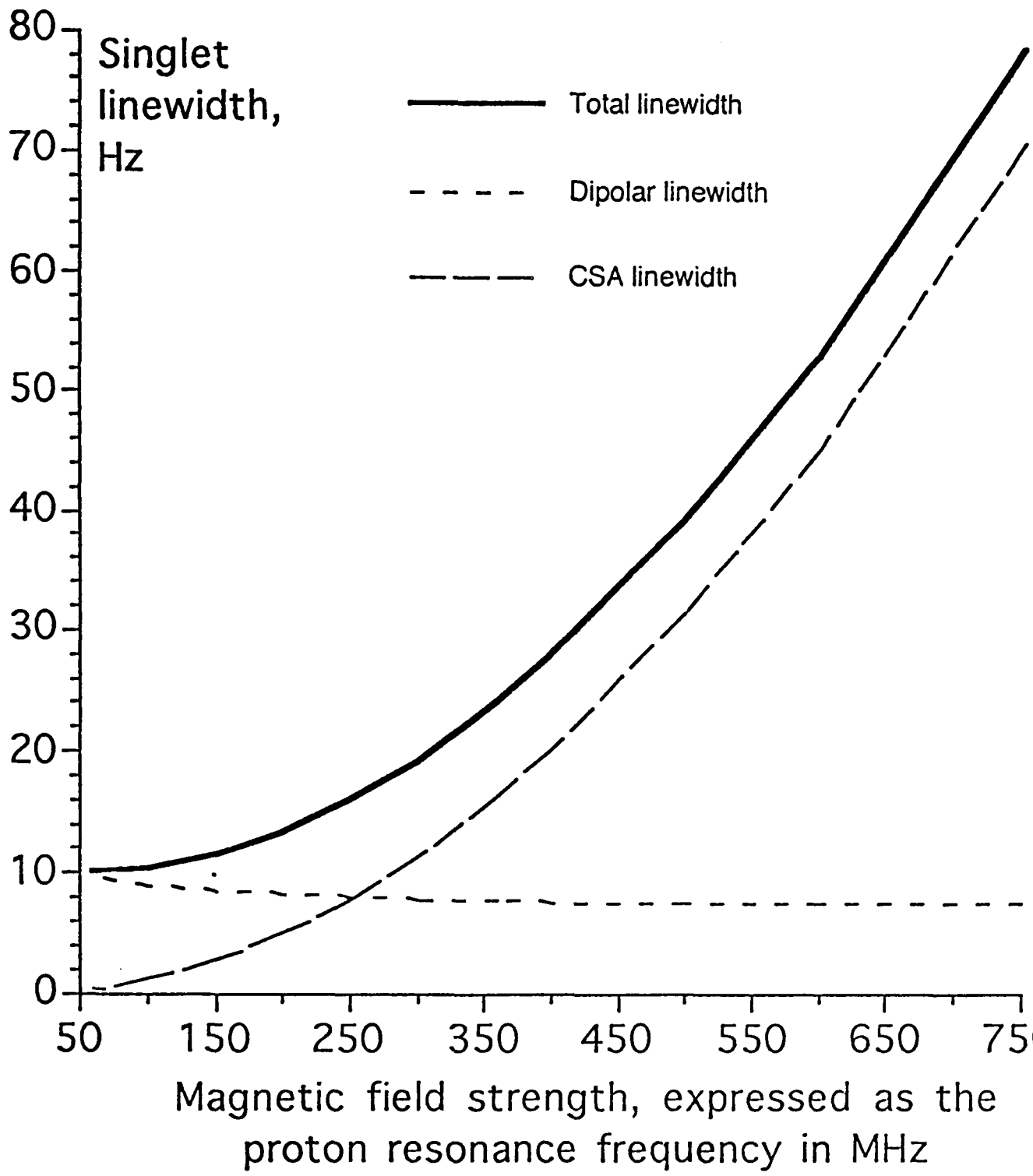

Contributions to the ^{19}F NMR half-height linewidths as a function of the magnetic field strength.
The contributions to the linewidths from dipolar and CSA relaxation have been calculated as $1/\pi T_2$ on the basis of the expressions in the text (Eqs. 4.4, 4.7, 4.10). A rotational correlation time of 17 ns has been used throughout (see section 4.5.1.4). The magnetic field strength is quoted as the proton NMR resonance frequency for the sake of familiarity. 100 MHz corresponds to a field strength of approximately 2.35 Tesla.

Figure 4.11

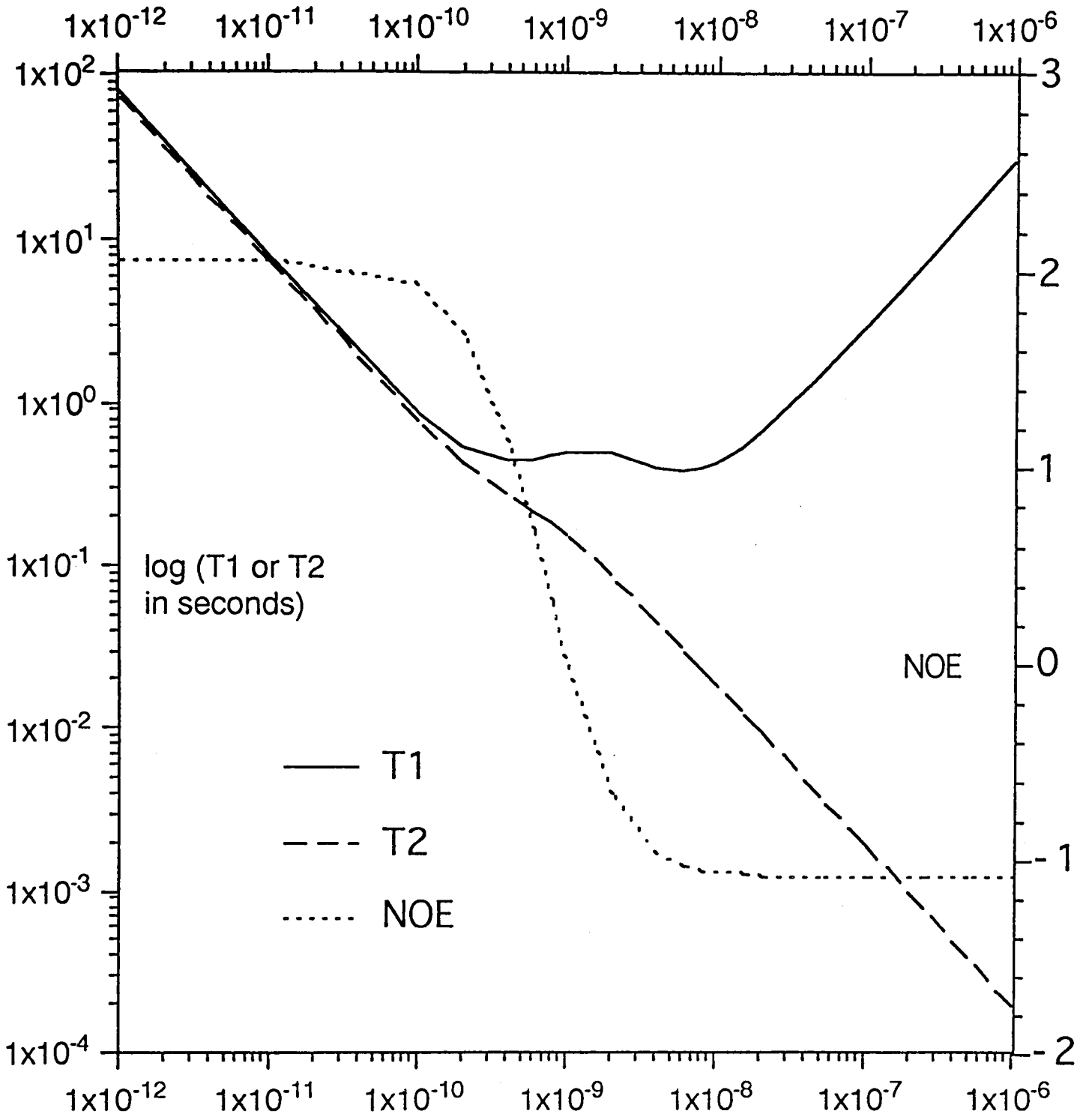

The ^{19}F NMR relaxation rate constants T_1 and T_2 and the nuclear Overhauser effect (NOE) as functions of the rotational correlation time. The left-hand y-axis is the log of T_1 or T_2 in seconds. The right-hand y-axis is the NOE factor. The factor represents the proportional increase in ^{19}F signal intensity with ^{1}H decoupling compared to that without. The values have been calculated according to the expressions in the text (Eqs. 4.3 to 4.11), using the proton matrix method to calculate the dipolar relaxation terms (Eq. 4.10). The magnetic field strength used was 9.4 T, corresponding to resonance frequencies of 400 and 376 MHz for ^{1}H and ^{19}F respectively.

Figure 4.12

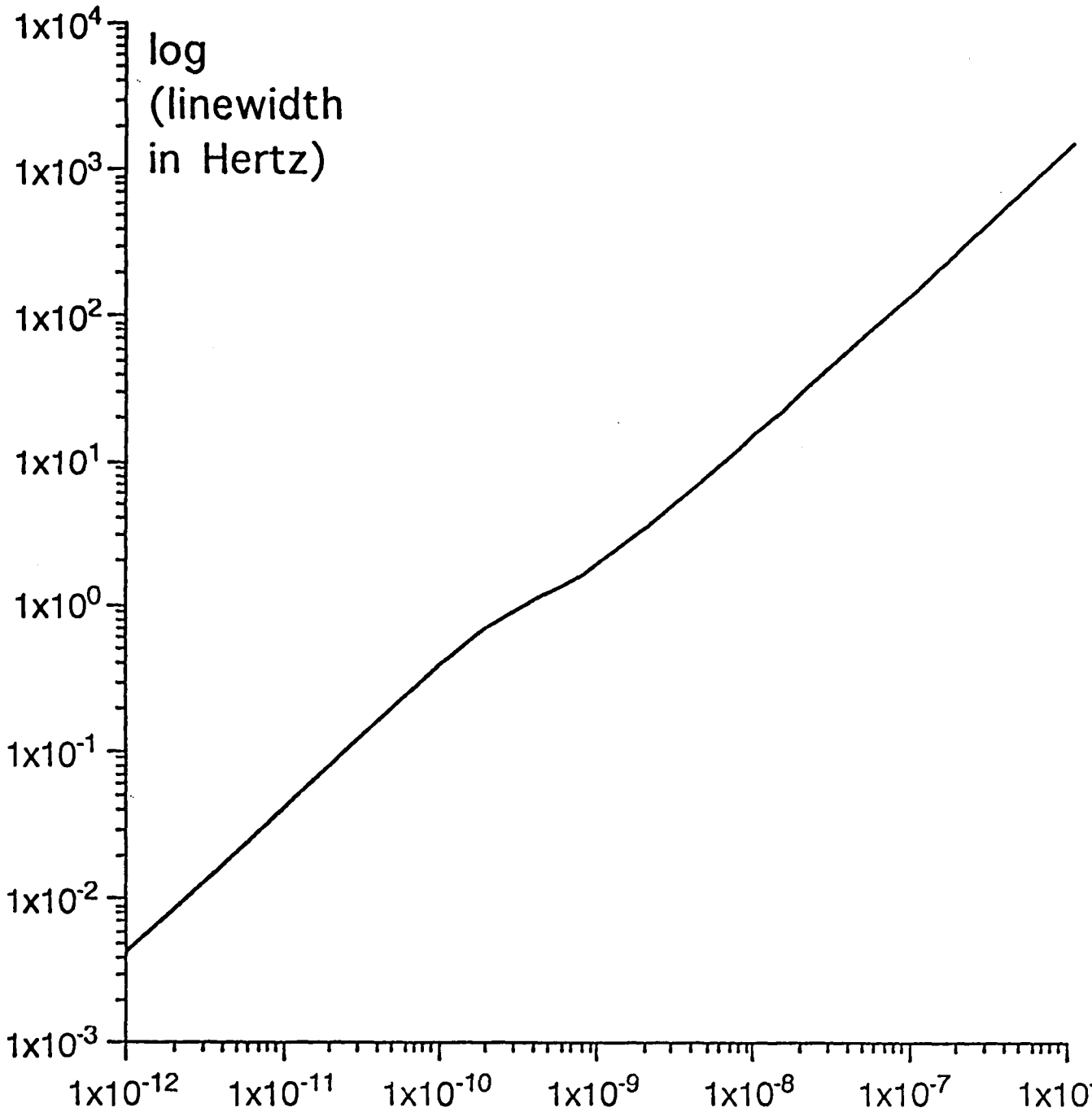

^{19}F NMR spectral linewidth at half-height as a function of the rotational correlation time, τ_c.
The half-height linewidths were calculated as $1/\pi T_2$ according to the expressions given in the text (Eqs. 4.4 to 4.10). The total linewidth is the sum of the linewidth from both dipolar and CSA relaxation processes. The dipolar contribution was calculated according to the proton-matrix model (Eq. 4.10). The magnetic field strength used was 9.4 T, corresponding to ^1H and ^{19}F resonance frequencies of 400 and 376 MHz respectively.

Figure 4.13

of 5-fluorotryptophan-labelled hexokinase are shown in Figure 4.14, which illustrates the changes in the spectra upon addition of glucose to the solution.

Table 4.8

	Sample description	Parameter		
		Name	Measured value	Predicted value
1	PGK in aq. soln., 18 °C, 7T	T_1	0.4 s	0.4 s
2	PGK in aq. soln., 18 °C, 7T	LW	31 Hz	33 Hz
3	PGK in aq. soln., 30 °C, 9.4 T	T_1	0.6 s	0.6 s
4	PGK in aq. soln., 30 °C, 9.4 T	LW	34 Hz	36 Hz
5	PGK in glycerol soln., η_r 1.9	LW	49 Hz	54 Hz
6	PGK in glycerol soln., η_r 10	LW	170 Hz	270 Hz
7	PK in glycerol soln., 25 °C	LW	315 Hz	310 Hz
8	PK in glycerol soln., 35 °C	LW	250 Hz	240 Hz
9	PK in glycerol soln., 45 °C	LW	190 Hz	195 Hz
10	PK in aq. soln., 20 °C	LW	110 Hz	240 Hz
11	Cell lysate containing HXK, 20 °C	LW	110 Hz	62 Hz
12	Cell lysate containing HXK, 20 °C	T_1	1.6s	1.1 s

Calculated and observed linewidths and T_1 values for a variety of samples.
All samples were approximately 30 mg/ml in protein and examined at 9.4 T except for the 7 T studies indicated. The predicted values are based on the spectral density functions for rigid spherical isotropic motion and use the proton-matrix rather than the two-proton assumption (see text). The radii of the PGK, PK and HXK were taken as 27 (see text), 55 (Müller *et al.* 1972) and 31 Å (McDonald *et al.* 1979) respectively.

Most of the predicted values in Table 4.8 agree very well with their experimentally-determined counterparts. This suggests that the motion of the 5-fluorotryptophan label is approximated reasonably well by considering it as being fixed on a rigid sphere, and that there is correspondingly little internal motion. Some discrepancies do remain, however, but these have not been investigated further yet.

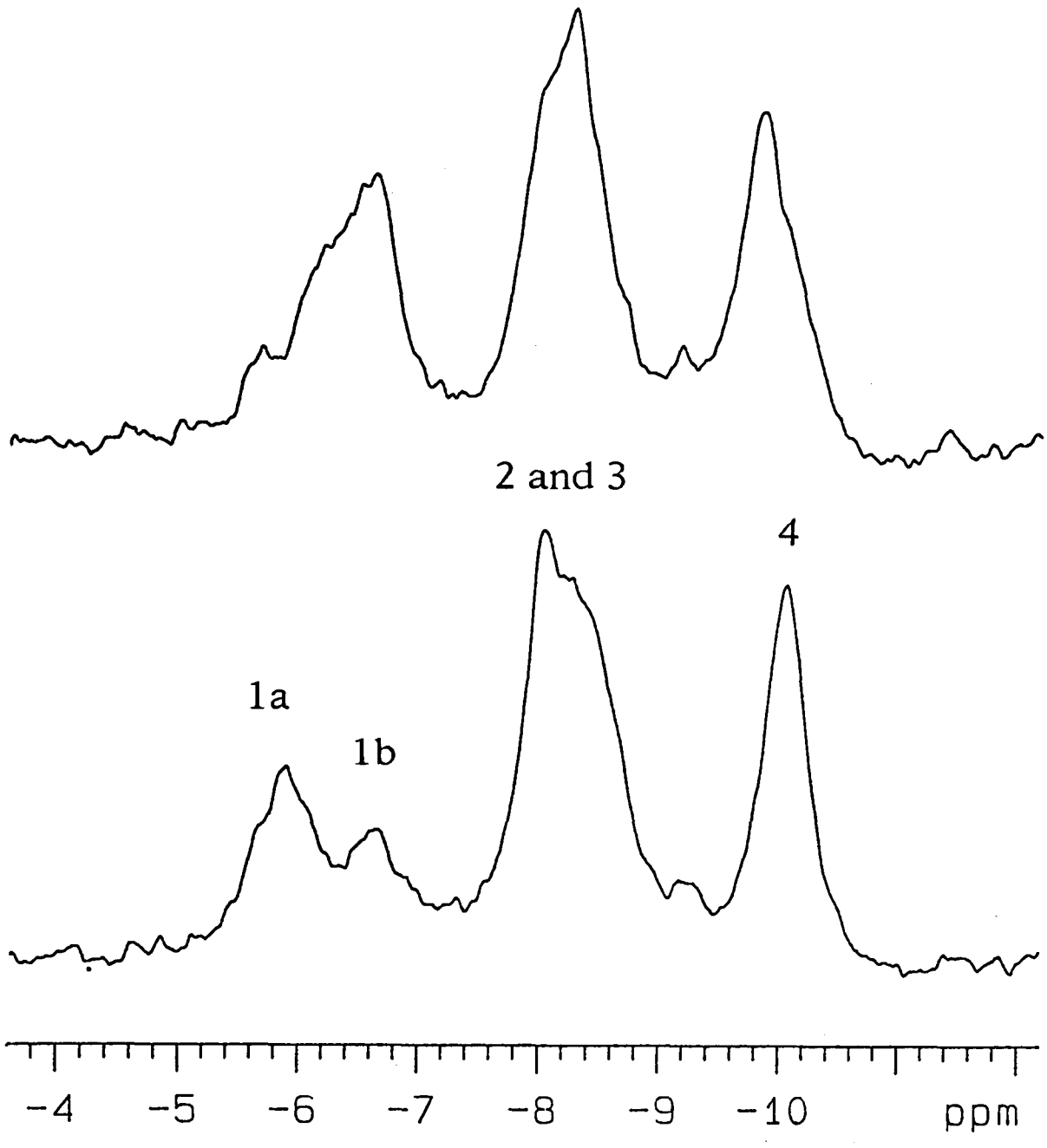

^{19}F NMR spectra of 5-fluorotryptophan-labelled yeast hexokinase B in the presence (top) and absence (bottom) of glucose.
Cell lysates were prepared by mechanical disruption of approximately 10 g yeast cells containing labelled hexokinase. The lysates were dialysed extensively against a buffer containing 10 mM MOPS and 5 mM EDTA neutralised to pH 7.0 with Tris base. The spectral width was 15000 Hz, the interpulse delay 20 s. Approximately 50 mM glucose was introduced to the 16 ml sample before acquiring the second spectrum. The spectra were acquired under fully-relaxed conditions to allow quantitation. Hexokinase contains 4 Trp residues, and the corresponding peaks in the spectrum are indicated on the figure.

Figure 4.14

In the case of pyruvate kinase in low-viscosity buffer (line 10), the observed linewidth is much smaller than that expected. It may be that the protein was unstable under the conditions used, and the observed linewidth does not arise from the homotetramer assumed for the calculations. Interestingly, the linewidth observed does correspond to that expected for a dimer of PK monomers. It may equally arise from a proteolytically degraded partial pyruvate kinase, although the preparation was derived from the protease-deficient strain BJ2168 (Jones 1990a). The actual explanation has not been pursued. The observation is certainly in accord with reports that PK must be kept in glycerol or similar solutions to preserve its activity (Kayne 1973).

The apparent linewidth of the labelled hexokinase preparation (lines 11,12) was much broader than that predicted for the monomer from the radius of gyration determined by small-angle x-ray scattering (McDonald *et al.* 1979). The linewidth observed does correspond to that expected for a hexokinase dimer. The x-ray scattering studies were performed at pH 8.6, when essentially no dimerisation was evident in the scattering experiments (McDonald *et al.* 1979). Under the conditions of the NMR experiment at pH 7.0, one would expect most of the hexokinase to exist as dimers (Derechin *et al.* 1972). The sample homogeneity was relatively poor, however. Although only a crude cell lysate, most of the DNA had been precipitated with protamine sulphate, so the viscosity of the solution should not have been very great. It may be that the observed linewidth is broadened by conformational and dimerisation exchange processes.

The PGK studied at lower viscosities (lines 1-5) gave experimental values in good agreement with the predicted values, but the observed linewidth at the higher viscosity (line 6) was much narrower than expected. The lineshapes have begun to look somewhat non-Lorentzian, perhaps because some material precipitated and contributed a broad hump to the spectrum. This

may reduce the accuracy of the measurement of the linewidths when fitting the spectral lines to Lorentzian shapes. However, the 100 Hz discrepancy is hard to account for on this basis alone.

Perhaps the changes in the internal motions that accompany changes in the solvent viscosity (Ghosh and McCammon 1987) removed motions that were previously at an effective relaxation frequency. It may simply be that the presence of the 59 % glycerol in the buffer altered the relaxation properties of the system, increasing the excited spin lifetime and hence reducing the linewidth. This has yet to be investigated.

4.5.3.3 Further work

For a large isotropically tumbling molecule, the T_1, T_2, and linewidths can be considered as a simple linear function of the viscosity of the medium. As Hull and Sykes have pointed out (Hull and Sykes 1974), the ratio of T_1/T_2 provides quite a sensitive measure of the correlation time, either through a change in the average isotropic correlation time or through the presence of internal motions in the protein. This has the added benefit of arriving at ratio values that are independent of the r^6 dipole-dipole distance term, thus removing the need to assume which protons are part of the relaxation pathway.

It is hoped that future measurements of NOEs, T_1 and T_2 in the intact cell and values derived from these parameters will allow more definitive conclusions about the freedom of cytosolic proteins to tumble in the cytoplasm.

The NOEs should enable the contribution of rapid internal motions to be assessed. It may be possible to follow the time course of protein breakdown in the cell by collecting NOE-weighted ^{19}F spectra; the signals from macromolecules would disappear upon ^{1}H irradiation, provided the internal

motions were negligible, while the signals from small molecules would be enhanced.

Work will continue with PGK, hexokinase and pyruvate kinase, which give a range of differently-sized molecules to use as probes. A smaller probe would clearly be useful. An ideal candidate would seem to be the C-terminal domain of PGK, whose radius is about 15 Å. This is a compact, globular domain that has already been successfully expressed in yeast and studied by ^{1}H NMR and circular dichroism (Fairbrother *et al.* 1989a). It contains both Trp residues and the ATP binding site. It would presumably be easier to detect NMR signals from this small probe in the intact cell since the peaks would be narrower and taller, and hence stand out better against the spectral noise. The rotational correlation time would be around 7 ns in water, giving a singlet linewidth of 12 Hz and T_1 of around 0.4 s.

The domain could even be expressed with leader sequences to direct it to chosen intracellular compartments to monitor the ATP/ADP concentrations and viscosity there, provided the compartment size was large enough to accommodate sufficient labelled material to observe. The motional properties of this compact unit may also be easier to reliably predict than for the multi-domain or oligomeric proteins, so a better model of the relaxation processes may be easier to generate.

5 Characterising the spectral changes: studies on isolated PGK

5.1 Introduction

There are many factors that influence the NMR spectra obtained from a labelled enzyme in the intact cell. Some of these, such as changes in the intracellular pH, can be studied non-invasively by NMR or other techniques. For some important parameters, such as the local concentrations of metabolites and macromolecules, there are no effective means of quantitating them *in situ*. Inevitably, the spectra from the labelled enzyme *in vivo* can not be wholly interpreted with observations of the intact cell.

A reductionist approach using *in vitro* studies requires considerable care. The main risk is of studying a system that is not sufficiently representative of the situation *in vivo*. This failing has important precedents in recent biochemical history. The most potent effector of 6-phosphofructo-1-kinase (PFK, EC 2.7.1.11), fructose-2,6-bisphosphate, was only discovered in 1980 after many years of active investigations into the control and operation of PFK (Van Schaftingen *et al.* 1980). Many studies have been plagued by difficulties in obtaining intact purified proteins, such as pyruvate kinase (Murcott *et al.* 1991).

Given that these limitations can be overcome, controlled studies of the isolated protein can give valuable information about the behaviour of the protein in the intact cell. The experiments outlined in this chapter aimed to evaluate the contributions of different changes in the cell to the ^{19}F NMR spectra recorded from labelled PGK in the intact cell.

5.2 Purification of PGK

5.2.1 General principles

The purification protocols employed are described fully in Chapter 2, the Materials and Methods section. They have been adapted from the literature (Scopes 1971; Fifis and Scopes 1978) to work on an appropriate scale and with starting materials enriched in the target protein by use of genetically manipulated strains (Scopes 1987; Deutscher 1990).

The yeast strain used, BJ2168 (pep4-3, prb1-1122, prc1-407), is also fully described in Chapter 2. It has mutations that virtually eliminate the activity of the general degradative pathways of proteolysis (Jones 1990a). This property allows the purification to be carried out virtually in the absence of the principal classes of protease responsible for protein degradation in cell lysates (Jones 1990a).

5.2.2 Results

5.2.2.1 Native, unlabelled PGK

Unlabelled PGK was successfully purified to apparent homogeneity in PAGE-SDS electrophoretic experiments. The specific activity of the final gel filtration fractions obtained in the preparations was between 400 and 500 U per mg protein, typically pooled to give a 450 U/mg stock, measured at room temperature (c. 20 to 22°C).

Sulphate at low concentrations (up to 100 mM) activates PGK up to four-fold and inhibits it at high concentrations. A similar effect occurs with other anions, and is probably caused by changes in the rate-limiting enzyme-product dissociation step (Scopes 1973; Scopes 1978b; Scopes 1978a). PGK is

commonly studied with c. 20 to 50 mM sulphate because it has non-Michaelis-Menten kinetics in the absence of sulphate, but the kinetics are simplified in the presence of sulphate (Scopes 1978b).

PGK activities are commonly cited without detailing the amounts of sulphate, from ammonium sulphate suspensions of the other enzymes used or from the stored stock of PGK, making direct comparisons of published activities difficult. Specific activities of up to 710 U/mg were determined in the presence of arbitrary amounts of sulphate, and specific activities of 250 to 350 U/mg were measured in the complete absence of sulphate. The assay mixture normally used in this work contained approximately 10 mM sulphate, arising from the 3.5M ammonium sulphate stock suspension of the coupling enzyme GAPDH.

The specific activity of the material obtained here was better than that measured on a commercial preparation of the same yeast enzyme (Boehringer Mannheim) under the same conditions, about 450 vs 380 U/mg. It is also comparable with the values reported by Scopes (Scopes 1978b) (700 U/mg at 25 °C, 40 mM [SO_4^{2-}]), by Fairbrother (Fairbrother *et al.* 1989b) (450 - 500 U/mg at 25 °C), by Minard (Minard *et al.* 1990) (c. 450 U/mg at 25 °C), and by Mas (Mas *et al.* 1988) (c. 825 U/mg at 25 °C, 50 mM [SO_4^{2-}], or c. 375 U/mg without sulphate according to Figure 4 of that paper).

5.2.2.2 5-fluorotryptophan–labelled 3-phosphoglycerate kinase

Labelled PGK was purified by the same methods as the unlabelled material. The fact that the specific activity (c. 300 to 400 U/mg) was almost the same as that measured for the unlabelled material and did not vary substantially with the fractional labelling of the PGK was taken to indicate that there was little difference in the specific activities of labelled and unlabelled proteins. The preparations with the lowest specific activities (c. 300 U/mg) were those

with the highest fractional labelling, but they were also some of the earliest and the specific activity was not significantly less than that of wild-type PGK prepared at that time. Some further experiments are required to draw definitive conclusions about the relative specific activities of the labelled and wild-type proteins.

Electrospray mass spectrometry was performed on a sample of labelled material by Andy Pitt, Cambridge, and this also showed that the preparation was not significantly contaminated with other proteins. As was seen with the unlabelled material, however, small amounts of a non-protein contaminant, probably nucleic acid, could be removed by passage over monoQ™ (Andy Pitt, Cambridge, personal communication). The mass distribution of the peak observed was a little wider than that expected from a similar-sized protein, and could reasonably be attributed to the presence of the non- mono- and di-fluorinated protein species. It was hoped to determine the distribution of the non-, mono- and di-fluorinated species, but this proved not quite possible on the VG Instruments machine then available. The experiment is feasible, however, and may be repeated on a newer Kratos Concept machine.

Interestingly, the precise mass of the labelled PGK determined by electrospray MS was about 100 Da in excess of its sequence-derived isotope-corrected mass. This has not been investigated further, but does accord with unpublished ^{31}P NMR observations that a small molecule is tightly bound to PGK and can be removed by dialysis against 3-phosphoglycerate (Hilary Muirhead, Bristol, personal communication). The mass result also suggests that the protein is not proteolytically clipped. The presence or absence of this component may be another source of the breadth of the peak seen in the electrospray mass spectrometry experiment.

5.3 Properties of PGK

5.3.1 Ligands of PGK

PGK has five natural ligands including the magnesium ion, participating in the reaction

$$1,3\text{-BPG} + \text{Mg.ADP} \underset{\text{(PGK)}}{\longleftrightarrow} \text{Mg.ATP} + 3\text{-PG}$$

The interactions of PGK and its natural ligands and ligand analogues have been widely studied by techniques such as equilibrium dialysis (Larsson-Raznikiewicz 1970; Minard *et al.* 1989), enzyme kinetic methods (Larsson-Raznikiewicz and Malmstrom 1961; Larsson-Raznikiewicz 1964; Larsson-Raznikiewicz 1970; Larsson-Raznikiewicz and Arvidsson 1971; Scopes 1978b; Tompa *et al.* 1986), gel filtration (Scopes 1978a), ^{1}H NMR spectroscopy (Fairbrother *et al.* 1988; Boyle *et al.* 1989; Fairbrother *et al.* 1989b; Fairbrother *et al.* 1990b; Fairbrother *et al.* 1990a; Graham and Williams 1991) and ^{31}P NMR spectroscopy (Rao *et al.* 1978; Ray and Rao 1988b; Ray and Rao 1988a; Ray *et al.* 1990), x-ray scattering (Pickover *et al.* 1979) and crystallography (Watson *et al.* 1982).

The binding properties of the nucleotides are relatively complex, since the apparent binding constant for a nucleotide depends on the pH, the ionic strength and the Mg^{2+} concentration, which affect the distribution of the various ionic forms of the molecule in solution, each of which will have its own "true" binding constants for the protein under that set of conditions (Bishop *et al.* 1990). The influence of pH, ionic strength and [free Mg^{2+}] on the equilibrium constants and kinetic properties of phosphate-transfer reactions has been demonstrated in several systems, including the PGK-GAPDH couple (Cornell *et al.* 1979; Lawson and Veech 1979; Veech *et al.*

1979). The important influence of these effects is ascribed mostly to their influence on the magnesium-nucleotide equilibria.

5.3.2 Important bulk properties of the intracellular environment

5.3.2.1 General principles

To mimic the ligand concentrations experienced by PGK in the intact cell, it is clearly necessary to perform experiments *in vitro* under the appropriate conditions of pH, ionic strength and [free Mg^{2+}]. Fortunately, good estimates of these parameters can be made.

A useful relationship exists between pH and the chemical shift of some phosphorus compounds, such as inorganic phosphate and the sugar phosphates, that are clearly visible in most ^{31}P NMR spectra of intact cells. The relationship is sufficiently sensitive and linear over the physiologically relevant range to allow good pH estimates to be made by this technique (Madden *et al.* 1991).

The intracellular pH was determined in this work from the chemical shift position of the cytoplasmic phosphate peak (Moon and Richards 1973), whereby the observed shift is interpreted by reference to the sigmoidal pH titration curve of the phosphate ^{31}P NMR chemical shift. The environment of the phosphate can have a significant effect on the accuracy of the pH determined (in some cases up to 0.5 pH unit) (Roberts *et al.* 1981). Particularly important parameters that can affect the titration curves include the ionic strength, the presence of divalent cations such as Mg^{2+}, the temperature and the concentrations of some proteins (Roberts *et al.* 1981; Seo *et al.* 1983). These considerations make it necessary that the pH titration curve used to determine the intracellular pH is itself produced under

conditions that mimic the intracellular environment in these important respects.

The ionic strength has been estimated in yeast as between 0.11 and 0.25 M, typically 0.15 M (Gancedo and Gancedo 1973) The influence of ionic strength, **I**, on chemical rates and equilibria involving charged species is governed by the Debye-Hückel relationship (Van Holde 1971), which states that the reaction rate is proportional to the square root of the ionic strength, so one need not be too concerned with its precise determination in each system examined.

Probably the most critical parameter influencing nucleotide binding is the free magnesium ion concentration. It is probably also the most difficult to determine using only natural endogenous probe molecules. There are a number of fluorescent and NMR techniques available that depend upon the introduction of synthetic probe molecules (such as fluorocitrate and FURA, or the newer NOTPME (Ramasamy *et al.* 1991)) to the system, and some that rely on the NMR observation of endogenous species such as citrate and ATP (London 1991).

The most accessible method of determining the intracellular free magnesium ion concentration is probably that based on measuring the chemical shift differences between peaks of the NTP resonances seen in the intact cell. This is particularly convenient since it can be performed on the same perifused cell sample and almost at the same time as acquiring the ^{19}F NMR data from the fluorine-labelled proteins in the intact cell. A suitable ^{31}P NMR spectrum can be obtained from the perifused cells in less than half an hour.

One method uses the α and β peaks of ATP, relying on the α resonance as an internal standard unaffected by Mg^{2+} complexation (Gupta *et al.* 1978). The other method uses the γ peak of ATP and the β peak of ADP (Tyler-Burt *et al.*

1990); although this method claims some advantages over the ATP method, its application in the cell systems studied in this work is prevented by being unable to adequately resolve the ATP and ADP signals, and by the undetectably low levels of ADP in many cells.

5.3.2.2 *Measurements of intracellular pH used in this work*

^{31}P NMR spectra obtained from perifused cells were used to determine the pH and estimate the free magnesium ion concentrations in the same cell populations used for the ^{19}F NMR studies. Typical ^{31}P NMR spectra of intact yeast cells under different metabolic conditions were shown in Figure 4.2 of Chapter 4.

The ^{31}P NMR chemical shift vs. pH titration curve used in this work was determined by Kevin Brindle *et al.* (Kevin Brindle, Manchester, personal communication) according to the method of den Hollander (den Hollander *et al.* 1981). It was based on a sample containing 30 mM NH_4Cl, 200 mM KCl, 20 mM $MgCl_2$ and 10 mM KH_2PO_4, and the chemical shifts referred to PCr. The solution was chosen to mimic the relevant intracellular conditions discussed in the preceding section. The titration curve has been parameterised and expressed as (Seo *et al.* 1983)

$$pH = pK_a + \log [((\delta PCr-\delta P_i)-\delta_{min}) / (\delta_{max}-(\delta PCr-\delta P_i))] \qquad \text{(Eq. 5.1)}$$

where δPCr and δP_i are the chemical shift positions of phosphocreatine and inorganic phosphate respectively, quoted as the distance upfield from an external MDP standard. The pK_a is 6.75. δ_{min} is the acid shift limit (3.27 ppm) and δ_{max} is the alkaline shift limit (5.69 ppm), both quoted as values downfield from PCr. The chemical shift of each individual MDP standard used was calibrated with respect to phosphocreatine by experiment. Typically, the PCr resonance was about 19.2 ppm upfield of the MDP resonance. The phosphate peak was typically around 14.4 ppm upfield of the MDP standard.

The function in Equation 5.1 is plotted in Figure 5.1, illustrating that chemical shift is relatively sensitive to pH changes in the physiological pH range.

5.3.2.3 *Measurements of free intracellular Mg^{2+} used in this work*

The free magnesium in the intact cells was determined from the titration of the NTP β phosphate peak relative to the NTP α peak (Gupta *et al.* 1978). It was assumed that it was appropriate to treat the NTP peaks seen in ^{31}P NMR spectra of the cells as if they were from ATP alone, since HPLC analysis of extracts had shown that the NTP present was over 80 % ATP. The titration curve used was that of Gupta (Gupta *et al.* 1983b). The sigmoidal titration curve can be parameterised and expressed as (Gupta *et al.* 1983a; London 1991)

$$Mg^{2+}_{free} = K_d^{MgATP} (\Delta_{obs} - \Delta_{free}) / (\Delta_{bound} - \Delta_{obs}) \qquad \text{(Eq. 5.2)}$$

where Δ_{obs} is the observed difference between δ_α and δ_β, the chemical shifts of the ATP α and β peaks respectively. Δ_{free} and Δ_{bound} are the limits of the difference under conditions of no complexation (8.432 ppm) and full complexation (10.778 ppm) respectively (Gupta *et al.* 1983a).

The value of K_d^{MgATP} is a composite dissociation constant incorporating terms for each of the various ionic species present (ATP^{4-}, $HATP^{3-}$ etc.). It is dependent on pH, ionic strength and temperature. The value used was 50 μM, being that determined under relatively physiological conditions, i.e. pH 7.2, **I** = 0.15M, 25 °C (Gupta *et al.* 1983a; Gupta *et al.* 1983b; London 1991).

The values of free magnesium determined by this technique depend critically on the values used for the K_d and the limiting shifts. In his recent review, London (London 1991) explains that literature values for the K_d vary widely (from around 38 to around 86 μM). More importantly, there is a significant

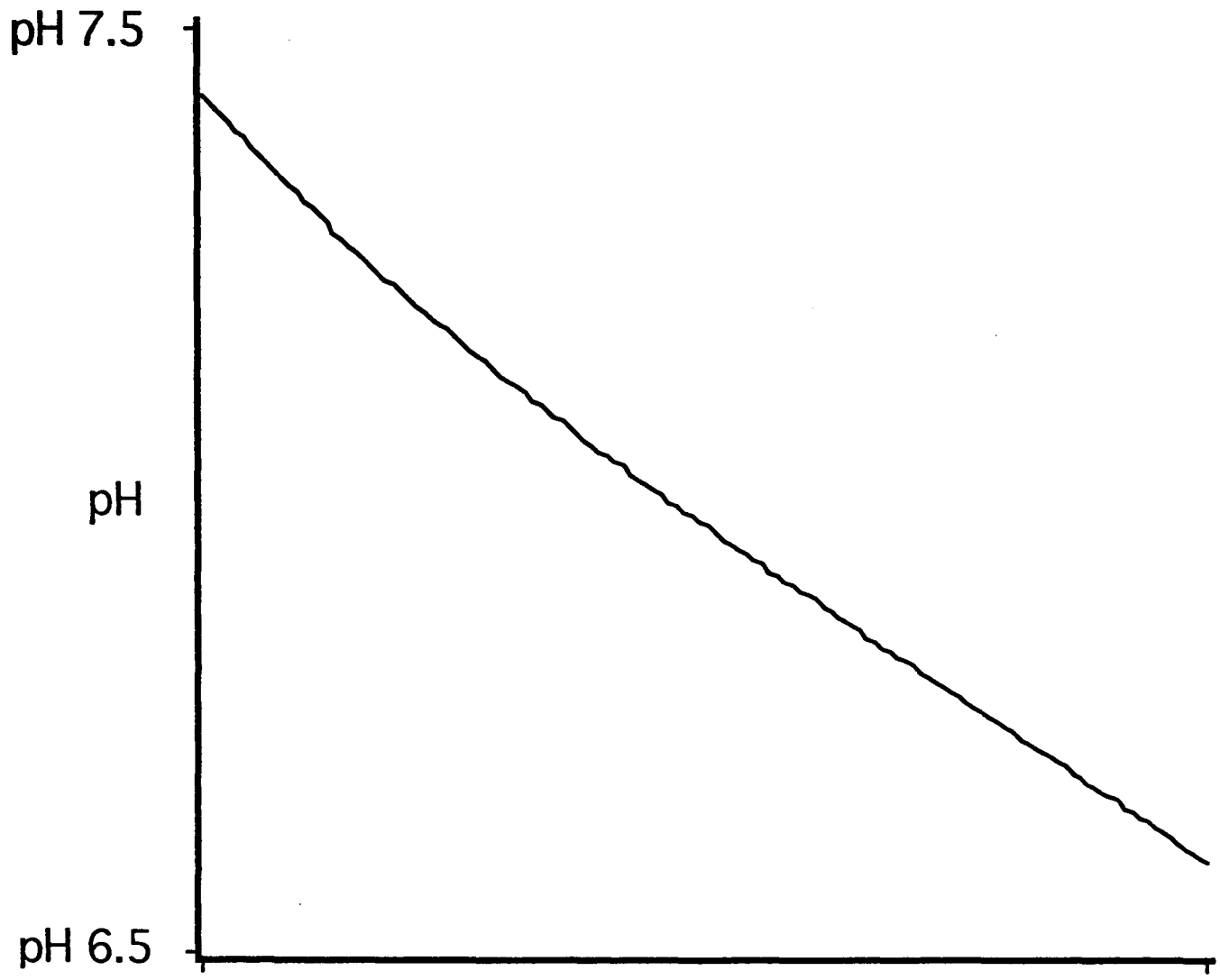

Theoretical curve calculated from Eq. 5.1, showing the variation of pH with the chemical shift position of the inorganic phosphate resonance.

The chemical shift of the phosphate is quoted as ppm upfield from the methylene diphosphonate standard.

Figure 5.1

mismatch between the K_d and the typical intracellular free magnesium concentrations. The values obtained are subject to large errors because the observed shift differences are so close to the (all bound) limit, and the titration curve is very steep in the region of interest. This difficulty is illustrated in Figure 5.2, which is a plot of Equation 5.2 highlighting the typical region of interest.

5.4 Effectors of the ^{19}F NMR spectrum from labelled PGK *in vitro*

5.4.1 ^{19}F NMR spectra

Spectra were acquired from solutions of PGK suspended in a 50 mM HEPES buffer containing 10 μM EDTA, 2 mM DTT and 10 % D_2O to act as field frequency lock. The pH was 7.2 (uncorrected for any deuterium isotope effect), the ionic strength 0.15 M with potassium acetate. Each sample was exchanged from a stock solution into the desired medium by gel filtration on a Pharmacia PD10 column.

To minimise the acquisition time needed to complete the experiments, the T_1 spin-lattice relaxation time of the sample was determined by an inversion-recovery experiment (Vold *et al.* 1968). This involves inverting the net z magnetisation (180° pulse), allowing the net magnetisation along the -z axis to decay for a time τ (by T_1 processes alone as there is no net xy magnetisation), "flipping" the net magnetisation in to the xy plane (90° pulse) and acquiring the resultant free induction decay. The magnitude of the signal depends on how far the relaxation processes had got before flipping and observing the signal.

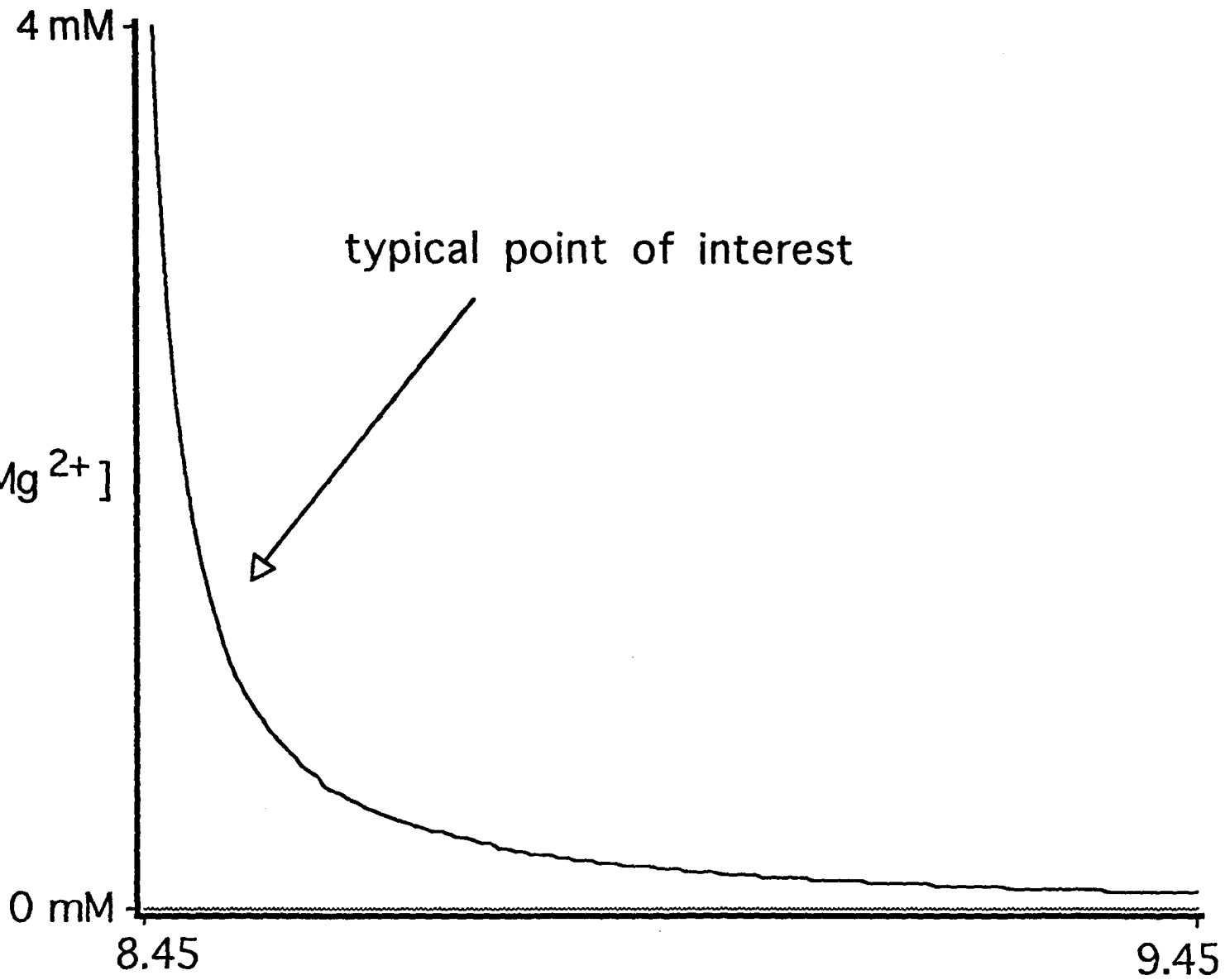

Theoretical curve calculated from Eq. 5.2, showing the variation of the free magnesium ion concentration with the ^{31}P NMR chemical shift difference between the α and β phosphate peaks of ATP.

For some cell types used in this thesis, typical apparent free Mg^{2+} levels were 0.2 to 1 mM. The BJ2168 cells used for the fluorine-labelled enzyme work had higher than average levels of free magnesium, around 2 to 4 mM. The difficulty in determining a reliable estimate of the free magnesium by this method is clear.

Figure 5.2

Schematically, the pulse sequence is d - 180° - τ - 90° - acquire, where d is a delay to allow re-equilibration of the spin system before each successive perturbation, 180° and 90° are broad-band pulses of those tip angles, and τ is the inversion recovery delay. Spectra were acquired at a series of τ values. The data are presented in Figure 5.3. The peak intensity decays exponentially with the delay τ, and the T_1 time constant can thus be determined by fitting the experimental peak intensities to an expression such as

$$I_t = I_0[1 - 2.Q.\exp(-\tau/T_1)] \qquad \text{(Eq. 5.3)}$$

where I_t and I_0 are the signal intensities observed with τ = t and τ = infinite (in practice, around 5 T_1) respectively, and Q is a constant determined by the quality of inversion (usually 1).

The signal collected in a given time is maximised when the pulse angle used is given by the expression (due to Richard Ernst, Zurich) (Derome 1987)

$$\cos \alpha_E = \exp(-\tau_R/T_1) \qquad \text{(Eq. 5.4)}$$

where τ_R is the time between pulses, T_1 is the spin-lattice relaxation time and α_E is the Ernst angle, the optimum pulse angle for the experiment. By setting τ_R equal to the data acquisition time and introducing no other delays, the signal-to-noise ratio of the acquisition is optimised. The T_1 value determined at 9.4 T was 0.6 ± 0.04s for each peak, and with a typical acquisition time of 0.67 s, α_E is 70°. At 7 T, a similar experiment showed the T_1 value was c. 0.4 s.

Typical spectra obtained from 5-fluorotryptophan-labelled PGK *in vitro* are presented in Figure 5.4. Note that the chemical shift difference between the two peaks can vary by at least 0.6 ppm.

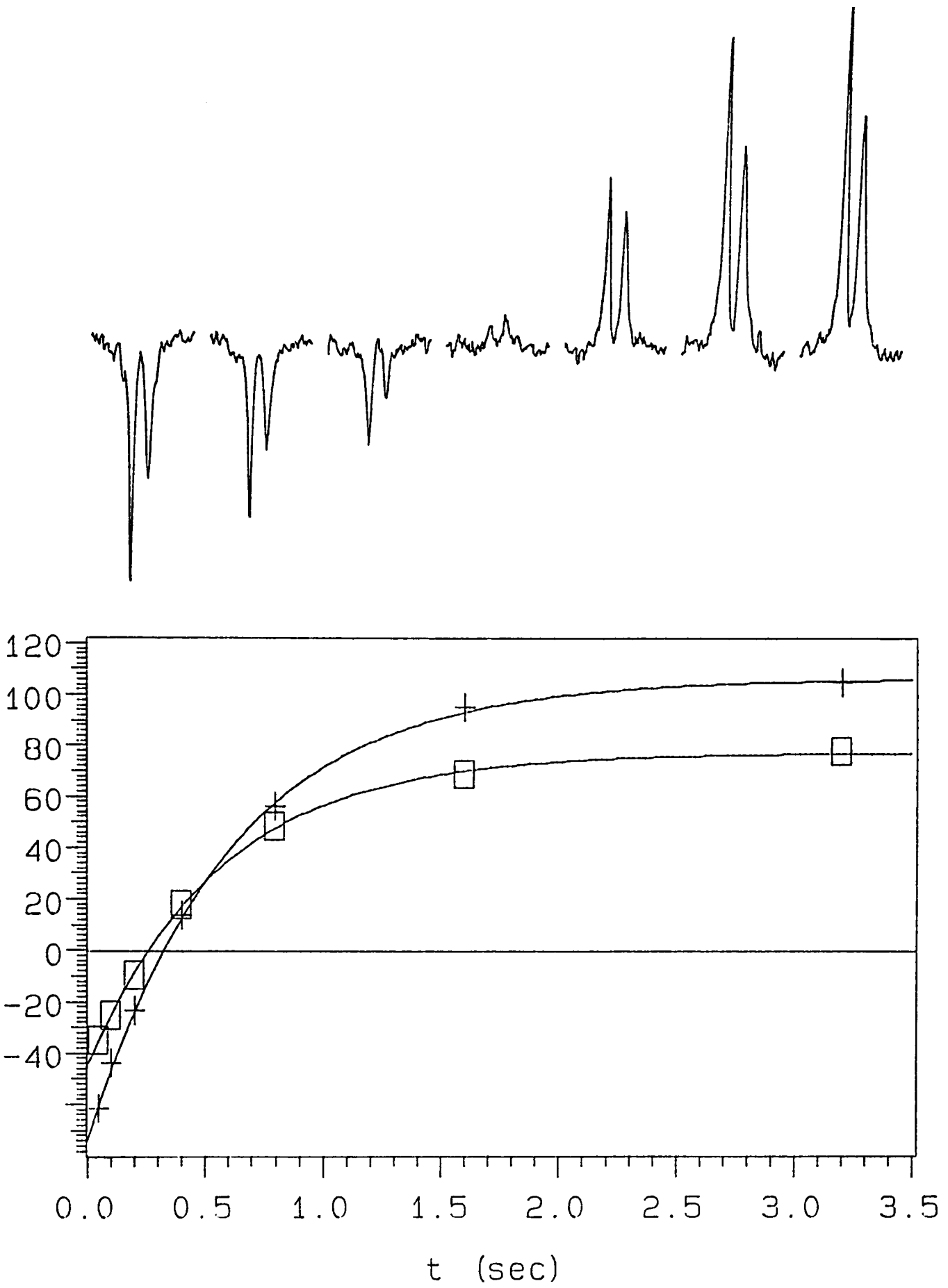

Inversion recovery experiment to determine the longitudinal relaxation time constant, T_1, for the peaks from the PGK. (Top): ^{19}F NMR spectra of 5-fluorotryptophan-labelled 3-phosphoglycerate kinase. (Bottom): a plot of the peak intensities as a function of the inversion recovery delay τ.

0.6 mM PGK was studied at 30 °C in a buffer at pH 7.2, I=0.15 M. The peak intensities were plotted as a function of τ, the inversion recovery delay, and fitted to an exponential function to determine the T_1s (see text). The results were the same whether based on peak heights or peak areas. The acquisition time was 0.67 s, the spectral width 9000 Hz. The d1 delay was 3 s, the d2 delay (τ) was varied over 7 steps from 50 ms to 3.2 s. Spectra were acquired in blocks of 100 transients, stepping through the τ list repeatedly until 1000 transients had been collected at each d1 value.

Figure 5.3

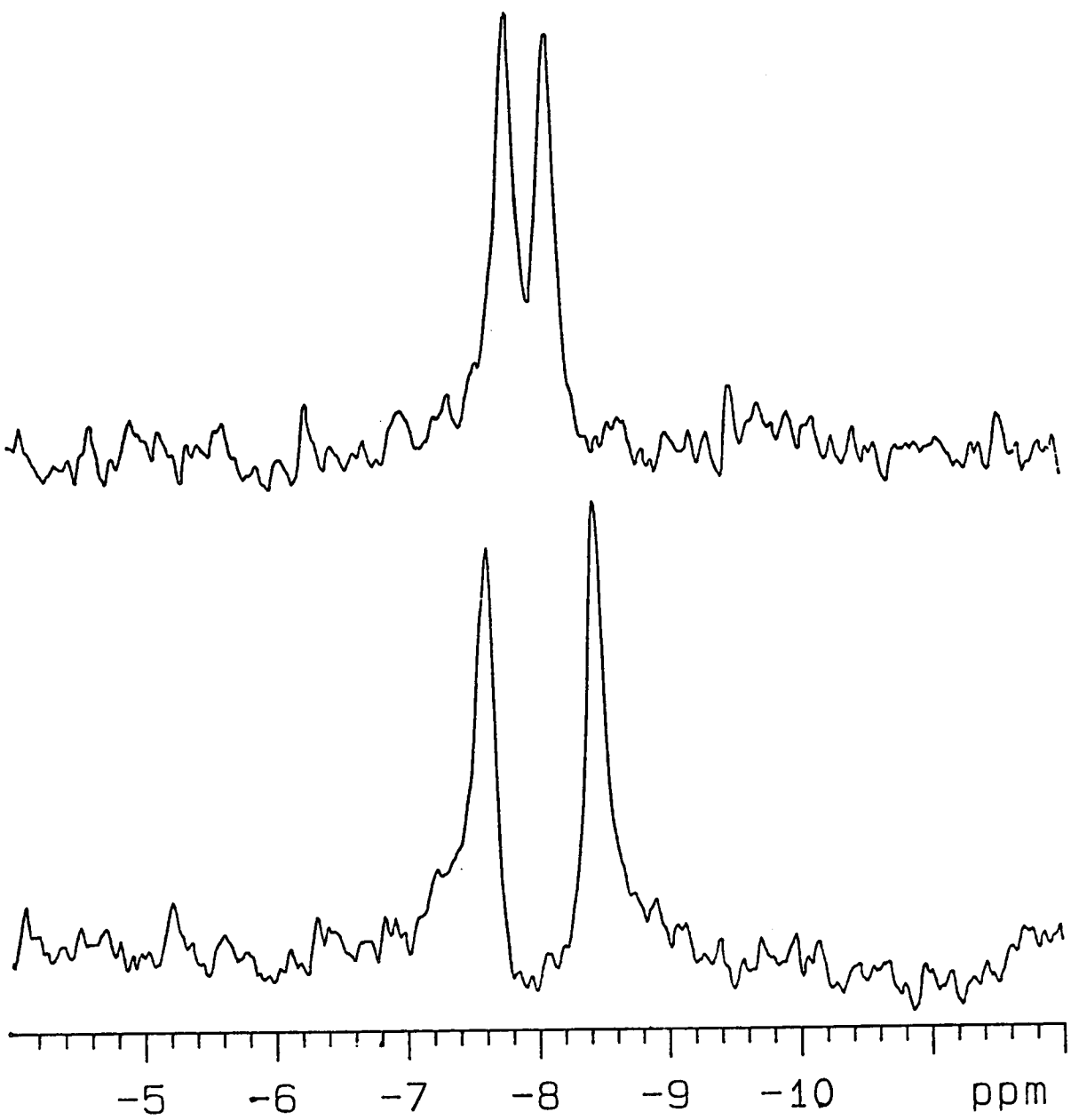

Sample ^{19}F NMR spectra obtained from purified 5-fluorotryptophan-labelled phosphoglycerate kinase studied at 9.4 T.
The spectra were acquired from a c. 0.5 mM PGK sample at 30 °C. The PGK was dissolved in a HEPES buffer at pH 7.2, I = 0.15 M. 2000 transients were collected over 20 minutes using a spectral width of 9000 Hz and 12000 digitisation points. The lower spectrum is of PGK alone; the upper spectrum was acquired in the presence of approximately 5mM MgADP. As discussed in Chapter 4, some spectral distortion is evident in the spectra presented. It originates from fluorinated material in the NMR probe, apparent at the high gain settings used, and could be eliminated with a very short (200μs) spin echo sequence.

Figure 5.4

5.4.2 pH

There were no significant differences between ^{19}F NMR spectra obtained from 5-fluorotryptophan-labelled PGK at pH 6.0, 7.0, 7.2, 7.5 and 8.0. It was inferred that pH was not an important direct effector in determining the chemical shifts observed in the intact cell.

5.4.3 3-phosphoglycerate and 1,3-bisphosphoglycerate

The chemical shifts of the two PGK peaks in the ^{19}F NMR spectrum were determined at 0, 5, 10, 50, 100 and 1000 μM 3-phosphoglycerate (3-PGA). The downfield peak moved only 0.05 ppm (upfield) during the titration, the upfield peak only 0.09 ppm (downfield). It was concluded that changes of 3-PGA in the physiological range (a steady-state value of up to c. 300 μM (Brindle 1988)) were not a very important effector in determining the chemical shifts observed in the intact cell.

1,3-bisphosphoglycerate (1,3-DPG) is unstable and cannot simply be added to the PGK solution. In the presence of MgATP and 3-PGA, however, the mixture will move toward an equilibrium mixture of ATP, ADP, 3-PGA and 1,3-DPG. The equilibrium constant at 38 °C, pH 7.0, I = 0.25 M, and free Mg^{2+} = 1 mM is c. 3.6 x 10^3 (Cornell *et al.* 1979). An experiment with 4 mM MgATP and 10 mM 3-PGA would thus give rise to about 1.7 mM 1,3-DPG and ADP in the equilibrium mixture.

When labelled PGK was studied with different ligands, the chemical shift difference between the two peaks moved from 0.93 ppm in the absence of ligands to 0.46 ppm in the presence of MgATP alone to 0.34 ppm in the presence of the equilibrium mixture. 1,3-DPG has been found to have a strong affinity for PGK, the K_d having been reported to be 50 nM by ^1H NMR (Fairbrother *et al.* 1990a) and 60 nM by a gel filtration technique (Scopes

1978a). However, its binding is not competitive with MgADP, which binds nearer to the tryptophan residues and certainly has a large effect on the chemical shifts, as discussed in the following section.

It was concluded that 1,3-DPG was unlikely to have a significant impact on the chemical shifts seen in the intact cell.

5.4.4 ATP, ADP and AMP

5.4.4.1 Defining the appropriate pH and [Mg^{2+}] to use

The influence of the important adenine nucleotides was investigated in a series of titration experiments. Since the binding of nucleotides is so heavily influenced by the pH and free Mg^{2+} concentration, these parameters were measured as described in the preceding sections by ^{31}P NMR in the intact BJ2168 cells used for the ^{19}F NMR experiments.

The intracellular pH was estimated as 7.15 in the anaerobic glucose-fed cells. The cytosolic pH appeared slightly more acidic (c. 0.03 pH units) in the ethanol-fed and starved cells, but measurements were not repeated to statistical significance. This value was slightly more acid than the 7.22 found in another cell line (see Chapter 6) and very close to the 7.17 found with a third cell line (Brindle 1988).

The free Mg^{2+} concentration was estimated from the chemical shift difference between the ATP α and β peaks as described. This was relatively simple in the glucose-fed cells where the ATP resonances were clearly visible, and somewhat less reliable in the case of the starved cells where there is virtually no visible ATP. Because the [Mg] versus chemical shift function is so steep in the region of interest, even adjacent data points in the digital data set gave [Mg] values varying by around 0.5 mM. The best estimates obtained were that

the free magnesium concentration lies between 1.9 and at least 3.7 mM, with some determinations giving values as high as 40 mM (almost certainly erroneous). A mid-point value of 3 mM was taken to be typical.

The estimate of 3 mM free magnesium in these cells (BJ2168) is higher than that determined by the same technique in two other cell lines (FY3-1 and BC3). Figures for this parameter in the literature also tend to be around 0.2 to 1 mM (Veloso *et al.* 1973; Veech *et al.* 1979; London 1991). This discrepancy seems reasonable given that these cells have such low levels of vacuolar polyphosphates. The polyphosphates are ordinarily involved in the complexing and homeostasis of magnesium in the vacuole (Okorokov *et al.* 1980; Klionsky *et al.* 1990), and the loss of polyphosphates could, therefore, be associated with an increase in the cytoplasmic free magnesium concentration.

Because of the remaining uncertainty in the free magnesium determinations, the nucleotide experiments were performed with both high and low concentrations of free magnesium.

5.4.4.2 The influence of ATP, ADP, and AMP on the ^{19}F NMR chemical shifts

Simple titration experiments were performed with PGK solutions that had the same pH and ionic strength as the yeast cytoplasm (pH 7.15, I=0.15 M). The PGK concentration used was 25 to 30 mg/ml (about 0.6 mM), the same as measured in the yeast cytoplasm (see Chapter 3). This high protein concentration is important, since the presence of the PGK nucleotide binding site may have a significant effect on the free nucleotide concentrations.

Typical titration curves are shown in Figure 5.5, which shows the chemical shift difference between the two peaks as a function of nucleotide concentration. The total magnesium concentration was maintained at 0.5 mM

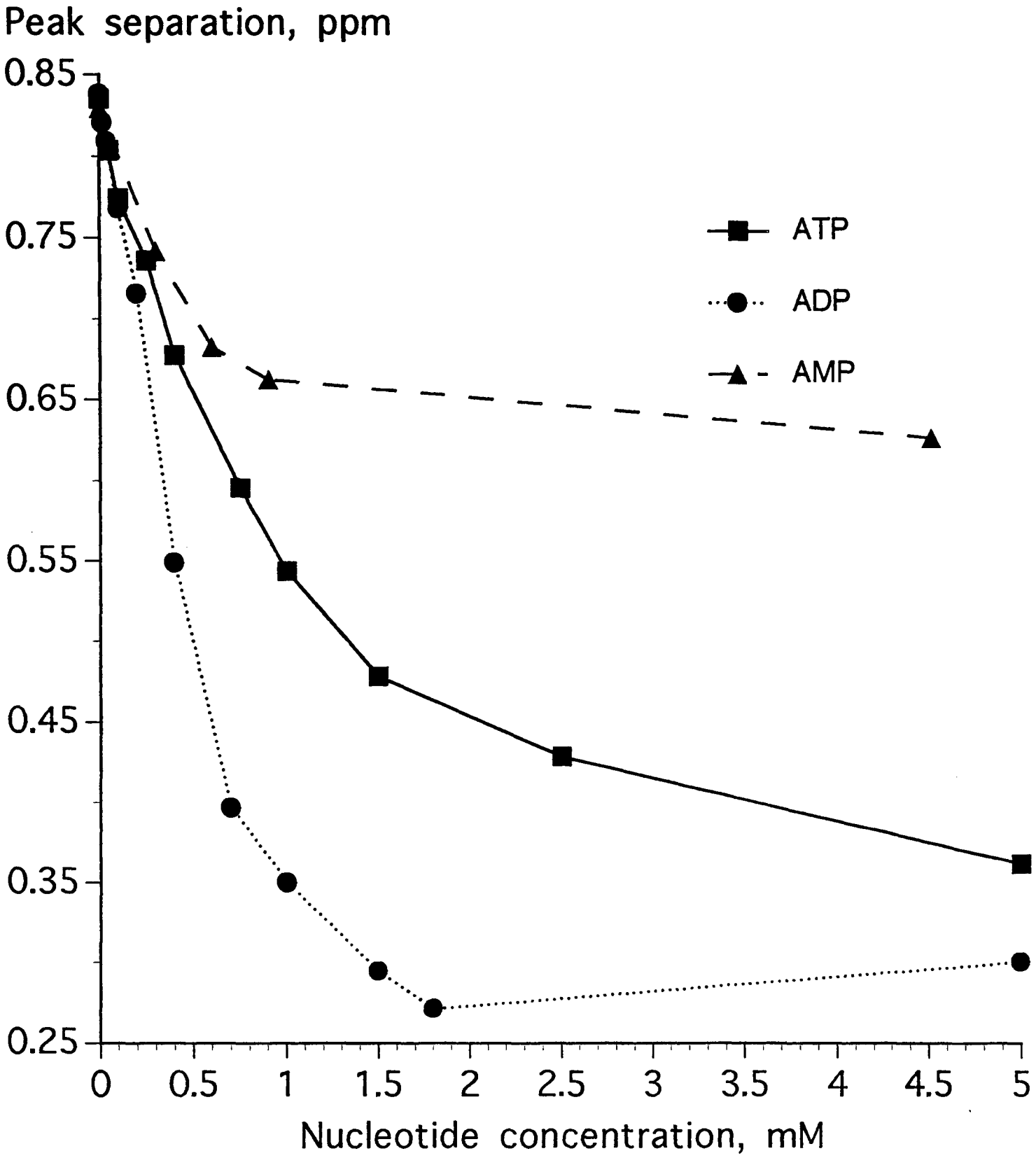

The chemical shift difference between the two peaks in ^{19}F NMR spectra of 5-fluorotryptophan-labelled PGK as a function of the nucleotide concentration.
PGK (c. 0.6 mM) was studied at 30 °C in a buffer at pH 7.2, I = 0.15 M. Concentrated, neutralised stock solutions of $MgCl_2$, AMP, ADP, or ATP were added to the enzyme solution to create mixtures with a series of nucleotide concentrations. The total magnesium ion concentration was maintained at 0.5 mM above the total nucleotide concentration at all points. The NMR spectra were acquired as described in the legend to Figure 5.4.

Figure 5.5

in excess of the total nucleotide concentration. The linewidths of the upfield peak showed a pronounced variation with the nucleotide concentration, presumably due to chemical exchange broadening. This was discussed as a possible source of line broadening in the intact cell in Chapter 4. The linewidths as a function of nucleotide concentration are plotted in Figure 5.6. The data is taken from the same experiment as that in Figure 5.5. The data points have been connected for clarity only, and not to indicate any interpolation of the data.

These data have only been treated in a qualitative way. There are at least ten different significant equilibria in operation in a mixture of PGK, Mg^{2+} and ATP (Fairbrother *et al.* 1990b), and the different effects of each component can not be trivially isolated. The situation is complicated because of the existence of a second, non-independent binding site for ATP (Larsson-Raznikiewicz 1973; Schierbeck and Larsson-Raznikiewicz 1979; Fairbrother *et al.* 1990b), that may be the general anion binding site.

As the Mg-nucleotide concentrations are increased beyond those shown in Figure 5.5, some small reversal of the trend toward smaller peak separations occurs. This is evident for ADP binding in Figure 5.6, but also occurs for ATP at MgATP concentrations in excess of around 10 mM. This effect may arise from the non-specific interaction of high concentrations of ATP or ADP at the general anion binding site (Fairbrother *et al.* 1990a). This behaviour is evident in the kinetic properties of PGK, where high concentrations of nucleotides inhibit the reaction in the absence of sulphate (Larsson-Raznikiewicz 1964)(Larsson-Raznikiewicz 1973; Schierbeck and Larsson-Raznikiewicz 1979).

Despite the difficulties with these experiments, it seems clear that the affinities of the nucleotides for PGK are different, with ADP > ATP >> AMP.

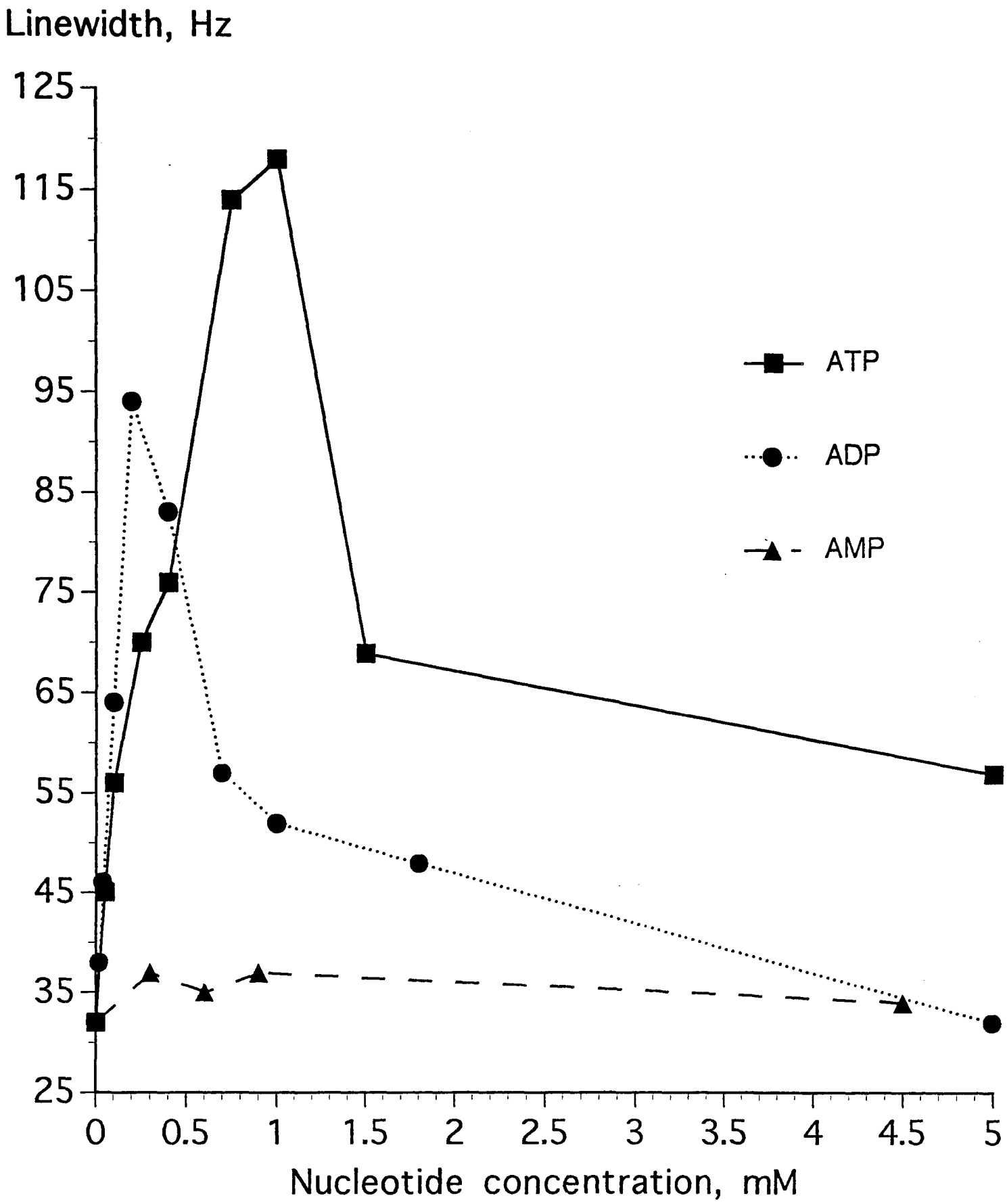

The linewidth of the upfield peak in ^{19}F NMR spectra of 5-fluorotryptophan-labelled PGK as a function of the nucleotide concentration.
The experimental details are as described in Figure 5.5. The linewidths were obtained by an iterative-fit procedure matching Lorenzian lines to the experimental data with Varian's VNMR utility software.

Figure 5.6

This trend is in agreement with previous measurements by gel filtration studies (Scopes 1978a) and inhibitor titrations (Larsson-Raznikiewicz and Arvidsson 1971).

5.4.5 The chemical shift changes expected from nucleotide binding

The changes in the ^{19}F NMR spectrum that accompany the binding of nucleotides may be wholly the result of solvation and conformational changes that accompany the binding. However, Trp 308 does lie close enough to the bound nucleotide in the crystal structure (Watson *et al.* 1982) to consider what effect the nucleotide itself may have.

A well-known phenomenon in NMR is the ring-current shift (Harris 1986). Considered in classical terms, the static B_0 field induces motion in the electron clouds above and below the plane of an aromatic ring. The motion of the electrons is such that the field produced opposes the applied static field to create localised disturbances in the field whose magnitude can be calculated from a knowledge of the aromatic systems involved. The geometry of the effect is such that the field is reduced ("deshielding") in the plane of the ring, and increased perpendicular to the plane ("shielding").

There are several theoretical approaches to calculating ring-current shifts, the best-known of which are probably the dipolar model of Pople (Pople 1956), the current-loop model of Johnson and Bovey (Johnson and Bovey 1958) and a quantum mechanical model of Haigh and Mallion (Haigh and Mallion 1972). Their application has been reviewed by Perkins (Perkins 1982). Each of the models is a function comprising intensity factors, proportionality constants and spatial geometric terms. In many biological applications, there is little to choose between the different models.

Perkins (Perkins 1982) has conveniently collected together many of the required constants into simple terms that allow the ready calculation of the ring-currents from molecules of biological interest. For multiple-ring systems such as adenine, one can satisfactorily approximate the situation by summing the effects from the component rings.

Using the dipolar approximation, where δR, the ring-current shift in ppm, is given by (Perkins 1982)

$$\delta R = \Sigma_i K_i (3 \cos^2 \theta - 1) r_i^{-3} \qquad \text{(Eq. 5.5)}$$

where K is a constant for a given ring system, θ is the dihedral angle between the plane of the ring and the vector connecting the affected nucleus and the centre of the ring, and r is the length of that vector, here in Angstroms.

For adenine, K = 19.654 for the 6-ring and 13.267 for the 5-ring (Perkins 1982). Taking approximate measurements from the crystal structure (Watson *et al.* 1982) gives the following geometric parameters: The distance between the fluorine atom on 5-fluorotryptophan at Trp 308 and the centre of the 6-ring in the ATP adenine is around 4.9 Å, at a dihedral angle of 72° The distance to the centre of the 5-ring is around 5.1 Å at a dihedral angle of 68°.

Evaluation of the expression in Eqn. 5.5 with the parameters given above leads to a predicted ring-current shift of $^{-}$0.17 ppm. Allowing for the actual distances being 10 % greater than the estimates used leads to value of $^{-}$0.13 ppm. These values are not large enough to account for the observed chemical shifts of around 0.5 ppm. Of greater significance is the sign of the result, which shows that the effect would be shielding, causing the peak to move upfield on binding ATP, the opposite of what is observed. If the indole or adenine rings were rotated through 90° relative to one another, such that the dihedral angles involved are now 18 and 22°, the expression now evaluates to a predicted ring-current shift of 0.44 ppm downfield, ignoring any change in

the interatomic distances. Even allowing for a 1.3 Å increase in the distance (arbitrarily chosen as the radius of the adenine 6-ring), the expression evaluates to 0.22 ppm.

The relative positions of the indole and adenine rings in the published crystal structure (Watson *et al.* 1982) were subject to relatively large errors, and it is not inconceivable that the relative orientation of the groups is as much as 90° different from that published (Herman Watson, Bristol, personal communication). It would be interesting to learn the true orientation of the groups involved, and if a ring-current shift is important. There seems to be no shift observed in the ^{1}H NMR spectrum at Trp 308 upon nucleotide binding (Fairbrother *et al.* 1989a), though the proton assigned to Trp 308 in the ^{1}H NMR spectrum may not be close to the relevant carbon-5 proton (Wayne Fairbrother, Oxford, personal communication). The fluorine nucleus is almost the nearest part of the indole ring to the adenine ring (see Figure 4.6).

It may be possible to improve the reliability of the structural information used to calculate the expected ring-current shifts and other parameters by performing energy minimisation calculations. The molecule needs to be simulated in an appropriately hydrated environment, with some care in the choice of minimisation parameters used. The crystal structure provides a good starting point, but the calculations have not yet been attempted.

5.4.6 Mimicking *in vitro* the spectra seen *in vivo*

5.4.6.1 Introduction

Because of the complexities of calculating the combined effects of the various parameters involved, an empirical approach has been taken to create

conditions *in vitro* under which the ^{19}F NMR spectrum of the 5-fluorotryptophan-labelled PGK are comparable to those seen *in vivo*.

Labelled PGK was studied at pH 7.15, ionic strength 0.15 M and varying free magnesium concentrations. The concentration of the PGK itself was also the same as that typically seen in the intact cell, around 25 mg/ml, i.e. c. 0.5 to 0.6 mM.

5.4.6.2 *Determining the intracellular nucleotide concentrations*

The nucleotide concentrations in the cell were determined from perchloric acid cell extracts prepared from cells perifused for 3 hours, i.e. to the midpoint of a typical cell perifusion used for collecting data from the intact cells. For each metabolic state studied (starved, ethanol-fed, glucose-fed) two extracts were prepared. The nucleotides were quantitated from ^{1}H-decoupled ^{31}P NMR spectra, examples of which are shown in Figure 4.8 in Chapter 4.

The mean nucleotide concentrations in the cell water of BJ2168 cells for each perifusion condition are shown below in Table 5.1.

Table 5.1

Metabolite	Starved cells	Ethanol-fed cells	Glucose-fed cells (anaerobic)	Glucose-fed cells (aerobic)
NTP	0.74	0.67	2.96	2.56
NDP	1.44	1.24	0.36	0.26
NMP	1.46	0.83	c. 0.1	c. 0.1

Cellular concentrations of nucleotide phosphates under different perifusion conditions
Perchloric acid cell extracts were quantitated with reference to an external standard in ^{1}H-decoupled ^{31}P NMR spectra. The different nucleotides cannot be individually quantitated by this technique, but HPLC analysis has shown that the adenine nucleotides predominate. The values are the means of two determinations, which were not significantly different from each other. The values are quoted as μmol per ml cell water, i.e. mM in the cell water.

5.4.6.3 *Calculating the total magnesium concentration*

To simulate the magnesium-nucleotide environment of the cell, the total nucleotide concentrations (Table 5.1) were combined with estimates of the free magnesium ion concentration to give the total magnesium ion concentration in the mixture. It was assumed that all the NTP measured was ATP. The equilibria were determined from the pH-corrected equilibrium constants (Lawson and Veech 1979) from

$$Mg.Nuc = (Mg^{free}.Nuc^{total}) / (Mg^{free} + K_d) \qquad \text{(Eq. 5.6)}$$

and

$$Mg.Nuc^2 - (Nuc^{total} + Mg^{total} + K_d).MgNuc + ... \\ Mg^{total}.Nuc^{total} = 0 \qquad \text{(Eq. 5.7)}$$

where Mg.Nuc, Nuc, and Mg are the concentrations of the magnesium-nucleotide, nucleotide and magnesium ion respectively. The superscripts are self-explanatory. K_d is the magnesium ion - nucleotide dissociation complex for the particular nucleotide in question.

The effective dissociation constants are derived from compound dissociation constants for the different ionic species and $[H^+]$ terms as

$$K_d^{nuc} = (K_a^{nuc} + [H^+]) / (K_a^{nuc}.k_{nuc} + k^+_{nuc}.[H^+]) \qquad \text{(Eq. 5.8)}$$

where K_d^{nuc} is the effective dissociation constant, K_a^{nuc} is the association constant for the H^+.Nuc/Nuc + H^+ equilibrium, and k_{nuc} and k^+_{nuc} are the association constants of magnesium for the unprotonated and protonated forms of the nucleotide, respectively. These parameters have been tabulated by Lawson and Veech (Lawson and Veech 1979), as shown in Table 5.2. The values are for a temperature of 38 °C. No correction for the temperature has been made in the calculations used in this work, which was performed at 30 °C.

Table 5.2

Nucleotide	Acid dissociation M	Magnesium association (unprotonated nucleotide) M^{-1}	Magnesium association (protonated nucleotide) M^{-1}	Mg.nucleotide K_d at pH 7.2
ATP	1.08×10^{-7}	1.39×10^{4}	35.5	115 μM
ADP	1.20×10^{-7}	1.32×10^{3}	32.4	1.14 mM
AMP	3.24×10^{-7}	6.01×10^{1}	9.31	15.4 mM

Acid dissociation and magnesium binding constants for phosphorylated intermediates, taken from Lawson and Veech (Lawson and Veech 1979)
These parameters were used with Equations 5.6 to 5.8 to calculate the free magnesium ion concentration in mixtures of magnesium ions and nucleotides at different pH values. The last column shows values of the K_ds calculated at pH 7.2.

5.4.6.4 *The spectra of labelled PGK in mixtures of magnesium nucleotides*

Samples of 5-fluorotryptophan-labelled PGK at physiological concentrations (c. 0.6 mM) were exchanged into buffers (pH 7.2, I=0.15 M) containing combinations of nucleotides at the same concentrations as those found in the starved, ethanol-fed and the anaerobic glucose-fed cells. The free magnesium concentration was set at 3 to 4 mM (see section 5.3.2.3). The samples also contained 10 % D_2O to act as a field frequency lock for the NMR experiments. The samples were studied at 30 °C.

The experiments were performed twice, and the mean results are tabulated in Table 5.3. There was no significant difference between the repeats.

Table 5.3

Metabolic condition	Simulated environment	Intact cell data
Starved	0.28	0.34
Ethanol-fed	0.28	0.41
Glucose-fed	0.28	0.55

^{19}F NMR spectra chemical shift differences, in ppm, between the two peaks of 5-fluorotryptophan-labelled PGK either in the intact cell or in a buffer of similar pH, ionic strength, enzyme, nucleotide and free magnesium concentration
The intact cell data are taken from Table 4.2 in Chapter 4. The simulated environment included c. 0.6 mM labelled PGK at pH 7.2, I=0.15 M. The nucleotide concentrations were determined in perchloric acid cell extracts, and are described in Table 5.1. The total magnesium concentration was 7 mM, and the free magnesium ion concentration in the simulations was approximately 3 to 4 mM, as determined from ^{31}P NMR spectra of the intact cells, described in section 5.3.2.3. For comparison, the shift difference in the absence of ligands is around 0.7 ppm.

Clearly, this simulated intracellular environment is not sufficiently akin to the true situation to reproduce the ^{19}F NMR spectra seen from the intact cell. One or more of the parameters used must be at fault. There is no suggestion that an effector is "missing" since the effect observed is greater than that seen in the intact cell. Since the pH and ionic strength can be estimated fairly accurately, the discrepancy presumably arises from the nucleotide or free magnesium concentrations. Relatively small errors in the free magnesium or nucleotide concentrations may account for the discrepancy with the starved or ethanol-fed situations, but there is a much greater discrepancy with the glucose-fed data.

A further series of experiments was carried out to investigate the effect of reducing the free magnesium ion concentration to the minimum plausible level of 0.5 mM and the ADP concentrations to lower values, concentrating on the glucose-fed situation. Since the AMP appears to be of little importance, this component was omitted from the subsequent experiments.

5.4.6.5 *Sequential studies of the effect of Mg^{2+} and ADP*

^{19}F NMR spectra were collected from solutions of 5-fluorotryptophan-labelled PGK as described in the previous section. The nucleotide and magnesium components of the mixture were added sequentially rather than simultaneously, though, and the free magnesium concentrations used were 0.5 and 3 mM. The experiments were performed so that combinations of high ADP / low magnesium and high magnesium / low ADP were present. The ATP concentration is more likely to have been correct than the ADP, because it can be observed as expected in the intact cell and is not likely to have been formed as an extraction artefact. The previous experiments have also shown a greater sensitivity to [ADP] than [ATP]. Consequently, the ATP concentration was not varied. The data are presented in Table 5.4.

Table 5.4

	[ATP], mM	[ADP], mM	[free Mg^{2+}], mM	$\Delta\delta$, ppm
1	0	0	0	0.86
2	2.9	0.05	0	0.82
3	2.9	0.05	0.5	0.62
4	2.9	0.1	0.5	0.53
5	2.9	0.05	3.0	0.50
6	2.9	0.3	0.5	0.46
7	2.9	0.1	3.0	0.42
8	2.9	0.3	3.0	0.36
9	2.9	0.3	> 7	0.33

The chemical shift difference, $\Delta\delta$, between the two peaks of FTrp-labelled PGK at different combinations of [ATP], [ADP], and [free Mg]
0.5 mM labelled PGK was studied at 30 °C in a buffer at pH 7.2, I=0.15 M. The ADP concentration includes 50 μM from the ATP solution. The ADP contamination of Boehringer Mannheim best-purity ATP used was assessed by ^{31}P NMR. The ADP appeared to be a true contaminant and not an artefact generated during the neutralisation of the ATP stock. ^{31}P NMR spectra of the samples showed broad signals from the enzyme-bound nucleotides and little inorganic phosphate, consistent with there being no significant hydrolysis of the ATP to ADP on the time scale of the measurements. Deproteinised extracts were not studied, however. For comparison, the chemical shift difference seen in intact glucose-fed BJ2168 cells was 0.55 ppm, and the ATP and ADP concentrations measured in cell extracts were 2.9 and 0.36 mM respectively.

Inspection of lines 2, 3, and 5 of Table 5.4 shows how important the free magnesium ion concentration is in this system. Note that the chemical shift difference *in vitro* most closely resembles that seen in the glucose-fed cells *in vivo* (0.55 ppm) when the ADP concentration is very low - see lines 3, 4, and 5. The free magnesium level of 0.5 mM is typical of that seen in some other cell types (see section 5.3.2.3), and measured in other cell lines by the same technique as part of this work. The value of 3 mM free magnesium is closer to that actually determined from ^{31}P NMR spectra of the intact glucose-fed cells used in this work.

5.4.7 Conclusions and discussion

Given that the concentration of ATP experienced by the labelled enzyme in the intact cell is the same as that apparent in ^{31}P NMR spectra of the intact cells or measured in cell extracts, one can place limits on the ADP or free magnesium concentrations experienced by the labelled enzyme. If the intracellular free magnesium ion concentration is as low as 0.5 mM, then the intracellular ADP concentration experienced by the labelled PGK must be around 100 μM (line 4 of Table 5.4). If the free magnesium concentration is nearer to 3 mM, then the ADP concentration experienced by the labelled PGK must be correspondingly lower, perhaps 50 μM (line 5 of Table 5.4). These values of [ADP] are approximately 3 to 7 times lower than observed in the cell extracts (0.36 mM).

Previous workers have observed a similar discrepancy between the amount of ADP observed in ^{31}P NMR spectra of intact tissues and the amounts determined in cell-free extracts of the same tissues (Gadian 1982; Iles *et al.* 1982). In muscle, actin-binding appears to offer an explanation, but in kidney and liver cellular compartmentation may be more relevant (Stubbs *et al.* 1984).

The intracellular free ADP concentration is an important parameter in regulating the activity of the cell, generally through the phosphorylation potential (Veech *et al.* 1979), directly at, for example, the adenine nucleotide translocator, and indirectly through the adenylate kinase-determined AMP concentration (Veech *et al.* 1979; Stubbs *et al.* 1984).

The data presented here, from ^{19}F NMR studies of intact cells and of isolated labelled PGK, suggest that the ADP pool available in the cytoplasm of the cells studied is around 100 μM. The amount of that ADP that is bound to the high concentration of PGK in the cell can be estimated from the K_d for the MgADP-

PGK equilibrium. Scopes gives a value for this K_d of 40 μM (Scopes 1978a). It can also be estimated from the *in vitro* experiments described above (section 5.4.4.2) as the [MgADP] which gives the greatest exchange broadening in the ^{19}F NMR spectra of the ADP - PGK titration (see Figure 5.6). This gives an estimated K_d of around 300 μM.

These values allow limits to be placed on the free ADP concentration in the intact cell, given that the PGK concentration is not less than 0.5 mM. Using an available ADP concentration of 100 μM, the high limit (K_d 300 μM, [PGK] 0.5 mM) is approximately 40 μM. At the low limit (K_d 40 μM, [PGK] say 1.25 mM), the free ADP in the cytoplasm is calculated to be just 3 μM.

Calculations of the equilibrium positions of the PGK-GAPDH couple in yeast (Brindle 1988) and creatine kinase in brain, liver and muscle (Veech *et al.* 1979) also suggest that the ADP concentration measured in cell extracts is greater than that participating in the equilibria in the intact cell; the free [ADP] estimate in yeast was around 50μM (Brindle 1988). Data obtained from the creatine kinase equilibrium studied by ^{31}P NMR in mouse liver (Brosnan *et al.* 1990) also suggest a similar cytoplasmic free ADP concentration of around 50 μM.

5.4.8 Further work

If the free ADP concentration is regulated, one would expect an increase in the concentration of ADP-binding components in the cell to cause an increase in total ADP. Preliminary further work has shown that the total ADP level measured in cell extracts does vary with the PGK concentration. A 50 % increase in [PGK] was accompanied by a c. 30 % increase in total [ADP]. ^{19}F NMR spectra showed that there was no change in the chemical shifts in the labelled PGK, implying an unchanged cytosolic pool of available ADP.

Harvesting the cells at different times after induction would allow a range of PGK concentrations to be established in the intact cell. A series of experiments could be performed at a range of PGK concentrations and under different metabolic conditions to examine the relationships between the free cytosolic ADP (from the ^{19}F NMR spectra of the labelled enzyme) and the total ADP (from cell extracts).

It would be interesting to repeat the work with the isolated C-terminal domain of PGK rather than the whole protein. As discussed in Chapter 4, this domain has been efficiently expressed in yeast and shown to have virtually the structure of the domain in the intact protein (Fairbrother *et al.* 1989a; Minard *et al.* 1989).

^{1}H NMR studies on the isolated C-domain have shown that it has a K_d for MgATP about three times higher than does the whole protein (Fairbrother *et al.* 1989a). The binding also becomes independent of the ionic strength (Fairbrother *et al.* 1989a), effectively removing one experimental variable. The isolated domain contains both Trp residues and the ATP binding site, but not the triose binding site, removing another experimental variable. Its smaller size should also make it possible to acquire spectra from the intact cell with better signal-to-noise ratios and at higher viscosities (see Chapter 4). Coupling the coding sequence for the domain with leader sequences to direct the protein to different cellular compartments may allow the measurement of the ADP concentration in compartments other than the cytoplasm.

6 Kinetics of PGK *in vivo*

6.1 Introduction

6.1.1 Background

An important goal of enzymology is to understand the operation of a metabolic pathway well enough to predict or even manipulate its properties in the intact cell. This requires a quantitative description of all its components, their environments and all the factors that influence their activities.

The outcome of some gross manipulation of an enzyme's activity might be very simple, even fatal. However, if subtler changes of metabolism are to be understood, then an enzyme must be considered as part of the whole of metabolism, subject to many influences in the cell.

The prediction of pathway fluxes *in vivo* is complicated by the need to know the detailed kinetic properties of each component in the system as it is *in situ*. Difficulties arise from the putative existence and operation of multienzyme complexes that may convey regulatory or rate-enhancing properties on the system (Srivastava and Bernhard 1986; Srere 1987; Keleti *et al.* 1989; Spivey and Merz 1989). These complexes may be defined in terms of novel intracellular compartments, co-localisation of components on a cytoskeletal or membrane structure, or the direct association of soluble enzymes in the cytoplasm.

The kinetic and regulatory properties of multienzyme complexes are the object of much research. A great deal of controversy surrounds both the

experimental and theoretical treatment of the problem. For example, the consequences of sequestering pathway intermediates within a complex and "channelling" the moieties from one active site to the next are unclear. It might be argued that channelling reduces the steady-state concentrations of the intermediates involved, reducing losses to spontaneous degradation or competing pathways. However, even the theoretical possibility of this effect under physiological conditions is disputed (Cornish-Bowden 1991; Mendes *et al.* 1992).

There is some experimental evidence for the association of the cytosolic enzyme glyceraldehyde-3-phosphate dehydrogenase (GAPDH) with lactate dehydrogenase (LDH) and with phosphoglycerate kinase (PGK) (Weber and Bernhard 1982; Srivastava and Bernhard 1986; Sukhodelets *et al.* 1988). However, much of the evidence is based on complex kinetic analyses of enzyme mixtures *in vitro* or on the visualisation of associations only apparent under non-physiological conditions. The validity of the kinetic evidence has been questioned by several workers (Chock and Gutfreund 1988; Kvassman and Petterson 1989a; Vas and Batke 1990; Wu *et al.* 1991).

The substantial difficulties in interpreting data from studies *in vitro* clearly make it desirable to manipulate the pathways of metabolism in the intact cell and to study the consequences *in situ*. The techniques of modern molecular genetics now make it relatively simple to manipulate the expression levels of a chosen enzyme, and the non-invasive techniques of NMR allow the consequences of these changes to be studied in the intact cell.

Kacser & Burns (Kacser and Burns 1973) and Heinrich & Rapoport (Heinrich and Rapoport 1974) were among the first to develop mathematical formulations of whole metabolic pathways that allow one to predict the consequences of small acute alterations in the activity of an enzyme or the

concentration of a metabolite. Using formal descriptions analogous to those of flow in hydraulic systems or in electrical circuits, they described pathways in terms of the metabolite flux they carry. The control of the enzymatic steps involved depends both on the inherent properties of a given enzyme and the concentrations of the metabolites it interacts with.

Metabolic control theory offers the prospect of evaluating the contribution of one enzyme to the control of flux under a given set of conditions through relatively simple experiments that can be performed *in vivo* (Kacser and Burns 1973; Kacser and Burns 1979; Torres *et al.* 1986; Kacser and Porteous 1987; Acerenza and Kacser 1990).

The effect of a change in an enzyme's activity is quantitated by comparing the (small) proportional change in enzyme activity with the resultant proportional change in flux. In the notation of control theory, the flux control coefficient, *C*, for an enzyme under a given set of conditions, is

$$C_i = (\delta J_i/J_i) / (\delta E_i/E_i) \qquad \text{(Eq. 6.1)}$$

where the subscript *i* indicates that the values are for the *i*th step in the pathway, δE and δJ are the changes in the enzyme activity and pathway fluxes respectively and E and J are the initial enzyme activity and pathway fluxes respectively. An important result in control theory is known as the summation theorem, which simply states that the sum of the control coefficients for all the steps in a pathway is unity.

There have been many extensions of the original theory that allow one to deal with further complications - branched pathways (Fell and Sauro 1985; Heinrich *et al.* 1987; Small and Fell 1989), one protein catalysing two steps (Cascante *et al.* 1990), situations where enzyme and substrate concentrations are similar (Fell and Sauro 1990), covalently modified enzymes (Small and Fell 1990), the effect of simultaneous changes in all the enzyme activities

(Acerenza and Kacser 1990), regulatory cascades (Kahn and Westerhoff 1991), and others.

To complement the direct studies of fluorine-labelled PGK in the intact cell, some functional studies of PGK's operation in the intact cell have been performed. The operation of PGK is of some interest because of the debate about its putative complex with GAPDH (Wu *et al.* 1991) and because the PGK-GAPDH couple is an important site of substrate-level phosphorylation and NAD^+ reduction (Scopes 1973).

The exchange process occurring between the γ-phosphate of ATP and P_i upon ATP hydrolysis or formation can be quantitated in the intact cell by ^{31}P NMR using the techniques of magnetisation transfer, reviewed by Brindle and Campbell (Brindle and Campbell 1987). A brief description of the technique is given in section 6.1.2. Comparison of the net metabolite flux with the rate of the exchange process reveals the reversibility of the reaction occurring at that step, and hence its state with respect to the equilibrium position. Under some circumstances, the exchange process can be attributed almost entirely to the function of the F_1F_0 mitochondrial ATP synthase. Under other circumstances, however, the total exchange process rate is dominated by the contribution from the PGK-GAPDH couple.

6.1.2 Measuring exchange fluxes by magnetisation transfer

Following a particular moiety as it is transferred from one molecule to another by chemical interconversion can be achieved by labelling experiments. Isotope-labelling involves the use of stable or radioisotope-labelled compounds, and the analysis of label distribution in the sample molecules. Temporary "labels" can be created *in situ* in the NMR experiment by selectively irradiating a particular population of nuclei. The label lasts

only as long as the net magnetisation of those nuclei remains significantly different from the others in the sample - essentially until they relax back to the pre-irradiation equilibrium state.

The time constants for these relaxation processes are typically of the order of seconds for small molecules, and magnetisation labelling techniques are thus well-suited to studies of processes on a similar timescale. Magnetisation labels have proved useful for examining the rates of chemical exchange processes *in vivo* and *in vitro* (reviewed in (Campbell *et al.* 1977; Alger and Shulman 1984)).

As the name suggests, the saturation transfer experiment involves the selective irradiation of a particular population eliminating the signal from that population at the next observe pulse. By chemical exchange, this saturation is passed into other chemical environments, with different chemical shifts.

In a simple two-site exchange system, A↔B, where A is irradiated and exchanges with B at forward and back rate constants k_a and k_b, the steady-state magnetisation of B depends both on its inherent relaxation rate and the rate of the exchange process. The expression for the ratio of intensities of B without and with irradiation of A, is (Forsén and Hoffman 1963; Mann 1977)

$$M_o/M_z = 1 + kT_{1B} \qquad \text{(Eq. 6.2)}$$

where k is the pseudo-first-order rate constant for the flux to A from B, M_o and M_z are the magnetisation levels of the B resonance without and with saturation of the A resonance respectively, and T_1 is the intrinsic longitudinal relaxation time constant for B in the presence of the exchange. This may also be expressed in terms of the fractional saturation, $\Delta M/M_o$, as

$$k = (\Delta M/M_o)/T_1{}^{obs}{}_B \qquad \text{(Eq. 6.3)}$$

since $(M_z/M_o) + (\Delta M/M_o) = 1$. The T_1 measured in an exchanging system, T_1^{obs}, will appear shorter than the intrinsic T_1 because of the exchange.

The intrinsic T_1 may be determined from

$$R_{1int} = R_{1obs} - k \qquad \text{(Eq. 6.4)}$$

where R_{1obs} and R_{1int} are the observed and intrinsic relaxation rates respectively. R_1 is the reciprocal of the relaxation time constant T_1. Alternatively,

$$R_{1int} = R_{1obs}\,(M_z/M_o) = R_{1obs}\,(1-[\Delta M/M_o]) \qquad \text{(Eq. 6.5)}$$

At the steady-state, the backward and forward rates are equal, and the exchange flux from A to B may simply be quantitated as k[B]. [B] can be determined from the signal intensity in control spectra by reference to a standard signal of known intensity; in this work, an external methylene diphosphonate sample was used as a chemical shift and intensity reference.

6.1.3 Previous studies of the PGK-GAPDH couple in the intact cell

A quantitative assessment of the importance of an enzyme in controlling a flux requires, according to the tenets of control theory, experiments in which small, finite, acute adjustments are made to the activity of the enzyme while the flux is measured. This might be achieved by the use of inhibitors or by genetic techniques. Genetic methods offer the prospect of wider applicability, greater selectivity and the prospects of elevating as well as depressing the enzyme activity. In practice, current genetic methodologies mean that it is in fact much easier to elevate rather than depress an enzyme's activity; in the foreseeable future, this may not be the case.

A previous study of the PGK-GAPDH couple *in vivo* and *in vitro* by Brindle used iodoacetate inhibition to depress the GAPDH activity and 2μ-based

plasmid expression vectors to elevate the activity of PGK (Brindle 1988). ^{31}P NMR studies of intact cells and test-tube mixtures of the two enzymes showed that neither enzyme has a significant flux control coefficient for glycolysis, but that PGK does have a high flux control coefficient for the γ-ATP$\leftrightarrow$P$_i$ exchange. The study also showed that any enzyme-enzyme interaction in the cell is also present at high dilution in the test-tube; it was inferred that any effect of the high enzyme concentration *per se* in the cell was unimportant.

These studies aimed to extend that work by examining cells in which the PGK level was lower than normal, to better define the importance of PGK in controlling the γ-ATP$\leftrightarrow$P$_i$ exchange and to gain some further insight into the environment of PGK in the cell.

6.2 Genetically depressing the level of an enzyme's activity in the intact cell

6.2.1 General principles

Many strategies might be devised to reduce the level of an enzyme's activity in the intact cell. The most promising developing methodologies appear to be "antisense RNA" (Takayama and Inouye 1990) and the use of "ribozymes" (Haseloff and Gerlach 1988). Ribozymes are RNA sequences with a highly-specific endoribonuclease activity. Antisense experiments involve the expression of RNA sequences complementary to the mRNA of the target enzyme, resulting in mutual binding and reduced expression. Although they may become techniques of choice in the future, these methods are not yet developed well enough to attempt using them in this work.

One available strategy for the reduction of an enzyme's activity in haploid yeast cells is to use gene deletion or disruption techniques to eliminate the

chromosomal gene for the enzyme, and then reintroduce the gene via a relatively inefficient expression system. This is the approach adopted in these studies.

In the yeast strain BC3(Piper *et al.* 1988; Piper and Curran 1990), the chromosomal PGK gene has been disrupted using homologous recombination by the insertion of a functional *TRP1* gene fragment into the PGK gene. The *pgk*$^-$ phenotype is slow-growing, cannot ferment glucose and can only slowly metabolise glycerol plus ethanol (Piper and Curran 1990). The choice of a suitable expression system in this yeast strain should allow cells with a range of subnormal PGK activities to be established.

6.2.2 Plasmid expression systems in yeast

6.2.21 2μ-based vectors

Many expression vectors used in yeast are derived from the 2μ circle that occurs in wild yeasts (Futcher and Cox 1984). It has a number of features that makes it attractive as the basis for artificial plasmids. 2μ circles exist in the cell at around 40 copies per cell, are distributed through a population of cells with good homogeneity and are relatively resistant to rearrangement (Rose and Broach 1990). The vectors designated pBF, pMA, and pKV in this work belong to this class of plasmid, as they all contain the origin of replication from the 2μ circle. They rely for some replicative functions on trans-acting factors from the endogenous 2μ circles.

When comparable numbers of both artificial and natural 2μ plasmids are present, successive rounds of plasmid division and segregation can lead to very inhomogenous distribution of the two plasmid types. Consequently, the stability of a low-copy-number artificial plasmid is compromised in *cir*$^+$ strains by the natural 2μ circle (Futcher and Cox 1984).

Raising the copy number of the artificial plasmid helps to improve its segregation and so helps maintain the population stability as well as elevating the level of expression of the other sequences on the plasmid.

The *LEU2* gene in the pMA27-based plasmids has a 29 base-pair deletion in the promoter region and is designated *LEU2-d*. The inefficiency of the *LEU2* gene expression causes the plasmid copy number to rise in compensation. In some plasmid and cell combinations the copy number can reach 300 per cell (Erhart and Hollenberg 1983). Even in the absence of *leu* selection pressure, it is stable in the cell population for around 30 generations (Melanie Dobson, Oxford, personal communication). Plasmid stability was experimentally verified with the strains used in this work.

Piper has reintroduced the PGK gene to the BC3 cell with a 2μ-based expression system carrying PGK promoter defects (Ogden *et al.* 1986) to reduce the expression level (Piper and Curran 1990). Unexpectedly, the plasmid copy number rose in compensation until normal levels of PGK expression were achieved, possibly by an increase in the mRNA stability (Piper and Curran 1990). It seems that the PGK gene itself had become the plasmid's selection marker, and that the underexpression of PGK would not be possible with 2μ-based plasmids. Piper went on to demonstrate that plasmids based on the yeast centromere rather than the episomal 2μ circle could, however, be used to achieve low, stable PGK levels.

6.2.2.2 Centromeric vectors

Piper prepared a number of centromeric plasmids carrying PGK under the control of various weakened promoters (Ogden *et al.* 1986; Piper and Curran 1990). They are based on the yeast centromeric origin of replication *CEN4* fragment and have very low copy numbers, around 1-5 copies per cell, while still retaining good stability and population homogeneity. They replicate once

during the cell cycle, unlike the 2μ-based plasmids that replicate independently of the cell cycle. (Resnick *et al.* 1990). The centromeric pYC plasmids used in this work are described in Chapter 2, Materials and Methods.

6.3 The physiological consequences of lowering the PGK activity in the intact cell

6.3.1 Genetic titration of PGK

Using the *pgk*$^-$ yeast strain BC3 transformed with various plasmids, it was possible to establish a collection of cell lines expressing PGK activities from as little as 5% of wild-type (plasmid pYC775) to over 20 times wild-type levels (plasmid pMA27). Wild-type levels of PGK activity are taken here to mean levels comparable to other yeast strains with intact chromosomal PGK genes, particularly the diploid parent yeast BC2.2 (Piper and Curran 1990). In the case of BC3, this seemed to correspond to transformation with the plasmid pMA777. The cell lines were generously provided by Peter Piper, University College, London.

6.3.2 The comparative metabolism of cells expressing normal or subnormal levels of PGK

6.3.2.1 Cell growth and perifusion

Cell cultures were stored on minimal media and grown in complete medium. The cells used for perifusion experiments were grown for 24 hours in glucose-containing YEPD complete medium (see chapter 2, Materials and Methods). The growth rates on minimal media were much slower. The distribution of the plasmids in the cell population after growth on complete

medium was experimentally verified by comparing colony counts on selective and non-selective media.

The growth rates of aerobic low-PGK and control cells were very similar on glucose, ethanol alone and on ethanol plus glycerol, indicating that not only are the small quantities of PGK sufficient for glycolysis but also for gluconeogenesis too.

Freshly-harvested cells were immobilised in fine agarose threads and perifused at 30 °C under various conditions in the bore of the magnet as described in Chapter 2, Materials and Methods. Perchloric acid cell extracts were prepared after perifusion and used to assay various metabolites by *in vitro* ^{31}P NMR and enzymatic assay. A representative spectrum with expansions of the phosphomonoester and α-nucleotide phosphate regions is shown in Figure 6.1. The net flux through the glycolytic pathway was estimated as the mean of the greatest and least possible values, i.e. from the net glucose consumption and from the net ethanol production. Better measurements are possible; this is discussed later.

^{31}P NMR spectra were acquired from the intact perifused cells and used to determine the cytosolic pH and the concentration of the phosphomonoesters, and P_i. Magnetisation transfer experiments were used to measure the net rate of the γ-ATP↔P_i exchange. Representative spectra are presented in Figure 6.2, showing the spectra with and without selective irradiation of the γ-NTP resonance and the difference between them. The chemical shift difference between the NTP α and β peaks suggests a free magnesium concentration of c. 0.2 mM (cf. values of several mM in the strain BJ2168 in Chapter 5).

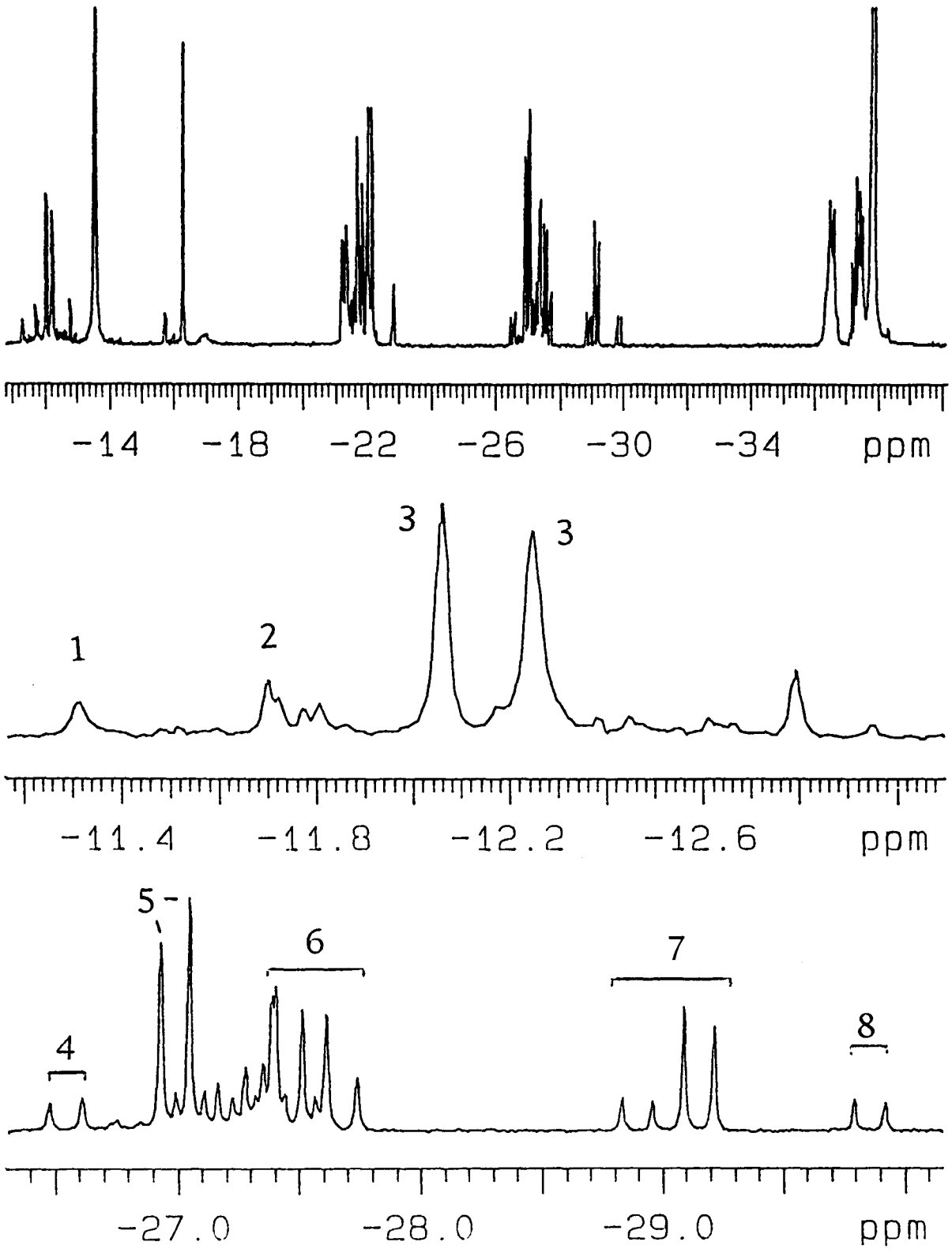

^{31}P NMR spectrum of a perchloric acid extract of BC3 cells perifused aerobically.

BC3 cells containing the plasmid pYC775 and expressing very low PGK levels were perifused aerobically with 50 mM glucose for five hours. The cells were rapidly frozen and extracted. The lyophilised extract was resuspended in triethanolamine buffer, pH 8, 30 °C. The sample contained 20 % v/v D_2O as a field frequency lock. 7500 transients were accumulated over 10.6 hours, using a 10000 Hz spectral window, 5.1 s delay between acquisitions and 22000 digitisation points. WALTZ-16 ^1H-decoupling was applied during the acquisition period. The resonances have been assigned by reference to previous work (den Hollander *et al.* (1986), Navon *et al.* (1979)) as follows: 1: α-FBP, 2: β+α G6P, 3: β-FBP, 4: αNDP, 5: α-NTP, 6: NAD^+, 7: UDP-sugars, 8: ADP-sugars.

Figure 6.1

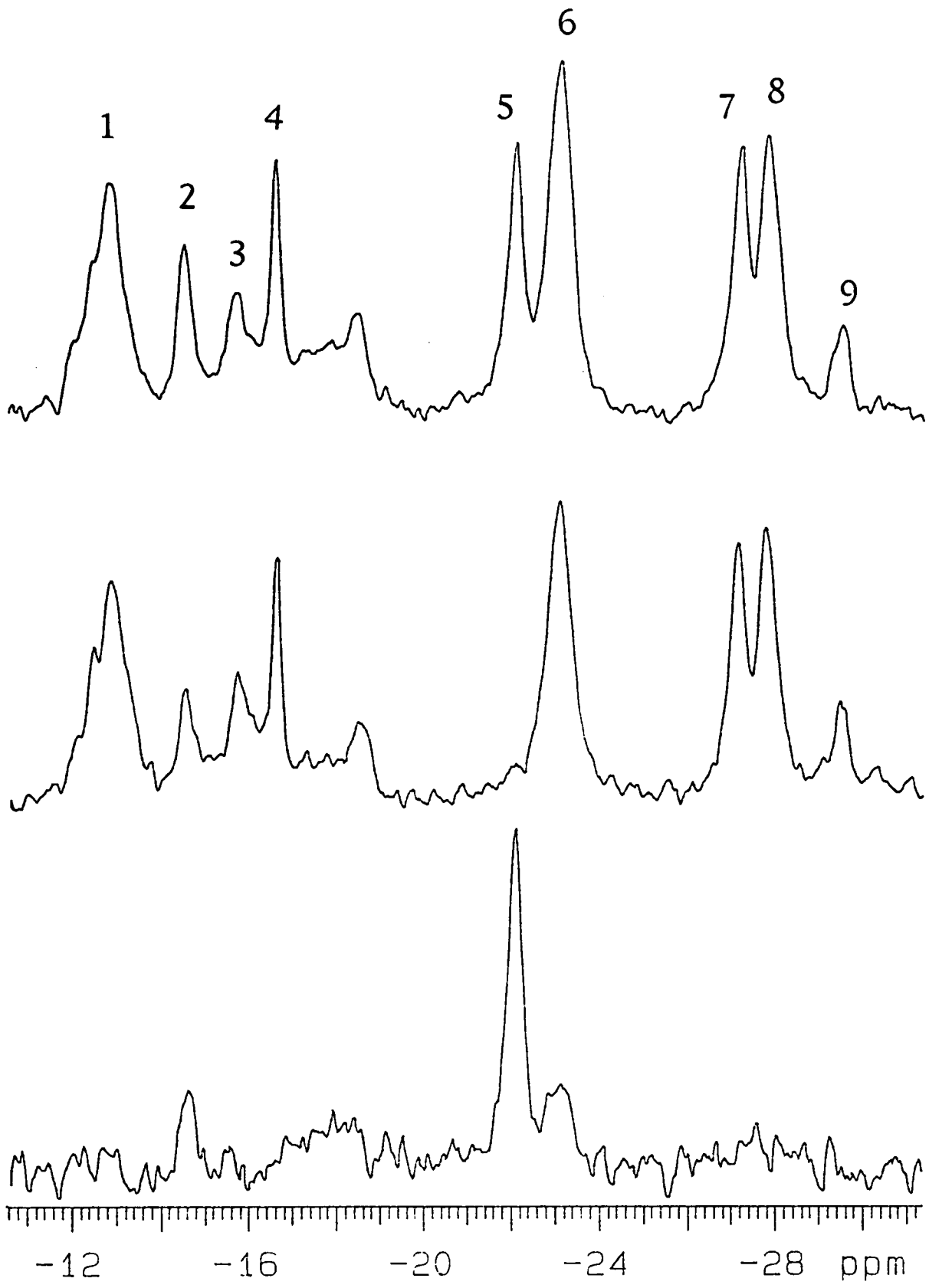

^{31}P NMR γ-ATP-P_i saturation tranfer experiment with aerobically perifused glucose-fed BC3 cells expressing very low PGK activity.
The top spectrum was acquired with selective irradiation at a control frequency as far downfield of P_i as γ-ATP is upfield. The middle spectrum was acquired with selective irradiation of the γ-ATP resonance. The bottom spectrum is the difference between the γ-ATP and control-irradiated spectra, at an enlarged vertical scale. 256 transients were collected in blocks of 16, alternating between γ-ATP and control irradiation. The selective irradiation was applied throughout the 5 s relaxation delay and gated off during the 0.4 s acquisition. The spectral window was 10000 Hz. The data were digitised into 8000 points. The spectra are shown with 20 Hz exponential line broadening. The resonances have been assigned by reference to previous work (Brindle (1988)) as follows:
1: phosphomonoesters (esp. sugar phosphates), 2: cytosolic P_i,
3: vacuolar P_i, 4: phosphodiesters, 5: γ-NTP/β-NDP, 6: polyphosphate (terminal), 7: α-NTP/NDP, 8: diphosphodiesters (esp. NAD), 9: UDP-sugars.

Figure 6.2

6.3.2.2 *Changes in metabolite concentrations*

The measurements made by enzymatic or NMR assay have been tabulated below in Table 6.1. Where the same parameter has been determined by NMR and enzymatic assay, both measurements are shown.

Table 6.1

Parameter group	Parameter	Plasmid name		
		pYC775	pYC763	pMA777
Enzyme levels	PGK (n=4)	38±8	107±13	1814±59
	GAPDH (n=2)	1471	1438	1307
Hexose phosphates (n=2)	Glc-6-P [2]	0.41	0.44	0.56
	Glc-6-P [1]	0.37	0.37	0.45
	Fru-6-P [2]	0.12	0.17	0.08
	Fru-1,6-BP [2]	2.97	2.51	1.87
	Fru-1,6-BP [1]	2.81	2.50	1.64
Triose phosphates (n=2)	DHAP + GAP [2]	1.0	0.92	1.1
	3-PGA [2]	0.038	0.045	0.061
Nucleotides (n=2)	NTP [1]	2.37	2.18	2.34
	NDP [1]	0.31	0.10	0.30
	NTP/NDP ratio	7.7	10.7	8.2
Intracellular pH [3]	pH (n=15, 8, 14)	7.13±0.01	7.17±0.00	7.20±0.02

Enzyme levels and metabolite concentrations measured in cell extracts of BC3 yeast cells transformed with different plasmids.
Cells were perifused anaerobically with 50 mM glucose for five hours prior to extraction. The abbreviated names of the metabolites are listed in the Abbreviations section. The enzyme activities are quoted in units per ml cell water. The metabolite concentrations are quoted in μmol per ml cell water. Values are mean figures where n=2 and means±standard error where n>2. [1] from ^{31}P NMR spectra of cell extracts. [2] from enzymatic assays of cell extracts. [3] from the chemical shift of the P_i resonance in ^{31}P NMR spectra of intact cells. Peak assignments in the NMR spectra were made by reference to previous work (Navon *et al.* 1979; den Hollander *et al.* 1981; den Hollander *et al.* 1986)

The results show an apparent cross-over effect in that lowering the PGK activity leads to an accumulation of fructose-1,6-bisphosphate and a depletion of 3-phosphoglycerate.

The concentrations of various phosphorylated metabolites measured in the intact anaerobic cells during perifusion are shown below in Table 6.2

Table 6.2

Cell type and condition	[PME] mM	$\Delta M/M_o$ PME	[P_i] mM	$\Delta M/M_o$ P_i
Anaerobic control [PGK] (n=3/15)	12.6 ± 1.3	0.13 ± 0.04	5.8 ± 0.3	0.39 ± 0.07
Anaerobic low [PGK] (n=3/15)	12.6 ± 0.7	0.09 ± 0.03	4.9 ± 0.3	0.14 ± 0.06
Aerobic low [PGK] (n=3/10)	9.3 ± 0.6	0.08 ± 0.02	3.6 ± 0.3	0.21 ± 0.03

The concentrations of phosphomonoesters (PME) and phosphate (P_i) in BC3 yeast cells perifused under the conditions indicated.
All values are quoted as μmol per ml cell water ± one standard error of the mean. n is the number of different cell batches/number of spectra. The anaerobic data were obtained during perifusions at 7 Tesla. The aerobic perifusions were performed some months later at 9.4 Tesla using a different perifusion apparatus. The aerobic cells are thus not strictly comparable with the anaerobic cells. The P_i depletion during aerobiosis has been reported previously (den Hollander *et al.* 1981). The concentrations and $\Delta M/M_o$ values were used to calculate γ-ATP to P_i and PME fluxes (see text).

6.3.2.3 *Changes in glycolytic rate and exchange flux*

Estimates of the glycolytic flux and measurements of the γ-ATP↔P_i exchange were made during anaerobic perifusions of 4 g of BC3 cells transformed with plasmids giving either very low (pYC775, pYC763) or control levels of PGK (pMA777). The γ-ATP↔P_i exchange flux was measured by comparing the intensity of the phosphate peak in spectra in spectra collected with and without selective irradiation of the γ-ATP peak.

These data were analysed as described in section 6.1.2 using an intrinsic T_1 value of 1 second for phosphate. The T_1 values were, unfortunately, not determined in this work. Determinations of the T_1 in the system used are clearly required before firm conclusions can be drawn. However, previously reported values of the intrinsic T_1 of phosphate measured in the intact yeast cell have not varied significantly from 1 second at magnetic field strengths of 4.3 T (Brindle and Krikler 1985), 7 T (Brindle 1988) or 8.5 T (Campbell-Burk *et al.* 1987b).

The results of these measurements and calculations are shown in Table 6.3 below.

Table 6.3

Flux measured	Plasmid name		
	pYC775 (PGK c. 40 U/ml cell water)	pYC763 (PGK c. 110 U/ml cell water)	pMA777 (PGK c. 1800 U/ml cell water)
Glucose consumption (n=4, 3, 4)	0.47±0.02	0.45±0.01	0.61±0.02
Ethanol production (n=4, 3, 4)	0.59±0.03	0.51±0.02	0.80±0.05
Net P_i consumption (n=4, 3, 4)	0.77±0.03	0.70±0.01	1.0±0.05
Net $P_i \rightarrow \gamma$–ATP flux (n=15, 8, 15)	0.8±0.3	0.7±0.3	3.7±0.5
Ratio of net P_i consumption to net $P_i \rightarrow \gamma$–ATP flux	c. 1	c. 1	c. 3 to 4

Pathway fluxes in anaerobic BC3 yeast transformed with plasmids giving different expression levels of PGK
Glucose consumption and ethanol production data were determined from assays of the perifusion medium. These data have been averaged to give a mean figure for the glycolytic rate, the net P_i consumption. The net $P_i \rightarrow \gamma$-ATP flux has been determined from ^{31}P NMR steady-state saturation transfer measurements in the intact cells (see text). All fluxes are quoted in units of μmol s^{-1} (ml cell water)$^{-1}$. The values are shown as the mean ± 1 standard error of the mean.

These data confirm previous findings that, in normal cells, the measured $P_i \rightarrow \gamma$–ATP flux exceeds the net glycolytic flux by a factor of three to four

(Brindle 1988). This observation suggested that the GAPDH/PGK step in glycolysis is near equilibrium *in vivo*, with significant forward and reverse fluxes. In the anaerobic case presented here, there is no contribution from the aerobic processes of oxidative phosphorylation to the total exchange flux measured. The measured exchange can therefore be attributed to the PGK/GAPDH couple (Campbell-Burk *et al.* 1987b; Brindle 1988).

Consistent with the suggestion that PGK has a high flux control coefficient for the $P_i \leftrightarrow \gamma$-ATP exchange reaction, the cells with significantly lowered PGK activities show a markedly reduced exchange flux. In the cells with very low levels of PGK, the exchange flux becomes comparable with the net metabolite flux, implying that there is no significant back reaction. The GAPDH/PGK couple under these conditions must be far from equilibrium, operating unidirectionally and with a relatively high flux control coefficient for glycolysis.

The estimated net P_i consumption in the cells expressing very little PGK is reduced by only 20 to 30 % compared to normal cells, despite containing only a few percent of the normal PGK activity. As an estimate for the effect on glycolysis, the ethanol production rate gives a worst-case estimate of approximately 25 to 35 %. This is consistent with the PGK having a low flux control coefficient for glycolysis (Brindle 1988), but could not, strictly, be predicted because the change in PGK activity was very large and not effected acutely.

Cells expressing low levels of PGK thus have the capacity for near-normal rates of glycolysis. The $P_i \leftrightarrow \gamma$-ATP exchange flux at the GAPDH/PGK step has the same value as the net glycolytic flux. This allows the glycolytic contribution to the total $P_i \leftrightarrow \gamma$-ATP exchange flux to be calculated. In aerobic systems, where the exchange flux can have contributions from both oxidative

phosphorylation and from glycolysis, the two components have previously been separated only by the use of inhibitors of glycolysis (iodoacetate) or oxidative phosphorylation (Campbell-Burk *et al.* 1987b)

In aerobic cells with low PGK activities one could use the measured glycolytic flux to quantitate the contribution of the GAPDH/PGK couple to the total $P_i \leftrightarrow \gamma$-ATP exchange flux. This would enable, for example, the calculation of the P:O ratio of oxidative phosphorylation in the intact cell since the total exchange flux less the glycolytic contribution may be attributed to oxidative phosphorylation.

This measurement has been attempted before in various tissues (heart (Matthews *et al.* 1981), kidney (Freeman *et al.* 1983) and maize root tips (Roberts *et al.* 1984)), but the results are compromised by the PGK-GAPDH contribution when a glycolytic flux is present (Brindle and Krikler 1985; Brindle and Radda 1987). A cell line with low PGK activity would allow this measurement without the need to block glycolysis with inhibitors.

6.3.2.4 ^{31}P NMR saturation transfer measurement of the P:O ratio in cells with very low PGK activities

^{31}P NMR saturation transfer measurements, oxygen consumption rates, glucose consumption and ethanol production rates were measured during aerobic cell perifusion experiments.

These measurements are tabulated in Table 6.4 below.

Unfortunately, the saturation transfer measurements of the $P_i \rightarrow \gamma$-ATP flux are subject to relatively large errors that propagate through to the calculated P:O ratios for oxidative phosphorylation (around ± 2 at 95 %). Inspection of Figure 6.2 shows how great the difficulty may be when there is little saturation transfer to measure. Nevertheless, the mean estimates of the P:O

ratio as c.2 to c.3 are in good agreement with measurements on isolated mitochondria (Mackler and Haynes 1973) and with previous studies in yeast, providing the glycolytic exchange has been taken into account (Brindle and Krikler 1985; Campbell-Burk *et al.* 1987b).

Table 6.4

	Mean value ± s.e.m. (n=3)
Glucose consumption	0.33 ± 0.04
Ethanol production	0.37 ± 0.03
Monooxygen consumption	0.155 ± 0.01
Saturation transfer $P_i \rightarrow \gamma$-ATP flux	0.76 ± 0.25
Calculated P:O ratio of the non-glycolytic $P_i \rightarrow \gamma$-ATP flux : glycolysis estimated as ethanol production	2.5 ± 0.25
Calculated P:O ratio of the non-glycolytic $P_i \rightarrow \gamma$-ATP: glycolysis estimated as 75 % of the glucose consumption	1.7 ± 0.25

Measurements of glycolytic flux and net $P_i \rightarrow \gamma$-ATP flux in glucose-fed aerobic BC3 yeast cells expressing very little PGK and the P:O ratios calculated from these data.
The P:O ratio of the non-glycolytic $P_i \rightarrow \gamma$-ATP flux is estimated twice: First, as the total $P_i \rightarrow \gamma$-ATP flux minus the ethanol production flux. Second, as the total flux minus 75 % of twice the glucose consumption rate. The 75 % correction factor is an estimate of the proportion of the glucose uptake that flows through phosphofructokinase (Campbell-Burk *et al.* 1987a).

Quantitating the glycolytic contribution is also problematic without a better estimate of the relevant glycolytic flux. Shulman and co-workers have used ^{13}C label distribution studies in yeast to examine the flux through the glycolytic pathway (den Hollander *et al.* 1986; Campbell-Burk *et al.* 1987a). Campbell-Burk *et al.* were able to estimate the proportion of glucose diverted away from glycolysis to trehalose and the phosphogluconate pathway, and quantitate the back-flux through fructose bisphosphatase. They estimated

that about 75 % of the flux through hexokinase went on through phosphofructokinase in anaerobic glucose-grown cells (Campbell-Burk *et al.* 1987a).

Similar measurements would clearly be useful in this work but have not been performed. Applying this correction to the P:O ratio calculations shown in Table 6.3 resulted in the ratio changing from 0.7 to 1.7. Clearly, this correction is substantial and the relevant flux through the triose phosphate section of glycolysis should be determined more accurately before drawing firm conclusions about the P:O ratio.

The oxygen consumption measured in these cells is somewhat lower than previously reported for glucose-grown derepressed yeast, being about 35 % (Brindle and Krikler 1985) to 70 % (Davies and Brindle 1992) of the rate measured in other yeast strains in this laboratory. Whether this difference is simply due to the yeast strain or to a deficiency in mitochondria has yet to be determined. The cells do show a significant Pasteur effect, and preliminary cytochrome c oxidase assays suggested that the mitochondrial content was similar to another strain, AH22. However, a controlled statistical comparison between glucose-grown and ethanol-grown cells has yet to be performed.

An alternative estimate of the glycolytic flux may be obtained from ^{31}P NMR measurements of saturation transfer from γ-ATP to the hexose phosphates in the early part of the glycolytic pathway. These measurements have been studied in detail in Shulman's laboratory (Campbell-Burk *et al.* 1987b). A knowledge of the proportions of the different components of the PME peak, their T_1 spin-lattice relaxation times, and ^{13}C labelling patterns to deduce the appropriate kinetic constants in the various exchange reactions are all required for a full analysis. These have not been determined, but a simpler comparison of the flux in normal and low-PGK cells is possible given that the

PME peak is dominated by fructose-1,6-bisphosphate, being around 70 % of the total PME.

The fractional saturation of the PME peak during selective irradiation was measured in the same spectra used to analyse the phosphate exchange flux. The intrinsic T_1 of the PME peak has been determined in yeast at 8.5 T as 0.9 ± 0.1 seconds (Campbell-Burk *et al.* 1987a), and a value of 1 s has been used here although it has not been measured in the cells studied.

Given that the [1-P] of fructose bisphosphate contributes at least 30 % of the PME peak intensity, the exchange flux at phosphofructokinase can be calculated from the data in Table 6.2. If the drop in PME intensity upon selective ATP irradiation is attributed entirely to changes in Fru-1,6-BP intensity, values for the underlying M_o and M_z for the Fru-1,6-BP can be calculated and used with Eq. 6.2 to determine the flux. The calculations are tabulated below in Table 6.5.

Table 6.5

	$\Delta M/M_o$ PME	[1-P FBP] (M_o)	M_z of [1-P FBP]	$\Delta M/M_o$ for [1-P FBP]	Implied Flux at PFK
Control	0.13	3.8	2.4	0.37	1.6
Low PGK	0.09	3.8	2.8	0.26	1.4

Calculated flux at PFK using saturation transfer data from the phosphomonoester peak measured in anaerobic BC3 cells expressing control or very low levels of PGK.
The calculations are based on fructose-1,6-bisphosphate being the predominant sugar present in the PME mixture. Flux is calculated using a T_1 value of 1 second. Concentrations are in mM, the fluxes in μmol s^{-1} (ml cell water)$^{-1}$. For comparison, the net glucose uptake rates were 0.47 and 0.61 μmol s^{-1} (ml cell water)$^{-1}$ in low PGK and control cells respectively.

These calculations suggest at face value that there is a significant reverse flux at PFK (presumably catalysed by fructose-1,6-bisphosphatase) since the γ-ATP to Fru-1,6-BP flux exceeds the glucose uptake rate by a factor of 2 to 3 in each

case. However, the fact that an assumed T_1 has been used and contributions from hexokinase have been ignored (glucose-6-phosphate may be up to 20 % of the PME peak in the control cells) makes it invalid to draw such a conclusion. ^{13}C NMR labelling studies have suggested that FBPase is inoperative in yeast cells under these conditions (Campbell-Burk *et al.* 1987a). However, it may be significant that the values are not very different from one another, again suggesting that lowering the PGK by some 95 % has had a disproportionately small effect on the net rate of glycolysis.

The resolution obtained in the ^{31}P NMR spectra of the intact cells was insufficient to resolve the individual sugar phosphates. However, the resolution in some spectra was good enough to suggest that there may be some benefit in ^{1}H-decoupling the spectra obtained from the intact cells. If effective, this would clearly be of great benefit in characterising the fluxes in the early part of glycolysis.

6.4 Discussion and further work

Further work should confirm that the effects seen following the reduction of PGK levels are due to the simple kinetic properties of the PGK:GAPDH couple and not due to other adaptive changes in the cell. This could be done by following the forward reaction kinetics spectrophotometrically at different PGK:GAPDH ratios, but this has yet to be done. If the results are confirmed, then it would be interesting to consider the implications for the operation of any kinetically significant GAPDH:PGK complex. The lowering of PGK to only 5 % of normal levels must have some impact on the existence of any complex, yet the flux change is relatively small (20 to 30 % decrease). This suggests that there is no significant kinetic rôle for any complex.

Another approach to probe the existence of any kinetically significant complex of PGK is to introduce into the cell a structurally intact but catalytically inert mutant PGK. Such an enzyme may be produced by site-directed mutagenesis. Finding a suitable mutant when there is no obvious critical residue, as is the case with PGK, is proving difficult, however (Herman Watson and Jennifer Littlechild, Bristol, personal communication).

Some preliminary work was undertaken using mutants of PGK (D372N, R21M) kindly supplied by Jennifer Littlechild, Bristol. The mutant enzymes were overexpressed in the AH22 cell type, in the expectation that they would reduce the rate of glycolysis if they became incorporated into a kinetically significant complex. Unfortunately, none of the mutants so far examined met both criteria required, i.e. having negligible activity but normal structure. A similar experiment has been performed with mutant mitochondrial citrate synthase and citrate-synthase-deficient cells (Sumegi *et al.* 1990). The data were interpreted as supporting the existence of a kinetically important complex in the mitochondria, the "metabolon".

The saturation transfer measurement of the exchange flux has a high error of measurement because of the relatively poor signal-to-noise ratios obtained in spectra of the intact cells. There is little that can be done to improve this situation, which requires large numbers of experiments to be performed in compensation. The measurement of the flux through the GAPDH:PGK couple could be determined rather more accurately than by the crude estimates of glucose consumption and ethanol production, especially by the use of ^{13}C labelling studies as demonstrated by Shulman *et al.* (den Hollander *et al.* 1986; Campbell-Burk *et al.* 1987a).

The finding that reduced levels of PGK can be used to abolish the $ATP \leftrightarrow P_i$ exchange flux at the GAPDH/PGK couple without substantially reducing the

metabolite flux may be useful. It allows the isolation of the exchange flux due to the aerobic contributions of oxidative phosphorylation. In combination with vectors expressing different levels of the adenine nucleotide translocase, this would be useful in addressing the long-standing question about the rôle of the adenine nucleotide transporter in limiting the rate of oxidative phosphorylation (Groen *et al.* 1982). The effect of the level of translocase on the rate of oxidative phosphorylation could be monitored directly, overcoming some of the difficulties of previous studies in this laboratory (Spickett 1990).

The measurement of the change in ATP demand during biosynthesis is of continuing interest in the biotechnology industry (see, for example, (Bu'Lock and Kristiansen 1987)). The combination of low-PGK cells and inducible expression systems should allow the ATP turnover to be measured directly during protein synthesis on different substrates, for example. These measurements could be extended to a range of cell types, including the commercially important mammalian cell lines.

The system used here to achieve very low expression levels of PGK relied upon the use of low copy-number plasmids. Although the population distribution of centromeric plasmids is good, typically 1 to 5 copies per cell (Resnick *et al.* 1990), there is still scope for large proportional differences in enzyme levels to arise. A better approach would be to integrate a vector into the genome. In yeast, it is relatively simple to achieve homologous recombination of the vector with the chromosomal gene (Botstein and Fink 1988; Rothstein 1990), thus achieving disruption of the chromosomal gene. This allows its replacement with a modified version, perhaps with an inefficient promoter or expressing a mutant protein.

The transformation procedure used to introduce DNA into yeast cells is itself mutagenic, causing substantial heritable changes in the growth characteristics of the cells (Danhash *et al.* 1991). Although efforts are made to control for this by selecting cells with "normal" phenotypes, there will inevitably be differences between different transformants. As has been shown in this work, there are some difficulties in maintaining a population of yeast in a constant state over many months, necessitating the use of different transformants from time to time. It may be easier to maintain a clonal cell line with chromosomal rather than episomal vectors, improving the stability of the cell populations used for experiments.

Further work would, therefore, concentrate on producing a cell line expressing low levels of PGK from a reintegrated vector and using that strain as the basis of studies of mitochondrial ATP synthase activity.

7 Conclusions and further work

7.1 Labelling a single protein in the intact cell

The work began with the aim of developing a method to selectively label a chosen protein in the intact cell and then study it *in situ* using the non-invasive techniques of NMR. As a model organism, the simple eukaryote *Saccharomyces cerevisiae* (baker's yeast) was chosen. The work used the glycolytic enzyme PGK as a model protein, and fluorine, incorporated as 5-fluorotryptophan, as a label.

It has been shown that a galactose-inducible expression system in yeast can be used to direct the synthesis of PGK in stationary phase cells, so that PGK is the predominant protein being actively synthesised. When this induced synthesis coincided with the presence of a fluorinated amino acid in the growth medium, 5-fluorotryptophan-labelled PGK was formed in the cells without significant labelling of other cellular proteins. The same strategy successfully produced 5-fluorotryptophan-labelled pyruvate kinase and hexokinase.

Three different protocols were employed to effect the induced PGK synthesis. They differed in the amount of total and labelled PGK that were produced within a cell, and in the number of cells that could be grown in a given size of culture. Enhancements to the original protocol have improved the quantity of labelled protein that can be produced in a culture by more than an order of magnitude and reduced the required culture time. This was achieved without a significant drop in the proportion of the PGK containing 5-fluorotryptophan, around 60 %, if the rich medium used is enzymatically

depleted of tryptophan. The expression levels achieved were quite high, the concentration of the induced PGK reaching 20 to 30 mg/ml in the cell water.

Further work will concentrate on enhancing the fractional labelling that can be achieved and applying the system to other proteins. The utility of co-expressing the GAL4 transcriptional activator protein will also be investigated further, with a view to increasing the rate of protein synthesis and final concentration of the target protein.

7.2 Studying the labelled protein in the intact cell

5-fluorotryptophan-labelled PGK was studied in the intact yeast cell during steady-state perifusion experiments. The ^{19}F NMR spectra showed characteristic changes in response to the metabolic condition of the cells. Two resonances were observed, corresponding to the two tryptophan residues of yeast PGK. Under circumstances where proteolysis might be expected, a third peak characteristic of free fluorotryptophan was observed.

All of the labelled PGK present in the cell was visible in the ^{19}F NMR spectra of the intact cells. The linewidths of the resonances from the labelled PGK indicated that it was freely tumbling in the cell and not immobilised or part of a large multienzyme complex. However, because the cells examined had a large excess of PGK over the wild-type levels, it can not firmly be concluded that this is so for the normal amount of PGK in the cell. The apparent relative viscosity of the cytoplasm, measured from the rotational diffusion of PGK, was around 4.

In initial ^{19}F NMR studies of 5-fluorotryptophan-labelled pyruvate kinase, no resonances could be detected in the intact cell, although there were strong signals from cell extracts. *In vitro*, labelled pyruvate kinase gave what appeared to be a single resonance, suggesting equivalence of the four

subunits, each with one tryptophan, of the homotetramer. The resonance was very sensitive to the presence of fructose bisphosphate, an allosteric effector of pyruvate kinase. The linewidth of the observed resonance was consistent with its origin from a protein the size of the pyruvate kinase tetramer.

Further work will continue the studies of pyruvate kinase and hexokinase in the intact cell. It is hoped that studies of hexokinase will yield information about the free glucose concentration in the cell and the position of the hexokinase monomer-dimer equilibrium under different conditions; preliminary studies *in vitro* suggested that this will be possible.

Studies of PGK will continue with the isolated C-terminal domain, which appears to offer a number of advantages over the whole protein. Its smaller size should allow its resonances to be detected with better signal-to-noise ratios, enabling its observation at lower concentration and at higher viscosities, perhaps within the mitochondrion. Expression of proteins with additional leader sequences should allow the direction of labelled enzymes or domains to particular intracellular compartments. Molecular dynamics calculations and modelling should allow better models of the motions of the 5-fluorotryptophan labels to be devised. These will allow a better definition of the motional properties of the whole protein in the intact cell.

7.3 Studies of labelled PGK *in vitro*

Titrations of 5-fluorotryptophan-labelled PGK with its substrates showed that the changes seen in its ^{19}F NMR spectrum *in vivo* were due to changes in the ADP and ATP concentrations in the cell. The chemical shifts of the resonances were most sensitive to ADP, in a markedly magnesium-dependent manner.

Comparisons between the spectra obtained in the intact cell and *in vitro* under semi-physiological conditions suggested that the concentration of

cytoplasmic ADP available to PGK was much lower than the total extractable ADP concentration. The "true" free ADP concentration in the cytoplasm appeared to be less than 50 μM, possibly much less. This has important implications in calculations of the phosphorylation potential, and in the levels of AMP (through adenylate kinase) and ADP available, for example, as regulators of enzyme activity.

7.4 Kinetics of PGK *in vivo*

The rôle of PGK in the PGK/GAPDH couple catalysing an exchange reaction between the γ-phosphate of ATP and inorganic phosphate was investigated. The exchange reaction was monitored by ^{31}P NMR saturation transfer techniques, and the PGK activity in the cell was lowered from wild type to less than 5 % of wild type by genetic means. This involved using a cell line containing a disrupted genomic copy of the PGK gene, and carrying low copy-number plasmids expressing low levels of PGK. Further work may address some of the limitations of this approach by using genomically integrated rather than episomal vectors.

The experiments showed that PGK has very little influence on the rate of glycolysis under the conditions used, but a very great influence on the exchange flux between the γ-phosphate of ATP and P_i. In cells with less than 5 % of normal PGK levels, glycolysis was depressed by less than 30 %. Under these conditions, the exchange flux was equal to the net flux, suggesting the enzyme is operating far from equilibrium and essentially unidirectionally. With normal levels of PGK, there was a large exchange flux, suggesting the enzyme was operating nearer to equilibrium and with a significant reverse flux.

The relatively small effect on glycolysis of a very large decrease in PGK activity might suggest that there is no functionally significant GAPDH:PGK complex. If a complex is present, then it is in such catalytic excess that any need for it as a rate-enhancement device is called into question, at least in the steady-state stationary phase cell.

It is hoped in further work to examine the functional significance of the PGK:GAPDH and other complexes using structurally intact but functionally inert enzymes, produced by site-directed mutation of the native enzyme. A detailed understanding of the enzyme's operation, probably from crystallographic studies and molecular modelling, is required to predict the necessary mutations. These would be expected to disrupt the function of a complex-dependent pathway, reducing the pathway flux, but have little effect on a pathway linked only by free diffusion.

Cells with near-normal glycolytic flux but little ATP and P_i exchange flux should be of great value in studies of mitochondrial ATP synthesis. One of the important difficulties in studying mitochondrial ATP synthesis by ^{31}P NMR saturation transfer is the complication caused by substrate-level phosphorylation at the GAPDH/PGK couple. In the low-PGK cells this contribution can be calculated easily because it is simply equal to the net glycolytic flux.

A preliminary application of the low-PGK cells to directly measuring the P:O ratio in the intact yeast cell gave P:O ratio estimates of around 2 to 3. Further work will extend these measurements of mitochondrial ATP synthesis to situations where the cell is in an altered state, perhaps during active protein synthesis or in the presence of overexpressed adenine nucleotide translocase.

Bibliography

Abragam, A. (1961) The Principles of Nuclear Magnetism. Oxford University Press, Oxford.

Acerenza, L. and Kacser, H. (1990) Enzyme kinetics and metabolic control. A method to test and quantify the effect of enzymic properties on metabolic variables. *Biochem. J.* 269 697-707.

Adams, B. and Pain, R.H. (1986) The effect of substrates on the inter-domain interactions of the hinge-bending enzyme 3-phosphoglycerate kinase. *FEBS Lett.* 196(*2*) 361-364.

Adams, S.E. (1989) Protocols for production and purification of hybrid Ty-VLPs. British Bio-technology Group PLC (Technical bulletin, 1989).

Adriaensens, P., Box, M.E., Martens, H.J., Onkelinx, E., Put, J. and Gelan, J. (1988) Investigation of protein structure by means of ^{19}F NMR. A study of hen egg-white lysozyme. *Eur. J. Biochem.* 177(*2*) 383-394.

Alger, J.R. and Shulman, R.G. (1984) NMR studies of enzymatic rates *in vitro* and *in vivo* by magnetization transfer. *Q. Rev. Biophys.* 17 83-124.

Arnold, D.L., Matthews, P.M. and Radda, G.K. (1984) Metabolic recovery after exercise and the assessment of mitochondrial function *in vivo* in human skeletal muscle by means of P-31 NMR. *Magnetic Resonance in Medicine* 1(*307-315*)

Avison, M.J., Hetherington, H.P. and Shulman, R.G. (1986) Applications of NMR studies to tissue metabolism. *Annu. Rev. Biophys. Chem.* 15 377-402.

Bachmair, A., Finley, D. and Varshavsky, A. (1986) In vivo half-life of a protein is a function of its amino-terminal residue. *Science (Washington, D.C.)* 234 179-186.

Baker, S.M., Johnston, S.A., Hopper, J.E. and Jaehning, J.A. (1987) Transcription of multiple copies of the yeast GAL7 gene is limited by specific factors in addition to GAL4. *Mol. Gen. Genet.* 208 127-134.

Baleja, J.D., Marmorstein, R., Harrison, S.C. and Wagner, G. (1992) Solution structure of the DNA-binding domain of Cd_2-GAL4 from *S. cerevisiae*. *Nature* 356 450-453.

Banks, R.D., Blake, C.C.F., Evans, P.R., Haser, R., Rice, D.W., Hardy, G.W., Merrett, M. and Phillips, A.W. (1979) Sequence, structure and activity of phosphoglycerate kinase: a possible hinge-bending enzyme. *Nature* 279 773-777.

Bergmeyer, H.U. and Gawehn, K., Ed. (1978) Principles of Enzymatic Analysis. Verlag Chemie, Weinheim.

Bishop, E.O., Miles, R. and Smith, B.E. (1990) A ^{31}P NMR study of the mechanism of and salt effect on Mg^{2+}-ATP exchange. *Biochim. Biophys. Acta* 1019 276-282.

Blake, C.C.F., Rice, D.W. and Cohen, F.E. (1986) A "helix-scissors" mechanism for the hinge-bending conformational change in phosphoglycerate kinase. *Int. J. Peptide Protein Res.* 27 443-448.

Bode, R., Kunze, G. and Birnbaum, D. (1985) Reversal of glyphosate-induced growth inhibition of *Candida maltosa* by several amino acids and pyruvate. *Biochem. Physiol. Pflanz.* 180(*8*) 613-619.

Bode, R., Schauer, F. and Birnbaum, D. (1986) Comparative studies on the enzymological basis for growth inhibition by glyphosate in some yeast species. *Biochem. Physiol. Pflanz.* 181(*1*) 39-46.

Botstein, D. and Fink, G.R. (1988) Yeast: an experimental organism for modern biology. *Science (Washington, D.C.)* 240 1439-1442.

Boyle, H.A., Fairbrother, W.J. and Williams, R.J.P. (1989) An NMR analysis of the binding of inhibitors to yeast phosphoglycerate kinase. *Eur. J. Biochem.* 184 535-543.

Bradford, M.M. (1976) A rapid and sensitive method for the quantitation of microgram quantities of protein utilizing the principle of protein-dye binding. *Anal. Biochem.* 72 248-254.

Brindle, K.M. (1988) ^{31}P NMR magnetization-transfer measurements of flux between inorganic phosphate and adenosine 5'-triphosphate in yeast cells genetically modified to overproduce phosphoglycerate kinase. *Biochemistry* 27 6187-6196.

Brindle, K.M. and Campbell, I.D. (1987) NMR studies of kinetics in cells and tissues. *Q. Rev. Biophys.* 19(*3/4*) 159-182.

Brindle, K.M., Davies, S.E.C. and Williams, S.-P. (1991) A combined n.m.r. and molecular biological approach to studying enzymes *in vivo*. *Biochem. Soc. Trans.* 19 997-1001.

Brindle, K.M. and Krikler, S. (1985) ^{31}P-NMR saturation transfer measurements of phosphate consumption in *Saccharomyces cerevisiae*. *Biochim. Biophys. Acta* 847 285-292.

Brindle, K.M. and Radda, G.K. (1987) ^{31}P NMR saturation transfer measurements of exchange between P_i and ATP in the reactions catalysed by glyceraldehyde-3-phosphate dehydrogenase and phosphoglycerate kinase in vitro. *Biochim. Biophys. Acta* 928 47-55.

Brindle, K.M., Williams, S.-P. and Boulton, M. (1989) ^{19}F NMR detection of a fluorine-labelled enzyme *in vivo*. *FEBS Lett.* 255(*1*) 121-124.

Broker, M., Bauml, O., Gottig, A., Ochs, J., Bodenbenner, M. and Amann, E. (1991) Expression of the human blood coagulation protein Factor XIIIa in *Saccharomyces cerevisiae:* dependence of the expression levels from host-vector systems and medium conditions. *Appl. Microbiol. Biotechnol.* 34 756-764.

Brosnan, M.J., Chen, L., Van Dyke, T.A. and Koretsky, A.P. (1990) Free ADP levels in transgenic mouse liver expressing creatine kinase. *J. Biol. Chem.* 265(*34*) 20849-20855.

Brown, F.F., Campbell, I.D., Kuchel, P.W. and Rabenstein, D.L. (1977) Human erythrocyte metabolism studied by ^{1}H spin echo NMR. *FEBS Lett.* 82 12-16.

Bu'Lock, J.D. and Kristiansen, B. (1987) Basic Biotechnology. Academic Press, London.

Bücher, T. (1947) Über ein phosphatübertragendes Gärungsferment. *Biochim. Biophys. Acta* 1 292-314.

Bücher, T. (1955) Phosphoglycerate kinase from brewer's yeast. *Methods Enzymol.* 1 415-422.

Campbell, A.K. (1990) Bioluminescent proteins; rainbow proteins. European Patent Office PCT/GB90/01131.

Campbell, I.D., Dobson, C.M., Ratcliffe, R.G. and Williams, R.J.P. (1977) Fourier transform NMR pulse methods for the measurement of slow exchange rates. *J. Magn. Reson.* 29(*397-405*)

Campbell-Burk, S.L., den Hollander, J.A., Alger, J.R. and Shulman, R.G. (1987a) ^{31}P NMR saturation-transfer and ^{13}C NMR kinetic studies of glycolytic regulation during anaerobic and aerobic glycolysis. *Biochemistry* 26 7493-7500.

Campbell-Burk, S.L., Jones, K.A. and Shulman, R.G. (1987b) ^{31}P NMR saturation-transfer measurements in *Saccharomyces cerevisiae*: Characterisation of phosphate exchange reactions by iodoacetate and antimycin A inhibition. *Biochemistry* 26 7483-7492.

Cantor, C.R. and Shimmel, P.R. (1980) Biophysical chemistry. W.H. Freeman, San Francisco.

Cascante, M., Canela, E.I. and Franco, R. (1990) Control analysis of systems having two steps catalyzed by the same protein molecule in unbranched chains. *Eur. J. Biochem.* 192 369-371.

Chance, B., Nioka, S., Kent, J., McCully, K., Fountain, M., Greenfield, R. and Holton, G. (1988) Time-resolved spectroscopy of hemoglobin and myoglobin in resting and ischemic muscle. *Anal. Biochem.* 174 698-707.

Chiang, H.-L. and Schekman, R. (1991) Regulated import and degradation of a cytosolic protein in the yeast vacuole. *Nature* 350 313-318.

Chock, P.B. and Gutfreund, H. (1988) Reexamination of the kinetics of the transfer of NADH between its complexes with glycerol-3-phosphate dehydrogenase and with lactate dehydrogenase. *Proc. Natl. Acad. Sci. USA* 85 8870-8874.

Cornell, N.W., Leadbetter, M. and Veech, R.L. (1979) Effects of free magnesium concentration and ionic strength on equilibrium constants for the glyceraldehyde phosphate dehydrogenase and phosphoglycerate kinase reactions. *J. Biol. Chem.* 254(*14*) 6522-6527.

Cornish-Bowden, A. (1991) Failure of channelling to maintain low concentrations of metabolic intermediates. *Eur. J. Biochem.* 195 103-108.

Cousens, D.J., Wilson, M.J. and Hinchcliffe, E. (1990) Construction of a regulated PGK expression vector. *Nucleic Acids Res.* 18(*5*) 1308.

CRC Handbook (1978) CRC Handbook of Chemistry and Physics. CRC Press Inc., West Palm Beach, Florida.

Danhash, N., Gardner, D.C.J. and Oliver, S.G. (1991) Heritable damage to yeast caused by transformation. *Biotechnology* 9(*2*) 179-182.

Daugherty, A., Becker, N.N., Scherrer, L.A., Sobel, B.E., Ackerman, J.J.H., Baynes, J.W. and Thorpe, S.R. (1989) Non-invasive detection of protein metabolsim by *in vivo* NMR spectroscopy. *Biochem. J.* 264 829-835.

Davies, S.E.C. and Brindle, K.M. (1992) Effects of overexpression of phosphofructokinase on glycolysis in the yeast *Saccharomyces cerevisiae*. *Biochemistry* 31 4729-4735.

den Hollander, J.A., Ugurbil, K., Brown, T.R. and Shulman, R.G. (1981) Phosphorus-31 Nuclear Magnetic Resonance Studies of the Effect of Oxygen upon Glycolysis in Yeast. *Biochemistry* 20 5871-5880.

den Hollander, J.A., Ugurbil, K. and Shulman, R.G. (1986) ^{31}P and ^{13}C NMR studies of intermediates of aerobic and anaerobic glycolysis in *Saccharomyces cerevisiae*. *Biochemistry* 25 212-219.

Derechin, M., Rustum, Y.M. and Barnard, E.A. (1972) Dissociation of yeast hexokinase under the influence of its substrates. *Biochemistry* 11(*10*) 1793-1797.

Derome, A.E. (1987) Modern NMR Techniques for Chemistry Research. Pergamon Books Ltd., Oxford.

Desmoulin, F., Cozzone, P.J. and Canioni, P. (1987) Phosphorus-31 NMR study of phosphorylated metabolites compartmentation, intracellular pH and phosphorylation state during normoxia, hypoxia and ethanol perfusion in the perfused rat liver. *Eur. J. Biochem.* 162 151-159.

Deutscher, M.P., Ed. (1990) Guide to Protein Purification. Academic Press, San Diego.

Dice, J.F. (1987) Molecular determinants of protein half-lives in eukaryotic cells. *FASEB J.* 1 349-357.

Difco Laboratories (1963) Difco manual of dehydrated culture media. Difco Laboratories,, Detroit, Michigan, USA.

Dix, J.A. and Verkman, A.S. (1990) Mapping of fluorescence anisotropy in living cells by ratio imaging. Application to cytoplasmic viscosity. *Biophys. J.* 57 231-240.

Dunn, T.F. and Leach, F.R. (1967) Incorporation of p-fluorophenylalanine into protein by a cell-free system. *J. Biol. Chem.* 242 2693.

Endre, Z.H., Chapman, B.E. and Kuchel, P.W. (1983) Intra-erythrocyte microviscosity and diffusion of specifically labelled [*glycyl-α* ^{13}C]glutathione by using ^{13}C n.m.r. *Biochem. J.* 216 655-660.

Erhart, E. and Hollenberg, C.P. (1983) The presence of a defective *LEU2* gene on 2*μ* DNA recombinant plasmids of *Saccharomyces cerevisiae* is responsible for curing and high copy number. *J. Bacteriol.* 156 625-635.

Fabry, M.E. and San George, R.C. (1983) Effect of magnetic susceptibilty on nuclear magnetic resonance signals arising from red cells: A warning. *Biochemistry* 22 4119-4125.

Fairbrother, W.J., Graham, H.C. and Williams, R.J.P. (1990a) An NMR study of anion binding to yeast phosphoglycerate kinase. *Eur. J. Biochem.* 190 161-169.

Fairbrother, W.J., Graham, H.C. and Williams, R.J.P. (1990b) The roles of ATP^{4-} and Mg^{2+} in control steps of phosphoglycerate kinase. *Eur. J. Biochem.* 190 407-414.

Fairbrother, W.J., Hall, L., Littlechild, J.A., Walker, P.A., Watson, H.C. and Williams, R.J.P. (1988) Probing the 3-phosphoglycerate-binding site of yeast phosphoglycerate kinase using site-specific mutants and ^{1}H nuclear magnetic resonance spectroscopy. *Biochem. Soc. Trans.* 16 724-725.

Fairbrother, W.J., Minard, P., Hall, L., Betton, J.-M., Missiakas, D., Yon, J.M. and Williams, R.J.P. (1989a) Nuclear magnetic resonance studies of isolated structural domains of yeast phosphoglycerate kinase. *Protein Engineering* 3(*1*) 5-11.

Fairbrother, W.J., Walker, P.A., Minard, P., Littlechild, J.A., Watson, H.C. and Williams, R.J.P. (1989b) NMR analysis of site-specific mutants of yeast phosphoglycerate kinase. An investigation of the triose-binding site. *Eur. J. Biochem.* 183 57-67.

Fawcett, C.P., Ciotti, M.M. and Kaplan, N.O. (1961) Inhibition of dehydrogenase reactions by a substance formed from diphosphopyridine nucleotide. *Biochim. Biophys. Acta* 54 210-212.

Fell, D.A. and Sauro, H.M. (1985) Metabolic control and its analysis. Additional relationships between elasticities and control coefficients. *Eur. J. Biochem.* 148 555-561.

Fell, D.A. and Sauro, H.M. (1990) Metabolic control analysis. The effects of high enzyme concentrations. *Eur. J. Biochem.* 192 183-187.

Fersht, A. (1984) Enzyme kinetics, 2nd ed., Freeman.

Fifis, T. and Scopes, R.K. (1978) Purification of 3-phosphoglycerate kinase from diverse sources by affinity elution chromatography. *Biochem. J.* 175 311-319.

Forsén, S. and Hoffman, R.A. (1963) Study of moderately rapid chemical exchange reactions by means of nuclear magnetic double resonance. *J. Chem. Phys.* 39(*11*) 2982-2901.

Foxall, D.L., Cohen, J.S. and Mitchell, J.B. (1984) Continuous perfusion of mammalian cells embedded in agarose gel threads. *Exp. Cell. Res.* 154 521-529.

Freeman, D., Bartlett, S., Radda, G. and Ross, B. (1983) Energetics of sodium transport in the kidney. Saturation transfer ^{31}P-NMR. *Biochim. Biophys. Acta* 762 325-336.

Freifelder, D. (1982) Physical Biochemistry. W.H. Freeman & Co., San Francisco.

Futcher, A.B. and Cox, B.S. (1984) Copy number and the stability of 2μm circle-based artificial plasmids of *Saccharomyces cerevisiae*. *J. Bacteriol.* 157 283-290.

Gadian, D.G. (1982) Nuclear magnetic resonance and its applications to living systems. Clarendon Press, OUP, Oxford.

Gamcsik, M.P., Gerig, J.T. and Gregory, D.H. (1987) Fluorine nuclear magnetic resonance spectra of rabbit carbonmonoxyhemoglobin. *Biochim. Biophys. Acta* 912 303-316.

Gancedo, J.M. and Gancedo, C. (1973) Concentrations of intermediary metabolites in yeast. *Biochimie* 55 205-211.

Gerig, J.T. (1989) Fluorine nuclear magnetic resonance of fluorinated ligands. *Methods Enzymol.* 177 3-23.

Gerig, J.T., Klinkenborg, J.C. and Nieman, R.A. (1983) Assignment of fluorine nuclear magnetic resonance signals from rabbit cyanomethemoglobin. *Biochemistry* 22 2076-2087.

Ghosh, I. and McCammon, J.A. (1987) Solvent viscosity effects on the rate of side-chain rotational isomerization in a protein molecule. *J. Phys. Chem.* 91 4878-4881.

Giessner-Prettre, C. and Pullman, B. (1970) Intermolecular nuclear shielding values for protons of purines and flavins. *J. Theor. Biol.* 27 87-95.

Gnaiger, E. and Forstner, H., Ed. (1983) Polarographic Oxygen Sensors. Springer Verlag, Berlin.

Graham, H.C. and Williams, R.J.P. (1991) The roles of ADP^{2-} and Mg^{2+} in control steps of phosphoglycerate kinase. *Eur. J. Biochem.* 197 81-91.

Griko, Y.V., Venyaminov, S.Y. and Privalov, P.L. (1989) Heat and cold denaturation of phosphoglycerate kinase (interaction of domains). *FEBS Lett.* 244(*2*) 276-278.

Groen, A.K., Wenders, R.J.A., Westerhoff, H.V., van der Meer, R. and Tager, J.M. (1982) Quantification of the contribution of various steps to the control of mitochondrial respiration. *J. Biol. Chem.* 257 2754-2757.

Gupta, R.K., Benovic, J.L. and Rose, Z.B. (1978) The determination of the free magnesium level in the human red blood cell by ^{31}P NMR. *J. Biol. Chem.* 253 6172-6176.

Gupta, R.K., Gupta, P., Yushok, W.D. and Rose, Z.B. (1983a) Measurement of the dissociation constant of MgATP at physiological nucleotide levels by a combination of ^{31}P NMR and optical absorbance spectroscopy. *Biochem. Biophys. Res. Commun.* 117(*1*) 210-216.

Gupta, R.K., Gupta, P., Yushok, W.D. and Rose, Z.B. (1983b) On the noninvasive measurement of intracellular free magnesium by ^{31}P NMR spectrocopy. *Physiol. Chem. Phys. Med. NMR* 15 265-288.

Gyubi, L., Chance, B., Ligeti, L., McDonald, G. and Cone, J. (1988) Correlated *in vivo* ^{31}P NMR and NADH fluorometric studies on gerbil brain in graded hypoxia and hyperoxia. *Am. J. Physiol.* 254(*C*) 699-708.

Haigh, C.W. and Mallion, R.B. (1972) New tables of "ring current" shielding in proton magnetic resonance. *Org. Magn. Reson.* 4 203.

Hames, B.D. and Rickwood, D., Ed. (1990) Gel electrophoresis of proteins: a practical approach. OUP/IRL Press, London.

Harris, R.K. (1986) Nuclear Magnetic Resonance Spectroscopy. A physicochemical view. Longman, Harlow, Essex.

Haseloff, J. and Gerlach, W.L. (1988) Simple RNA enzymes with new and highly specific endoribonuclease activities. *Nature* 334(*6183*) 585-591.

Heinrich, R., Holzhütter, H.-. and Schuster, S. (1987) A theoretical approach to the evolution and structural design of enzymatic networks; linear enzymatic chains, branched pathways and glycolysis of erythrocytes. *Bull. Math. Biol.* 49 539.

Heinrich, R. and Rapoport, T.A. (1974) A linear steady-state treatment of enzymatic chains: general properties, control and effector strength. *Eur. J. Biochem.* 42 89.

Henry, G.D., Weiner, J.H. and Sykes, B.D. (1986) Backbone dynamics of a model membrane protein: ^{13}C NMR spectroscopy of alanine methyl groups in detergent-solubilized M13 coat protein. *Biochemistry* 25 590-598.

Hess, B. (1973) Organisation of glycolysis: oscillatory and stationary control. *Symp. Soc. Exp. Biol.* 27 105-131.

Hestenes, D. (1986) New Foundations for Classical Mechanics. D. Reidel Publishing Co., Dordrecht.

Hinnen, A., Hicks, J.B. and Fink, G.R. (1978) Transformation of yeast. *Proc. Natl. Acad. Sci. USA* 75 1929-1933.

Ho, C., Pratt, E.A. and Rule, G.S. (1989) Membrane-bound D-lactate dehydrogenase of *Escherichia coli* : a model for protein interactions in membranes. *Biochim. Biophys. Acta* 988 173-184.

Hu, C.Q. and Sturtevant, J.M. (1987) Thermodynamic study of yeast phosphoglycerate kinase. *Biochemistry* 26 178-182.

Hull, W.E. and Sykes, B.D. (1974) Fluorotyrosine alkaline phosphatase. ^{19}F nuclear magnetic resonance relaxation times and molecular motion of the individual fluorotyrosines. *Biochemistry* 13(*17*) 3431-3437.

Hull, W.E. and Sykes, B.D. (1975) Dipolar nuclear spin relaxation of ^{19}F in multispin systems. Application to ^{19}F labeled proteins. *J. Chem. Phys.* 63(*2*) 867-880.

Iles, R.A., Stevens, A.N. and Griffiths, J.R. (1982) NMR studies of metabolites in living tissue. *Prog. Nucl. Magn. Reson. Spectrosc.* 15 49-200.

Jackson, S.A., Thomson, M.J. and Clegg, J.S. (1990) Glycolysis compared in intact, permeabilized and sonicated L-929 cells. *FEBS Lett.* 262 212-214.

Jarema, M.A.C., Lu, P. and Miller, J.H. (1981) Genetic assignment of resonances in the NMR spectrum of a protein: *lac* repressor. *Proc. Natl. Acad. Sci. USA* 78(*5*) 2707-2711.

Jenkins, B.G. (1991) Detection of site-specific binding and co-binding of ligands to macromolecules using ^{19}F NMR. *Life Sciences* 48 1227-1240.

Johnson, C.E. and Bovey, F.A. (1958) Calculation of nuclear magnetic resonance spectra of aromatic hydrocarbons. *J. Chem. Phys.* 29 1012-1014.

Johnston, M. (1987) A model fungal gene regulatory mechanism: the GAL genes of *Saccharomyces cerevisiae. Microbiol. Rev.* 51 458-476.

Johnston, S.A. and Hopper, J.E. (1982) Isolation of the yeast regulatory gene GAL4 and analysis of its dosage effects on the galactose/melibiose regulon. *Proc. Natl. Acad. Sci. USA* 83 6971-6975.

Jones, E.W. (1990a) *Tackling the protease problem in Saccharomyces cerevisiae.* pp 428-453 in Guide to Yeast Genetics and Molecular Biology, ed by Guthrie, C. and Fink, G.R., Academic Press, San Diego.

Jones, E.W. (1990b) *Vacuolar proteases in yeast Saccharomyces cerevisiae.* pp 372-386 in Gene Expression Technology, ed by Goeddel, D.V., Academic Press, San Diego.

Jue, T. and Anderson, S. (1990) ^{1}H NMR observation of tissue myoglobin: an indicator of cellular oxygenation *in vivo*. *Magnetic Resonance in Medicine* 13(*3*) 524-528.

Kacser, H. and Burns, J.A. (1973) The control of flux. *Symp. Soc. Exp. Biol.* 27 65-104.

Kacser, H. and Burns, J.A. (1979) Molecular democracy: Who shares the controls? *Biochem. Soc. Trans.* 7 1149-1167.

Kacser, H. and Porteous, J.W. (1987) Control of metabolism: what do we have to measure. *Trends Biochem. Sci.* January 5-14.

Kahn, D. and Westerhoff, H.V. (1991) Control Theory of Regulatory Cascades. *J. Theor. Biol.* 153 255-285.

Kay, L.E., Ikura, M., Zhu, G. and Bax, A. (1991) 4-dimensional heteronuclear triple resonance NMR of isotopically enriched proteins for the sequential assignment of backbone atoms. *J. Magn. Reson.* 91(*2*) 422-428.

Kayne, F.J. (1973) *Pyruvate kinase.* pp 353-382 in The Enzymes, ed by Boyer, P.D., Academic Press, New York.

Keilin, D. (1925) On cytochrome, a respiratory pigment, common to animals, yeast, and higher plants. *Proc. Roy. Soc. London, series B* 98 312-320.

Keleti, T., Ovádi, J. and Batke, J. (1989) Kinetic and physico-chemical analysis of enzyme complexes and their possible role in the control of metabolism. *Prog. Biophys. Molec. Biol.* 53 105-152.

Kim, H.-W., Perez, J.A., Ferguson, S.J. and Campbell, I.D. (1990) The specific incorporation of labelled aromatic amino acids into proteins through growth of bacteria in the presence of glyphosate; application to fluoro-tryptophan labelling of the H^{+} ATPase of *Escherichia coli* and NMR studies. *FEBS Lett.* 272 34-36.

Kingsman, S.M., Cousens, D., Stanway, C.A., Chambers, A., M., W. and Kingsman, A.J. (1990) *High efficiency yeast expression vectors based on the promoter of the phosphoglycetate kinase gene.* pp 329-341 in Gene Expression Technology, ed by Goeddel, D.V., Academic Press, San Diego.

Kirk, K. and Kuchel, P.W. (1988) Physical basis of the effect of hemoglobin on the ^{31}P NMR chemical shifts of various phosphoryl compunds. *Biochemistry* 27 8803-8810.

Kirschenlohr, H.L., Metcalfe, J.C., Morris, P.G. and Rodrigo, G.C. (1988) Ca^{2+} transient, Mg^{2+}, and pH measurements in the cardiac cycle by ^{19}F NMR. *Proc. Natl. Acad. Sci. USA* 85 9017-9021.

Klionsky, D.J., Herman, P.K. and Emr, S.D. (1990) The fungal vacuole: composition, function, and biogenesis. *Microbiol. Rev.* 54(*3*) 266-292.

Knight, M.R., Campbell, A.K., Smith, S.M. and Trewevas, A.J. (1991) Transgenic plant aequorin reports the effects of touch and cold-shock and elicitors on cytoplasmic calcium. *Nature* 352 524-526.

Kraulis, P.J., Raine, A.R.C., Gadhavi, P.L. and Laue, E.D. (1992) Structure of the DNA-binding domain of zinc GAL4. *Nature* 356 448-450.

Kvassman, J. and Petterson, G. (1989a) Evidence that 1,3-bisphosphoglycerate dissociation from phosphoglycerate kinase is an intrinsically rapid reaction step. *Eur. J. Biochem.* 186 261-264.

Kvassman, J. and Petterson, G. (1989b) Mechanism of 1,3-bisphosphoglycerate transfer from phosphoglycerate kinase to glyceraldehyde-3-phosphate dehydrogenase. *Eur. J. Biochem.* 186 265-272.

Laemmli, U.K. (1970) Cleavage of structural proteins during the assembly of the head of bacteriophage T4. *Nature* 227 680-685.

Larsson-Raznikiewicz, M. (1964) Kinetic studies on the reaction catalysed by phosphoglycerate kinase. I. The effect of Mg^{2+} and adenosine 5'-triphosphate. *Biochim. Biophys. Acta* 85 60-68.

Larsson-Raznikiewicz, M. (1970) The phosphoglycerate kinase reaction and its metal ion specificity. *Eur. J. Biochem.* 17 183-192.

Larsson-Raznikiewicz, M. (1973) Graphical Analyses on Binding of Ligands to a Two-Sited System. Theoretical Treatments Exemplified on Yeast Phosphoglycerate Kinase. *Arch. Biochem. Biophys.* 158 754-762.

Larsson-Raznikiewicz, M. and Arvidsson, L. (1971) Inhibition of phosphoglycerate kinase by products and product homologues. *Eur. J. Biochem.* 22 506-512.

Larsson-Raznikiewicz, M. and Malmstrom, B.G. (1961) The metal-ion activation of 3-phosphoglycerate kinase in correlation with metal-binding studies. *Arch. Biochem. Biophys.* 92 94-99.

Laughton, A., Driscoll, R., Wills, N. and Gesteland, R.F. (1984) Identification of two proteins encoded by the *Saccharomyces cerevisiae* GAL4 gene. *Mol. Cell. Biol.* 4 268-275.

Lawson, J.W.R. and Veech, R.L. (1979) Effects of pH and free Mg^{2+} on the K_{eq} of the creatine kinase reaction and other phosphate hydrolyses and phosphate transfer reactions. *J Biol Chem* 254(*14*) 6528-6537.

Lepock, J.R., Cheng, K.-H., Campbell, S.D. and Kruuv, J. (1983) Rotational diffusion of tempone in the cytoplasm of Chinese hamster lung cells. *Biophys. J.* 44 405-412.

London, R. (1991) Methods for measurement of intracellular magnesium: NMR and fluorescence. *Annu. Rev. Physiol.* 53 241-258.

London, R.E. and Gabel, S.A. (1989) Determination of membrane potential and cell volume by ^{19}F NMR using trifluoroacetate and trifluoroacetamide probes. *Biochemistry* 28 2378-2382.

Luby-Phelps, K., Taylor, D.L. and Lanni, F. (1986) Probing the structure of cytoplasm. *J. Cell. Biol.* 102 2015-2022.

Luck, L.A. and Falke, J.J. (1991) ^{19}F NMR studies of the D-galactose chemosensory receptor. 1. Sugar binding yields a global structural change. *Biochemistry* 30 4248-4256.

Mackler, B. and Haynes, B. (1973) Studies of oxidative phosphorylation in *Saccharomyces cerevisiae* and *Saccharomyces carlsbergensis. Biochim. Biophys. Acta* 292 88-91.

Madden, A., Leach, M.O., Sharp, J.C., Collins, D.J. and Easton, D. (1991) A quantitative analysis of pH measurement accuracy: Assessment of the NMR methodology. *NMR in Biomedicine* 4(*1*) 1-11.

Mann, B.E. (1977) The application of the Forsén-Hoffman spin-saturation method of measuring rates of exchange to the ^{13}C NMR spectrum of N,N-dimethylformamide. *J. Magn. Reson.* 25 91-94.

Marmorstein, R., Carey, M., Ptashne, M. and Harrison, S.C. (1992) DNA recognition by GAL4: structure of a protein-DNA complex. *Nature* 356 408-414.

Mas, M.T., Bailey, J.M. and Resplandor, Z.E. (1988) Site-directed mutagenesis of histidine-388 in the hinge region of yeast 3-phosphoglycerate kinase: Effects on catalytic activity and activation by sulfate. *Biochemistry* 27 1168-1172.

Mas, M.T., Chen, C.Y., Hitzeman, R.A. and Riggs, A.D. (1986) Active human-yeast chimeric phosphoglycerate kinases engineered by domain interchange. *Science (Washington, D.C.)* 233 788-790.

Mas, M.T. and Resplandor, Z.E. (1988) Structure-function relationships in 3-phosphoglycerate kinase: Role of the carboxy-terminal peptide. *Proteins* 4 56-62.

Mas, M.T., Resplandor, Z.E. and Riggs, A.D. (1987) Site-directed mutagenesis of glutamate-190 in the hinge region of yeast 3-phosphoglycerate kinase: Implications for the mechanism of domain movement. *Biochemistry* 26 5369-5377.

Mastro, A.M., Babich, M.A., Taylor, W.D. and Keith, A.D. (1984) Diffusion of a small molecule in the cytoplasm of mammalian cells. *Proc. Natl. Acad. Sci. USA* 81 3414-3418.

Matthews, P.M., Bland, J.L., Gadian, D.G. and Radda, G.K. (1981) The steady-state rate of ATP synthesis in the perfused rat heart measured by ^{31}P NMR saturation transfer. *Biochem. Biophys. Res. Commun.* 103 1052-1059.

McDonald, R.C., Steitz, T.A. and Engelman, D.M. (1979) Yeast hexokinase in solution exhibits a large conformational change upon binding glucose or glucose-6-phosphate. *Biochemistry* 18(*2*) 338-342.

Mellor, J., Dobson, M.J., Roberts, N.A., Kingsman, A.J. and Kingsman, S.M. (1985) Factors affecting heterologous gene expression in *Saccharomyces cerevisiae*. *Gene* 33 215-226.

Mellor, J., Dobson, M.J., Roberts, N.A., Tuite, M.F., Emtage, J.S., White, S., Lowe, P.A., Patel, T., Kingsman, A.J. and Kingsman, S.M. (1983) Efficient synthesis of enzymatically active calf chymosin in *Saccharomyces cerevisiae*. *Gene* 24 1-14.

Mendes, P., Kell, D.B. and Westerhoff, H.V. (1992) Channelling can decrease pool size. *Eur. J. Biochem.* 204 257-266.

Metzler, D.E. (1977) Biochemistry, the chemical reactions of living cells. Academic Press, New York.

Millikan, G.A. (1937) Experiments on muscle haemoglobin *in vivo*; the instantaneous measurement of muscle metabolism. *Proc. Roy. Soc. London, series B* 123 218-241.

Minard, P., Bowen, D.J., Hall, L., Littlechild, J.A. and Watson, H.C. (1990) Site-directed mutagenesis of aspartic acid 372 at the ATP binding site of yeast phosphoglycerate kinase: over-expression and characterisation of the mutant enzyme. *Protein Engineering* 3(*6*) 515-521.

Minard, P., Hall, L., Betton, J.-M., Missiakas, D. and Yon, J.M. (1989) Efficient expression and characterisation of isolated structural domains of yeast phosphoglycerate kinase generated by site-directed mutagenesis. *Protein Engineering* 3(*1*) 55-60.

Moon, R.B. and Richards, J.H. (1973) Determination of intracellular pH by ^{31}P magnetic resonance. *J. Biol. Chem.* 248(*20*) 7276-7278.

Müller, K., Kratky, O., Röschlau, P. and Hess, B. (1972) X-ray small-angle scattering of the allosteric yeast pyruvate kinase. *Hoppe-Seylers Z. Physiol. Chem.* 353 803-809.

Murcott, T.H.L., McNally, T., Allen, S.C., Fothergill-Gilmore, L.A. and Muirhead, H. (1991) Purification, characterisation and mutagenesis of highly expressed recombinant yeast pyruvate kinase. *Eur. J. Biochem.* 198 513-519.

Murphy, E., Gabel, S.A., Funk, A. and London, R.E. (1988) NMR observability of ATP: Preferential depletion of cytosolic ATP during ischemia in perfused rat liver. *Biochemistry* 27 526-528.

Navon, G., Shulman, R.G., Yamane, T., Eccleshall, T.R., Lam, K.-B., Baronofsky, J.J. and Marmur, J. (1979) Phosphorus-31 nuclear magnetic resonance studies of wild-type and glycolytic pathway mutants of *Saccharomyces cerevisiae*. *Biochemistry* 18(*21*) 4487-4499.

Nimmo, H.G. and Cohen, P.T.W. (1987) Applications of recombinant DNA technology to studies of metabolic regulation. *Biochem. J.* 247 1-13.

Offord, R. (1991) Going beyond the code. *Protein Engineering* 4(*7*) 709-710.

Ogden, J., Stanway, C., Kim, S., Mellor, J., Kingsman, A.J. and Kingsman, S.M. (1986) Efficient expression of the *Saccharomyces cerevisiae PGK* gene depends on an upstream activation sequence but does not require TATA sequnces. *Mol. Cell. Biol.* 6(*12*) 4335-4343.

Okorokov, L.A., Lichko, L.P. and Kulaev, I.S. (1980) Vacuoles: main compartments of potassium, magnesium, and phosphate ions in *Saccharomyces carlsbergensis* cells. *J. Bacteriol.* 144(*2*) 661-665.

Ovádi, J. (1991) Physiological significance of metabolite channeling. *J. Theor. Biol.* 152(*1*) 1-22.

Perkins, S.J. (1982) Application of Ring Current Calculations to the Proton NMR of Proteins and transfer RNA. *Biol. Magn. Reson.* 4 193-336.

Pickover, C.A., McKay, D.B., Engelman, D.M. and Steitz, T.A. (1979) Substrate binding closes the cleft between the domains of yeast phosphoglycerate kinase. *J. Biol. Chem.* 254(*22*) 11323-11329.

Piper, P.W., Curran, B., Davies, M.W., Hirst, K., Lockheart, A., Ogden, J.E., Stanway, C.A., Kingsman, A.J. and Kingsman, S.M. (1988) A heat shock element in the phoglycerate kinase gene promoter of yeast. *Nucleic Acids Res.* 16(*4*) 1333-1348.

Piper, P.W. and Curran, B.P.G. (1990) When a glycolytic gene on a yeast 2μ ORI-*STB* plasmid is made essential for growth its expression level is a major determinant of plasmid copy number. *Curr. Genet.* 17 119-123.

Pople, J.A. (1956) Proton magnetic resonance of hydrocarbons. *J. Chem. Phys.* 24 1111.

Post, J.F.M., Cottam, P.F., Simplaceanu, V. and Ho, C. (1984) Fluorine-19 nuclear magnetic resonance study of 5-fluorotryptophan-labeled histidine-binding Protein J of *Salmonella typhimurium. J. Mol. Biol..* 179 729-743.

Radda, G.K. (1986) The use of NMR spectroscopy for the understanding of disease. *Science (Washington, D.C.)* 233 640-645.

Ramasamy, R., Lazar, I., Brucher, E., Sherry, A.D. and Malloy, C.R. (1991) NOTPME: a ^{31}P NMR probe for measurement of divalent cations in biological systems. *FEBS Lett.* 280 121-124.

Rao, B.D.N., Cohn, M. and Scopes, R.K. (1978) ^{31}P NMR study of bound reactants and products of yeast 3-phosphoglycerate kinase at equilibrium and the effect of sulfate ion. *J. Biol. Chem.* 253(*22*) 8056-8060.

Rao, D.R. and Oesper, P. (1961) Purification and properties of muscle phosphoglycerate kinase. *Biochem. J.* 81 405-411.

Ray, B.D., Moore, J.M. and Rao, B.D.N. (1990) ^{31}P NMR studies of enzyme-bound substrate complexes of yeast 3-phosphoglycerate kinase: 3. Two ADP binding sites and their Mg(II) affinity; effects of vanadate and arsenate on enzymic complexes with ADP and 3-P-glycerate. *J. Inorg. Biochem.* 40 47-57.

Ray, B.D. and Rao, B.D.N. (1988a) ^{31}P NMR studies of enzyme-bound substrate complexes of yeast 3-phosphoglycerate kinase. 1. Effects of sulfate and pH. Mg(II) affinity at the two ATP sites. *Biochemistry* 27 5574-5578.

Ray, B.D. and Rao, B.D.N. (1988b) ^{31}P NMR studies of enzyme-bound substrate complexes of yeast 3-phosphoglycerate kinase. 2. Structure measurements using paramagnetic relaxation effects of Mn(II) and Co(II). *Biochemistry* 27 5579-5585.

Reeck, G. (1976) *Amino acid composition of selected proteins.* pp 504-510 in Handbook of Biochemistry and Molecular Biology, ed by Fasman, G.D., CRC Press, Inc., West Palm Beach, Florida.

Resnick, M.A., Westmoreland, J. and Bloom, K. (1990) Heterogeneity and maintenance of centromere plasmid copy number in *Saccharomyces cerevisiae. Chromosoma* 99 281-288.

Roberts, J.K.M., Wade-Jardetzky, N. and Jardetzky, O. (1981) Intracellular pH measurements by ^{31}P NMR. Influence of factors other than pH on ^{31}P chemical shifts. *Biochemistry* 20 5389-5394.

Roberts, J.K.M., Wemmer, D. and Jardetzky, O. (1984) Measurement of mitochondrial ATPase activity in maize root tips by saturation transfer ^{31}P nuclear magnetic resonance. *Plant Physiol.* 74 632-639.

Roschlau, P. and Hess, B. (1972) Purification and crystallisation of yeast pyruvate kinase. *Hoppe-Seylers Z. Physiol. Chem.* 353 435-440.

Rose, A.B. and Broach, J.R. (1990) *Propagation and expression of cloned genes in yeast: 2μ circle-based vectors.* pp 234-279 in Gene Expression Technology, ed by Goeddel, D.V., Academic Press, San Diego.

Ross, W.N. (1989) Changes in intracellular calcium during neuron activity. *Annu. Rev. Physiol.* 51 491-506.

Rothstein, R. (1990) *Targeting, Disruption, Replacement, and Allele Rescue: Integrative DNA Transformation in Yeast.* pp 281-301 in Guide to Yeast Genetics and Molecular Biology, ed by Guthrie, C. and Fink, G.R., Academic Press, San Diego.

Rule, G.S., Pratt, E.A., Simplaceanu, V. and Ho, C. (1987) Nuclear magnetic resonance and molecular genetic studies of the membrane-bound D-lactate dehydrogenase of *Escherichia coli. Biochemistry* 26 549-556.

Sambrook, J., Fritsch, E.F. and Maniatis, T. (1989) Molecular Cloning: A laboratory manual. Cold Spring Harbor.

Sanders, J.K.M. and Hunter, B.K. (1987) Modern NMR Spectroscopy. Oxford University Press, Oxford.

Santi, D.V. and Danenberg, P.V. (1971) Phenylalanyl transfer ribonucleic acid synthetase from *Escherichia coli.* Analysis of the phenylalanine binding site. *Biochemistry* 10 4812.

Scheffler, J.E. and Cohn, M. (1986) Photochemically induced dynamic nuclear polarisation NMR study of yeast and horse muscle phosphoglycerate kinase. *Biochemistry* 25 3788-3796.

Schierbeck, B. and Larsson-Raznikiewicz, M. (1979) Product inhibition studies of yeast phosphoglycerate kinase evaluating properties of multiple substrate binding sites. *Biochim. Biophys. Acta* 568 195-204.

Schultz, L.D., Hofmann, K.J., Mylin, L.M., Montgomery, D.L., Ellis, R.W. and Hopper, J.E. (1987) Regulated overproduction of the GAL4 gene product greatly increases expression from galactose-inducible promoters on multi-copy expression vectors in yeast. *Gene* 61 123-133.

Scopes, R.K. (1971) An improved procedure for the isolation of 3-phosphoglycerate kinase from yeast. *Biochem. J.* 122 89-92.

Scopes, R.K. (1973) *3-Phosphoglycerate kinase.* pp 335-351 in The Enzymes, ed by Boyer, P.D., Academic Press, New York.

Scopes, R.K. (1978a) Binding of substrates and other anions to yeast phosphoglycerate kinase. *Eur. J. Biochem.* 91 119-129.

Scopes, R.K. (1978b) The steady-state kinetics of yeast phosphoglycerate kinase. *Eur. J. Biochem.* 85 503-516.

Scopes, R.K. (1987) Protein purification. Principles and practice. Spinger-Verlag, New York.

Seo, Y., Murakami, M., Watari, H., Imai, Y., Yoshizaki, K., Nishikawa, H. and Morimoto, T. (1983) Intracellular pH determination by a ^{31}P NMR technique. The second dissociation constant of phosphoric acid in a biological system. *J. Biochem.* 94(*729-734*)

Shaka, A.J., Keeler, J., Frenkiel, T. and Freeman, R. (1983) An improved sequence for broadband decoupling: WALTZ-16. *J. Magn. Reson.* 52 335-338.

Sharman, F., Fink, G.R. and Hicks, J.B. (1986) Laboratory Course Manual for Methods in Yeast Genetics. Cold Spring Harbor Laboratory.

Shearwin, K. and Masters, C. (1990) The binding of glycolytic enzymes to the cytoskeleton - influence of pH. *Biochem. Int.* 22(*4*) 735-740.

Shearwin, K., Nanhua, C. and Masters, C. (1990) Interactions between glycolytic enzymes and cytoskeletal structure - the influence of ionic strength and molecular crowding. *Biochem. Int.* 21(*1*) 53-60.

Sixl, F., King, R.W., Bracken, M. and Feeney, J. (1990) ^{19}F NMR studies of ligand-binding to 5-fluorotryptophan- and 3-fluorotyrosine-containing cyclic AMP receptor protein from *Escherichia coli. BJ* 266 545-552.

Small, J.R. and Fell, D.A. (1989) The matrix method of metabolic control analysis: its validity for complex pathway structures. *J. Theor. Biol.* 136 181.

Small, J.R. and Fell, D.A. (1990) Covalent modification and metabolic control analysis. *Eur. J. Biochem.* 191 405-411.

Spickett, C.M. (1990) NMR studies of cellular bioenergetics. D. Phil. thesis, University of Oxford.

Spivey, H.O. and Merz, J.M. (1989) Metabolic compartmentation. *BioEssays* 10(*4*) 127-130.

Srere, P.A. (1987) Complexes of sequential metabolic enzymes. *Annu. Rev. Biochem.* 56 89-124.

Srere, P.A. and Ovadi, J. (1990) Enzyme-enzyme interactions and their metabolic role. *FEBS Lett.* 268(*2*) 360-364.

Srivastava, D.K. and Bernhard, S.A. (1986) Enzyme-enzyme interactions and the regulation of metabolic reaction pathways. *Curr. Top. Cell. Regul.* 28 1-68.

Stubbs, M., Freeman, D. and Ross, B.D. (1984) Formation of n.m.r.-invisible ADP during renal ischaemia in rats. *Biochem. J.* 224 2421-246.

Sukhodelets, M.V., Muronetz, V.I., Tsuprun, V.L., Kaftanova, A.S. and Nagradova, N.K. (1988) Association of rabbit muscle glyceraldehyde-3-phosphate dehydrogenase and 3-phosphoglycerate kinase. The biochemical and electron-microscope evidence. *FEBS Lett.* 238(*1*) 161-166.

Sumegi, B., Sherry, A.D. and Malloy, C.R. (1990) Channeling of TCA cycle intermediates in cultured *Saccharomyces cerevisiae. Biochemistry* 29 9106-9110.

Sykes, B.D. and Weiner, J.H. (1980) *Biosynthesis and ^{19}F NMR characterization of fluoroamino acid containing proteins.* pp 171-196 in Magnetic Resonance in Biology, ed by Cohen, J.S., Wiley, New York.

Takayama, K.M. and Inouye, M. (1990) Antisense RNA. *CRC Crit. Rev. Biochem. and Mol. Biol.* 25(*3*) 155-184.

Tao, T. (1969) Time-dependent fluorescence depolarization and Brownian rotational diffusion coefficients of macromolecules. *Biopolymers* 8 609-632.

Tompa, P., Hong, P.T. and Vas, M. (1986) The phosphate group of 3-phosphoglycerate accounts for conformational changes occurring on binding to 3-phosphoglycerate kinase. Enzyme inhibition and thiol reactivity studies. *Eur. J. Biochem.* 154 643-649.

Torres, N.V., Mateo, F., Melendez-Hevia, E. and Kacser, H. (1986) Kinetics of metabolic pathways. A system *in vitro* to study the control of flux. *Biochem. J.* 234 169-174.

Turnock, G., Ed. (1991) Biotechnological innovations in health care. Butterworth-Heineman, Oxford.

Tyler-Burt, C., Cheng, H.-M., Gabel, S. and London, R.E. (1990) ATP, ADP, and Magnesium Mixed Solutions: *In vitro* ^{31}P NMR Characterisation and *in vivo* Applications to Lens. *J. Biochem.* 108 441-448.

Van Holde, K.E. (1971) Physical Biochemistry. Prentice-Hall, New Jersey.

Van Schaftingen, E., Davies, D.R. and Hers, H. (1980) Fructose-2,6-bisphosphatase from rat liver. *Eur. J. Biochem.* 124 143-149.

Vas, M. and Batke, J. (1990) Kinetic misinterpretaion of a coupled enzyme reaction can lead to the assumption of an enzyme-enzyme interaction. The example of 3-phospho-D-glycerate kinase and glyceraldehyde-3-phosphate dehydrogenase couple. *Eur. J. Biochem.* 191 679-683.

Veech, R.L., Lawson, J.W.R., Cornell, N.W. and Krebs, H.A. (1979) Cytosolic phosphorylation potential. *J. Biol. Chem.* 254(*14*) 6538-6547.

Veloso, D., Guynn, R.W., Oskarsson, M. and Veech, R.L. (1973) The concentrations of free and bound magnesium in rat tissues. *J. Biol. Chem.* 248(*13*) 4811-4819.

Vold, R.L., Waugh, J.S., Klein, M.P. and Phelps, D.E. (1968) Measurement of spin relaxation in complex systems. *J. Chem. Phys.* 48 3831-3832.

Walsh, J.L. and Knull, H.R. (1987) Heteromerous interactions among glycolytic enzymes and of glycolytic enzymes with F-actin: effects of poly(ethylene glycol). *Biochim. Biophys. Acta* 952 83-91.

Wang, Z.Y., Noyszewski, E.A. and Leigh, J.S. (1990) *In vivo* MRS measurement of deoxymyoglobin in human forearms. *Magnetic Resonance in Medicine* 14(*3*) 562-567.

Wasylewski, Z. and Eftink, M.R. (1987) Frequency domain fluorescence studies of yeast phosphoglycerate kinase and its ternary complex. *Eur. J. Biochem.* 167 513-518.

Watson, H.C., Walker, N.P.C., Shaw, P.J., Bryant, T.N., Wendell, P.L., Fothergill, L.A., Perkins, R.E., Conroy, S.C., Dobson, M.J., Tuite, M.F., Kingsman, A.J. and Kingsman, S.M. (1982) Sequence and structure of yeast phosphoglycerate kinase. *EMBO J.* 1(*12*) 1635-1640.

Weber, J.P. and Bernhard, S.A. (1982) Transfer of 1,3-diphosphoglycerate between glyceraldehyde-3-phosphate dehydrogenase and 3-phosphoglycerate kinase via an enzyme-substrate-enzyme complex. *Biochemistry* 21 4189-4194.

Wilson, H.R., Williams, R.J.P., Littlechild, J.A. and Watson, H.C. (1988) NMR analysis of the interdomain region of yeast phosphoglycerate kinase. *Eur. J. Biochem.* 170 529-538.

Wittebort, R.J. and Szabo, A. (1978) Theory of NMR relaxation in macromolecules: restricted diffusion and jump models for multiple internal rotations of amino acid side chains. *J. Chem. Phys.* 69(*4*) 1722-1736.

Wu, X., Gutfreund, H., Lakatos, S. and Chock, P.B. (1991) Substrate channeling in glycolysis: A phantom phenomenon. *Proc. Natl. Acad. Sci. USA* 88 497-501.